RELIABILITY BASED SINGLE AND MULTI-OBJECTIVE OPTIMIZATION OF CONCRETE MIX DESIGN PARAMETERS

A Ph. D. Thesis
Submitted in Fulfillment of the
Requirements for the Award of the Degree of

DOCTOR OF PHILOSOPHY

By:

Ms. Rachna Aggarwal

Reg. No.: 950911006

Supervisors

Dr. M. K. Sharma	**Dr. R. K. Sharma**	**Dr. Maneek Kumar**
Associate Professor School of Mathematics	Professor Department of Computer Science & Engineering	Professor Department of Civil Engineering

SCHOOL OF MATHEMATICS

THAPAR UNIVERSITY

(Declared as Deemed-to-be-University u/s 3 of UGC act of 1956)

PATIALA – 147 004

July 2015

To my parents and my lovely family

CERTIFICATE

I, **Rachna Aggarwal** hereby certify that the work which is being presented in this thesis entitled, "RELIABILITY BASED SINGLE AND MULTI-OBJECTIVE OPTIMIZATION OF CONCRETE MIX DESIGN PARAMETERS", in partial fulfillment of the requirements for the award of degree of **DOCTOR OF PHILOSOPHY** in the School of Mathematics, Thapar University, Patiala, is an authentic record of my own work carried out under the supervision of **Dr. M.K. Sharma** (Associate Professor, SoM, Thapar University, Patiala), **Dr. R.K.Sharma** (Professor, CSED, Thapar University, Patiala) and **Dr. Maneek Kumar** (Professor, CED, Thapar University, Patiala)

The matter presented in this thesis has not been submitted either in part or full to any other university or institute for the award of any other degree.

Rachna Aggarwal 16/7/15

(**Rachna Aggarwal**)
Signature of candidate

This is certified that the above statement made by the candidate is correct to the best of our knowledge.

16/7/15

Dr. M. K. Sharma
Associate Professor
School of Mathematics
Thapar university
Patiala-147004
India
Supervisor

R.K.Sharma 16.7.15

Dr. R. K. Sharma
Professor
Department of Computer Science & Engineering
Thapar university
Patiala-147004
India
Supervisor

Maneek 16/7/15

Dr. Maneek Kumar
Professor
Department of Civil Engineering
Thapar university
Patiala-147004
India
Supervisor

ACKNOWLEDGEMENTS

I would like to express my special appreciation and thanks to my advisors Dr. M.K. Sharma, Dr. R.K.Sharma and Dr. Maneek Kumar, who have been tremendous mentors for me. I shall ever remain indebted to them for encouraging my research and for allowing me to grow as a research scientist. I would like to thank them for their meticulous guidance, constructive criticism, keen interest and constant encouragement. I would also like to express my gratitude to Dr. Amit Kumar and Dr. Naveen Kwatra for serving as my committee members.

Special words of appreciation go to Mr. Gourav Gupta, my student and research scholar at SoM who supported me unconditionally all through my research.

A special thanks to my family. Words cannot express how grateful I am to all of my family members, for all of the prayers that they've made on my behalf. Their prayer for me was what sustained me thus far.

The blessings of my father Sh. Narinder Kumar Aggarwal and my brother Sh. Rishi Kumar were always there with me which helped me do better each day. The moral support and encouragement given by my mother Smt. Vidya Gupta and my sister Smt. Sangeeta Singla helped me tackle all the problems and work harder.

I wholeheartedly thank my mother-in-law Smt. Sudesh Gupta and my sister-in-laws for providing me moral support during the course of work.

At the end I would like express appreciation to my husband Mr. Sumit Aggarwal who spent sleepless nights and was always my support in the moments of distress. My son Aneesh Aggarwal always stood by my side and kept my morale high. He deserves all admiration.

(RACHNA AGGARWAL)

ABSTRACT

Concrete is a composite construction material made by water; Portland cement; and fine and coarse aggregates in desired proportions. Additional components such as chemical and mineral admixtures may be added to the basic mix constituents to enhance certain properties of fresh or hardened concrete. The process of selecting suitable ingredients for concrete and their relative amount with the objective of producing concrete of required strength, durability and workability as economically as possible is termed as mix design. However, concrete mix design is always under the effect of random environment, and the sources of randomness are variations in quality of materials, mixing and transporting procedures, major methods of placing concrete; and methods of curing and testing procedures. As such actual compressive strength of concrete in a structure is always different from the specimen obtained under controlled laboratory conditions. This gap between the expected performance and obtained performance is even larger when the mix design is deterministically optimized since Deterministic Design Optimization (DDO) typically yields optimal designs that are pushed to the limits of design constraint boundaries; leaving no room for uncertainties in manufacturing imperfections, modeling and design variables.

In the present work, a reliability based design optimization strategy has been developed for finding reliable optimal concrete mix proportions under single and multi-objective environments. The steps considered in this strategy are: statistical analysis of the data; developing models for concrete mix parameters; and reliability based single and multi-objective optimization of concrete mix proportions. In statistical analysis step, experimental data generated by Kumar (2002) has been explored to identify the input parameters for developing models for compressive strength of concrete. Selected parameters have been analyzed to study inter-dependency among them.

In the second step, Ordinary Least Square Regression (OLSR), Principal Component Regression (PCR), Traditional Ridge Regression (TRR) and Generalized Ridge Regression (GRR) techniques have been employed to develop models for prediction of compressive strength of concrete for different curing ages. The models are then incorporated into the Reliability Based Design Optimization (RBDO) model.

In the third step, the efficient and well-known RBDO method, namely, Sequential

Optimization and Reliability Assessment (SORA) method is employed to determine reliable optimal concrete mix proportions in single objective environment. Safety factor based DDO designs have also been obtained using Sequential Quadratic Programming (SQP) technique. Reliabilities of DDO designs have been computed using Advanced Mean Value (AMV) algorithm. It is seen that reliability of RBDO designs are more than that of DDO designs. Elitist Non-Dominated Sorting Algorithm (NSGA-II) developed by Deb *et al*. (2002) has been used to study the tradeoff between cost of concrete and reliability of compressive strength constraint satisfaction in multi-objective environment.

The optimal concrete mix proportions obtained in this work satisfy compressive strength requirement constraint with desired reliability. Results from this research suggest that the RBDO methodology could be a valuable tool for minimizing the number of trial batches required to identify the optimal concrete mix proportions having desired properties and reliability.

CONTENTS

LIST OF TABLES

LIST OF FIGURES

CHAPTER 1
INTRODUCTION

==========

1.0 GENERAL

Concrete is a ubiquitous building material that has been in use for millennia. It has experienced a modern revival since the discovery of Portland cement in the 1800s. It is used extensively for building roadways, bridges, buildings, walkways, and numerous other structures. Conventional concrete is a mixture of water; Portland cement; and fine and coarse aggregates. Additional components such as chemical and mineral admixtures may be added to the basic mixture to enhance certain properties of fresh or hardened concrete. The process of selecting suitable ingredients for concrete and their relative amount with the objective of producing concrete of required strength, durability and workability as economically as possible is termed as mix design. Earlier, concrete manufacturers used to employ a variety of concrete mix designs having different strengths, slumps and other properties, which are optimized through trial and error and/or through standard mix design tables. But, given the extremely large number of possible concrete mix designs, coupled with the practical inability to test even a small fraction of such mix designs, the likelihood of identifying the optimum mix design through trial and error and/or through the use of standard tables is very small. So, various proportioning methods have been explored by researchers to achieve optimum mix design proportions. The objective of any proportioning method is to determine an adequate and economic rate for the materials making-up the concrete, which can be used in its production, giving as close to possible the desired properties of strength and durability, with the lowest cost. A mix design must fulfill a number of different criteria, such as cost, performance and durability, leading to conflicting requirements to be simultaneously satisfied. Therefore, the challenge in the design process is how to achieve the best compromise between contradictory design requirements. Optimization

techniques play an important role in finding the optimal characteristics of mix design leading to greatly improved performance.

However, a concrete mix design obtained after optimization is acceptable only if there is sufficient confidence that this design will fulfill the design requirements, as the effect of uncertainties in any structural design problem cannot be ignored.

1.1 UNCERTAINTIES IN STRUCTURAL DESIGN

The performance of a structure is assessed by its safety, serviceability and economy over its life cycle. However, the information about the input variables is never certain and/or complete. The uncertainties owe themselves to inherent randomness, limited information, imperfect knowledge and errors. With these uncertainties, to estimate absolute safety of a structure is impossible due to, mainly, the unpredictability of loads on the structure during its life cycle, in-place material strengths and human errors. Structural idealizations in formulating the mathematical model of the structure to predict its response or behavior and the limitations of numerical techniques also hamper the accurate estimation of the structural safety. These factors lead to some risk with regard to the unacceptable performance of the structure. In the conventional deterministic analysis and design procedures, it is assumed that all parameters (loads, strength of materials *etc*.) are not subjected to probabilistic variations. However, it is well known that loads (live loads on floors, wind loads, earthquake loads *etc*.) coming on the structure are random in nature. Similarly, the strengths of materials (concrete, steel *etc*.) and the geometric properties (sectional dimensions, effective depth, diameter of bars *etc*.) are subjected to statistical variations. So, role of uncertainties while designing a structure cannot be ignored (Kumar, 2002).

1.2 OPTIMIZATION WITH UNCERTAINTY

Concrete mix design is always under the effect of random environment. The sources of randomness are variations in quality of materials, mixing and transporting procedures, placing of concrete, methods of curing and testing procedures. As such actual compressive strength of concrete in a structure is always different from that of the concrete specimen obtained under controlled laboratory conditions. This gap between the expected and obtained performances is even larger when the mix design is deterministically optimized since Deterministic Design Optimization (DDO) typically yields optimal designs that are pushed to the limits of design constraint boundaries;

leaving no room for uncertainties in manufacturing imperfections, modeling and design variables. In DDO, the uncertainties are usually accounted for by the introduction of safety factors as described by the design codes of practice *IS 456* (2000). As a matter of fact, these safety factors are calibrated for average design situations and cannot ensure consistent reliability levels for specific design conditions. They may even lead to poor design, as the optimization procedure will search for the weakest region in the domain covered by the code of practice. This weakest region often presents not only the lowest cost but ironically, the lowest safety. The deterministic optimal design is pushed to the admissible domain boundaries, leaving very little space for safety margins in design, manufacturing and operating processes. Moreover, the optimization process leads to redistribution of the roles of uncertainties which can only be controlled by reliability assessment on the basis of the sensitivity measures. For these reasons, DDO cannot ensure appropriate reliability levels. If the DDO solution is more reliable than required, the losses can be avoided in construction and manufacturing costs; however, if the reliability is lower than required, the economic solution is not really achieved, because of the increase of the failure rate, leading to failure losses higher than the expected money saving. In this sense, the Reliability Based Design Optimization (RBDO) becomes a very powerful tool for robust and cost effective designs (Frangopol 1995).

In RBDO problem, additional probabilistic constraints are imposed in order to take various random parameters into account. Probabilistic constraints define the feasible region of the design space by restricting the probability that a constraint is violated within the allowable probability of violation. As such RBDO is a very powerful tool because of the explicit consideration of safety level and the optimal solution obtained is less sensitive to system uncertainties.

1.3 AIMS AND OBJECTIVES OF PRESENT STUDY

The aim of the present study is to develop a reliability based optimization methodology for proportioning of concrete mixtures. The concrete mix data used for analysis is based on the experiments conducted by Kumar (2002). The experimental data generated in the controlled laboratory conditions for the compressive strength of concrete is available for probabilistic analysis and subsequent reliability based design optimizations. The data has been summarized in *Appendix A.*

The objectives of the present study were explicitly fixed as:

a) To carry out the statistical analysis of various parameters on compressive strength and cost of concrete for the existing experimentally generated data.
b) To propose regression equations based on different parameters to predict the compressive strength of concrete.
c) To develop single-objective and multi-objective reliability based optimization models for prediction of various concrete related parameters.
d) To propose an efficient reliability based optimization methodology for concrete mix design.

The following section gives details of regression techniques that have been used in the present work for development of compressive strength prediction models for concrete.

1.4 REGRESSION TECHNIQUES FOR MODEL DEVELOPMENT

1.4.1 Ordinary least square regression

In matrix notation, the multiple linear regression model can be expressed as:

$$\boldsymbol{Y} = \boldsymbol{X}\boldsymbol{\beta} + \boldsymbol{\varepsilon} \tag{1.1}$$

where $\boldsymbol{Y}$ is a $n \times 1$ vector for response variable, $\boldsymbol{X}$ is a $n \times (p+1)$ matrix. First column of $\boldsymbol{X}$ consists of ones and remaining p columns are for explanatory variables or predictors, $\boldsymbol{\beta}$ is a $(p+1) \times 1$ vector for unknown regression coefficients and $\boldsymbol{\varepsilon}$ is a $n \times 1$ vector of experimental errors with mean 0 and variance σ^2. OLSR estimators of regression coefficients are given as:

$$\widehat{\boldsymbol{\beta}} = (\boldsymbol{X}'\boldsymbol{X})^{-1}\boldsymbol{X}'\boldsymbol{Y} \tag{1.2}$$

A unique solution of (1.2) may exist even when the predictor variables have linear dependencies on each other, *i.e.*, the matrix $\boldsymbol{X}'\boldsymbol{X}$ is ill conditioned. However, in such nearly singular cases, the solution is very unstable. Also, OLSR estimates have large variances in such cases (Rawling *et al*., 1998). This greatly affects the prediction accuracy of OLSR model which is an important aspect for model development, especially when the developed model is to be used for further analysis. This problem of linear dependence among predictor variables is termed as multi-collinearity.

The problem of multi-collinearity is often solved by removing the highly correlated variables. But, removing one or more such predictors to reduce multi-collinearity may not be a safe strategy as this sometimes leads to loss of important information. The

methods that can be employed to tackle multi-collinearity in presence of all the predictors are biased regression methods. Here, biasedness refers to the difference between the expected value given by the method and the true value of the parameter being estimated. OLSR method is considered as the method that leads to unbiased estimators which means that the parameter estimates yielded by this method are very close to true parameters. But, according to Ngo *et al*. (2004), the unbiased property is meaningful only if the fitted model is the true model, and most often this may not be guaranteed and as such unbiased property should not be over emphasized. Further, Hoerl and Kennard (1970) argued that in OLSR, parameter estimates based on minimum residual sum of squares have a high probability of being far away from true parameter values, if prediction variables suffer from multi-collinearity. However, in biased regression methods, a small bias in parameter estimates is introduced that may result in an estimation for which the sum of variance of the estimator and squared bias is smaller than the variance of the unbiased estimator. In that case the biased estimator is closer on average to true parameter values than the unbiased estimator (Rawling *et al.*, 1998). However, success of these methods is dependent upon choice of the bias introduced.

Ridge regression (RR) proposed by Hoerl and Kennard (1970) and Principal Component Regression (PCR) given by Massy (1965) are two commonly used biased regression methods to tackle the problem of multi-collinearity. RR attacks this problem by reducing the apparent magnitude of the correlations, whereas PCR deals with this problem by regressing depending variable on the important Principal Components (PCs) and then parceling out the effect of PC variables to the original variables.

Following sub sections explain both the RR and PCR techniques.

1.4.2 Ridge regression

Ridge regression technique is a biased regression technique that shrinks regression coefficients and hence, reduces the variance of the regression coefficients. This technique produces stable regression coefficients and improves the prediction accuracy of the model.

Ridge regression estimates are given as:

$$\widehat{\boldsymbol{\beta}}_{\boldsymbol{RR}} = (\boldsymbol{X}'\boldsymbol{X} + k\boldsymbol{I})^{-1}\boldsymbol{X}'\boldsymbol{Y} \qquad (1.3)$$

where $k \geq 0$ is called the ridge parameter and $\boldsymbol{I}$ is the identity matrix of order $(p+1) \times (p+1)$. Regression estimates given by (1.3) are termed as Traditional Ridge Regression (TRR) estimates. Hoerl and Kennard (1970) also proposed an improvement on TRR in the form of Generalized Ridge Regression (GRR). GRR estimates of the regression coefficients are given as:

$$\widehat{\boldsymbol{\beta}}_{\boldsymbol{GRR}} = (\boldsymbol{X'X} + \boldsymbol{K})^{-1}\boldsymbol{X'Y} \tag{1.4}$$

where $\boldsymbol{K}$ is a $(p+1) \times (p+1)$ diagonal matrix. Diagonal entries of $\boldsymbol{K}$ are called ridge parameters. GRR gives the user some flexibility with regard to the shrinkage of each regression coefficient, as it may be desirable to treat the coefficients differently (Ryan, 1996).

If all the ridge parameters are taken to be equal to k, then ridge estimates obtained using (1.4) are same as TRR estimates. For $\boldsymbol{K} = \boldsymbol{0}$, the ridge regression coefficients are identical to OLSR coefficients.

Cross validation criterion employed by Yan (2008) has been used to find optimal ridge parameters for TRR and GRR models that minimizes the Mean Square Error (MSE) of prediction for validation set given as:

$$MSE = (\boldsymbol{y_t} - \tilde{\boldsymbol{y}}_{\boldsymbol{t}})'(\boldsymbol{y_t} - \tilde{\boldsymbol{y}}_{\boldsymbol{t}})/n_t \tag{1.5}$$

where $\boldsymbol{y_t}$ denotes vector of dependent variable for validation set, $\tilde{\boldsymbol{y}}_{\boldsymbol{t}}$ denotes predicted values of $\boldsymbol{y_t}$ and n_t denotes the number of observations in the validation set.

1.4.3 Principal component regression

PCR is a technique that handles the problem of multi-collinearity and thus produces stable and meaningful estimates of regression coefficients. If multi-collinearity is severe, there will be at least one eigen value of correlation matrix of predictors approaching to zero. The dimension of the sample space corresponding to this eigen value has the least contribution in explaining the sample space dispersion. In PCR, original predictors are transformed into a new set of orthogonal or uncorrelated variables called Principal Components (PCs) of the correlation matrix. These PCs are the linear combinations of the centered and scaled original variables. The principal component matrix contains exactly the same information as the original centered and scaled data set. This transformation categorizes the new orthogonal variables in order of their importance in explaining the variance of the sample space. PCR is a dimension reduction technique in which principal components are eliminated until the remaining

components explain some pre-selected percentage of total variance. A number of other stopping rules have also been suggested in literature for this elimination. Most commonly used rule is that the PCs associated with eigen values greater than 1 should be considered. This rule is referred as Kaiser-Gutman rule. Guiot *et al.* (1982) proposed the selection rule that keeps the PCs corresponding to which the product of eigen values is greater than 1. Another method is scree test in which number of PCs is plotted against eigen values of correlation matrix of predictor variables. The eigen value decreases with number of components and the curve makes an elbow. The heuristic method is to drop the components after the one starting the elbow shape.

Jollife (2002) presented the point of view that deletion of components with small eigen values may sometimes result in removal of PCs having high predictive power for the dependent variable. Removal of low variance components having high predictive power could be dangerous for regression analysis. Thus, the two objectives of deleting PCs with small variances and of retaining PCs that are good predictors of the dependent variables should simultaneously be achieved. The selected PCs are then used to develop a regression model to estimate the response variable using OLSR technique. The regression coefficients obtained for PCs are then transformed back into a new set of coefficients corresponding to original correlated set of independent variables.

Computational technique for PCR

Let $\boldsymbol{X}^*$ denotes the $n \times p$ matrix of centered and scaled predictor variables without the column of ones. Firstly, $p \times p$ correlation matrix of predictor variables is calculated using (1.6).

$$\boldsymbol{C} = \boldsymbol{X}^{*\prime}\boldsymbol{X}^* \tag{1.6}$$

(1.7) is employed to compute the p eigen values $\lambda_1 > \lambda_2 > \lambda_3 > \cdots > \lambda_p$, of the correlation matrix $\boldsymbol{C}$.

$$|\boldsymbol{C} - \lambda \boldsymbol{I}| = 0 \tag{1.7}$$

Then, p eigen vectors $\boldsymbol{v}_1, \boldsymbol{v}_2, \boldsymbol{v}_3 \ldots, \boldsymbol{v}_p$ associated with each eigen value are calculated using (1.8).

$$(\boldsymbol{C} - \lambda \boldsymbol{I})\boldsymbol{V} = \boldsymbol{0} \tag{1.8}$$

where $\boldsymbol{V} = (\boldsymbol{v}_1, \boldsymbol{v}_2, \boldsymbol{v}_3 \ldots, \boldsymbol{v}_p)$ is a $p \times p$ matrix whose each column denotes an eigen vector.

Principal components are given by the relation (1.9).

$$\boldsymbol{Z} = \boldsymbol{X}^{*}\boldsymbol{V} \tag{1.9}$$

where $\boldsymbol{Z}$ is a $n \times p$ matrix with each column representing a PC. It is worth mentioning here that the PCs are orthogonal to each other and are arranged in descending order on the basis of variance of the sample space explained by them. Using one of the PCs selection rules as explained earlier, let $k < p$, PCs are eliminated. Thus, only the first $(p-k)$ PCs are left. The OLSR is then used to regress the dependent variable against selected PCs. Let $\hat{\boldsymbol{\alpha}}$ denotes $(p-k) \times 1$ vector of regression coefficients of PCs. Then, coefficients of centered and scaled original predictors $\boldsymbol{\beta}^{*}_{\boldsymbol{pc}} = (\beta^{*}_{1,pc}, \beta^{*}_{2,pc}, \beta^{*}_{pc}, \dots, \beta^{*}_{p,pc})'$ are given by (1.10).

$$\boldsymbol{\beta}^{*}_{\boldsymbol{pc}} = \boldsymbol{V}_{k\times p-k}\hat{\boldsymbol{\alpha}}_{p-k\times 1} \tag{1.10}$$

here, $\boldsymbol{V}_{k\times p-k}$ denotes the matrix of first $(p-k)$ eigen vectors. Finally, vector of original predictor variables $\boldsymbol{\beta}_{\boldsymbol{pc}} = (\beta_{0,pc}, \beta_{1,pc}, \beta_{2,pc}, \dots, \beta_{p,pc})'$ is obtained using Eqs. (1.11) and (1.12).

$$\beta_{j,pc} = \frac{\beta^{*}_{j,pc}}{S_j} \qquad j = 1,2,\dots,p \tag{1.11}$$

$$\beta_{0,pc} = \bar{y} - \sum_{j=1}^{p} \frac{\beta^{*}_{j,pc}\bar{x_j}}{S_j} \tag{1.12}$$

Herein, $S_j = \sqrt{\sum_{i=1}^{n}\left(x_{ji} - \bar{x_j}\right)^2}$, $\bar{x_j}$ denotes the mean of jth predictor variable and $\bar{y}$ denotes the mean of response variable.

The following section explains the basic formulation of RBDO problem.

1.5 FORMULATION OF RBDO PROBLEM

RBDO deals with obtaining best designs while explicitly considering the unavoidable effects of uncertainty. In RBDO problems, there is a trade-off between obtaining higher reliability and lowering cost.

Traditionally, the RBDO problem has been formulated as a double loop optimization problem. In a typical RBDO formulation, the hard constraints from the deterministic formulation are replaced by reliability constraints. A RBDO formulation is given in (1.13).

$$\left.\begin{aligned} & \underset{\boldsymbol{d},\boldsymbol{\mu_x}}{Minimize}\, f(\boldsymbol{d},\boldsymbol{X},\boldsymbol{P}) \\ Subject\ to: \quad & F_{g_i}(0) = Prob\{g_i(\boldsymbol{d},\boldsymbol{X},\boldsymbol{P}) \le 0\} \ge R_i \quad (i = 1,2,\dots,m) \\ & h_j(\boldsymbol{d},\boldsymbol{X},\boldsymbol{P}) \le 0 \qquad\qquad (j = 1,2,\dots,n) \\ & \boldsymbol{d}_l \le \boldsymbol{d} \le \boldsymbol{d}_u \\ & \boldsymbol{X}_l \le \boldsymbol{X} \le \boldsymbol{X}_u \end{aligned}\right\} \quad (1.13)$$

where f is the objective function, $\boldsymbol{d}$ is the vector of deterministic design variables, $\boldsymbol{X}$ is the vector of random design variables, $\boldsymbol{P}$ is the vector of random design parameters. $\boldsymbol{d}$ and $\boldsymbol{\mu_x}$ are the design variables where $\boldsymbol{\mu_x}$ is the mean of the random design variables $\boldsymbol{X}$. $g_i(\boldsymbol{d},\ \boldsymbol{X},\ \boldsymbol{P})\ \ (i = 1,2,\dots,m)$ and $h_j(\boldsymbol{d},\boldsymbol{X},\boldsymbol{P})(j = 1,2,\dots,n)$ are the performance functions. $F_{g_i}(0)$ represents the probability of constraint satisfaction or reliability of i^{th} constraint. R_i is the required minimum reliability of i^{th} constraint. The last two constraints in (1.13) are the boundary constraints.

However, two formulations of reliability constraints in (1.13) are given in (1.14) and (1.15).

$$P_i \le P_{allow,i} \quad (1.14)$$

$$\beta_i \ge \beta_{t,i} \quad (1.15)$$

where P_i is the probability of failure of i^{th} constraint and $P_{allow,i}$ is the allowable probability of failure for this constraint. β_i is the reliability index for i^{th} constraint and $\beta_{t,i}$ is the minimum required value of reliability index for this constraint. The relationship between the three measures of reliability can be expressed as:

$$P_i = \Phi(-\beta_i) = 1 - F_{g_i}(0) \quad (1.16)$$

wherein, Φ denotes the Cumulative Distribution Function (CDF) of a standard normal variable.

The next subsection explains briefly the reliability analysis techniques.

1.5.1 Reliability analysis techniques

Analytically, reliability, *i.e.*, the probability of constraint satisfaction is computed using the integral (1.17).

$$F_{g_i}(0) = \int \dots \int_{g_i(\boldsymbol{d},\boldsymbol{X},\boldsymbol{P}) \le 0} h_{\boldsymbol{X},\boldsymbol{P}}(\boldsymbol{x},\boldsymbol{p})\ d\boldsymbol{x}\, d\boldsymbol{p} \quad (1.17)$$

where, $h_{\boldsymbol{X},\boldsymbol{P}}(x,p)$ is the joint probability density function of $\boldsymbol{X}$ and $\boldsymbol{P}$.

Thus, reliability analysis requires the evaluation of multiple integral as shown in (1.17). One of the alternatives to evaluate this integral is Monte Carlo simulation. However, when the reliability is very high (approaching 1.0), the computational effort of Monte Carlo simulation is prohibitively expensive (Du and Chen, 2000).

Because it is difficult to solve (1.17) analytically, some approximate probability integration methods have also been developed to provide efficient solutions, such as the First-Order Reliability Method (FORM) and Second-Order Reliability Method (SORM) (Madson *et al*., 1986; Palle and Michael, 1982). The FORM often provides adequate accuracy and is widely used for RBDO applications. Reliability analysis requires a transformation called Rosenblatt Transformation (Rackwitz and Fiessler, 1978; Hohenbichler and Rackwitz, 1981) from the original random parameter space $\boldsymbol{X}$ to the independent and standard normal random parameter space $\boldsymbol{U}$. The performance function $g_i(\boldsymbol{d}, \boldsymbol{X}, \boldsymbol{P})$ in *X*-space can then be mapped onto $g_i(\boldsymbol{d}, \boldsymbol{U}, \boldsymbol{P})$ in $\boldsymbol{U}$-space. The point on the constraint boundary surface that has minimum distance from origin is called the Most Probable Point (MPP) of failure. To find MPP of failure, optimization problem given in (1.18) is solved.

$$\left.\begin{array}{ll} minimize & \|\boldsymbol{U}\| \\ Subject\ to: & g_i(\boldsymbol{d}, \boldsymbol{U}, \boldsymbol{P}) = 0 \end{array}\right\} \tag{1.18}$$

Let $\boldsymbol{u}^*$ be the solution of (1.18), then reliability index β_i is given as:

$$\beta_i = -\frac{\boldsymbol{\alpha_i}^T \boldsymbol{u}^*}{\|\boldsymbol{\alpha_i}\|} \tag{1.19}$$

where $g_i(\boldsymbol{d}, \boldsymbol{U}, \boldsymbol{P}) \approx \boldsymbol{\alpha_i}^T \boldsymbol{u} + \beta_i$ is the approximate first order Taylor series expansion of the performance function. Then, Probability of failure of i^{th} constraint can be calculated using (1.16). This method of estimating probability of failure is called FORM. However, in SORM the performance function is approximated as a second order surface. This approach for handling reliability constraint using (1.18) is referred to as Reliability Index Approach (RIA).

Tu *et al*. (1999) proposed Performance Measure Approach (PMA) in which reliability constraint is expressed as:

$$g_i^* = F_{g_i}^{-1}\left(\Phi\left(\beta_{t,i}\right)\right) \leq 0 \tag{1.20}$$

where g_i^* is termed as probabilistic performance measure for the i^{th} probabilistic constraint.

The first-order probabilistic performance measure g_i^* is obtained from a nonlinear optimization problem (Tu *et al*., 1999) in $\boldsymbol{U}$-space defined as:

$$\left.\begin{matrix} minimize & g_i(\boldsymbol{d},\boldsymbol{U},\boldsymbol{P}) \\ Subject\ to: & \|\boldsymbol{U}\| = \beta_{t,i} \end{matrix}\right\} \tag{1.21}$$

According to Tu *et al*. (1999), solving RBDO by the PMA formulation is usually more efficient and robust than the RIA formulation where the reliability is evaluated directly. The efficiency lies in the fact that the search for the MPP of an inverse reliability problem is easier to solve than the search for the MPP corresponding to an actual reliability. The RIA and the PMA approaches for RBDO are essentially inverses of one another and would yield the same solution if the constraints are active at the optimum (Tu *et al*., 1999). The Advanced Mean Value (AMV) method is well suited for solving optimization problem (1.21) (Wu *et al*., 1990; Wu, 1994) due to its simplicity and efficiency.

Advanced mean value method

AMV method begins with the starting point which is defined as:

$$\boldsymbol{u}_{iMV}^* = \beta_{t,i}\boldsymbol{n}_i(\boldsymbol{0}) \tag{1.22}$$

where

$$\boldsymbol{n}_i(\boldsymbol{0}) = -\frac{\nabla_X g_i(\boldsymbol{d},\boldsymbol{\mu},\boldsymbol{P})}{\|\nabla_X g_i(\boldsymbol{d},\boldsymbol{\mu},\boldsymbol{P})\|} = -\frac{\nabla_U g_i(\boldsymbol{d},\boldsymbol{0},\boldsymbol{P})}{\|\nabla_U g_i(\boldsymbol{d},\boldsymbol{0},\boldsymbol{P})\|} \tag{1.23}$$

This means that in order to minimize the performance function $g_i(\boldsymbol{d},\boldsymbol{U},\boldsymbol{P})$, the normalized steepest descent direction $\boldsymbol{n}_i(\boldsymbol{0})$ is defined at the mean value. The AMV method iteratively updates the direction of vector of steepest descent at the probable point $\boldsymbol{u}_{iAMV}^{(k)}$, initially obtained using mean value method. Thus, the AMV method can be formulated as given in (1.24).

$$\boldsymbol{u}_{iAMV}^{(1)} = \boldsymbol{u}_{iMV}^*, \quad \boldsymbol{u}_{iAMV}^{(k+1)} = \beta_{t,i}\boldsymbol{n}_i(\boldsymbol{u}_{iAMV}^{(k)}) \tag{1.24}$$

where

$$\boldsymbol{n_i}\left(\boldsymbol{u}_{iAMV}^{(k)}\right) = -\frac{\nabla_U g_i(\boldsymbol{d},\boldsymbol{u}_{iAMV,}^{(k)}\boldsymbol{P})}{\left\|\nabla_U g_i(\boldsymbol{d},\boldsymbol{u}_{iAMV}^{(k)},\boldsymbol{P})\right\|} \tag{1.25}$$

This method has been employed in the present study to perform reliability analysis of designs obtained by multi-objective design optimization and deterministic single-objective design optimization.

In the present work, Sequential Optimization and Reliability (SORA) method developed by Du and Chen (2004) has been employed to carry out single-objective reliability based design optimization of concrete mix parameters. The subsequent subsection explains the SORA method.

1.5.2 Sequential optimization and reliability assessment method

SORA method replaces probability formulation of RBDO described in (1.13) by percentile formulation given as:

$$\left.\begin{aligned} & \underset{\boldsymbol{d},\boldsymbol{\mu_x}}{Minimize}\, f(\boldsymbol{d},\boldsymbol{X},\boldsymbol{P}) \\ Subject\ to: \quad & g_i^{R_i}(\boldsymbol{d},\boldsymbol{X},\boldsymbol{P}) \le 0 \quad (i = 1,2,\dots,m) \\ & h_j(\boldsymbol{d},\boldsymbol{X},\boldsymbol{P}) \le 0 \quad (j = 1,2,\dots,n) \\ & \boldsymbol{d}_l \le \boldsymbol{d} \le \boldsymbol{d}_u \\ & \boldsymbol{X}_l \le \boldsymbol{X} \le \boldsymbol{X}_u \end{aligned}\right\} \tag{1.26}$$

where $g_i^{R_i}$ is the R_i-percentile of $g_i(\boldsymbol{d},\boldsymbol{X},\boldsymbol{P})$, namely,

$$Prob\{g_i(\boldsymbol{d},\boldsymbol{X},\boldsymbol{P}) \le g_i^{R_i}\} = R_i \tag{1.27}$$

Concept of R-percentile for i^{th} constraint has been demonstrated in Figure 1.1. This figure has been taken from the work of Du and Chen (2004). If the shaded area is equal to the desired reliability R_i, then the left ending point $g_i^{R_i}$ on the g_i axis is called R_i-percentile of function g_i. In Figure 1.1, $g_i^{R_i} \le 0$ indicating that $Prob\{g_i(\boldsymbol{d},\boldsymbol{X},\boldsymbol{P}) \le 0\} \ge R_i$ which means that this constraint is feasible. Thus, in this formulation the original constraints that require reliability assessment are replaced by constraints that evaluate R-percentile. The advantage of percentile formulation is that reliability assessment is performed only upto a necessary level, represented by desired reliability R. This formulation results in saving a lot of computational cost used in finding the actual reliability of a limit state function.

$g_i^{R_i}$ is given as:

$$g_i^{R_i} = g_i(\boldsymbol{d},\boldsymbol{u}_{MPPi},\boldsymbol{P}_{MPPi}) = g_i(\boldsymbol{d},\boldsymbol{X}_{MPPi},\boldsymbol{P}_{MPPi}) \tag{1.28}$$

where $(\boldsymbol{d},\boldsymbol{u}_{MPPi},\boldsymbol{P}_{MPPi})$ denotes the solution of (1.21) and $(\boldsymbol{d},\boldsymbol{X}_{MPPi},\boldsymbol{P}_{MPPi})$ is the solution obtained by transforming the standardized variables back to original variables. Thus, the model given by (1.26) becomes

$$\left.\begin{array}{ll} & \underset{\boldsymbol{d},\boldsymbol{\mu_x}}{Minimize}\, f(\boldsymbol{d},\boldsymbol{X},\boldsymbol{P}) \\ Subject\ to: & g_i(\boldsymbol{d},\boldsymbol{X}_{MPPi},\boldsymbol{P}_{MPPi}) \le 0 \quad (i = 1,2,\dots,m) \\ & h_j(\boldsymbol{d},\boldsymbol{X},\boldsymbol{P}) \le 0 \quad (j = 1,2,\dots,n) \\ & \boldsymbol{d}_l \le \boldsymbol{d} \le \boldsymbol{d}_u \\ & \boldsymbol{X}_l \le \boldsymbol{X} \le \boldsymbol{X}_u \end{array}\right\} \quad (1.29)$$

Thus, this method establishes a correspondence between probabilistic optimization and deterministic optimization.

Figure 1.2 shows the flow chart of SORA method given by Du and Chen (2004). In the first cycle of optimization, $\boldsymbol{X}_{MPPi}$ and $\boldsymbol{P}_{MPPi}$ are taken as mean values of random design variables $(\boldsymbol{\mu}_x)$ and random parameters $(\boldsymbol{\mu}_p)$, respectively. This is because no information about MPPs is available in the first cycle. Let $\boldsymbol{\mu}_x^{(k)}$denotes the optimal solution and $\boldsymbol{X}_{MPPi}^{(k)}$ denotes the MPP corresponding to i^{th} constraint in k^{th} cycle. Then, optimization problem (1.30) is solved in $(k+1)^{\text{th}}$ cycle.

$$\left.\begin{array}{ll} & \underset{\boldsymbol{d},\boldsymbol{\mu_x}}{Minimize}\, f(\boldsymbol{d},\boldsymbol{X},\boldsymbol{P}) \\ Subject\ to: & g_i\left(\boldsymbol{d},\boldsymbol{\mu}_x - \boldsymbol{s}_i^{(k+1)},\boldsymbol{P}_{MPPi}^{(k)}\right) \le 0 \quad (i = 1,2,\dots,m) \\ & h_j(\boldsymbol{d},\boldsymbol{X},\boldsymbol{P}) \le 0 \quad (j = 1,2,\dots,n) \\ & \boldsymbol{d}_l \le \boldsymbol{d} \le \boldsymbol{d}_u \\ & \boldsymbol{X}_l \le \boldsymbol{X} \le \boldsymbol{X}_u \end{array}\right\} \quad (1.30)$$

Here, $\boldsymbol{s}_i^{(k+1)}$ is called shift vector for i^{th} constraint in cycle $(k+1)$ and is given as:

$$\boldsymbol{s}_i^{(k+1)} = \boldsymbol{\mu}_x^{(k)} - \boldsymbol{X}_{MPPi}^{(k)} \quad (1.31)$$

With the introduction of shift vectors, the constraints boundaries are shifted towards the feasible region in each cycle of optimization. The optimization stops when all the constraints are satisfied and difference in objective function values in two consecutive cycles is very small.

The next section elaborates the main objectives of any Multi-Objective Optimization (MOO) strategy and gives details of the MOO technique used in the present study.

1.6 MULTI-OBJECTIVE OPTIMIZATION STRATEGY

Most real world problems involve simultaneous optimization of multiple competing objectives. While in single-objective optimization the optimal solution is usually clearly defined, this does not hold for MOO problems. Instead of a single optimum, there is rather a set of alternative trade-offs, generally known as Pareto-optimal solutions. These solutions are optimal in the wider sense that no other solutions in the search space are superior to them when all objectives are considered. However, three main tasks of any MOO strategy are:

(I) To find solutions as close to true Pareto-optimal front as possible.

(II) To maintain as many widely spread non-dominated solutions as possible.

(III) Emphasize elites to provide a faster and reliable convergence near the true Pareto-optimal front. Here, Elitism means that a good solution once found should not be lost.

Elitist Non-Dominated Sorting Algorithm (NSGA-II) developed by Deb *et al*. (2000a, 2000b) employs an efficient elite-preservation strategy by combining both offspring and parent population before performing non-dominated sorting of solutions. This elitism mechanism does not allow an already found Pareto-optimal solution to be deleted. Also, the diversity among the solutions in a non-dominated front is introduced by using crowded distance metric which is the measure of the density of solutions in the neighbourhood of a given solution. Thus, NSGA-II efficiently targets all the three main objectives of MOO and is used to locate Pareto-optimal fronts in present work.

1.6.1 NSGA-II

Initially, a random parent population P_0 of size N is created. This population is sorted into different non-domination levels. Each solution is assigned a fitness equal to its non-domination level with 1 as the best level. Thus, minimization of fitness is assumed. Binary tournament selection, recombination and mutation operators are used to create an offspring population Q_0 of size N. To introduce elitism, both parent and offspring are combined together before non-dominated sorting after initial step.

The step by step procedure of NSGA-II is highlighted in Figure 1.3. Firstly, parent population P_t and offspring population Q_t are combined to create a population R_t, where t denotes current generation. The population R_t is of size $2N$. The population is sorted according to non-domination. Since R_t includes members of both current and previous generation, the elitism is ensured. The non-domination approach proposed by

Deb *et al*. (2000a, 2000b) is explained in subsection 1.6.1.1. The solutions belonging to the best non-dominated front set Φ_1 are the best solutions from the combined population and therefore, are emphasized more than any other solution. If the size of Φ_1 is smaller than N, all the members of Φ_1 are chosen for the new population P_{t+1}. The remaining members of P_{t+1} are chosen from subsequent non-dominated fronts in order of their ranking. Thus, solutions are chosen next from the set Φ_2, followed by Φ_3 and so on. The procedure continues till no more sets can be accommodated. If the total number of solutions found in the selected non-dominated fronts are larger than N, the solutions from the last selected front are sorted using crowded comparison operator $\prec_n$ in descending order and best solutions in this front are chosen to make the population size exactly N. Crowded comparison operator $\prec_n$ is explained in subsection 1.6.1.2.

The new population P_{t+1} is then used for selection, crossover and mutation to create a new population Q_{t+1}. This method uses a binary tournament selection operator based on crowded comparison operator $\prec_n$ for selection process. The crowded comparison procedure introduces diversity among the non-dominated solutions during the selection process.

1.6.1.1 Non-domination approach

In this approach, every solution from the given population is tested with a partially filled population for domination. Let the given population be noted as P. In step I, the first solution from P is kept in a set P'. Afterwards, each solution p from P is compared with all members of the set P' one by one. If the solution p dominates any member q of P', then the solution q is removed from P'. Otherwise, if solution p is dominated by any member q of P', then the solution p is ignored. If solution p is not dominated by any member q of P', then the solution p is also entered in P'.Thus, when all the solutions are compared, P'consists of best non-dominated solutions from the given population and is called the first non-dominated front.

After, first non-dominated front is obtained; the process is repeated again with remaining members of population P to find all non-dominated fronts in decreasing order of importance.

1.6.1.2 Crowded comparison operator

The Crowded comparison operator $\prec_n$ directs the selection process at various stages of the NSGA-II algorithm towards a uniformly spread out Pareto-optimal front. It assumes

that every solution i has two attributes, namely, non-domination rank (r_i) and a local crowding distance (d_i). The partial order $\prec_n$ is defined as:

$$i \prec_n j \qquad if\ (r_i < r_j)\ or\ ((r_i = r_j)\ and\ (d_i > d_j)) \tag{1.32}$$

This means a solution i wins a tournament with another solution j if any one of the given two conditions is true. First condition ensures that the chosen solution lies in a better non-dominated front. The second condition resolves the tie of both the solutions, if they lie in same non-dominated front based on their crowded distance. The solution which lies in less crowded area wins the tournament. This helps in maintaining diversity among the solutions.

To calculate crowded distance the population in a given non-dominated front is arranged in increasing order of magnitude according to each of the objective function values. Then, for each objective, the boundary solutions are assigned infinite distance. All other intermediate solutions are assigned a distance equal to the absolute difference in function value of two adjacent solutions. The overall crowding distance is taken as the sum of individual distance values corresponding to each objective.

1.7 ORGANIZATION OF THESIS

The thesis is presented in six chapters as detailed below:

Chapter-2 presents literature review of the work done by various researchers in the direction of development of techniques for finding efficient solutions of RBDO and MOO problems. Also, the work done in the direction of regression model development of concrete mix parameters; single and multi-objective optimization of concrete mix parameters and application of RBDO in structural design problems has been reviewed.

Chapter-3 deals with linear and pure quadratic regression model development for compressive strength of concrete using different regression methods. The models have been built up for concrete with or without fly ash for curing ages of 28 days, 56 days and 91 days. The performance of developed models has been assessed on the basis of their $MSEs$.

Chapter-4 presents the formulation of RBDO model for concrete mix parameters with cost of concrete as an objective function. This objective is minimized satisfying a ratio constraint, an absolute volume constraint, boundary constraints on input variables and a

reliability constraint on compressive strength requirement. SORA method has been employed to find reliability based optimal design of concrete mix proportions. Extensive experimentation has been done to include three reliability levels, three curing ages and different compressive strength models. Experiments have also been conducted by replacement of 15% cement by fly ash. Comparison of RBDO results and safety factor based DDO results has been presented. Variation of design variables for different design requirements has also been studied.

Chapter-5 describes the optimal concrete mix proportions satisfying the requirements of two objectives which are conflicting in nature under certain restrictions. The first objective is to minimize the cost of concrete and the second objective is to design a mix having compressive strength for a given curing age above a specified level with minimum probability of failure. The multi-objective RBDO problem has been solved using NSGA-II. Optimizations have been performed for concrete without fly ash and for concrete with 15% replacement of cement by fly ash by varying the parameters of curing age, target compressive strength and probability of failure.

Chapter-6 concludes the thesis with an overview of the major research results and contributions. In addition, future research recommendations are also presented in this chapter.

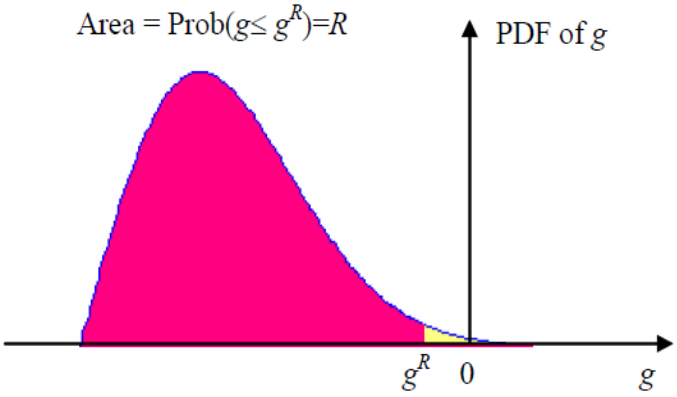

Figure 1.1 *R*-percentile of a constraint function

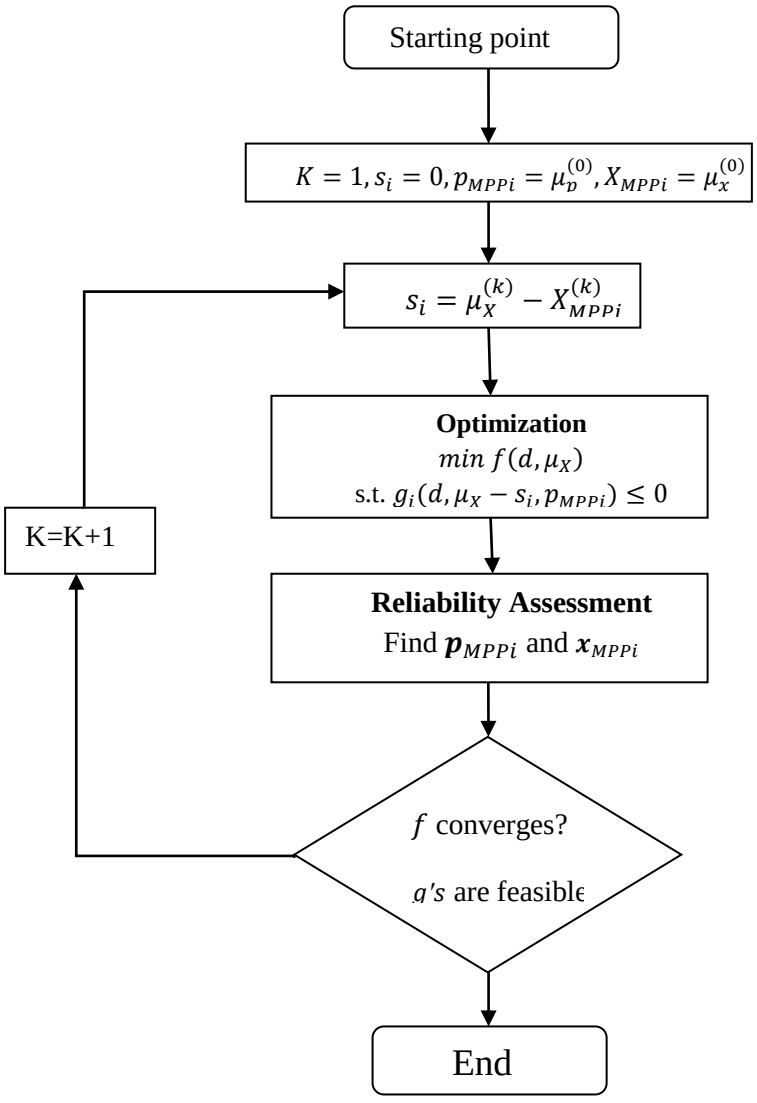

Figure 1.2 Flow chart of SORA method

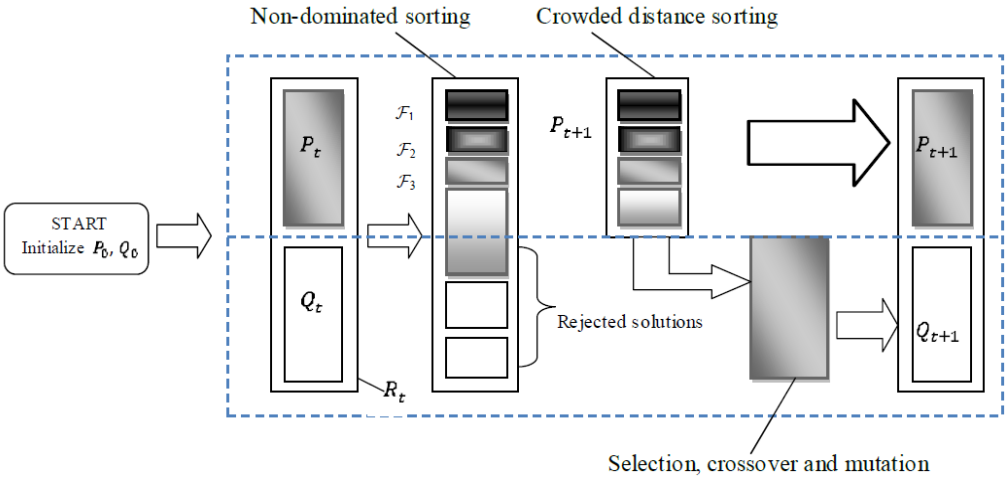

Figure 1.3 Step by step procedure of NSGA-II

CHAPTER 2
LITERATURE REVIEW

==========

2.0 GENERAL

The chapter herein presents literature review of the work done by various researchers in the direction of development of techniques for finding efficient solutions of RBDO and MOO problems. Also, the work done in the area of regression model development of concrete mix parameters; single and multi-objective optimization of concrete mix parameters and application of RBDO in structural design problems has been reviewed.

2.1 RBDO APPROACHES

A survey of the literature reveals that the various RBDO methods can, in general, be divided into three broad categories. A brief review of the literature related to the same is presented in the succeeding sub-sections.

2.1.1 Double loop method for RBDO

Typically, an RBDO problem is a double loop problem that employs nested optimization and reliability analysis loops, in which the reliability of a constraint is estimated inside the optimization loop. Reliability of a constraint is evaluated using either the RIA or PMA approach. This double loop approach has been employed by many researchers to solve various design problems.

Nikolaidis and Burdisso (1988) applied the concept of safety index approach developed by Hasofer and Lind (1974) by expanding the performance function at the point of maximum likelihood known as the most probable failure point. An advanced first order second moment method is used for evaluating the probabilities of violation of constraints. Enevoldsen and Sørensen (1994) investigated different formulations of the RBDO problem such as reliability-based optimal design of structural systems with component or systems reliability constraints, reliability-based optimal inspection

planning and reliability-based experiment planning. Component and system reliabilities are evaluated using FORM. The finite element method is included as the response evaluation tool. Special emphasis is laid on the sensitivity analysis and stability of optimization process.

Reddy *et al*. (1994) developed a simplified safety index approach based on advanced second moment method to find optimal designs of complex structures. The safety indices are interpolated using information at mean and MPP. They showed that minimum weight design with improved safety index limit is achieved by using extended interior penalty method of optimization. Li and Yang (1994) formulated RBDO problem as a linear programming problem. Linear approximation of the reliability index is constructed using information about sensitivities. Grandhi and Wang (1998) proposed to replace the performance function by a two-point adaptive nonlinear approximation. The nonlinear approximation is constructed by using the function values and the first-order gradients at two points of the limit-state function, and its nonlinearity index is automatically changed for different problems. The reduction in computational cost realized in safety index calculation and optimization are demonstrated through two structural problems.

However, the overall RBDO is still a nested double-loop optimization procedure. Such formulations are computationally intensive for problems where the function evaluations are expensive. To alleviate the computational cost associated with the nested formulation, unilevel and sequential RBDO methods have been developed.

2.1.2 Unilevel method for RBDO

This approach avoids the double loop by taking advantage of Karush-Kuhn-Tucker (KKT) optimality conditions and Lagrange's multipliers. Chen *et al*. (1997) developed single loop single design vector approach based on the quantile approximation of the limit state. It is reported that this method completely eliminates the need of inner optimization loop and does not increase the number of design variables. So, it resulted in modest increase of computational cost over that of deterministic design optimization.

Kuschel and Rackwitz (1997, 2000) proposed a unilevel formulation in which the direct FORM problem is replaced by the corresponding first order KKT optimality conditions. Kirjner-Neto *et al*. (1998) reformulated the RBDO problem as a standard semi-infinite optimization problem. This reformulation tackles the shortcomings of both the RIA approach as well as the bi-level approach. However, this approach is applicable only to

series system problems with a separate reliability constraint imposed on each of its failure modes. Outer approximation algorithms are used to find solutions of reformulated problem.

Wang and Kodiyalam (2002) demonstrated the efficiency of the single-level approach for both reliability based optimization and robust design with non-normal distributions. They used normal tail transformation to find the equivalent means and standard deviations for non-normally distributed variables. Kharmanda *et al*. (2002) and Mohsine *et al*. (2006) developed a procedure that leads to parallel convergence of reliability and optimization problems in hybrid design space that contains both design and random variables. The two optimization problems, namely, design optimization and reliability solution were solved simultaneously by minimizing a function of cost and reliability levels, under deterministic, limit state and reliability constraints. The objective function is represented as the product of cost and reliability of the structure.

Agarwal (2004) and Agarwal *et al*. (2007) proposed a unilevel formulation for RBDO where the first order KKT conditions corresponding to each probabilistic constraint are enforced directly at the system level optimizer, thus eliminating the lower level optimizations used to compute probabilistic constraints. The proposed formulation is solved in an augmented design space that consists of the original decision variables, the MPPs of failure and Lagrange's multipliers corresponding to each lower level optimization. It is shown that this formulation is computationally equivalent to the original nested optimization formulation if lower level optimization problem is solved by satisfying the KKT conditions. However, the major limitation of this formulation is that it is accompanied by a large number of equality constraints which poses numerical difficulty to the gradient based optimizers. However, Kanakasabai and Dhingra (2012) proposed to use an exterior penalty based cross entropy method to overcome the problem of equality constraints in unilevel RBDO problem.

Liang *et al*. (2008) introduced a single level RBDO approach for both normal and non-normal random variables. The algorithm collapsed the nested optimization loops into an equivalent single-loop optimization process by using KKT optimality conditions of the reliability loops in the outer optimization loop. As a result, the double loop RBDO problem is transformed into an equivalent deterministic design optimization problem. It is reported that the algorithm does not increase the number of design variables and equality constraints. Also, it does not require second order derivatives. Thus, its accuracy is comparable with the double loop approach and efficiency is equivalent to

deterministic optimization. Marti and Kaymaz (2006) and Kaymaz and Marti (2007) developed a one level RBDO formulation for elastoplastic mechanical structures by explicitly considering the parameter optimization problem for computation of β-point. However, the one-level RBDO formulation increases the total design variables since the Lagrange variables appearing in the KKT are also considered as design variables.

Shan and Wang (2008) introduced the concept of Reliable Design Space (RDS), within which every design satisfies reliability requirements. Thus, the RBDO problem transforms into a deterministic one restricted to find the solution in RDS. The RDS is identified by using the partial derivatives at the current design point as an approximation of the derivatives at its corresponding MPP on the limit state function. The reliability analysis loop is completely eliminated using this approach.

2.1.3 Sequential method for RBDO

The basic concept behind sequential RBDO techniques is to decouple the upper level optimization from the reliability analysis to avoid a nested optimization problem. In sequential RBDO methods, the main optimization and reliability analysis is performed separately and the procedure is repeated until desired convergence is achieved.

Wu and Wang (1998) used the concept of safety factor approach in order to replace the RBDO by a series of deterministic optimizations. Royset *et al*. (2001) proposed a decoupling approach that employs a reformulation of RBDO problem in which reliability terms are replaced by deterministic functions. The reformulation is done by replacing the reliability index for each component by a function that denotes the minimum of the corresponding limit state function within a ball of specified radius. The reformulated problem can be solved by the existing semi-infinite optimization algorithms. They showed that the reformulated problems produced exact solutions when the limit state functions are affine. For non-affine limit state functions, the solutions are correct to the first order approximation when the reliability constraints are active.

Qu and Haftka (2004) introduced the concept of probabilistic sufficiency factor that combines safety factor and probability of failure. They showed that this factor does not suffer from accuracy problems in regions of low probability of failure or safety index when calculated by Monte Carlo simulation. Agarwal (2004) proposed a sequential RBDO methodology in which sensitivities of the MPPs with respect to the design

variables are used to update them during the deterministic optimization phase. However, it is reported that this approach may suffer from convergence problem.

Chen and Du (2004) proposed Sequential Optimization and Reliability Assessment (SORA) methodology that employs a single loop strategy with a serial of cycles of deterministic optimization and reliability assessment. In each cycle, optimization and reliability assessment are decoupled from each other; the reliability assessment is only conducted after the deterministic optimization to verify constraint feasibility under uncertainty. The key to the proposed method is to shift the boundaries of violated constraints to the feasible direction based on the reliability information obtained in the previous cycle. The design is quickly improved from cycle to cycle and the computational efficiency is improved significantly.

In the present work, SORA method has been employed to carry out single objective optimization of concrete mix parameters.

Zou and Mahadevan (2006) developed a direct decoupling approach where reliability constraints in the RBDO problem are approximated using simulation based methods such as Monte Carlo simulation. A deterministic optimization is then performed using the approximated reliability constraints. The reliability analysis and optimization loops are performed sequentially until desired convergence is achieved.

2.2 MULTI-OBJECTIVE OPTIMIZATION TECHNIQUES

Traditionally, Multi-Objective Optimization (MOO) problems are solved using classical methods in which Pareto-optimal set is generated by combining the objectives into a single, parameterized objective. Some of the classical methods are weighted sum method, ε- constraint method (Haimes *et al*., 1971), weighted metric method, Benson's method (Benson, 1978), value function method and goal Programming method (Steuer, 1986).

In weighted sum method, multiple objectives are replaced by a single objective by pre-multiplying each objective with a user supplied weight. This method has the simplest approach and therefore, is most widely used. However, success of this approach depends largely on the precise value of weights for each objective. ε- constraint method suggested to reformulate the MOO problem by just keeping one of the objectives and restricting the rest of the objectives within user specified values.

In weighted metric method, multiple objectives are replaced by a single objective, which is taken as the weighted distance of any point in the objective space from the

ideal point, and this objective is minimized. However, different objectives may have different orders of magnitude and therefore, objective functions are required to be normalized. This normalization can be done only if minimum and maximum values of all the objectives are known (Deb, 2001). Benson's method starts with choosing a random solution from the feasible region. The sum of the non-negative differences of each objective from the chosen solution is then maximized. Value function method or utility function method considers a user supplied mathematical value function relating all the objectives as the objective function which is to be maximized.The main idea in goal programming method is to find solutions that attain a pre-specified target for one or more objective functions. If the pre-specified targets for all the objectives are not achieved, then the solutions that minimize the weighted sum of deviations from target values are found. Concept of symmetric duality to solve multi-objective programming problems was employed by Gulati *et al*. (1997, 2005).

The above referred classical methods are very popular because of the fact that well studied algorithms for single objective optimization can be used. However, Deb (2001) refers to some of the difficulties that can arise in finding Pareto-optimal front using these classical methods. These difficulties are:

a) Only one Pareto-optimal solution can be found in one simulation run.
b) All algorithms require some prior knowledge, such as suitable weights or ε or target values.

In past two decades, Evolutionary Algorithms (EAs) that mimic the principle of natural evolution have been established as an alternative to classical methods. The main features of EAs are:

a) They are capable of finding multiple solutions in one single run.
b) They are capable of handling large search spaces to generate global optimal solution.
c) They work on two distinct operations, namely, selection and search. In the selection operation, better solutions to the current population are emphasized by duplicating them in mating pool. In the search operation, new solutions are created by exchanging some information among the solutions in mating pool and by perturbing them in their neighborhood.
d) No prior knowledge regarding the importance of objectives is required.

A number of multi-objective evolution algorithms have been developed by various researchers. Some of them include vector evaluated genetic algorithm (Schaffer, 1984),

vector optimized evolution strategy (Kursawe, 1990), weighted-based genetic algorithm (Hajela and Lin, 1993), multi-objective genetic algorithm (Fonseca and Fleming, 1993), non-dominated sorting genetic algorithm (Srinivas and Deb, 1994), niched-pareto genetic algorithm (Horn *et al*., 1994) and predator-prey evolution strategy (Laumanns *et al*., 1998).

The common aspect of these algorithms is that none of them have used an elite-preserving operator that can speed up the performance of EA significantly and can help in preventing the loss of good solutions once they are found. However, NSGA-II developed by Deb *et al*. (2000a, 2000b) employs an efficient elite-preservation strategy by combining both offspring and parent population before performing non-dominated sorting of solutions.

2.3 REGRESSION MODEL DEVELOPMENT FOR CONCRETE MIX PARAMETERS

OLSR technique and its variants have been traditionally used by researchers to develop models to predict concrete mix parameters. Saluja *et al*. (1992) suggested a rational method based on experimental observations to predict compressive strength of fibrous concrete considering the effect of variable fibre content and aspect ratio. Bhanja and Sengupta (2002) developed regression models to predict ratios of 28 days compressive strength of silica fume based control concrete with pre-fixed silica fume percentages. The developed model was independent of specimen parameters as it involved non-dimensional variables. They concluded that predictions were obtained within 7.5% of experimental observations. Namyong *et al*. (2004) studied 1442 compressive strength results at construction sites from the specimens having 59 different kinds of mixtures, covering a wide range of input parameters and compressive strength. Multiple regression models for predicting compressive strength of concrete for 7 days and 28 days curing period are developed in the study. Water-cement ratio, cement content and cement-aggregate ratio were selected as predictors, based on the correlation analysis of various parameters with compressive strength, but effect of correlation among the predictors is not considered.

Tangtermsirikul *et al.* (2004) proposed a 28 days compressive strength prediction model of roller compacted concrete with fly ash in order to minimize the process of trial mixing. The model is formulated based on quantities of concrete ingredients, chemical compositions and physical properties of cement and fly ash. The researchers

found that at room temperature of $28^{\circ}C \pm 3^{\circ}C$, the proposed model gave satisfactory results to predict compressive strength of the tested mixtures of roller-compacted concrete with fly ash designed for dams and road pavements at the ages between 3 and 91 days. Mathematical regression models are elaborated by Kazerbuk and Lelusz (2007) to study the development of compressive strength of concrete with fly ash replacements upto 30%. They evaluated the effect of addition of fly ash content, time of curing and type of cement on compressive strength of concrete. It is concluded that fly ash addition, in considered range of fa/c values, has no significant effect on specific gravity and water absorbability of concrete. Also, the rate of strength increase of fly ash concrete is slower and sustains for longer period. The concrete mixes containing fly ash are capable of developing more strength than Portland cement concrete and blast furnace slag concrete.

Pande and Gupta (2007) analyzed proportions of ingredients and revealed that water to cementitious component ratio and cementitious component to inert component ratios play significant role in compressive strength development. Abd and Zain (2009) built power models to predict slump and compressive strength of concrete at different curing ages. Mix proportion elements, *i.e.*, cement, fly ash, silica fume, water, coarse aggregate and fine aggregate are considered as predictor variables. Also, slump test results and density of concrete are included in the model. Compressive strength models for different curing ages of 3, 7, 14, 28 and 91 days are developed. It is seen that cement, water, coarse aggregate and fine aggregate have significant correlation with compressive strength of concrete irrespective of the curing age. Chakraverty *et al*. (2008) applied two dimensional orthogonal polynomials in the regression analysis to develop a relationship of product parameters such as compressive strength, bulk density and water absorption of fly ash cement bricks with percentages of fly ash, sand and cement. Chakraverty *et al*. (2008) introduced regression models of different orders to predict compressive strength at different curing periods with ternary systems of fly ash, cement and sand by using simplex lattice design for building bricks. They concluded that three parameter third order regression model constructed by using the proposed design points accurately predicted the compressive strength.

Abdullahi *et al*. (2009) showed on the basis of Analysis of Variance (ANOVA) that a polynomial model is adequate to predict the slump, air-density and compressive strength of palm oil clinker concrete using mix ingredients as predictors. Regression

modeling is done at 95% confidence interval using forward selection approach. They used a central composite design method to design 20 trial mixes at different factor and level combinations. They concluded that the slump decreases with an increase in water-cement ratio, an increase in cement content, and an increase in fine-total aggregate ratio. The air-dry density decreases with an increase in water-cement ratio, a decrease in cement content, and an increase in fine-total aggregate ratio. The strength shows a decrease with an increase in water-cement ratio and a decrease in fine-total aggregate ratio. The fine-total aggregate ratio has significant effect on the strength of lightweight concrete since failure of lightweight concrete is mainly governed by the strength of the aggregate rather than the quality of the hardened cement paste.

Qadi *et al*. (2009) developed linear, interaction, pure quadratic and full quadratic models for modulus of elasticity and compressive strength of Self-Compacting Concrete (SCC) at various curing ages. Influence of key mixture parameters, namely, cement, water-powder ratio, fly ash and super plasticizer on hardened properties affecting the performance of SCC is studied. The models are evaluated on the basis of level prediction, residual error, residual mean square error and correlation coefficients. It is shown that full quadratic models performed best in case of each response variable. Atici (2011) applied multiple regression analysis and Artificial Neural Network (ANN) in estimating the compressive strength of concrete that contains various amounts of blast furnace slag and fly ash. Riad *et al*. (2011) used data from 70 different class K concrete mixes that were cast in field conditions to predict concrete initial setting times through multivariate regression analysis. Two prediction models are achieved, corresponding to the addition of set retarding and set accelerating admixtures. It is demonstrated with the help of field tests that concrete initial setting times can be accomplished with 2% error, provided the most accurate temperature forecast is given during the curing period.

You *et al*. (2012) developed dynamics modulus prediction models for asphalt mixes using weighted least square nonlinear multiple regression method. Ahmed (2012) built up prediction model for compressive strength of concrete containing different matrix mixture at fixed age or at different curing periods. Eight different parameters, namely, time, water, cement, metakaolin, silica fume, sand, aggregate and superplasticizer are examined for matrix mixture. It is shown that predicted values are highly correlated with experimental values of compressive strength. Lofty *et al*. (2014) conducted a response surface method based experimental study to model the influence of key

parameters on the properties of Extended Clay Light Weight Self Compacting Concrete (EC-LWSCC) mixtures. They identified three key parameters, namely, water to binder ratio, high rate water reducing admixture percent, and total binder content to derive mathematical models for evaluating fresh and hardened concrete properties. Slump flow diameter, V-funnel flow time, J-ring flow diameter, J-ring height difference, L-box ratio, filling capacity, sieve segregation, fresh/28-day air/oven dry unit weights and 7- and 28-day compressive strengths were evaluated to analyze the influence of mix design parameters and develop the models. The developed models were utilized to formulate three optimum EC-LWSCC mixtures with high statistical desirability. EC-LWSCC mixtures, thus produced, satisfy the European EFNARC criteria.

If the data used for development of regression models is not taken from a statistically designed experiment, which ensures the predictor variables to be independent, the regression analysis may suffer from the serious problem of multi-collinearity. However, multi-collinearity is not a problem in regression analysis if the only purpose of the regression analysis is to predict the compressive strength of concrete for the same combination of the predictor values which are in the sample and are used to obtain the parameter estimates. But, if the purpose of regression analysis is estimation and control of compressive strength of concrete with predictors as random variables so that the model may give reasonably good predictions for the interpolation of data points within the sample, then effect of multi-collinearity needs to be considered. In that case, results obtained by OLSR can be misleading. In the presence of multi-collinearity, OLSR may result in regression coefficients with different signs and inflated variances (Ryan, 1996). The problem of multi-collinearity is often solved by removing the highly correlated variables. Wu *et al*. (2010) used variable selection and variable transformation methods to get rid of the problem of multi-collinearity in the data and developed a parsimonious model with 84.37% coefficient of determination to predict compressive strength of concrete. Cevik *et al*. (2010) presented the application of two techniques, namely, genetic programming and stepwise regression for formulating strength enhancement of carbon-fiber-reinforced polymer confined concrete cylinders. Stepwise regression technique uses variable selection method to select best possible subset of predictors by checking at every step the significance of all subsequently included variables. Ramugade (2010) resolved the problem of multi-collinearity by removing highly correlated variables and proposed regression models for predicting compressive strength of concrete. But, removing one or more such predictors to reduce

multi-collinearity may not be a safe strategy as this sometimes leads to loss of important information.

2.4 SINGLE-OBJECTIVE OPTIMIZATION OF CONCRETE MIX PARAMETERS

Yeh (1999, 2003) proposed a methodology for finding optimal proportions for concrete mixes for a given workability and compressive strength. Their methodology consisted of three steps. First step was to build accurate models for workability and strength using ANNs and experimental data. Specific properties of a given mix are evaluated using developed models in the second step. Optimal concrete mix proportions using nonlinear programming technique were found in the third step.

Lim *et al*. (2004) proposed to use Genetic Algorithm (GA) technique to design optimal High Performance Concrete (HPC) mixtures to reduce the number of trial mixes with desired properties in the field test. The factors affecting compressive strength of concrete are taken as water-binder ratio, water content, fine aggregate ratio, replacement ratio of fly ash, replacement ratio of silica fume and content of air-entertaining agent. Also, the factors affecting slump are considered as, water-binder ratio, water content, fine aggregate ratio, replacement ratio of fly ash and replacement ratio of silica fume and content of superplasticizer. 181 sets of concrete mixtures are used for development of fitness functions for compressive strength and slump and 8 mixtures are used for verification of results. 181 set of mixtures are further divided into two sets of 104 and 77 mixtures on the basis of compressive strength. First set of mixtures have compressive strength lying between 40 MPa to 80 MPa, while, the second set mixtures has compressive strength lying between 80 MPa to 120 MPa. Four GA programs are implemented to find optimal concrete mix proportions for specified values of compressive strength and slump. Applicability of proposed methodology is demonstrated by comparison of optimal mixture proportions for a specified value of compressive strength or slump with experimental values.

Özbay *et al*. (2006) used Taguchi method and GA to find optimal concrete mix proportions for maximum compressive strength of concrete. They designed experiments using an orthogonal array technique L_{27} array with seven factors, namely, water content, water to cementitious content ratio, fine aggregate to total aggregate percent, fly ash percent, AE content, SP and silica fume content. Compressive strength of concrete is modeled using nonlinear regression method. The optimal mix proportions

obtained using the two methods are tested experimentally. It is found that GAs produce better results. Rajasekaran *et al*. (2006) employed evolution strategies to find optimal mix design for HPC that minimize the cost of concrete subjected to strength and slump of concrete. Penalty function method is used as constraint handling technique which converts the constrained optimization problem into unconstrained optimization problem. The relationship between strength, slump and input parameters is established using sequential learning neural network. It is concluded that the developed program can find optimal mix of HPC irrespective of the geographic location, provided the current rates for constituents for HPC are used.

Yeh (2007) proposed Computer-Aided Design (CAD) tool to find optimal concrete mix proportions. CAD tool mainly consisted of modeling module and optimization module. In modeling module, strength and slump of concrete were modeled using ANNs. In optimization module, optimization was performed using nonlinear programming technique and GA. Variations of optimal concrete mix constituents with required compressive strength of concrete have been studied. Yeh (2009) integrated three technologies, namely, Design of Experiments (DOE), ANN and Mathematical Programming (MP) to find optimal mix proportions of concrete. DOE and ANN are employed to reduce the number of test mixes and specimens without sacrificing the accuracy of evaluating the effects and interactions of variations of the components on workability and compressive strength. The function of MP is to optimize the mixture to lower the cost while keeping the concrete to satisfy required properties. He concluded that the early strength requirement played the dominant role in low and medium strength concrete while late strength requirement played the dominant role in high strength concrete.

Parichatprecha and Nimityongskul (2009) developed a cost based High Performance Concrete (HPC) mix optimization system based on an integrated approach using ANN and GA. ANN is used to predict the three main properties of HPC, namely workability, strength and durability, which are used to evaluate fitness and constraint violations in the GA process. The correlation between concrete components and its properties is established. GA is employed to arrive at an optimal mix proportion of HPC by minimizing its total cost. They also validated the proposed model with the help of trial batches. Jayaram *et al*. (2009) proposed elitist GA models for optimization of HVFAC mix. The data is firstly analyzed to elicit upper and lower bounds of certain range and ratio constraints. Then, elitist GA is applied to find the quantities of cement, fly ash and

water for maximized concrete strength of mix corresponding to five ranges of 28 days compressive strength.

Lee *et al*. (2009) presented an enhanced design methodology for optimal mixture proportions of concrete composition with respect to accuracy in the case of using prediction models based on a limited data base. The methodology is demonstrated using a convex hull, an ANN and a GA technique. Convex hull is used to find an evaluation model for the effective region. ANN is used to model material properties and GA is used as an optimization tool. It is found that results obtained are very accurate and practically feasible. Ozbay *et al*. (2010) generated high strength concrete data according to Taguchi design of experiments method. Mechanical properties of concrete are modeled using Genetic Programming. HSC mix having minimum cost while satisfying requirements of strength and workability is obtained using GA.

2.5 MULTI-OBJECTIVE OPTIMIZATION OF CONCRETE MIX PARAMETERS

Karihaloo and Kornbak (2001) used compromise programming technique for simultaneous optimization of tensile strength and ductility for a given compressive strength in the design of fibre reinforced concrete mixes. In this technique, multiple objectives are combined to form a single objective using maximum and minimum values for each objective. Modified method of feasible directions is employed to find optimal solutions. It is seen that the most effective parameters controlling the mix properties are fibre aspect ratio and volume fraction of fibre. Maruyama *et al*. (2001) and Maruyama *et al*. (2002) applied GA to find optimal concrete mix proportions under multi-criteria environment. Two mix proportioning problems are dealt in their work. First problem deals with a compromise between delayed setting time and high flowability in hot weather and the second problem studies the tradeoff between accelerated setting time and high flowability in cold weather.

Noguchi *et al*. (2003) solved two concrete mix proportioning problems using GA. First problem deals with cost optimization of concrete having a strength of 60 MPa, whereas, the second problem deals with finding optimal concrete mix for mass concrete in cold weather at the coast. Baykasoğlu *et al*. (2009) followed a two-step approach to optimize HSC parameters. In first step, HSC parameters, namely, compressive strength, slump and cost are modeled using regression analysis, neural networks and Gene Expression Programming (GEP) and in the second step, multi-objective optimization

models based on GEP and regression models are solved. Multiple objectives are handled using weighing method and hierarchical method in combination with GA. It is seen that GA using weighted method generated more Pareto-optimal solutions than the GA using hierarchical method for both GEP and regression based models. Also, Pareto-optimal solutions generated using regression based model are higher. Nehzad *et al*. (2010) performed multi-objective optimization considering two conflicting objectives, namely, concrete diffusion factor and 28 days compressive strength. They proposed a new diversity preserving algorithm called ε- elimination to enhance the performance of NSGA II for optimization purpose. Park *et al*. (2013) and Park (2013) optimized mix proportions for recycled aggregate concrete using GA under multi-criteria environment. Several optimum mix proportions for recycled aggregate concrete that meets required performances were obtained.

Whereas the optimization of concrete mix proportions have been investigated in detail in literature, But, the effect of various uncertainties *e.g.* modeling uncertainties, manufacturing uncertainties *etc*. on the concrete mix design has not been fully accounted for. The present work proposes to perform safety factor based deterministic optimization and reliability based single and multi-objective optimizations of concrete mix parameters with the aim of designing concrete mixes with lowest cost and maximum reliability.

Reliability based design optimization techniques have been successfully employed in structural design problems to obtain reliable designs of concrete structures, and a brief review of the same is presented in the succeeding section.

2.6 APPLICATION OF RBDO IN STRUCTURAL DESIGN OPTIMIZATION

RBDO has been successfully applied to various structural design problems to produce better designs than those obtained by the deterministic design optimization.

Koskisto and Ellingwood (1997) presented a decision model for minimizing the life cycle cost of prefabricated concrete elements and structures, taking into account the building design, manufacturing, construction and service life as a whole. Their model utilized principles of engineering economic analysis under uncertainty in considering various costs. Frangopol *et al*. (1997) presented a reliability based approach to design Reinforced Concrete (RC) bridge girders that are under corrosion attack. They investigated the effect of corrosion on both moment and shear reliabilities and minimized the total material cost considering corrosion effect. Bland (1998) applied

Tabu search to find optimal structural design in terms of weight minimization of a space truss. He showed how the effects of variations in material strength and applied loadings may be analyzed. Barakat *et al*. (2003) presented a single objective reliability based optimization approach for Prestressed Concrete Beam (PCB). Permissible tensile and compressive stresses at both initial and final stages, prestressing losses, ultimate shear strength, ultimate flexural strength, cracking moment, crack width, and the immediate deflection and the final long term deflection are considered as limit states. Optimal overall cost of the PCB in terms of concrete, pre-stressing steel, mild steel, and formwork is obtained subjected to 11 reliability constraints and four geometrical constraints.

Almeida *et al*. (2008) compared DDO and RBDO of RC plane frames. Sequential Quadratic Programming (SQP) and Sequential Linear Programming (SLP) are used as optimization techniques. Reliability analysis is performed by FORM using RIA and PMA. They concluded that DDO may lead to structures with inadequate level of reliability while RBDO gives an optimal design with a target reliability index. Aoues and Chateauneuf (2008) proposed a methodology for system RBDO of reinforced concrete structures. The method is based on adaptive target reliabilities for structural components instead of specifying identical predefined component targets. Over designed components are avoided by pulling down the target reliabilities for low sensitivity components with respect to overall system safety. Zou *et al*. (2008) presented RBDO technique for base-isolated concrete building structures under spectrum loading. This technique integrates response spectrum seismic analysis, reliability analysis, isolation strategies and an optimization technique. The total cost of the base-isolated building is minimized subject to multiple design performance criteria such as inter-story drift of the superstructure and the lateral displacement of the isolation system or corresponding reliability constraints. Drift responses and corresponding reliability indexes are explicitly formulated using principle of virtual work. Integrated optimization problem is solved using optimality criteria method. It is reported that this technique is capable of achieving the optimal balance between the costs of the superstructure and isolation systems whilst the seismic drift performance or corresponding reliability of the building can be simultaneously considered.

Lopez *et al*. (2011) developed a RBDO methodology based on safety factors derived from KKT optimality conditions of the RIA. This methodology is coupled with particle swarm optimization to find designs for laminated composite structures. The optimal

designs are validated using Monte Carlo simulation. Luo *et al*. (2011) formulated reliability based design optimization (RBDO) of adhesive bonded steel concrete composite beams as a double loop problem considering probabilistic and non-probabilistic uncertainties. The PMA is employed to improve the convergence and the stability in solving the inner-loop. Moreover, the double-loop optimization problem is transformed into a series of approximate deterministic problems by incorporating the sequential approximate programming and the iteration scheme. Finally, reliability-based optimization designs of a single span adhesive bonded steel–concrete composite beam with different loading cases are achieved through integration of the present systematic method, the finite element analysis and the optimization package.

Song *et al*. (2011) dealt with RBDO of a riser support installed on a floating production storage and offloading unit under operation, extreme, damaged, one line failure cases and installation loading conditions. They minimized the weight of the riser support structure subjected to stress constraints for a given target reliability. Probabilistic optimal solutions are obtained by moving least square method for RBDO using response surface metamodel. Inequality constraint functions of stresses are modeled employing constraint-feasible moving least square method. Beaurepaire *et al*. (2012) presented a method for determining optimal maintenance scheduling of metallic structures considering uncertainties related to fatigue crack initiation and crack propagation. They showed that cost associated with such structures is mainly affected by the time of inspection and in less degree by the quality of inspection.

Khatibinia *et al*. (2013) introduced a new discrete gravitational search algorithm and a meta-modeling framework for RBDO of RC structures. The Monte-Carlo Simulation method is used to estimate probabilities of reliability. The meta-model consisted of a weighted least square support vector machine and a wavelet Kernel function. They concluded that the proposed method performed efficiently when applied to numerical problems. Behnam and Eamon (2013) conducted RBDO on three types of ductile hybrid fibre reinforced polymer bars, which are cost minimized for different bridge deck and building beam design states considering strength, deflection, ductility and reliability constraints. It is found that the optimized designs were approximately 10-30% less expensive than the base design considered.

Salehghaffari *et al*. (2013) proposed an evidence based approach for optimization of structural components under material parameter uncertainty. The approach is applied to evidence based design optimization of externally stiffened circular tubes under axial

impact load. The component is divided into three different regions for representation of spatial uncertainties in material properties. Radial basis function metamodelling approach and Latin hypercube sampling are used to develop surrogate models for the response functions. They concluded that inclusion of spatial uncertainty makes the task of uncertainty representation and propagation much more complex than the assumption of uniform uncertainty throughout the structure. Aoues *et al*. (2013) proposed a new RBDO method for RC structures. The RBDO problem is decomposed into several cycles of deterministic optimization based on a new safety factor called Optimal System Safety Factor (OSSF). At each cycle of DDO, the system reliability analysis is performed to verify the reliability of optimal design. The OSSF are computed on the basis of the previous system reliability analysis, Then the updated OSSF are provided for the next cycle of DDO. They showed that the numerical application of proposed method is equivalent to DDO.

2.7 SUMMARY

This chapter presents a historical chronology of development of RBDO methods and MOO techniques. Also, work done by researchers in the area of regression model development of concrete mix parameters; single and multi-objective optimization of concrete mix parameters and application of RBDO in structural design problems has been reviewed. A detailed review of literature reveals that biased regression methods like ridge regression method and principal component regression method has not been explored by researchers to model concrete mix parameters, in presence of multi-collinearity in the data. Further, it is seen that effect of uncertainties while optimizing concrete mix proportions has not been investigated.

In the present work, prediction models for compressive strength of concrete have been developed using biased regression methods. Reliability based optimal designs of concrete mix proportions have been obtained under single and multi-objective environment.

CHAPTER 3
PREDICTION MODELS FOR COMPRESSIVE STRENGTH OF CONCRETE

==========

3.0 GENERAL

In an optimization process, simplified mathematical models are needed that could provide efficient representation of various concrete mix parameters. The compressive strength of concrete is a nonlinear function of its constituents as it is known only through its discrete outcomes. Thus, form and degree of the model for compressive strength is not known. The success of prediction model depends on proper form of the model as well as on the proper values of the parameters of the model. A second order polynomial is most often employed by many researchers for the response surface (Melchers 2002). However, in polynomial models predictor variables are linearly dependent on each other because of form of the model. Thus, the data inherently suffers from multi-collinearity. In this chapter, linear and pure quadratic models for compressive strength of concrete have been developed using OLSR, TRR, GRR and PCR techniques. The models have been built up for concrete with or without fly ash for curing ages of 28 days, 56 days and 91 days.

3.1 FACTORS INFLUENCING COMPRESSIVE STRENGTH OF CONCRETE FOR DETERMINING PREDICTOR VARIABLES

Concrete, as mentioned earlier, is obtained by mixing cement, water, fine aggregates, coarse aggregates and some admixtures like fly ash, super plasticizers *etc.* in required proportions. The mixture when placed in forms and allowed to cure, hardens like a rock-like mass which grows stronger with age. The ingredients of concrete can be classified into two groups, namely, active and inactive. The active group consists of cement and water, whereas, the inactive group consists of fine and coarse aggregates. The main function of cement is primarily to bind the fine and coarse aggregates together in addition to the filling the voids between fine and coarse aggregates to form a

compact mass. Water is the most important and least expensive ingredient of concrete. A part of mixing water is utilized in the hydration of cement to form the binding matrix in which the inert aggregates are held in suspension until the matrix has hardened. The remaining water serves as a lubricant between fine and coarse aggregates and makes concrete workable, *i.e.*, readily placeable in forms.

Aggregates are much cheaper than cement and impart greater volume, stability and durability to concrete. The most important function of fine aggregate is to assist in producing a workable and homogenous concrete mix and also, it helps the cement paste to hold the coarse aggregates particles in suspension. The aggregates are used primarily for providing bulk to the concrete and increase the density of resulting mix. The aggregates provide about 75% of the body of concrete and hence their role is extremely important.

Further, admixtures like fly ash are used as a partial replacement of cement in concrete. This replacement produces concrete that is much more resistant to the action of salt, sulphate or acidic water. However, presence of fly ash also results in reduction of the rate of development of compressive strength in normal concrete. According to Gambhir (1995), the major factors influencing the compressive strength of concrete are:

a) Type of cement and age
b) Type of aggregates and admixture.
c) Degree of compaction
d) Concrete mix proportions, i.e., cement content, fine aggregate-cement ratio, coarse aggregate-cement ratio, amount of air voids and water-cement ratio
e) Type and temperature of curing
f) Nature of loading to which the specimen is subjected, i.e., static, sustained dynamic *etc*.
g) Type of stress situation that may exist, viz., uniaxial, biaxial and triaxial.

However, as mentioned earlier, the data for compressive strength of concrete had been generated in controlled laboratory conditions. Thus, type of constituent materials, type of curing, type of stress situation and temperature of curing are within the preset limits and only the concrete mix proportions had been varied. Hence in the present work, the variation in compressive strength of concrete is attributed primarily to variation in the mix proportion. As such compressive strength of concrete has been modeled as a function of concrete mix proportions and cement content.

It is worth mentioning here that exact form of relationship between compressive strength of concrete and its ingredients is still not known. In the present work, linear and pure quadratic approximation models for compressive strength of concrete have been developed. Compressive strength of concrete has been considered for curing periods of 28 days, 56 days and 91 days. Separate models for concrete mixes without fly ash and for concrete with 15% replacement of cement with fly ash have been developed using OLSR, TRR, GRR and PCR techniques.

3.2 COMPRESSIVE STRENGTH PREDICTION MODELS FOR CONCRETE WITHOUT FLY ASH

The data set consists of 49 different concrete mix proportions. Concrete is composed of water (w), cement (c), fine aggregate (fa) and coarse aggregates ($ca-I, ca-II$, $ca-III$), all measured in kg/m^3. Compressive strength of concrete without fly ash has been modeled considering water-cement ratio (w/c), fine aggregate-cement ratio (fa/c), ratio of coarse aggregates and cement content ($ca-I/c$, $ca-II/c$, $ca-III/c$) and cement content (c) as predictor variables. Models have been developed for 28 days compressive strength ($st28$), 56 days compressive strength ($st56$) and 91 days compressive strength ($st91$), all measured in MPa. It is worth mentioning here that quadratic term for c, i.e. c^2 has not been considered in development of quadratic models. This has been done to avoid the problem of very high difference of order of magnitude of predictor variables that may affect the performance of regression models severely.

3.2.1 Sample data analysis

To analyze multi-collinearity among the sample data, Ryan (1996) suggested to examine the correlations between the pairs of predictor variables and the Variance Inflation Factor (VIF) of predictor variables. A pair wise correlation matrix of predictor variables might be insufficient to identify collinearity problem because linear dependencies may exist among combinations of predictors. Hence, it is necessary to examine VIFs also. Following Ryan (1996), the VIF_i of i^{th} predictor variable x_i (say) has been considered as:

$$VIF_i = \frac{1}{1-R_i^2} \tag{3.1}$$

where R_i^2 is the squared multiple correlation coefficient that results from regression of x_i against all other predictors. It is clear that if x_i has a strong linear relationship with other predictor variables, R_i^2 is close to 1 and VIF value tends to be very high. In the absence of linear relationship among predictor variables, R_i^2 is zero and VIF equals 1. As a rule of thumb, multi-collinearity is said to exist if VIF value for a predictor variable is more than 10.

Table 3.1 shows the correlation among the predictor variables and also, their correlation with compressive strength for various ages.

It can be noted from Table 3.1 that compressive strength for any given age is influenced by w/c, fa/c and c. Coarse aggregates to cement content ratios do not have any significant effect on compressive strength. Table 3.1 reveals that w/c has correlations numerically greater than 0.500 with fa/c and c. $ca-I/c$ has strong negative correlation with $ca-III/c$. c has negative correlations numerically greater than 0.500 with w/c and fa/c. These results indicate that the given data set suffers from multi-collinearity. Also, it can be noted from the Table 3.2 that VIF values for all the predictors exceed 10 except for c and $ca-II/c$ and thus provide enough evidence for presence of multi-collinearity. Further, being quadratic models, strong multi-collinearity is present because of form of the models.

3.2.2 OLSR and RR models

The total sample set consists of 49 concrete mix composition observations. Total sample set is randomly divided into training set of 33 observations and validation set of 16 observations. In order to illustrate the performance of developed models, MSE for validation set is calculated using (1.5).

For RR models, MSE is calculated for optimal value of $\boldsymbol{K}$ which is obtained using Differential Evolution (DE) algorithm. However, for linear OLSR (LOLSR) model and pure quadratic OLSR (QOLSR) model, $\boldsymbol{K}=\boldsymbol{0}$. In order to obtain the optimal ridge parameters for TRR and GRR models, DE algorithm was employed using parameters $N_p=50$, $Cr=0.9$, $F=0.85$ and $g_{max}=500$. Here, N_p symbolizes the number of individuals in a population, $Cr\epsilon\,[0,1]$ is the crossover probability, $F\,\epsilon\,[0,2]$ denotes the mutation probability, and maximum number of generations are denoted by g_{max}. DEMAT, a MATLAB program developed by Price *et al*. (2005) is used to carry out DE algorithm.

The optimal ridge parameters obtained for linear TRR (LTRR) model, pure quadratic TRR (QTRR) model, linear GRR (LGRR) model and pure quadratic GRR (QGRR) model for 28 days, 56 days and 91 days compressive strength are given in Tables 3.3(a)-(c). The regression coefficients of the developed models are summarized in Tables 3.4(a)-(c). It can be noted from Tables 3.3(a) and 3.3(c) that ridge parameters for LTRR and QTRR model for 28 days compressive strength and for LTRR model for 91 days concrete compressive strength are negligibly small. That is the reason why TRR models developed in these cases are same as corresponding OLSR models (Tables 3.4(a) and 3.4 (c)).

To demonstrate the performances of developed compressive strength models, the MSE values of each of the developed models are listed in Table 3.5.

It can be seen from Table 3.5 that QGRR model has the least value of MSE for 28 and 91 days compressive strength models. LGRR model is the second best performing models for 28 and 91 days compressive strength. For 56 days compressive strength, least value of MSE is obtained for QTRR model followed by QGRR model.

3.2.3 PCR models

Tables 3.6 and 3.7 show the eigen values of correlation matrix of predictor variables and corresponding percentage of variance explained by each PC for linear PCR (LPCR) and pure quadratic PCR (QPCR) models. It can be seen from the Tables 3.6 and 3.7 that eigen values are nearly zero corresponding to 5^{th} and higher components, indicating the presence of strong multi-collinearity. Also, it can be noted from the tables that first four PCs explain 99.671 % and 99.394% variance of sample space for linear and quadratic models, respectively. The limited dispersion in remaining PCs dimensions inflates the variances of OLSR coefficients for all the independent variables involved in near singularities.

Kaiser-Gutman rule suggests that first two PCs should be selected for linear models and three PCs for quadratic models, but they together explain less than 95% variance in the sample space. Guiot's method advocates the use of first four PCs in each case. The scree plots shown in Figures 3.1 and 3.2 suggest the use of first four PCs for LPCR model and QPCR model. Thus, first four PCs are selected for linear and quadratic model development of concrete compressive strength. Further, it is also ensured that the dropped PCs do not have any predictive importance for concrete mix parameters. For

this purpose, compressive strength at various ages is regressed against each of the dropped PCs and the value of coefficient of determination (r^2) which is the measure of variance in response variable explained by the predictor variables is found out to be lying between 0.000 and 0.051. Very low values of r^2 validates that dropped PCs do not affect prediction ability of the models. Subsequently, least square regression is carried out to develop regression models to estimate the concrete compressive strength using selected PCs as predictors. Finally, the regression coefficients of the PCs are transformed back to find coefficients of original variables. The results of PCR are summarized in Table 3.8. The MSE values of each of the developed models are listed in Table 3.9. On comparison of $MSEs$ listed in Tables 3.5 and 3.9 for the developed concrete compressive strength prediction models, it is found that the MSE for PCR models is higher than that for GRR, TRR and OLSR models for 28 days curing age. This value is less only for LTRR and LOLSR model for 56 days compressive strength. For 91 days concrete compressive strength, PCR models are better than QOLSR and QTRR models. This can be attributed to the fact that ridge parameters for GRR and TRR models have been selected in such a way that the prediction error for validation set is minimized.

3.3 COMPRESSIVE STRENGTH PREDICTION MODELS FOR CONCRETE WITH 15% REPLACEMENT OF CEMENT BY FLY ASH

There are 27 concrete mixes composed of $w, fa, ca-I, ca-II, ca-III$ and cementitious content (cm), all measured in kg/m^3. Here, cementitious content cm is a mixture consisting of 85 percent cement content and 15 percent fly ash. Compressive strength of concrete without fly ash has been modeled considering water-cementitious content ratio (w/cm), fine aggregate-cementitious content ratio (fa/cm), ratio of coarse aggregates and cementitious contents ($ca-I/cm, ca-II/cm, ca-III/cm$) and cm as predictor variables. Linear and pure quadratic models have been developed for $st28$, $st56$ and $st91$, all measured in MPa. Again, as explained in section 3.2, cm^2 has not been considered as a predictor variable for concrete compressive strength in pure quadratic models.

3.3.1 Sample data analysis

The pair wise correlation between the selected predictor variables listed in Table 3.10 shows that w/cm has strong correlation with fa/cm. $ca-I/cm$ has correlation numerically greater than 0.500 with $ca-III/cm$. Remaining pair wise correlations between predictor variables are very small. These results indicate that the given data set does not suffer much from multi-collinearity. Also, it can be noted from the Table 3.11 that VIF values for w/cm, fa/cm, $ca-I/cm$ and $ca-III/cm$ are greater than 10. This also gives the idea that the data suffers from moderate multi-collinearity. However, in quadratic models, strong multi-collinearity is present because of form of the models.

3.3.2 OLSR and RR models

The total sample set consists of 27 concrete mix composition observations. Total sample set is randomly divided into training set of 18 observations and validation set of 9 observations. In order to illustrate the performance of developed models, MSE for validation set is calculated using (1.5).

For RR models, MSE is calculated for optimal value of optimal value of $\boldsymbol{K}$ which is obtained using Differential Evolution (DE) algorithm. However, for OLSR models, $\boldsymbol{K}=\mathbf{0}$. In order to obtain the optimal ridge parameters for TRR and GRR models, DE algorithm was employed using the same parameter values as used for concrete without fly ash. The optimal ridge parameters obtained for linear and pure quadratic TRR and GRR models for 28 days, 56 days and 91 days compressive strength are given in Tables 3.12(a)-(c). The regression coefficients of the developed models are summarized in Table 3.13(a)-(c). It can be noted from Tables 3.12(b) and 3.12(c) that ridge parameters for LTRR models for 56 days and 91 days compressive strength are negligibly small. That could be the reason why TRR models developed in these cases are same as corresponding OLSR models (Tables 3.13(b) and 3.13 (c)). The MSE values of each of the developed models are listed in Table 3.14. It can be seen from the table that QOLSR model performs worst in each case. QGRR model give the least value of MSE among various compressive strength models for curing ages of 28 days and 91 days, whereas for 56 days compressive strength, best prediction is given by QTRR model.

3.3.3 PCR models

Tables 3.15 and 3.16 show the eigen values of correlation matrix of predictor variables and corresponding percentage of variance explained by each PC for linear and pure quadratic models. It can be seen from the Tables 3.15 and 3.16 that eigen values are nearly zero corresponding to 5^{th} and higher components, indicating the presence of strong multi-collinearity. Also, it can be noted from the tables that first four PCs explain 99.390 % and 99.288% variance of sample space for linear and quadratic models, respectively. The limited dispersion in remaining PCs dimensions inflates the variances of OLSR coefficients for all the independent variables involved in near singularities.

As explained earlier, Kaiser-Gutman rule suggests the selection of first two PCs for LPCR model and first three PCs for QPCR models, but they together explain less than 95% variance in the sample space. Guiot's method advocates the use of first four PCs in each case. The scree plot shown in Figs. 3.3 and 3.4 also suggest the use of first four PCs. Thus, first four PCs are selected for linear and quadratic model development of concrete compressive strength. Further, it is also ensured that the dropped PCs do not have any predictive importance for concrete mix parameters. For this purpose, compressive strength at various ages is regressed against each of the dropped PCs and it is found that value of r^2 lies between 0.000 and 0.037. These very low values of r^2 validates that dropped PCs do not affect the prediction ability of the models. Subsequent to this, least square regression is carried out to develop regression models to estimate compressive strength using selected PCs as predictors. Finally, the regression coefficients of the PCs are transformed back to find coefficients of original variables. The results of PCR are summarized in Table 3.17.

The MSE values of each of the developed models are listed in Table 3.18. On comparing the Tables 3.14 and 3.18, it is observed that MSE for PCR models is higher than that for GRR, TRR and OLSR models in each case except for QOLSR models for 28 days and 91 days compressive strength.

3.4 SUMMARY

In this chapter, models for compressive strength of concrete with or without fly ash have been developed using OLSR, TRR, GRR and PCR techniques for different curing ages. Performance of the developed models has been assessed on the basis of MSE of

validation set. It is seen that QGRR model is best for 28 and 91 days compressive strength of concrete with or without fly ash. QTRR model gives best performance for 56 days compressive strength of concrete with or without fly ash. However, all of these developed models will be incorporated in the RBDO models to study their impact on optimization results.

Table 3.1 Correlation matrix for concrete without fly ash parameters

Parameter	w/c	fa/c	$ca-I/c$	$ca-II/c$	$ca-III/c$	c (kg/m^3)	$st28$ (MPa)	$st56$ (MPa)	$st91$ (MPa)
w/c	1.000	0.960	0.085	0.481	0.114	-0.734	-0.968	-0.941	-0.958
fa/c		1.000	0.184	0.490	-0.031	-0.637	-0.900	-0.872	-0.888
$ca-I/c$			1.000	0.122	-0.934	-0.438	-0.186	-0.209	-0.177
$ca-II/c$				1.000	-0.225	-0.416	-0.378	-0.334	-0.344
$ca-III/c$					1.000	0.197	-0.060	-0.044	-0.071
c(kg/m^3)						1.000	0.821	0.816	0.808

Table 3.2 VIF values of predictor variables for concrete without fly ash

Parameter	VIF value
w/c	68.616
fa/c	40.134
$ca-I/c$	95.639
$ca-II/c$	8.378
$ca-III/c$	99.329
c	9.741

Table 3.3(a) Optimal ridge parameters for 28 days compressive strength models for concrete without fly ash

	TRR model		GRR model	
	Linear	Pure Quadratic	Linear	Pure Quadratic
Intercept	3.76E-15	5.91E-14	0.000000	0.000000
w/c	3.76E-15	5.91E-14	0.000000	0.000028
fa/c	3.76E-15	5.91E-14	0.007888	0.000000
$ca-I/c$	3.76E-15	5.91E-14	0.000000	1.000000
$ca-II/c$	3.76E-15	5.91E-14	0.290825	0.000000
$ca-III/c$	3.76E-15	5.91E-14	1.000000	1.000000
c	3.76E-15	5.91E-14	1.000000	0.999983
$(w/c)^2$		5.91E-14		0.000000
$(fa/c)^2$		5.91E-14		0.091078
$(ca-I/c)^2$		5.91E-14		1.000000
$(ca-II/c)^2$		5.91E-14		1.000000
$(ca-III/c)^2$		5.91E-14		1.000000

Table 3.3(b) Optimal ridge parameters for 56 days compressive strength models for concrete without fly ash

	TRR model		GRR model	
	Linear	Pure Quadratic	Linear	Pure Quadratic
Intercept	0.000373	0.000139	0.000000	0.000000
w/c	0.000373	0.000139	0.000000	0.999993
fa/c	0.000373	0.000139	1.000000	0.006149
$ca-I/c$	0.000373	0.000139	0.000000	0.011388
$ca-II/c$	0.000373	0.000139	0.207472	1.000000
$ca-III/c$	0.000373	0.000139	1.000000	1.000000
c	0.000373	0.000139	1.000000	1.000000
$(w/c)^2$		0.000139		0.003538
$(fa/c)^2$		0.000139		0.000000
$(ca-I/c)^2$		0.000139		1.000000
$(ca-II/c)^2$		0.000139		1.000000
$(ca-III/c)^2$		0.000139		1.000000

Table 3.3(c) Optimal ridge parameters for 91 days compressive strength models for concrete without fly ash

	TRR model		GRR model	
	Linear	Pure Quadratic	Linear	Pure Quadratic
Intercept	6.97E-15	0.031653	0.000000	0.005646
w/c	6.97E-15	0.031653	0.000000	1.000000
fa/c	6.97E-15	0.031653	0.094689	1.000000
$ca-I/c$	6.97E-15	0.031653	1.000000	0.000000
$ca-II/c$	6.97E-15	0.031653	0.000000	0.000000
$ca-III/c$	6.97E-15	0.031653	1.000000	0.000000
c	6.97E-15	0.031653	0.000000	0.000000
$(w/c)^2$		0.031653		0.000000
$(fa/c)^2$		0.031653		0.000000
$(ca-I/c)^2$		0.031653		0.125024
$(ca-II/c)^2$		0.031653		1.000000
$(ca-III/c)^2$		0.031653		1.000000

Table 3.4(a) Regression coefficients for 28 days compressive strength models for concrete without fly ash

	Regression Coefficients					
	Linear OLSR model	Pure Quadratic OLSR model	Linear TRR model	Pure Quadratic TRR model	Linear GRR model	Pure Quadratic GRR model
Intercept	113.503278	25.880527	113.503278	25.880528	109.857188	62.299505
w/c	-186.852348	197.596807	-186.852348	197.596797	-181.034035	32.373875
fa/c	11.088042	-23.540387	11.088042	-23.540386	10.009904	7.506371
$ca-I/c$	-1.365693	11.016013	-1.365693	11.016014	-0.882352	0.183190
$ca-II/c$	2.231068	4.386100	2.231068	4.386101	2.245465	1.502309
$ca-III/c$	-1.170294	13.126752	-1.170294	13.126753	-0.452704	-0.133433
c	0.016932	0.018415	0.016932	0.018415	0.020358	0.015581
$(w/c)^2$		-334.399294		-334.399284		-218.821083
$(fa/c)^2$		9.558913		9.558913		0.759037
$(ca-I/c)^2$		-4.281801		-4.281802		-0.523348
$(ca-II/c)^2$		-1.782398		-1.782398		0.225892
$(ca-III/c)^2$		-6.837795		-6.837795		-0.107460

Table 3.4(b) Regression coefficients for 56 days compressive strength models for concrete without fly ash

	Regression Coefficients					
	Linear OLSR model	Pure Quadratic OLSR model	Linear TRR model	Pure Quadratic TRR model	Linear GRR model	Pure Quadratic GRR model
Intercept	118.342929	74.058639	96.744801	49.570076	84.735277	51.254378
w/c	-220.608187	-204.944378	-131.277625	-57.984279	-111.940496	-0.119420
fa/c	19.244303	12.784851	5.675433	-1.513162	0.615533	-4.533880
$ca-I/c$	0.207654	33.461960	-2.187322	30.239378	-0.451967	4.764800
$ca-II/c$	4.399315	23.937600	1.792348	19.866236	3.113438	-0.092384
$ca-III/c$	1.934267	53.743343	-3.265029	45.820142	-0.666811	-0.414163
c	0.019856	0.020407	0.027238	0.022075	0.038946	0.041101
$(w/c)^2$		58.651904		-65.353606		-35.303776
$(fa/c)^2$		-1.936972		1.980518		-2.105360
$(ca-I/c)^2$		-10.645468		-9.950632		-2.655529
$(ca-II/c)^2$		-9.237605		-7.939531		-0.164341
$(ca-III/c)^2$		-27.782201		-23.666559		-0.330883

Table 3.4(c) Regression coefficients for 91 days compressive strength models for concrete without fly ash

	Regression Coefficients					
	Linear OLSR model	Pure Quadratic OLSR model	Linear TRR model	Pure Quadratic TRR model	Linear GRR model	Pure Quadratic GRR model
Intercept	124.186600	127.703926	124.186600	18.463761	100.899061	50.749372
w/c	-185.308907	-67.004666	-185.308907	2.327911	-134.543743	0.053341
fa/c	13.467012	-17.755753	13.467012	1.840064	3.808650	0.028106
$ca-I/c$	-1.627032	-8.066776	-1.627032	9.360048	-0.343672	6.451018
$ca-II/c$	1.662256	-11.311923	1.662256	6.216220	2.751441	6.066895
$ca-III/c$	-1.472594	-11.273903	-1.472594	4.837750	-0.138983	8.257680
c	0.004458	0.007570	0.004458	0.075560	0.023626	0.048365
$(w/c)^2$		-138.881641		-1.501680		-155.314191
$(fa/c)^2$		13.063057		-6.978775		2.450309
$(ca-I/c)^2$		2.200704		-2.841729		-1.045570
$(ca-II/c)^2$		5.8035099		-1.6581150		-0.0831826
$(ca-III/c)^2$		5.6786881		0.5200014		-0.2157994

Table 3.5 Mean square error for validation set for concrete without fly ash

Name of the model	MSE		
	For 28 days compressive strength	For 56 days compressive strength	For 91 days compressive strength
Linear OLSR model	0.41	1.48	1.23
Pure Quadratic OLSR model	0.65	0.97	1.66
Linear TRR model	0.41	1.34	1.23
Pure Quadratic TRR model	0.65	0.95	1.58
Linear GRR model	0.37	1.11	1.05
Pure Quadratic GRR model	0.34	0.96	0.92

Table 3.6 Eigen analysis for linear model for concrete without fly ash

Component	Eigen value	% of Variance explained
1	3.24162	54.02695
2	1.69720	28.28660
3	0.64626	10.77094
4	0.39521	6.58677
5	0.01618	0.26970
6	0.00354	0.05905

Table 3.7 Eigen analysis for pure quadratic model for concrete without fly ash

Component	Eigen value	% of Variance explained
1	5.77701	52.51825
2	3.25341	29.57647
3	1.38239	12.56714
4	0.52054	4.73216
5	0.04119	0.37443
6	0.01376	0.12510
7	0.00525	0.04771
8	0.00421	0.03828
9	0.00196	0.01778
10	0.00028	0.00255
11	0.00001	0.00012

Table 3.8 Regression coefficients for PCR models of compressive strength of concrete without fly ash

	Regression Coefficients					
	28 days compressive strength		56 days compressive strength		91 days compressive strength	
	Linear model	Pure Quadratic model	Linear model	Pure Quadratic model	Linear model	Pure Quadratic Model
Intercept	63.946459	60.500434	61.633483	60.064527	70.706788	67.094767
w/c	-60.905993	-33.306926	-53.771591	-29.894544	-53.284047	-28.961017
fa/c	-10.556191	-4.417460	-8.543007	-3.340762	-9.373301	-3.904988
$ca-I/c$	-0.518270	-0.304035	-0.535338	-0.319980	-0.419060	-0.243229
$ca-II/c$	2.589462	0.714107	3.120992	0.963646	2.338326	0.673034
$ca-III/c$	-1.687023	-1.165708	-1.758145	-1.219817	-1.498873	-1.035780
c	0.053230	0.043570	0.055939	0.045979	0.044563	0.036930
$(w/c)^2$		-34.690465		-31.259069		-30.145144
$(fa/c)^2$		-1.715160		-1.302455		-1.515102
$(ca-I/c)^2$		-0.484677		-0.509451		-0.409203
$(ca-II/c)^2$		0.280828		0.379307		0.266642
$(ca-III/c)^2$		-1.357937		-1.420030		-1.198083

Table 3.9 Mean square error for validation set using PCR models for concrete without fly ash

Name of the model	MSE		
	For 28 days compressive strength	For 56 days compressive strength	For 91 days compressive strength
Linear PCR model	0.70	1.22	1.28
Pure Quadratic PCR model	0.69	1.22	1.37

Table 3.10 Correlation matrix for concrete with fly ash parameters

Parameter	w/cm	fa/cm	$ca-I/cm$	$ca-II/cm$	$ca-III/cm$	cm (kg/m^3)	$st28$ (MPa)	$st56$ (MPa)	$st91$ (MPa)
w/cm	1.000	0.929	-0.344	0.233	0.390	-0.157	-0.953	-0.953	-0.981
fa/cm		1.000	-0.121	0.307	0.133	-0.038	-0.862	-0.845	-0.903
$ca-I/cm$			1.000	0.051	-0.963	-0.353	0.200	0.312	0.270
$ca-II/cm$				1.000	-0.239	-0.074	-0.158	-0.070	-0.186
$ca-III/cm$					1.000	0.221	-0.295	-0.400	-0.343
$cm(kg/m^3)$						1.000	0.370	0.256	0.263

Table 3.11 VIF values of predictor variables for concrete with fly ash

Parameter	VIF value
w/cm	35.514
fa/cm	27.073
$ca-I/cm$	78.698
$ca-II/cm$	5.146
$ca-III/cm$	89.111
cm	3.486

Table 3.12(a) Optimal ridge parameters for 28 days compressive strength models for concrete with fly ash

	TRR model		GRR model	
	Linear	Pure Quadratic	Linear	Pure Quadratic
Intercept	0.000031	0.00006311	0.000000	0.000000
w/cm	0.000031	0.00006311	0.000012	0.030368
fa/cm	0.000031	0.00006311	0.000000	0.000001
$ca-I/cm$	0.000031	0.00006311	0.309175	0.932429
$ca-II/cm$	0.000031	0.00006311	1.000000	0.000302
$ca-III/cm$	0.000031	0.00006311	0.000000	0.000060
cm	0.000031	0.00006311	1.000000	0.905408
$(w/cm)^2$		0.00006311		0.000037
$(fa/cm)^2$		0.00006311		0.000765
$(ca-I/cm)^2$		0.00006311		0.002861
$(ca-II/cm)^2$		0.00006311		0.000034
$(ca-III/cm)^2$		0.00006311		0.010662

Table 3.12(b) Optimal ridge parameters for 56 days compressive strength models for concrete with fly ash

	TRR model		GRR model	
	Linear	Pure Quadratic	Linear	Pure Quadratic
Intercept	2.38E-14	0.000001	0.000000	0.003108
w/cm	2.38E-14	0.000001	0.000000	1.000000
fa/cm	2.38E-14	0.000001	0.000000	1.000000
$ca-I/cm$	2.38E-14	0.000001	1.000000	1.000000
$ca-II/cm$	2.38E-14	0.000001	0.000000	1.000000
$ca-III/cm$	2.38E-14	0.000001	0.000000	0.000000
cm	2.38E-14	0.000001	0.000003	0.000000
$(w/cm)^2$		0.000001		0.000000
$(fa/cm)^2$		0.000001		1.000000
$(ca-I/cm)^2$		0.000001		0.000000
$(ca-II/cm)^2$		0.000001		0.000000
$(ca-III/cm)^2$		0.000001		0.000000

Table 3.12(c) Optimal ridge parameters for 91 days compressive strength models for concrete with fly ash

	TRR model		GRR model	
	Linear	Pure Quadratic	Linear	Pure Quadratic
Intercept	2.17E-15	0.000031	0.000000	0.000000
w/cm	2.17E-15	0.000031	0.000005	0.000000
fa/cm	2.17E-15	0.000031	1.000000	1.000000
$ca-I/cm$	2.17E-15	0.000031	1.000000	1.000000
$ca-II/cm$	2.17E-15	0.000031	1.000000	1.000000
$ca-III/cm$	2.17E-15	0.000031	0.000000	0.000000
cm	2.17E-15	0.000031	1.000000	0.999996
$(w/cm)^2$		0.000031		0.000000
$(fa/cm)^2$		0.000031		0.999999
$(ca-I/cm)^2$		0.000031		0.000000
$(ca-II/cm)^2$		0.000031		1.000000
$(ca-III/cm)^2$		0.000031		1.000000

Table 3.13(a) Regression coefficients for 28 days compressive strength models for concrete with fly ash

	Regression Coefficients					
	Linear OLSR model	Pure Quadratic OLSR model	Linear TRR model	Pure Quadratic TRR model	Linear GRR model	Pure Quadratic GRR model
Intercept	103.069240	241.293796	96.071049	126.345829	96.675656	100.905721
w/cm	-164.333277	-326.429813	-141.993278	-74.321706	-153.392103	-0.278395
fa/cm	3.815868	-60.860698	0.044291	-64.511974	1.804144	-71.493052
$ca-I/cm$	-2.289220	-51.581446	-2.430339	-11.003796	-1.448217	0.042470
$ca-II/cm$	0.349431	-54.655701	0.097192	-3.240662	0.365318	11.349818
$ca-III/cm$	-2.755949	-96.532608	-3.373876	-32.191616	-1.660422	-9.344565
cm	0.025835	0.031382	0.029817	0.032584	0.031569	0.026466
$(w/cm)^2$		158.778028		-70.563795		-153.352565
$(fa/cm)^2$		29.383104		27.603219		30.930717
$(ca-I/cm)^2$		16.267525		2.288855		-1.480732
$(ca-II/cm)^2$		25.523421		0.626547		-6.311867
$(ca-III/cm)^2$		58.986421		21.695799		6.170875

Table 3.13(b) Regression coefficients for 56 days compressive strength models for concrete with fly ash

	Regression Coefficients					
	Linear OLSR model	Pure Quadratic OLSR model	Linear TRR model	Pure Quadratic TRR model	Linear GRR model	Pure Quadratic GRR model
Intercept	120.649523	494.045923	120.649523	265.717820	119.038645	55.918774
w/cm	-190.543844	-2541.852099	-190.543844	-654.646862	-194.260051	0.034518
fa/cm	7.155821	236.022769	7.155821	35.549539	7.509842	-0.045985
$ca-I/cm$	-0.786478	24.634249	-0.786478	-46.369692	-0.081891	0.071681
$ca-II/cm$	2.067952	11.638222	2.067952	-50.483636	2.724764	0.106702
$ca-III/cm$	-0.511819	63.512448	-0.511819	-67.589772	0.694958	3.387063
cm	0.008559	0.027377	0.008559	0.016396	0.011174	0.043447
$(w/cm)^2$		2514.634892		485.195849		-159.185292
$(fa/cm)^2$		-95.414217		-10.507139		-0.296722
$(ca-I/cm)^2$		-6.776302		16.098171		1.071778
$(ca-II/cm)^2$		-1.744969		25.951024		2.617886
$(ca-III/cm)^2$		-41.822132		36.845349		-0.648986

Table 3.13(c) Regression coefficients for 91 days compressive strength models for concrete with fly ash

	Regression Coefficients					
	Linear OLSR model	Pure Quadratic OLSR model	Linear TRR model	Pure Quadratic TRR model	Linear GRR model	Pure Quadratic GRR model
Intercept	100.153598	47.761380	100.153598	128.017698	104.053090	147.859037
w/cm	-116.764696	1042.020775	-116.764696	-49.940612	-128.551213	-319.407294
fa/cm	-2.406605	-153.804573	-2.406605	-27.962185	-0.035227	-0.010403
$ca-I/cm$	-0.587557	-107.764736	-0.587557	-32.746239	-0.421183	-0.039300
$ca-II/cm$	1.075808	-94.747361	1.075808	-18.089863	0.446093	0.113565
$ca-III/cm$	-0.708211	-184.926556	-0.708211	-52.764535	-0.344599	-0.543854
cm	0.017857	0.017866	0.017857	0.023837	0.015793	0.015778
$(w/cm)^2$		-1255.493814		-66.161252		208.632393
$(fa/cm)^2$		65.289932		10.720141		-0.021162
$(ca-I/cm)^2$		35.853006		11.127556		-0.322635
$(ca-II/cm)^2$		44.713175		9.302762		0.217565
$(ca-III/cm)^2$		108.207792		29.759160		-0.010758

Table 3.14 Mean square error for validation set for concrete with fly ash

Name of the model	MSE		
	For 28 days compressive strength	For 56 days compressive strength	For 91 days compressive strength
Linear OLSR model	0.20	0.98	0.35
Pure Quadratic OLSR model	0.50	1.15	0.93
Linear TRR model	0.19	0.98	0.35
Pure Quadratic TRR model	0.15	0.65	0.41
Linear GRR model	0.18	0.92	0.28
Pure Quadratic GRR model	0.12	0.85	0.27

Table 3.15 Eigen analysis for linear model for concrete with fly ash

Component	Eigen value	% of Variance explained
1	2.67568	44.59468
2	1.66763	27.79388
3	0.89611	14.93510
4	0.74077	12.34625
5	0.01439	0.23986
6	0.00541	0.09025

Table 3.16 Eigen analysis for pure quadratic model for concrete with fly ash

Component	Eigen value	% of Variance explained
1	5.29507	48.13701
2	2.91382	26.48925
3	1.85577	16.87062
4	0.87776	7.97959
5	0.03256	0.29601
6	0.01922	0.17473
7	0.00329	0.02989
8	0.00143	0.01304
9	0.00104	0.00948
10	0.00003	0.00030
11	0.00001	0.00006

Table 3.17 Regression coefficients for PCR models of compressive strength of concrete with fly ash

	Regression Coefficients					
	28 days compressive strength		56 days compressive strength		91 days compressive strength	
	Linear model	Pure Quadratic model	Linear model	Pure Quadratic model	Linear model	Pure Quadratic model
Intercept	62.757182	54.356914	77.004202	67.603745	79.081669	70.837919
w/cm	-70.019715	-37.295301	-70.760091	-36.969041	-60.872758	-31.773608
fa/cm	-13.630350	-6.260579	-14.175369	-6.713877	-12.437221	-5.906859
$ca-I/cm$	-0.075884	-0.079925	0.150268	0.055090	0.024903	-0.009047
$ca-II/cm$	1.870134	0.684730	2.277816	0.977095	1.334803	0.509323
$ca-III/cm$	-0.752456	-0.461259	-1.032561	-0.586507	-0.664393	-0.382741
cm	0.055509	0.051871	0.037307	0.034707	0.032108	0.029710
$(w/cm)^2$		-40.850094		-40.374259		-34.672111
$(fa/cm)^2$		-2.732770		-2.929584		-2.573572
$(ca-I/cm)^2$		-0.185962		-0.086237		-0.096615
$(ca-II/cm)^2$		0.339992		0.4863089		0.257236
$(ca-III/cm)^2$		-0.644551		-0.747891		-0.516001

Table 3.18 Mean square error for validation set using PCR models for concrete with fly ash

Name of the model	MSE		
	For 28 days compressive strength	For 56 days compressive strength	For 91 days compressive strength
Linear PCR model	0.42	1.37	0.48
Pure Quadratic PCR model	0.40	1.39	0.46

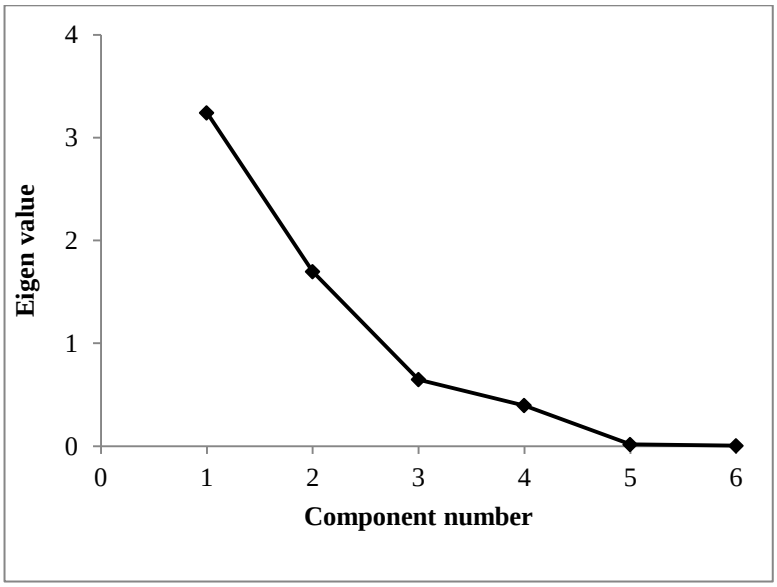

Figure 3.1 Scree plot for linear model for concrete without fly ash

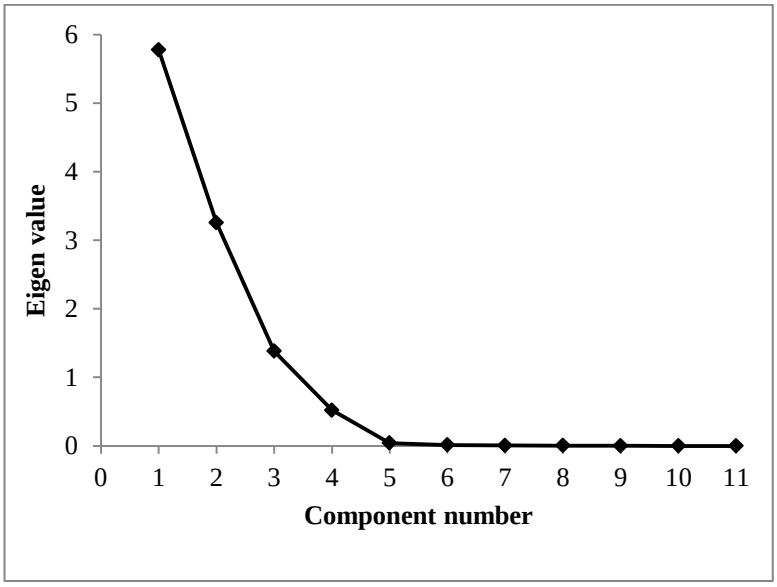

Figure 3.2 Scree plot for pure quadratic model for concrete without fly ash

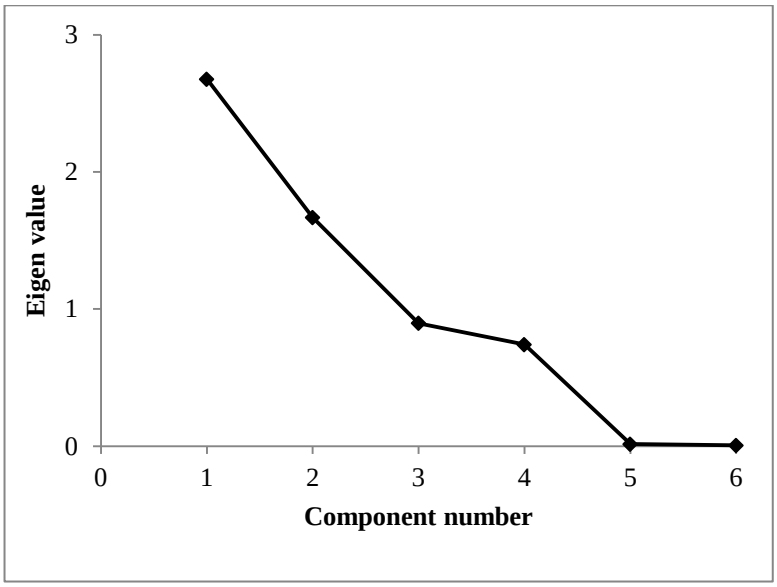

Figure 3.3 Scree plot for linear model for concrete with fly ash

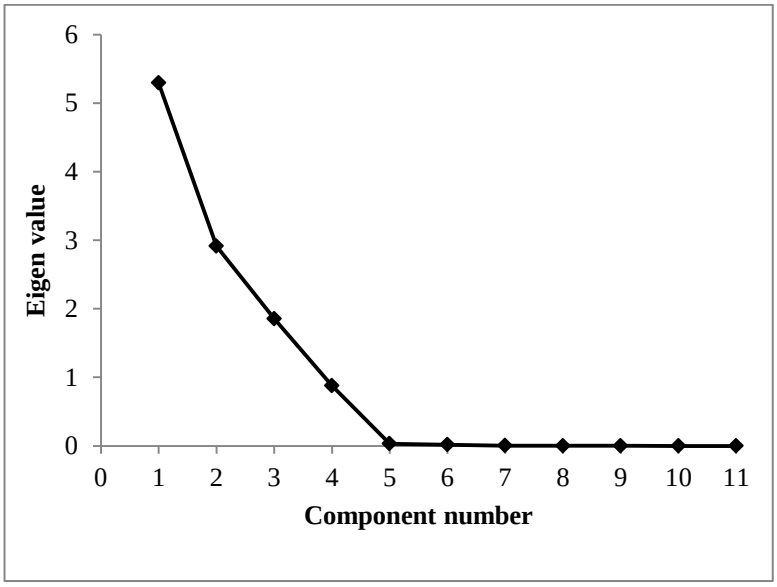

Figure 3.4 Scree plot for pure quadratic model for concrete with fly ash

CHAPTER 4

RELIABILITY BASED SINGLE-OBJECTIVE DESIGN OPTIMIZATION OF CONCRETE MIX PARAMETERS

==========

4.0 GENERAL

This chapter presents the reliability based optimal designs of concrete mix proportions for a desired compressive strength considering different modeling techniques, replacement of 15% cement by fly ash, variation in reliability levels and three curing ages. The performance of concrete compressive strength prediction models is evaluated to identify the best model. A comparison of RBDO results and safety factor based DDO results has been presented. Variation in concrete mix parameters with target compressive strength requirements and reliability level has been studied. A comparison of optimal results for concrete without or with fly ash has been presented.

4.1 FORMULATION OF RBDO MODEL FOR CONCRETE MIX PARAMETERS

The RBDO model for concrete mix parameters is formulated with cost of concrete as objective function. This objective is minimized satisfying a ratio constraint, an absolute volume constraint, boundary constraints on input variables and a reliability constraint on compressive strength requirement. The input variables $w, fa, ca-I, ca-II, ca-III$ and b have been considered as random variables that follow normal distribution with their respective means and standard deviations listed in Table 4.1 and 4.2. Here, the input variable b represents the binder content. This component is cement content c for concrete without fly ash and is cementitious content cm for concrete with fly ash. As described in chapter-3, cm is a mixture consisting of 85 percent cement content and 15 percent fly ash. The design variables for the proposed RBDO problem have been taken as the mean values of water content, fine aggregate content, coarse

aggregate contents and binder content denoted as μ_w, μ_{fa}, μ_{ca-I}, μ_{ca-II}, μ_{ca-III} and μ_b, respectively.

The RBDO problem formulated for concrete mix cost optimization is given below:

$$\left.\begin{array}{rl} Minimize_{\mu_w,\, \mu_{fa},\, \mu_{ca-I},\mu_{ca-II},\mu_{ca-III},\mu_b} & cost\,(fa, ca-I, ca-II, ca-III, b) \\ Subject\ to: & \mathrm{Prob}\big(cst_t(\mathrm{w}, fa, ca-I, ca-II, ca-III, b) \geq f_{c,t}\big) \geq R \\ & 0.42 \leq {}^{w}/_{b} \leq 0.55 \\ & v = 1.00 \\ & w_l \leq w \leq w_u \\ & fa_l \leq fa \leq fa_u \\ & ca-I_l \leq ca-I \leq ca-I_u \\ & ca-II_l \leq ca-II \leq ca-II_u \\ & ca-III_l \leq ca-III \leq ca-III_u \\ & b_l \leq b \leq b_u \end{array}\right\} \quad (4.1)$$

where,

$cost$ - Cost of concrete per m^3. In this study, no cost is associated with the water content and cost of concrete is a linear function of its ingredients. The cost of various ingredients of concrete per kg is given in *Appendix A.*

Hence, for concrete without fly ash cost of concrete is given by the following equation:

$$cost = 0.500 * fa + 0.550 * ca-I + 0.570 * ca-II + 0.700 * ca-III + 5.000 * c \quad (4.2)$$

Cost of concrete with 15% replacement of cement by fly ash is given by:

$$cost = 0.500 * fa + 0.550 * ca-I + 0.570 * ca-II + 0.700 * ca-III + 4.314 * cm \quad (4.3)$$

cst_t - Compressive strength of concrete for a given curing age t; (t = 28, 56, 91 days)

$f_{c,t}$ - Target compressive strength of concrete for a given curing age t

$\mathrm{Prob}(.)$ - Probability of constraint satisfaction

R - Target reliability level

w/b - Water-binder content ratio

v - Absolute volume of components of concrete. Relations for determining absolute volume of concrete without and with fly ash are given in equations (4.4) and (4.5), respectively.

For concrete without fly ash:

$$v = \left(w + \frac{fa}{\mathrm{G}_{fa}} + \frac{ca-I}{\mathrm{G}_{ca-I}} + \frac{ca-II}{\mathrm{G}_{ca-II}} + \frac{ca-III}{\mathrm{G}_{ca-III}} + \frac{c}{\mathrm{G}_c}\right) * 0.001 + 0.02 \quad (4.4)$$

For concrete with 15% replacement of cement by fly ash:

$$v = \left(w + \frac{fa}{\mathrm{G}_{fa}} + \frac{ca-I}{\mathrm{G}_{ca-I}} + \frac{ca-II}{\mathrm{G}_{ca-II}} + \frac{ca-III}{\mathrm{G}_{ca-III}} + \frac{0.85 * cm}{\mathrm{G}_{c}} + \frac{0.15 * cm}{\mathrm{G}_{FA}} \right) * 0.001 + 0.02 \qquad (4.5)$$

G_{fa} , G_{ca-I}, G_{ca-II}, G_{ca-III}, G_c and G_{FA} are the specific gravities of w, fa, $ca-I$, $ca-II$, $ca-III$, c and fly ash (FA), respectively

w_l, fa_l, $ca-I_l$, $ca-II_l$, $ca-III_l$ and b_l are the lower bounds for w, fa, $ca-I$, $ca-II$, $ca-III$ and b, respectively

w_u, fa_u, $ca-I_u$, $ca-II_u$, $ca-III_u$ and b_u are the upper bounds for w, fa, $ca-I$, $ca-II$, $ca-III$ and b, respectively

The first constraint in (4.1) is the reliability constraint on compressive strength of concrete which ensures that cst_t is more than a specified value of compressive strength $f_{c,t}$ with a target reliability R. The second constraint is a deterministic constraint which ensures that w/b ratio lies between 0.42 and 0.55, whereas, the third constraint is an absolute volume equation which represents a condition that the total volume of components of concrete should be equal to 1 m^3. In the equations (4.4) and (4.5) for volume of concrete, 0.02 signifies the percentage of air content present in concrete mix. Last six constraints are boundary constraints for design variables. The specific gravities, lower bounds and upper bounds for the design variables are given in Tables 4.1 and 4.2.

Using SORA method, RBDO problem formulated in (4.1) is replaced by deterministic optimization problem given in (4.6) with definition of shift factors provided in (4.7).

$$\left.\begin{array}{c} \underset{\mu_w, \mu_{fa}, \mu_{ca-I}, \mu_{ca-II}, \mu_{ca-III}, \mu_b}{Minimize} \quad cost\,(fa, ca-I, ca-II, ca-III, b) \\ Subject\ to: \quad cst_t\left(\mu_w - s_w^{(k)}, \mu_{fa} - s_{fa}^{(k)}, \mu_{ca-I} - s_{ca-I}^{(k)}, \mu_{ca-II} - s_{ca-II}^{(k)}, \mu_{ca-III} - s_{ca-III}^{(k)}, \mu_b - s_b^{(k)}\right) \geq f_{c,t} \\ 0.42 \leq {}^{w}/_{b} \leq 0.55 \\ v = 1.00 \\ w_l \leq w \leq w_u \\ fa_l \leq fa \leq fa_u \\ ca-I_l \leq ca-I \leq ca-I_u \\ ca-II_l \leq ca-II \leq ca-II_u \\ ca-III_l \leq ca-III \leq ca-III_u \\ b_l \leq b \leq b_u \end{array}\right\} \qquad (4.6)$$

where k denotes the cycle number and $s_w, s_{fa}, s_{ca-I}, s_{ca-II}, s_{ca-III}, s_b$ are called shift factors described in (4.7).

$$\begin{bmatrix} s_w^{(k)} \\ s_{fa}^{(k)} \\ s_{ca-I}^{(k)} \\ s_{ca-II}^{(k)} \\ s_{ca-III}^{(k)} \\ s_b^{(k)} \end{bmatrix} = \begin{cases} \mathbf{0}, & k = 1 \\ \begin{bmatrix} \mu_{\boldsymbol{w}}^{(k-1)} - w_{\text{MPP}}^{(k-1)} \\ \mu_{fa}^{(k-1)} - fa_{\text{MPP}}^{(k-1)} \\ \mu_{ca-I}^{(k-1)} - ca - I_{\text{MPP}}^{(k-1)} \\ \mu_{ca-II}^{(k-1)} - ca - II_{\text{MPP}}^{(k-1)} \\ \mu_{ca-III}^{(k-1)} - ca - III_{\text{MPP}}^{(k-1)} \\ \mu_b^{(k-1)} - b_{\text{MPP}}^{(k-1)} \end{bmatrix}, & k \geq 2 \end{cases} \tag{4.7}$$

Here, $(w_{\text{MPP}}, fa_{\text{MPP}}, ca - I_{\text{MPP}},\ ca - II_{\text{MPP}}, ca - III_{\text{MPP}}, b_{\text{MPP}})$ denotes the inverse Most Probable Point (MPP) of failure of compressive strength constraint corresponding to the given reliability level R at deterministic optimal solution$(\mu_w, \mu_{fa}, \mu_{ca-I}, \mu_{ca-II}, \mu_{ca-III}, \mu_b)$. The deterministic optimization problem in each cycle is updated on the basis of MPP information obtained from the previous cycle. The above procedure is repeated cycle by cycle until the $cost$ function converges and the reliability requirement for compressive strength constraint is achieved.

4.2 FORMULATION OF SAFETY FACTOR BASED DDO MODEL FOR CONCRETE MIX PARAMETERS

In deterministic design procedures, safety margin is set before the optimization process. As per *IS 10262* (2009), for a specified target compressive strength of $f_{c,t}$, the concrete mix should be proportioned for an average compressive strength not less than $(f_{c,t} + 1.65s)$, so that, no more than 5% of the results will fall below $f_{c,t}$. Here, s denotes the assumed standard deviation of the compressive strength data, which is dependent upon the quality control expected at the site of construction. So, in DDO problem based on safety factor approach, probabilistic constraint given in (4.1) is replaced by the deterministic constraint given below:

$$cst_{\text{t}}(\text{w}, fa, ca - I, ca - II, ca - III, b) \geq f_{c,t} + 1.65\text{s} \tag{4.8}$$

Also, the design variables w, fa, $ca - I$, $ca - II$, $ca - III$ and b are taken as deterministic design variables.

4.3 RESULTS AND DISCUSSION

RBDO models based on various compressive strength models developed using OLSR, TRR, GRR and PCR techniques in chapter 3 have been solved by SORA method. SORA method has been implemented using Altair Hyperstudy 10.0. Optimizations have been performed for concrete without fly ash and for concrete with 15%

replacement of cement by fly ash by varying the parameters of curing age, reliability level and target compressive strength. The variation in parameters is listed in Table 4.3. The value of target reliability R is chosen by the decision maker based upon the importance of the structure where concrete is to be used. This value is taken as 0.90 for ordinary structures, approximately 0.95 for multi-storeyed buildings, residential complexes *etc*. and around 0.99 for important structures like hospitals, water towers and tanks, power houses, schools, cinema halls *etc*. So, RBDO problem has been considered for three target reliability levels of 0.90, 0.95 and 0.99. The optimizations have been performed for target compressive strength ranging from 25 to 55 MPa as this represents a fairly representative group covering all the ranges of practical use of concrete. The minimum value has been taken as 25 MPa for 28 days compressive strength and 30 MPa for 56 days and 91 days compressive strength. However, QOLSR models failed to give any optimal solution for 28 days and 91 days compressive strength for concrete with fly ash. The optimal mix proportions obtained in all the remaining cases are presented in Table 4.4-4.44.

Safety factor based DDO model has been solved only for 28 days compressive strength using sequential quadratic programming method. As per *IS 10262* (2009), assumed standard deviations for different grades of concrete are listed in Table 4.45. It can be noted from Table 4.45 that the value of s is 4 MPa for target compressive strength of 25 MPa and this value is 5 MPa for target compressive strength $\geq$ 30 MPa. As such, the safety margin is taken 6.60 MPa for target compressive strength of 25 MPa and 8.25 MPa in all the remaining cases.

The results of safety factor based deterministic design optimization are summarized in Tables 4.46-4.59. Reliability analysis using mean value approximation method is carried out at DDO optimal designs and computed reliabilities are also reported in Tables 4.46-4.59.

4.3.1 Discussion of results for concrete without fly ash

In this section, it is intended to study the influence of modeling technique and reliability level on optimal concrete mix proportions. Also, variation of parameters like cement content, water-cement ratio and aggregate-cement content ratio has been studied. It can be seen from Tables 4.11, 4.13 and 4.17 that for 56 days curing age and reliability levels of 0.90, 0.95 and 0.99, predicted values of $st56$ using QTRR model, QOLSR

model and LOLSR model go as high as 79.21 MPa, 82.54 MPa and 71.35 MPa, respectively. The predicted values obtained are much beyond the range of experimentally generated data used for analysis. This observation demonstrates the inadequacy of these three 56 days compressive strength models. So, results obtained using these three models have not been considered in remaining study.

(a) Comparison of compressive strength models

Figures 4.1(a)-(c), 4.2(a)-(c) and 4.3(a)-(c) show the variation of cost with target compressive strength considering the parameters of curing age, reliability level and modeling technique.

It can be seen from Figures 4.1(a)-(c) that for 28 days curing age and for reliability levels of 0.90, 0.95 and 0.99, the optimal cost is the least for QTRR/QOLSR model. On the other hand, both the PCR models give highest optimal cost for a given target compressive strength. On observing the figures for R = 0.90 and 0.95, it is noted that the curves for QGRR model, LGRR model and LTRR/LOLSR model more or less overlap each other. For R = 0.99, all the curves except the curves for PCR models have nearly same optimal cost for a given target strength. Curves corresponding to LGRR model and LTRR/LOLSR model are overlapping and lie slightly above the curve for QTRR/QOLSR model. Thus, it can be said that the QTRR/QOLSR model offers best cost effective concrete mix designs for curing age of 28 days.

Figures 4.2(a)-(c) reveal that for 56 days curing age and reliability level of 0.90, 0.95 and 0.99, curves obtained for all the five models are very close to each other. Figure 4.2(a) illustrates that the most cost effective designs are obtained with QGRR model, LGRR model and LTRR model for R = 0.90. Similarly, it can be noted from Tables 4.2(b) and 4.2(c) that for R = 0.95 and 0.99, best performance from the view point of cost effectiveness is given by LGRR model, LPCR model and QGRR model.

Figures 4.3(a) and 4.3(b) demonstrate that for 91 days curing age and R = 0.90 and 0.95, QGRR model, LTRR/LOLSR model and LGRR model yielded best cost effective optimal designs. Figure 4.3(c) shows that for R = 0.99, all the three linear models perform better than quadratic models.

Thus, it is seen that QTRR/QOLSR model performs best for 28 days concrete compressive strength, both the GRR models perform better than other models for 56

days concrete compressive strength and LGRR give better results than other models for 91 days concrete compressive strength.

(b) Effect of reliability level on optimal cost

The variation of optimal cost with target compressive strength and reliability level for different compressive strength models has been demonstrated in Figures 4.4(a)-(f), 4.5(a)-(e) and 4.6(a)-(g). It can be seen from the figures that rise of optimal cost with reliability level is not uniform. To raise reliability level from 0.95 to 0.99 is costlier than to raise it from 0.90 to 0.95 which clearly indicates that the increase in cost is much more at higher reliability levels. The percentage increase in cost as reliability level is raised from 0.90 to 0.95 and from 0.95 to 0.99, for each curing age and for each compressive strength model is listed in Tables 4.60-4.62. This observation suggests that optimal cost is not linearly related to the reliability. So, there is a need to study the tradeoff between optimal cost and reliability to establish a relationship between these two factors. The next chapter of the present work is devoted to fulfill this aim by converting the single objective concrete mix design problem into multi-objective by taking reliability as the second objective, rather than only a constraint.

(c) Comparison of RBDO approach with safety factor based DDO approach

Results obtained by safety factor based DDO approach for 28 days curing age has also been plotted in Figure 4.4(a)-(f) to have a comparison between the two approaches. It can be noted from the figure that optimal costs for safety factor based DDO designs are less than those obtained for RBDO designs in each corresponding case and for each reliability level.

In particular, for reliability level of 0.95 for which safety factor based DDO designs are obtained, comparison shows that optimal costs achieved for RBDO designs are 2.18% to 9.48% more than the optimal costs obtained using the safety factor based designs. However, Tables 4.46-4.51 reveal that in safety factor based DDO results, optimal designs do not meet the reliability requirement of 0.95 in all the cases although reliability improves as target compressive strength increases.

Thus, it can be concluded that using DDO approach, required reliability levels cannot be maintained. The disadvantage of safety factor based DDO approach is that recommended safety margins are not always suitable for the given system. But, as already mentioned, RBDO process modulates the safety margins within the

optimization process taking into account uncertainty effect for each variable. Hence, the resulting designs obtained by RBDO approach are the best solution relative to the designs obtained by safety factor based DDO approach as the objective is to provide best compromise between cost and safety.

(d) Variation of w/c ratio and cement content with compressive strength and reliability level

It can be noted from Tables 4.4-4.24 and Figures 4.7(a)-(f), 4.10(a)-(e) and 4.13(a)-(g) that w/c ratio decreases as the target strength increases for a given reliability in all the cases except for two models for 56 days compressive strength. The two models, which are exception to the case are QGRR model and LPCR model for R = 0.99. Thus, there are only two cases in all where this well established trend of concrete mix design process that lower the w/c ratio greater is the compressive strength of concrete and vice-versa has not been followed indicating their non-suitability for the case. It is also observed that the decrease in of w/c ratio with compressive strength follows a parabolic path in most of the cases. This indicates that in lower strength regions the fall is not as sharp as in high strength regions for a given curing age.

Moreover, Figures 4.7(a)-(f), 4.10(a)-(e) and 4.13(a)-(g) reveal that for a given target strength, w/c ratio falls as reliability level increases in each case. This is due to the reason that to maintain higher reliability levels, higher safety margins are assumed by the RBDO process. So, concrete mixes are designed for higher strengths which result in low w/c ratio.

Figures 4.8(a)-(f), 4.11(a)-(e) and 4.14(a)-(g) demonstrate the variation of cement content with target strength and reliability level in each case for concrete without fly ash. Cement content c increases according to target strength and reliability level with only one exception. The case is for 91 days QTRR compressive strength model with R = 0.99, where cement content falls from 473.97 kg/m^3 to 470.48 kg/m^3 as target $st91$ increases from 45 MPa to 50 MPa (Table 4.19), which clearly makes it an exception to the case, thus proving its non-suitability. Further, rise of cement content with compressive strength follows a linear path for 28 days curing age and an upwards open parabolic path for 56 days and 91 days strength for all the models except for QTRR and LPCR models with 28 days and 91 days curing age.

Thus, it can be said that, in most of the cases w/c ratio falls and cement content increases with rise in target compressive strength and reliability level. These observations are as per already proven trends for concrete mix design. It further strengthens the idea that the formulated RBDO model behaves in accordance with the existing standards and hence is of great practical importance.

(e) Variation of aggregate ratios with compressive strength and reliability level

It can be seen from Figures 4.9(a)-(f), 4.12(a)-(e) and 4.15(a)-(g) that fa/c ratio falls with increase in compressive strength requirement for each curing age except for few exceptions. Also, the rate of decrease is less than that observed for w/c ratio. This indicates that dependency of compressive strength of concrete on fa/c ratio is lesser than that for w/c ratio. This observation is in accordance with correlation of these two ratios with compressive strengths for different curing ages. Also, the figures reveal that for a given target strength, fa/c ratio falls as reliability level increases in each case.

Further, the Figures 4.9(a)-(f), 4.12(a)-(e) and 4.15(a)-(g) show the variation of total coarse aggregate content to cement content ratio (ca/c) ratio with compressive strength and reliability levels for different curing ages as well. Here, ca consists of all the three coarse aggregate components, *i.e.*, $ca-I$, $ca-II$ and $ca-III$. It can be seen from the figures that variation of ca/c ratio does not follow any particular trend with rise in compressive strength in all the cases. Also, it can be observed from the figures that ca/c ratio falls as reliability level is raised for a given curing age except for the results obtained using LPCR model for each curing age and QTRR model for 91 days curing age. These results for aggregate ratios indicate that aggregate-cement ratio has to be decreased to maintain higher reliability levels.

Further, Percentage proportion of three types of coarse aggregates, namely, $ca-I$, $ca-II$ and $ca-III$ with respect to total coarse aggregate content is calculated in each case. The range of variation in percentage proportion is given in Tables 4.63-4.65 for each curing age. It was observed that in most of the cases, the percentage of $ca-I$, $ca-II$ and $ca-III$ is approximately 31%, 47% and 22%, respectively. However, different compositions are obtained for high compressive strength requirements.

(f) Variation of predicted compressive strength with target compressive strength

Figure 4.16 shows the variation of predicted 28 days compressive strength with target 28 days compressive strength for R = 0.95 for different prediction models. Also, the observations from actual experimental data set generated by Kumar (2002) have been plotted as the experimental data has been generated for 95% reliability. It can be seen from the Figure that curves for both PCR model are nearer to experimental data curve than the remaining models. It is indicated that safety margins taken by GRR and TRR/OLSR models are much higher than that for PCR models. Very high safety margins may result in over-conservative designs for concrete mix proportions which is not a desirable situation. Also, Tables 4.46-4.51 show that reliabilities for PCR models based DDO results are higher than that for remaining models except for target $st28$ of 25 MPa. So, it can be concluded that although PCR models are not cost effective for 28 days curing age case, but the optimal designs given by them assume realistic safety margins. So, it may not be judicious to reject PCR models solely on the basis of cost.

4.3.2 Discussion of results for concrete with 15% replacement of cement by fly ash

In this section, Tables 4.25-4.44 have been examined to study the influence of various factors on the optimization results obtained for concrete with 15% replacement of cement by fly ash. It can be seen from Tables 4.33 and 4.40 that QTRR model based RBDO model converged only for target compressive strengths of 25 MPa with R = 0.90, 0.95 and for target compressive strengths of 30 MPa with R = 0.90 for 56 and 91 days curing age. Also, in each of these cases predicted values of $st56$ and $st91$ are very high. Also, Tables 4.35 and 4.37 show that for 56 days curing age and for each reliability level, predicted values of $st56$ vary from 59.1 MPa to 73.89 MPa for QOLSR model and from 62.69 MPa to 72.01 MPa for LTRR/LOLSR model. The predicted values obtained are much beyond the range of experimentally generated data used for analysis. These observations establish the inadequacy of the above discussed compressive strength models. Thus, results obtained by these models will not be considered in remaining study.

(a) Comparison of compressive strength models

Figures 4.17(a)-(c), 4.18(a)-(c) and 4.19(a)-(c) show the variation of the optimal cost with target compressive strength for different curing ages and reliability levels.

Figure 4.17(a) depicts that QTRR model gives much higher optimal costs than remaining models for reliability level of 0.90. A careful investigation of curves divulges that QGRR model gives best results for small values of target 28 days strength followed by LTRR and LPCR models. However, as target strength increases QGRR curves goes above the curves for LTRR and LPCR models. Also, it can be noted from the figure that LOLSR based curve goes downwards as target $st28$ increases from 25 MPa to 30 MPa. However, this observation is contrary to the theory according to which cost is expected to rise with the compressive strength.

Figure 4.17(b) demonstrates that for reliability level of 0.95, QTRR model again shows worst performance and QGRR model gives best results. Curves for remaining models are crossing each other. Both PCR models give higher costs than all the models except QTRR model upto target strength of around 34 MPa. Beyond this value of target strength, QPCR model is the best followed by LPCR model. Also, both PCR models give the optimal solutions upto 40 MPa target strength while remaining models converged only upto 35 MPa target strength. OLSR based curve shows downwards trend as target $st28$ increases from 25 MPa to 30 MPa indicating the non-applicability of the LOLSR model. Figure 4.17(c) depicts that for reliability level of 0.99, LPCR model covers a wider range with lesser cost than other models. QTRR model based RBDO yields only one optimal point and that too with highest optimal cost. Curves corresponding to remaining models are intersecting each other and therefore, cannot be categorized on the basis of cost.

It can be seen from Figure 4.18(a) that for reliability level of 0.90, performance of all the 56 days compressive strength models is comparable. Curves for both the PCR models more or less overlap each other. Both PCR models and LGRR model give almost same optimal solutions upto target $st56$ of 33 MPa and the optimal costs are less than that for QGRR model in this range. Both PCR models assign higher optimal costs than both GRR models from 33 MPa to 40 MPa. Beyond 40 MPa, PCR models provide lesser optimal costs than GRR models. Figure 4.18(b) reveals that optimal cost falls as target $st56$ rises from 35 MPa to 40 MPa in case of QPCR model based results. However, as mentioned earlier this is not desirable. LGRR model performs better than LPCR model beyond target $st56$ of 30 MPa. Figure 4.18(c) shows that QPCR model performs better than LPCR model and LGRR model performs better than QGRR model for curing age 56 days and reliability level of 0.99. Comparison of

performance of QPCR model and LGRR model depicts that below target $st56$ of 27 MPa and above 36 MPa, QPCR model is better while performance of LGRR model is the best between 27 MPa and 36 MPa.

Figures 4.19(a) and 4.19(b) demonstrate that for curing age of 91 days and reliability levels 0.90 and 0.95, QGRR model yields the best optimal results upto target strength of 45 MPa. Both PCR models show best results beyond 45 MPa. Also, curves for both PCR models cover each other completely. All the models give same optimal cost for target $st91$ of 25 MPa. Also, for target strength of 45 MPa, the optimal costs obtained for all the models are nearly equal. Figure 4.19(c) shows that for curing age of 91 days and reliability level of 0.99, curve for QPCR model has negative slope for target $st91$ lying between 35 MPa and 40 MPa which is not in accordance with the theory as already mentioned. Similar trend is noticed for linear PCR model for target $st91$ lying between 40 MPa and 45 MPa. Out of remaining three models QGRR model performs best followed by LTRR/LOLSR and LGRR models. Both LTRR/LOLSR and LGRR models give nearly same optimal solutions.

It was seen that LPCR, LGRR and QGRR models perform fairly better than other models for curing ages of 28 days, 56 days and 91 days, respectively.

(b) Effect of reliability level on optimal cost

Variation of optimal cost with target compressive strength and reliability level has been demonstrated in Figures 4.20(a)-(g), 4.21(a)-(d) and 4.22(a)-(e). Percentage rise in cost as reliability level is raised from 0.90 to 0.95 and from 0.95 to 0.99 for each curing age and each compressive strength model is listed in Tables 4.66-4.68. It can be noted from the figures that the results obtained are similar to the results obtained in case of concrete without fly ash in the sense that relationship between optimal cost and reliability is not linear.

However, in some cases unacceptable observations are made. Figure 4.20(b) shows that optimal cost for R = 0.95 is more than the optimal cost for R = 0.99 for 28 days target strength of 30 MPa for QTRR model based RBDO results. Similar situation has been encountered in 28 days curing age RBDO results based on LPCR model shown in Figure 4.20(f) where optimal cost for target $st28$ of 25 MPa for R = 0.99 is less than the optimal cost for R = 0.95.

Figs. 4.21(a) and 4.21(c) reveal that for 56 days curing age, QGRR model and LGRR model based results exhibit similar pattern where optimal cost rises with reliability level for a given target strength. However, the gap between the three curves for different reliability levels is very small upto target $st56$ of 35 MPa. The gap between 0.90 and 0.95 reliability curves widens beyond 40 MPa and gap between 0.95 and 0.99 reliability curves widens beyond 35 MPa. Also, there is a sharp rise in optimal costs beyond the two stages mentioned above. Figure 4.21(b) shows the optimal cost for target 56 days strength of 40 MPa decreases as reliability level is raised from 0.90 to 0.95 for QPCR model based RBDO results. It can be seen from Figs. 4.22(a), 4.22(c) and 4.22(d) that for 91 days curing age, QGRR model, LGRR model and LTRR/LOLSR model based results follow similar pattern where optimal cost rises with reliability level for a given target strength and the gap between the three curves for different reliability levels is very small suggesting that higher reliability levels can be assured by a little rise in the cost.

(c) Comparison of RBDO approach with safety factor based DDO approach

Results obtained by safety factor based DDO approach for 28 days curing age has also been plotted in Figure 4.32 to compare the two approaches. It can be noted from Figures 4.20(a), 4.20(b), 4.20(d) and 4.20(g) that optimal costs for safety factor based DDO designs for QGRR model, QTRR model, LGRR model and LOLSR model are less than that for RBDO designs in each corresponding case and for each reliability level. In particular, for reliability level of 0.95 for which safety factor based DDO designs are obtained, comparison shows that optimal costs achieved for RBDO designs are 0.69% to 5.13% more than optimal costs for safety factor based designs obtained in these cases. Also, Tables 4.52, 4.53, 4.56, 4.59 reveal that in safety factor based DDO results, optimal designs do not meet the reliability requirement of 0.95 in any of these cases.

Figure 4.20(c) divulges that safety factor based DDO based on 28 days QPCR model give higher optimal cost than that for RBDO with R = 0.90 and 0.95 for target $st28$ of 35 MPa and 40 MPa. This observation can be attributed to the fact that reliabilities of deterministic optimal designs at these points are greater than 0.95 (Table 4.54). Figure 4.20(e) reveals that safety factor based DDO curve based on 28 days LTRR model goes above the RBDO curve for R = 0.90 for target $st28$ of 33 MPa and above indicating

that deterministic concrete mix designs are costlier than reliability based designs for R = 0.90 in this region. However, reliabilities of deterministic optimal designs for target $st28$ of 35 MPa and 40 MPa are 0.894 and 0.921 (Table 4.57), respectively. Thus, higher cost of DDO design is justified for target strength of 40 MPa. But, for target strength of 35 MPa RBDO solution is better. Figure 4.20(f) depicts that for LPCR model, safety factor based DDO curve gives least cost upto 33 MPa. This curve goes above the RBDO curves for R = 0.90 and 0.95 for target $st28$ above 33 MPa. Finally at $st28$ = 40 MPa, DDO gives optimal cost slightly less than that for reliability based design with R = 0.95. However, Table 4.58 shows that reliabilities of DDO designs are above 0.95 for target 28 days compressive strengths of 30 MPa, 35 MPa and 40 MPa suggesting that DDO gives better solutions for $st28$ lying between 30 MPa and 40 MPa.

(d) Variation of w/cm ratio and cementitious content with compressive strength and reliability level

It can be noted from Tables 4.25-4.44 and Figures 4.23(a)-(g), 4.26(a)-(d) and 4.29(a)-(e) that water-cementitious content ratio falls as target strength increases for a given reliability in all the cases. Also, for a given target strength, w/cm ratio falls as reliability level increases in each case except for two cases. The first case is that from QPCR model based results for 56 days curing age with target strength of 25 MPa where w/cm ratio rises from 0.459 to 0.468 as reliability level is raised from 0.95 to 0.99 (Table 4.34). The second case is that from LPCR model based results for 91 days curing age with target strength of 40 MPa where w/cm ratio rises from 0.525 to 0.550 as reliability level is raised from 0.95 to 0.99 (Table 4.44). However, it is seen that fall of w/cm ratio is not as sharp as is in the case of w/c ratio for concrete without fly ash.

Figures 4.24(a)-(g), 4.27(a)-(d) and 4.30(a)-(e) reveal that cementitious content rises as target compressive strength and reliability level increases for a given curing age in almost every case. The cases where this trend is broken are that of LPCR model for each curing age, QPCR model for 56 and 91 days curing age. In the remaining cases, it is observed that gain in cm content with target strength is very low upto a certain value of target strength depending upon curing age and reliability level and beyond that level there is a sudden rise in value of cm content. Also, it is observed that upto the limit of compressive strength mentioned above, reliability level has no significant effect on cm

content values for 56 and 91 days curing age. It indicates that addition of fly ash as a replacement of cement produces concrete mix designs having high reliabilities for 56 and 91 days curing age.

(e) Variation of aggregate ratios with compressive strength and reliability level

It can be noted from Figures 4.25(a)-(g), 4.28(a)-(d) and 4.31(a)-(e) that fa/cm ratio falls as 28 days compressive strength requirement increases except for both TRR models with R = 0.90 and LOLSR model for each reliability level. Figures 4.40 and 4.43 reveal that for 56 and 91 days curing age fa/cm falls as compressive strength requirement increases for a given reliability level. However, no particular pattern is observed for LGRR models in case of 56 and 91 days curing age. It is also observed that curves corresponding to all the three levels of reliability nearly overlap each other in most of the cases indicating that fa/cm ratio is not much affected by reliability level in case of concrete with fly ash.

Also, Figures 4.25(a)-(g), 4.28(a)-(d) and 4.31(a)-(e) show that ca/cm ratio firstly rises and then falls as target compressive strength increases for a given reliability level in almost every case. Also, reliability level does not seem to have much impact on ca/cm ratio.

Percentage proportion of three types of coarse aggregates, namely, $ca-I$, $ca-II$ and $ca-III$ with respect to total coarse aggregate content is calculated in each case. The range of variation in percentage proportion is given in Tables 4.69-4.71 for each curing age. However, no particular combination of coarse aggregates is found as was found in case of concrete without fly ash.

(f) Variation of predicted compressive strength with target compressive strength

Figure 4.32 shows the variation of predicted 28 days compressive strength with target 28 days compressive strength for R = 0.95 for different prediction models. Also, the observations from actual experimental data set have been plotted as the experimental data has been generated for 95% reliability. It can be seen from the Figure that curves for both PCR models are nearly covering the experimental data curve implying that safety margins assumed by RBDO process for these models are roughly same as margins taken for safety factor based DDO approach. This observation suggests that for

concrete with fly ash safety margins calibrated by Design codes of practice (*IS 456*(2000)) are sufficient to take care of desired reliability level in case of PCR models. The curves corresponding to QTRR model lies much above the experimental data curve indicating that safety margins assumed by this model are exceptionally high. This further strengthens the idea that QTRR model does not behave well for concrete with fly ash and 28 days curing age. Curves for remaining models lie close to each other above PCR curves indicating that safety margins taken by them are slightly greater than that for PCR curves.

4.3.3 Comparison of results for concrete without and with fly ash

The variation in cost of concrete with target compressive strength for best three models for each curing age with or without fly ash has been presented in Figures 4.33(a)-(c), 4.34(a)-(c) and 4.35(a)-(c). It is observed that for a given curing age, reliability level and target strength, 15% replacement of cement by fly ash results in concrete mix designs that are more economical than the corresponding mix designs for concrete without fly ash. Comparison of optimal costs for various curing ages for concrete with or without fly ash shows that concrete without fly ash results in 0.9%-6.4%, 2.0%-7.3% and 3.6%-9.2% rise in optimal cost for 28 days, 56 days and 91 days curing age, respectively.

However, for concrete without fly ash, maximum target strength that can be attained for a given reliability level is greater than or equal to that for concrete with fly ash in all the cases except two cases. The cases are that of 28 days and 91 days curing age with R = 0.99 where LPCR model for concrete with fly ash converged upto 40 MPa and 50 MPa, respectively while models for concrete without fly ash converged upto 35 MPa and 40 MPa, respectively in these cases (Figures 4.35 and 4.41).

4.4 SUMMARY

It is seen that QOLSR model and QTRR model performed poorly in every case for concrete with or without fly ash except for one case. The case is that of concrete without fly ash for 28 days curing age. However, LOLSR and LTRR models produce good results for concrete without fly ash with 28 and 91 days curing age and for concrete with fly ash with 91 days curing age. Both linear and quadratic PCR models are not cost effective for concrete without fly ash although safety margins assumed by

them are moderate. However, these models perform better for concrete with fly ash. Linear compressive strength models developed using GRR technique yield low cost designs of concrete mixes without fly ash for each curing age and that of concrete mixes with fly ash and 56 days curing age. The models that worked well and produced reliable and economical designs of concrete mixes in each and every case are the pure quadratic compressive strength models built up using GRR technique.

Thus, effect of multi-collinearity is evident in performance of pure quadratic OLSR models. However, multi-collinearity does not influence the working of linear OLSR models to that extent. TRR models appear to fail in most of the cases indicating that TRR technique does not provide a good alternative to tackle multi-collinearity. But, PCR and GRR models deal with multi-collinearity in an efficient manner. Further, 15% replacement of cement by fly ash results in concrete mixes which are cost effective in comparison to the concrete mixes obtained without fly ash.

Table 4.1 Descriptive statistics for concrete without fly ash

Variable	Minimum (kg/m^3)	Maximum (kg/m^3)	Mean (kg/m^3)	Standard deviation (kg/m^3)	Specific gravity
w	179.90	229.95	202.45	12.67	1.00
fa	416.93	642.18	535.64	57.29	2.54
$ca-I$	0.00	802.93	478.49	316.32	2.68
$ca-II$	343.91	626.03	461.84	91.48	2.68
$ca-III$	0.00	472.80	124.51	199.20	2.60
c	350.00	475.00	424.49	37.32	3.12
$st28$	31.66	54.49	45.80	5.42	-
$st56$	37.18	58.65	51.11	5.03	-
$st91$	43.92	63.07	53.88	4.97	-

Table 4.2 Descriptive statistics for concrete with fly ash

Variable	Minimum (kg/m^3)	Maximum (kg/m^3)	Mean (kg/m^3)	Standard deviation (kg/m^3)	Specific gravity
w	179.78	229.95	204.43	13.42	1.00
fa	416.93	626.85	520.59	58.70	2.54
$ca-I$	0.00	783.85	433.48	321.19	2.68
$ca-II$	343.91	614.25	451.41	88.79	2.68
$ca-III$	0.00	450.68	142.33	205.35	2.60
cm	400.00	475.00	450.93	21.35	3.12 of c 1.99 of fly ash
$st28$	35.23	49.41	41.83	3.72	-
$st56$	40.05	53.58	47.56	3.87	-
$st91$	46.11	58.19	52.75	3.20	-

Table 4.3 Variation in parameters

Parameter	For concrete without fly ash	For concrete with 15% replacement of concrete by fly ash
Curing age	28, 56, 91 days	28, 56, 91 days
Target Reliability	0.90, 0.95, 0.99	0.90, 0.95, 0.99
Target compressive strength	25, 30, 35,40, 45, 50, 55 MPa	25, 30, 35,40, 45, 50, 55 MPa

Table 4.4 Reliability based design optimization results for concrete without fly ash for 28 days curing age using QGRR model

Target Reliability R	Target $st28$ (MPa)	$cost$ $(Rs.)$	Predicted $st28$ (MPa)	w $\left(kg/m^3\right)$	fa $\left(kg/m^3\right)$	$ca-I$ $\left(kg/m^3\right)$	$ca-II$ $\left(kg/m^3\right)$	$ca-III$ $\left(kg/m^3\right)$	c $\left(kg/m^3\right)$	w/c
0.90	25	2768.22	43.56	180.00	575.50	376.08	576.16	274.96	350.55	0.513
	30	2828.73	46.58	180.00	573.46	372.83	573.35	271.76	363.98	0.495
	35	2895.36	49.69	180.00	576.31	367.31	569.90	265.04	378.96	0.475
	40	2943.68	53.23	180.00	642.18	335.24	511.32	275.74	390.75	0.461
	45	3065.08	56.09	180.00	583.45	352.66	560.98	248.83	417.09	0.432
	50	-	-	-	-	-	-	-	-	-
0.95	25	2842.08	47.20	180.00	573.00	372.14	572.73	271.03	366.94	0.491
	30	2900.75	49.91	180.00	575.95	367.16	569.68	264.78	380.16	0.473
	35	2967.69	52.68	180.00	580.10	361.11	566.12	257.27	395.25	0.455
	40	3049.41	55.47	180.00	579.11	355.93	562.15	251.98	413.45	0.435
	45	3134.51	58.54	182.64	628.61	318.07	551.60	223.55	434.87	0.420
	50	-	-	-	-	-	-	-	-	-
0.99	25	2975.18	52.89	180.00	577.96	361.65	565.97	257.74	396.85	0.454
	30	3036.84	55.06	180.00	578.74	357.22	562.89	252.74	410.65	0.438
	35	3108.68	57.27	180.00	578.31	352.52	559.37	247.81	426.67	0.422
	40	-	-	-	-	-	-	-	-	-
	45	-	-	-	-	-	-	-	-	-

Table 4.5 Reliability based design optimization results for concrete without fly ash for 28 days curing age using QTRR/QOLSR model

Target Reliability R	Target $st28$ (MPa)	$cost$ $(Rs.)$	Predicted $st28$ (MPa)	w $\left(kg/m^3\right)$	fa $\left(kg/m^3\right)$	$ca-I$ $\left(kg/m^3\right)$	$ca-II$ $\left(kg/m^3\right)$	$ca-III$ $\left(kg/m^3\right)$	c $\left(kg/m^3\right)$	w/c
0.90	25	2765.82	48.01	180.00	575.21	376.34	576.30	275.33	350.00	0.514
	30	2765.82	48.01	180.00	575.21	376.34	576.30	275.33	350.00	0.514
	35	2804.77	49.57	180.00	574.59	374.47	573.64	273.13	358.67	0.502
	40	2888.50	52.42	180.00	573.13	371.07	567.32	268.54	377.30	0.477
	45	3005.00	55.57	180.00	578.65	367.09	551.66	260.16	403.44	0.446
	50	3105.52	58.30	180.00	521.40	549.16	343.97	326.92	423.58	0.425
0.95	25	2765.82	48.01	180.00	575.21	376.34	576.30	275.33	350.00	0.514
	30	2815.09	49.95	180.00	574.40	373.94	573.06	272.49	360.97	0.499
	35	2890.35	52.44	180.04	571.97	370.32	568.66	268.69	377.69	0.477
	40	2990.80	55.22	180.00	578.13	366.78	555.27	260.12	400.28	0.450
	45	3131.30	57.96	181.37	552.27	388.97	523.27	266.61	431.27	0.421
	50	3311.84	60.38	199.08	417.33	532.12	372.27	331.42	473.26	0.421
0.99	25	2920.86	53.34	180.00	571.35	368.67	567.11	266.92	384.46	0.468
	30	3008.73	55.58	180.00	577.28	362.24	558.14	259.31	404.24	0.445
	35	3110.42	57.83	180.00	416.93	509.36	625.87	197.40	425.38	0.423
	40	-	-	-	-	-	-	-	-	-
	45	-	-	-	-	-	-	-	-	-

Table 4.6 Reliability based design optimization results for concrete without fly ash for 28 days curing age using QPCR model

Target Reliability R	Target $st28$ (MPa)	$cost$ $(Rs.)$	Predicted $st28$ (MPa)	w $\left(kg/m^3\right)$	fa $\left(kg/m^3\right)$	$ca-I$ $\left(kg/m^3\right)$	$ca-II$ $\left(kg/m^3\right)$	$ca-III$ $\left(kg/m^3\right)$	c $\left(kg/m^3\right)$	w/c
0.90	25	2772.89	37.19	180.00	574.19	376.32	576.68	274.73	351.56	0.512
	30	2858.77	40.87	180.00	568.63	372.77	573.79	270.84	370.56	0.486
	35	2954.84	44.66	180.00	559.43	370.18	573.63	265.24	391.78	0.459
	40	3064.95	48.54	180.00	548.14	367.07	573.40	259.81	416.06	0.433
	45	3159.85	52.58	183.63	471.99	388.01	626.03	239.30	437.22	0.420
	50	-	-	-	-	-	-	-	-	-
0.95	25	2838.06	40.01	180.00	570.20	373.53	574.27	271.83	365.98	0.492
	30	2923.86	43.43	180.00	564.06	370.29	572.08	267.60	384.95	0.468
	35	3019.70	46.97	180.00	554.23	368.04	572.77	261.56	406.12	0.443
	40	3157.31	51.03	184.51	539.97	359.37	565.75	253.03	438.01	0.421
	45	3302.00	54.25	199.45	507.89	347.22	560.87	232.82	474.88	0.420
	50	-	-	-	-	-	-	-	-	-
0.99	25	2958.55	44.78	180.00	560.04	369.80	573.17	264.73	392.63	0.458
	30	3042.24	47.81	180.00	550.47	368.36	575.08	258.66	411.11	0.438
	35	3162.16	51.00	185.76	543.09	356.84	561.38	251.95	439.60	0.423
	40	-	-	-	-	-	-	-	-	-
	45	-	-	-	-	-	-	-	-	-

Table 4.7 Reliability based design optimization results for concrete without fly ash for 28 days curing age using LGRR model

Target Reliability R	Target $st28$ (MPa)	$cost$ $(Rs.)$	Predicted $st28$ (MPa)	w $\left(kg/m^3\right)$	fa $\left(kg/m^3\right)$	$ca-I$ $\left(kg/m^3\right)$	$ca-II$ $\left(kg/m^3\right)$	$ca-III$ $\left(kg/m^3\right)$	c $\left(kg/m^3\right)$	w/c
0.90	25	2765.82	42.72	180.00	575.21	376.34	576.30	275.33	350.00	0.514
	30	2813.67	45.06	180.05	573.63	373.70	574.02	272.72	360.65	0.499
	35	2894.22	48.90	180.00	574.67	368.01	570.05	266.20	378.64	0.475
	40	2982.67	52.81	180.00	577.73	360.88	565.49	257.82	398.50	0.452
	45	3077.23	56.78	180.00	586.55	350.70	560.21	245.95	419.92	0.429
	50	-	-	-	-	-	-	-	-	-
0.95	25	2808.29	45.05	180.00	582.89	370.69	565.59	275.38	359.56	0.501
	30	2888.16	48.54	180.00	572.13	369.39	570.52	268.21	377.20	0.477
	35	2967.34	52.16	180.00	577.28	362.16	566.28	259.13	395.07	0.456
	40	3055.29	55.84	180.00	582.75	354.15	561.59	249.33	414.90	0.434
	45	3147.47	59.54	184.42	642.18	294.25	574.83	202.13	439.08	0.420
	50	-	-	-	-	-	-	-	-	-
0.99	25	2946.90	51.27	180.00	576.51	363.94	567.34	261.00	390.48	0.461
	30	3020.08	54.44	180.00	581.64	357.15	563.39	252.38	407.01	0.442
	35	3105.59	57.64	180.00	580.45	351.84	559.28	246.87	426.05	0.422
	40	-	-	-	-	-	-	-	-	-
	45	-	-	-	-	-	-	-	-	-

Table 4.8 Reliability based design optimization results for concrete without fly ash for 28 days curing age using LTRR/LOLSR model

Target Reliability R	Target $st28$ (MPa)	$cost$ $(Rs.)$	Predicted $st28$ (MPa)	w $\left(kg/m^3\right)$	fa $\left(kg/m^3\right)$	$ca-I$ $\left(kg/m^3\right)$	$ca-II$ $\left(kg/m^3\right)$	$ca-III$ $\left(kg/m^3\right)$	c $\left(kg/m^3\right)$	w/c
0.90	25	2765.82	42.84	180.00	575.21	376.34	576.30	275.33	350.00	0.514
	30	2817.18	45.41	180.01	573.66	373.49	573.89	272.49	361.42	0.498
	35	2896.23	49.24	180.00	575.26	367.63	569.96	265.66	379.11	0.475
	40	2950.42	54.12	180.13	642.18	337.70	562.72	220.70	393.67	0.458
	45	3073.34	57.10	180.00	589.14	349.88	560.48	244.47	419.15	0.429
	50	-	-	-	-	-	-	-	-	-
0.95	25	2817.82	45.44	180.00	573.64	373.48	573.87	272.46	361.55	0.498
	30	2890.64	48.97	180.00	574.77	368.22	570.27	266.35	377.85	0.476
	35	2969.24	52.56	180.00	578.44	361.55	566.22	258.21	395.54	0.455
	40	3054.62	56.24	180.00	584.75	353.35	561.68	248.03	414.82	0.434
	45	3122.03	60.10	181.53	642.18	315.19	553.48	215.75	432.22	0.420
	50	-	-	-	-	-	-	-	-	-
0.99	25	2952.23	51.81	180.00	577.49	363.17	567.10	259.94	391.71	0.460
	30	3023.55	54.97	180.00	583.24	356.24	563.28	251.04	407.84	0.441
	35	3107.55	58.15	180.00	582.56	350.82	559.23	245.31	426.57	0.422
	40	-	-	-	-	-	-	-	-	-
	45	-	-	-	-	-	-	-	-	-

Table 4.9 Reliability based design optimization results for concrete without fly ash for 28 days curing age using LPCR model

Target Reliability R	Target $st28$ (MPa)	$cost$ $(Rs.)$	Predicted $st28$ (MPa)	w $\left(kg/m^3\right)$	fa $\left(kg/m^3\right)$	$ca-I$ $\left(kg/m^3\right)$	$ca-II$ $\left(kg/m^3\right)$	$ca-III$ $\left(kg/m^3\right)$	c $\left(kg/m^3\right)$	w/c
0.90	25	2765.82	36.28	180.00	575.21	376.34	576.30	275.33	350.00	0.514
	30	2853.09	39.91	180.10	568.55	372.93	573.84	271.48	369.32	0.488
	35	2959.55	44.04	180.00	559.56	369.31	571.83	266.86	392.78	0.458
	40	2984.82	48.46	180.00	416.93	458.36	624.39	273.28	395.41	0.455
	45	3169.68	52.57	194.31	434.52	384.29	626.03	249.61	441.90	0.440
	50	3291.61	56.91	199.47	416.93	526.63	626.03	88.57	474.93	0.420
0.95	25	2820.83	38.56	180.50	570.76	373.85	574.37	272.59	362.32	0.498
	30	2915.87	42.38	180.00	563.61	370.73	572.45	268.78	383.15	0.470
	35	3020.47	46.33	180.00	551.63	368.27	572.96	263.76	406.18	0.443
	40	3160.67	50.63	185.06	536.92	358.70	564.73	255.70	438.81	0.422
	45	3301.92	54.37	199.27	498.55	348.76	563.62	239.07	474.44	0.420
	50	-	-	-	-	-	-	-	-	-
0.99	25	2936.90	43.18	180.00	561.89	370.00	572.01	267.79	387.79	0.464
	30	3030.90	46.71	180.00	550.25	368.15	573.26	263.06	408.48	0.441
	35	3159.82	50.46	185.39	541.59	357.07	561.11	255.12	438.84	0.422
	40	3191.44	54.27	186.35	416.93	418.80	625.99	253.37	443.69	0.420
	45	-	-	-	-	-	-	-	-	-

Table 4.10 Reliability based design optimization results for concrete without fly ash for 56 days curing age using QGRR model

Target Reliability R	Target $st56$ (MPa)	$cost$ $(Rs.)$	Predicted $st56$ (MPa)	w $\left(kg/m^3\right)$	fa $\left(kg/m^3\right)$	$ca-I$ $\left(kg/m^3\right)$	$ca-II$ $\left(kg/m^3\right)$	$ca-III$ $\left(kg/m^3\right)$	c $\left(kg/m^3\right)$	w/c
0.90	30	2765.82	44.03	180.00	575.21	376.34	576.30	275.33	350.00	0.514
	35	2789.90	44.90	180.30	573.19	375.01	575.34	274.31	355.42	0.507
	40	2890.58	48.30	180.00	565.63	370.63	572.66	271.30	377.52	0.477
	45	2963.63	52.47	180.00	466.25	407.85	611.78	287.55	391.24	0.460
	50	3083.43	56.17	180.00	416.93	403.58	626.03	307.53	416.18	0.433
	55	3287.55	59.87	196.44	416.93	382.41	592.831	274.56	467.73	0.420
0.95	30	2774.42	44.31	180.00	574.93	376.19	576.28	275.31	351.77	0.512
	35	2859.06	47.28	180.00	568.47	371.57	573.593	272.34	370.57	0.486
	40	2959.83	50.38	180.00	560.79	366.49	570.899	269.21	392.80	0.458
	45	3036.33	54.39	180.00	459.51	402.25	611.91	286.40	407.21	0.442
	50	3152.31	57.44	180.93	416.93	357.20	625.97	337.99	430.80	0.420
0.99	30	2917.19	49.08	180.14	565.19	367.45	571.77	270.36	383.47	0.470
	35	2945.31	50.55	217.21	425.53	279.28	626.03	338.52	397.03	0.547
	40	3097.44	54.11	180.06	547.08	353.95	572.98	268.10	422.99	0.426
	45	3176.75	57.55	191.49	431.41	373.97	610.36	285.66	441.50	0.434
	50	-	-	-	-	-	-	-	-	-

Table 4.11 Reliability based design optimization results for concrete without fly ash for 56 days curing age using QTRR model

Target Reliability R	Target $st56$ (MPa)	$cost$ $(Rs.)$	Predicted $st56$ (MPa)	w $\left(kg/m^3\right)$	fa $\left(kg/m^3\right)$	$ca-I$ $\left(kg/m^3\right)$	$ca-II$ $\left(kg/m^3\right)$	$ca-III$ $\left(kg/m^3\right)$	c $\left(kg/m^3\right)$	w/c
0.90	30	2765.82	66.65	180.00	575.21	376.34	576.30	275.33	350.00	0.514
	35	2765.82	66.65	180.00	575.21	376.34	576.30	275.33	350.00	0.514
	40	2765.85	66.68	180.00	575.05	376.92	575.63	275.58	350.00	0.514
	45	2815.52	71.73	180.00	566.10	482.57	398.89	345.93	359.51	0.501
	50	2894.75	72.49	180.03	542.59	421.00	514.36	302.28	377.42	0.477
	55	2888.88	73.05	180.00	468.70	522.91	415.38	379.51	372.90	0.483
	60	3137.22	78.68	180.27	482.70	472.84	441.89	340.13	429.17	0.420
	65	3132.12	79.21	180.03	424.46	555.44	377.74	385.21	425.89	0.423
0.95	30	2810.30	68.31	180.00	570.96	378.86	569.46	275.81	359.76	0.500
	35	2828.71	70.07	180.00	555.37	407.81	537.70	292.13	363.15	0.496
	40	2908.48	72.79	180.21	538.90	424.01	513.95	300.62	380.49	0.474
	45	2872.79	72.70	180.00	476.99	512.44	431.37	367.94	369.80	0.487
	50	3110.72	78.09	180.00	488.18	462.81	461.59	330.55	423.52	0.425
	55	3055.77	77.70	180.00	445.28	538.30	405.18	369.86	409.44	0.440
0.99	30	2957.36	75.31	180.00	455.44	536.71	421.27	360.78	388.35	0.463
	35	3144.39	79.01	181.00	456.22	515.57	423.64	340.40	430.59	0.420
	40	3081.87	77.81	181.37	416.93	583.74	374.33	373.99	415.44	0.437
	45	-	-	-	-	-	-	-	-	-
	50	-	-	-	-	-	-	-	-	-

Table 4.12 Reliability based design optimization results for concrete without fly ash for 56 days curing age using QPCR model

Target Reliability R	Target $st56$ (MPa)	$cost$ $(Rs.)$	Predicted $st56$ (MPa)	w $\left(kg/m^3\right)$	fa $\left(kg/m^3\right)$	$ca-I$ $\left(kg/m^3\right)$	$ca-II$ $\left(kg/m^3\right)$	$ca-III$ $\left(kg/m^3\right)$	c $\left(kg/m^3\right)$	w/c
0.90	30	2765.82	43.35	180.00	575.21	376.34	576.30	275.33	350.00	0.514
	35	2817.62	45.35	180.41	571.52	373.91	574.59	272.39	361.60	0.499
	40	2921.11	49.12	180.00	564.79	370.05	572.50	267.147	384.37	0.468
	45	3010.90	53.06	180.00	517.85	382.84	619.48	240.90	403.94	0.446
	50	3193.32	56.97	187.79	529.19	356.92	573.50	242.83	447.11	0.420
	55	-	-	-	-	-	-	-	-	-
0.95	30	2793.74	44.44	180.29	573.18	374.97	575.32	273.69	356.28	0.506
	35	2883.01	47.80	180.00	567.46	371.57	573.40	269.10	375.94	0.479
	40	2986.09	51.32	180.00	558.83	368.17	573.64	261.99	398.76	0.451
	45	3075.68	55.04	180.00	511.24	381.25	621.67	235.15	418.28	0.430
	50	3252.53	58.70	194.19	491.54	359.75	607.60	216.29	462.23	0.420
0.99	30	2916.28	48.95	180.00	565.50	370.17	572.47	267.23	383.31	0.470
	35	3003.92	51.96	180.00	555.88	368.43	576.92	258.23	402.75	0.447
	40	3108.41	55.10	180.00	548.27	364.48	575.55	251.91	425.88	0.423
	45	3217.40	58.34	190.28	483.31	371.42	626.03	213.32	453.06	0.420
	50	-	-	-	-	-	-	-	-	-

Table 4.13 Reliability based design optimization results for concrete without fly ash for 56 days curing age using QOLSR model

Target Reliability R	Target $st56$ (MPa)	$cost$ $(Rs.)$	Predicted $st56$ (MPa)	w $\left(kg/m^3\right)$	fa $\left(kg/m^3\right)$	$ca-I$ $\left(kg/m^3\right)$	$ca-II$ $\left(kg/m^3\right)$	$ca-III$ $\left(kg/m^3\right)$	c $\left(kg/m^3\right)$	w/c
0.90	30	2765.82	70.22	180.00	575.21	376.34	576.30	275.33	350.00	0.514
	35	2765.85	70.25	180.00	575.09	376.76	575.76	275.57	350.00	0.514
	40	2876.72	75.29	180.00	558.55	397.61	535.43	291.48	373.91	0.481
	45	2969.22	80.29	180.00	599.67	487.37	353.99	321.10	394.96	0.456
	50	2969.22	80.29	180.00	599.67	487.37	353.99	321.10	394.96	0.456
	55	-	-	-	-	-	-	-	-	-
0.95	30	2820.84	72.61	180.04	567.59	382.62	562.86	279.94	361.96	0.497
	35	2935.66	79.21	180.00	553.22	477.92	392.81	347.82	385.76	0.467
	40	2900.19	76.78	180.09	537.51	423.02	507.10	311.76	378.30	0.476
	45	3004.28	79.75	180.20	520.32	435.23	482.91	322.06	400.81	0.450
	50	-	-	-	-	-	-	-	-	-
0.99	30	3122.03	82.79	180.00	477.08	472.91	437.16	354.44	425.22	0.423
	35	3113.07	82.56	180.00	445.45	521.63	394.09	383.99	422.01	0.427
	40	3163.59	82.54	181.78	416.93	570.29	349.84	395.00	433.11	0.420
	45	-	-	-	-	-	-	-	-	-
	50	-	-	-	-	-	-	-	-	-

Table 4.14 Reliability based design optimization results for concrete without fly ash for 56 days curing age using LGRR model

Target Reliability R	Target $st56$ (MPa)	$cost$ $(Rs.)$	Predicted $st56$ (MPa)	w $\left(kg/m^3\right)$	fa $\left(kg/m^3\right)$	$ca-I$ $\left(kg/m^3\right)$	$ca-II$ $\left(kg/m^3\right)$	$ca-III$ $\left(kg/m^3\right)$	c $\left(kg/m^3\right)$	w/c
0.90	30	2765.82	45.92	180.00	575.21	376.34	576.30	275.33	350.00	0.514
	35	2780.14	46.53	180.00	574.82	375.47	576.25	273.96	353.20	0.510
	40	2881.33	50.47	180.00	569.69	370.59	572.16	269.23	375.61	0.479
	45	2993.69	54.50	180.00	565.75	364.15	570.62	260.21	400.63	0.449
	50	3078.57	58.67	180.00	642.18	328.92	626.03	142.92	423.94	0.425
	55	-	-	-	-	-	-	-	-	-
0.95	30	2765.82	45.92	180.00	575.21	376.34	576.30	275.33	350.00	0.514
	35	2849.87	49.28	180.00	571.17	372.19	573.21	270.97	368.63	0.488
	40	2950.74	53.01	180.00	567.50	366.55	571.46	263.23	391.08	0.460
	45	3063.27	56.84	180.00	564.04	359.75	570.84	253.01	416.18	0.433
	50	3284.80	60.40	198.45	541.04	302.09	626.03	184.06	472.49	0.420
0.99	30	2888.17	50.73	180.00	569.40	370.31	571.83	268.90	377.13	0.477
	35	2979.89	54.00	180.02	565.43	365.50	569.18	263.14	397.50	0.453
	40	3080.83	57.39	180.00	563.12	359.10	569.61	252.53	420.06	0.429
	45	3284.99	60.37	198.66	540.95	302.18	626.03	183.40	472.62	0.420
	50	-	-	-	-	-	-	-	-	-

Table 4.15 Reliability based design optimization results for concrete without fly ash for 56 days curing age using LTRR model

Target Reliability R	Target $st56$ (MPa)	$cost$ $(Rs.)$	Predicted $st56$ (MPa)	w $\left(kg/m^3\right)$	fa $\left(kg/m^3\right)$	$ca-I$ $\left(kg/m^3\right)$	$ca-II$ $\left(kg/m^3\right)$	$ca-III$ $\left(kg/m^3\right)$	c $\left(kg/m^3\right)$	w/c
0.90	30	2765.82	46.12	180.00	575.21	376.34	576.30	275.33	350.00	0.514
	35	2805.30	47.76	180.26	573.67	374.04	574.46	272.88	358.86	0.502
	40	2899.10	51.66	180.00	571.39	368.93	570.82	267.08	379.63	0.474
	45	2994.46	55.65	180.00	583.75	357.86	569.48	248.24	401.48	0.448
	50	3116.47	59.66	180.00	578.74	350.39	564.78	242.64	428.52	0.420
	55	-	-	-	-	-	-	-	-	-
0.95	30	2791.72	47.20	180.18	574.18	374.83	575.08	273.72	355.81	0.506
	35	2876.38	50.76	180.00	571.93	370.25	571.74	268.57	374.58	0.481
	40	2968.95	54.43	180.00	574.51	363.13	568.84	258.28	395.39	0.455
	45	3072.00	58.19	180.00	578.36	354.77	565.82	246.04	418.59	0.430
	50	3264.52	61.68	198.58	642.18	284.50	564.67	158.13	470.88	0.422
0.99	30	2922.25	52.64	180.00	573.68	366.63	570.35	263.00	384.91	0.468
	35	3005.18	55.87	180.00	578.24	359.47	568.12	251.82	403.65	0.446
	40	3102.80	59.15	180.00	576.42	353.61	564.30	244.95	425.40	0.423
	45	3281.30	61.83	199.98	642.18	230.22	583.13	186.53	474.13	0.422
	50	-	-	-	-	-	-	-	-	-

Table 4.16 Reliability based design optimization results for concrete without fly ash for 56 days curing age using LPCR model

Target Reliability R	Target $st56$ (MPa)	$cost$ $(Rs.)$	Predicted $st56$ (MPa)	w $\left(kg/m^3\right)$	fa $\left(kg/m^3\right)$	$ca-I$ $\left(kg/m^3\right)$	$ca-II$ $\left(kg/m^3\right)$	$ca-III$ $\left(kg/m^3\right)$	c $\left(kg/m^3\right)$	w/c
0.90	30	2765.82	42.70	180.00	575.21	376.34	576.30	275.33	350.00	0.514
	35	2808.99	44.31	180.31	571.82	374.40	574.96	273.15	359.64	0.501
	40	2922.49	48.38	180.00	563.31	370.22	572.68	268.11	384.62	0.468
	45	3013.84	52.68	180.00	508.48	383.18	616.13	253.30	404.07	0.445
	50	3168.68	56.96	195.07	453.35	373.06	626.03	238.65	442.59	0.441
	55	3268.83	61.35	198.29	416.93	623.50	626.03	0.00	472.12	0.420
0.95	30	2765.82	42.70	180.00	575.21	376.34	576.30	275.33	350.00	0.514
	35	2869.92	46.54	180.00	567.50	372.22	573.72	270.55	373.01	0.483
	40	2984.34	50.51	180.00	556.34	368.58	573.56	264.63	398.26	0.452
	45	3023.97	54.74	180.00	416.93	482.61	626.03	240.16	405.03	0.444
	50	3223.71	58.76	190.51	457.23	377.33	626.03	233.34	453.48	0.420
0.99	30	2884.38	47.05	180.00	566.45	371.66	573.38	269.85	376.20	0.478
	35	2986.65	50.59	180.00	555.88	368.64	573.89	264.33	398.76	0.451
	40	3095.39	54.27	180.00	537.66	367.63	581.34	256.79	422.65	0.426
	45	3210.05	58.04	196.91	449.60	370.95	626.03	231.40	452.48	0.435
	50	-	-	-	-	-	-	-	-	-

Table 4.17 Reliability based design optimization results for concrete without fly ash for 56 days curing age using LOLSR model

Target Reliability R	Target $st56$ (MPa)	$cost$ $(Rs.)$	Predicted $st56$ (MPa)	w $\left(kg/m^3\right)$	fa $\left(kg/m^3\right)$	$ca-I$ $\left(kg/m^3\right)$	$ca-II$ $\left(kg/m^3\right)$	$ca-III$ $\left(kg/m^3\right)$	c $\left(kg/m^3\right)$	w/c
0.90	30	2765.82	52.45	180.00	575.21	376.34	576.30	275.33	350.00	0.514
	35	2765.82	52.45	180.00	575.21	376.34	576.30	275.33	350.00	0.514
	40	2842.23	56.07	180.00	574.79	371.24	572.28	270.43	367.03	0.490
	45	2914.00	59.98	180.00	589.30	360.08	566.17	258.58	383.52	0.469
	50	3001.02	63.89	180.00	597.95	350.27	560.14	248.68	403.21	0.446
	55	3098.52	67.84	180.00	606.88	339.12	553.41	238.55	425.23	0.423
0.95	30	2770.05	52.79	180.00	577.35	375.16	575.75	273.97	351.02	0.513
	35	2845.18	56.20	180.00	574.64	371.12	572.15	270.30	367.68	0.490
	40	2916.36	59.78	180.00	583.50	362.46	566.95	261.16	383.86	0.469
	45	2991.72	63.44	180.00	596.10	351.84	560.95	250.04	401.08	0.449
	50	3087.43	67.07	180.00	598.58	344.05	555.40	242.59	422.50	0.426
	55	3135.65	71.35	180.00	642.18	45.31	626.03	414.20	428.57	0.420
0.99	30	2914.84	59.66	180.00	582.38	363.16	567.23	261.67	383.48	0.469
	35	2979.46	62.82	180.00	593.06	354.22	562.12	252.06	398.25	0.452
	40	3060.12	65.94	180.00	595.03	347.74	557.49	245.79	416.30	0.432
	45	3102.37	69.59	180.00	642.18	317.90	546.57	228.11	427.04	0.422
	50	-	-	-	-	-	-	-	-	-

Table 4.18 Reliability based design optimization results for concrete without fly ash for 91 days curing age using QGRR model

Target Reliability R	Target $st91$ (MPa)	$cost$ $(Rs.)$	Predicted $st91$ (MPa)	w $\left(kg/m^3\right)$	fa $\left(kg/m^3\right)$	$ca-I$ $\left(kg/m^3\right)$	$ca-II$ $\left(kg/m^3\right)$	$ca-III$ $\left(kg/m^3\right)$	c $\left(kg/m^3\right)$	w/c
0.90	30	2765.82	55.14	180.00	575.21	376.34	576.30	275.33	350.00	0.514
	35	2765.82	55.14	180.00	575.21	376.34	576.30	275.33	350.00	0.514
	40	2787.40	55.95	180.00	574.23	375.25	575.27	274.40	354.78	0.507
	45	2863.59	59.57	180.00	642.18	283.93	472.98	379.86	370.17	0.486
	50	2997.13	62.61	180.00	571.77	360.83	562.79	264.15	401.42	0.448
	55	3130.85	66.36	180.00	588.41	275.65	501.46	366.69	428.50	0.420
0.95	30	2765.82	55.14	180.00	575.21	376.34	576.30	275.33	350.00	0.514
	35	2795.64	56.25	180.00	573.96	374.82	574.84	274.00	356.61	0.505
	40	2878.55	59.13	180.00	577.26	367.70	568.59	268.11	375.18	0.480
	45	2979.31	62.12	180.00	572.65	362.47	563.59	264.16	397.49	0.453
	50	3100.70	65.24	180.00	565.86	356.71	558.01	259.75	424.34	0.424
	55	-	-	-	-	-	-	-	-	-
0.99	30	2868.22	59.21	180.00	642.18	399.78	475.94	260.84	374.68	0.480
	35	2947.88	61.76	180.00	642.18	344.26	496.70	280.46	391.60	0.460
	40	3056.24	64.14	180.00	568.27	359.89	560.09	260.35	414.54	0.434
	45	-	-	-	-	-	-	-	-	-
	50	-	-	-	-	-	-	-	-	-

Table 4.19 Reliability based design optimization results for concrete without fly ash for 91 days curing age using QTRR model

Target Reliability R	Target $st91$ (MPa)	$cost$ $(Rs.)$	Predicted $st91$ (MPa)	w $\left(kg/m^3\right)$	fa $\left(kg/m^3\right)$	$ca-I$ $\left(kg/m^3\right)$	$ca-II$ $\left(kg/m^3\right)$	$ca-III$ $\left(kg/m^3\right)$	c $\left(kg/m^3\right)$	w/c
0.90	30	2765.82	45.89	180.00	575.21	376.34	576.30	275.33	350.00	0.514
	35	2785.51	46.69	180.17	572.50	376.16	575.58	274.90	354.37	0.508
	40	2880.40	50.49	182.46	555.42	375.89	571.60	272.63	375.86	0.485
	45	2992.27	54.48	183.18	531.42	380.24	569.326	272.90	400.38	0.458
	50	3177.80	59.37	186.82	507.05	373.27	561.25	268.05	442.29	0.422
	55	3060.88	61.09	230.00	416.93	600.83	393.09	199.23	431.69	0.533
0.95	30	2770.19	46.21	180.62	572.75	376.78	575.95	275.21	351.13	0.514
	35	2860.23	49.76	182.33	558.73	376.26	571.94	272.59	371.42	0.491
	40	2961.78	53.43	183.13	538.65	379.80	569.08	271.77	393.79	0.465
	45	3071.30	57.18	182.69	509.36	390.20	568.29	274.04	417.25	0.438
	50	3221.61	61.19	191.78	481.10	382.17	557.94	267.24	453.16	0.423
	55	3311.67	64.88	199.17	416.93	428.80	539.67	268.73	474.33	0.420
0.99	30	2755.60	51.94	192.60	474.90	452.11	576.31	271.59	350.18	0.550
	35	3019.45	55.61	182.77	520.72	391.08	567.35	271.52	406.11	0.450
	40	3185.69	59.06	186.75	519.42	371.89	555.73	260.44	444.47	0.420
	45	3254.58	62.60	230.00	465.95	360.30	516.82	227.13	473.97	0.485
	50	3272.03	63.43	198.03	416.93	784.84	343.91	119.21	470.48	0.421

Table 4.20 Reliability based design optimization results for concrete without fly ash for 91 days curing age using QPCR model

Target Reliability R	Target $st91$ (MPa)	$cost$ $(Rs.)$	Predicted $st91$ (MPa)	w $\left(kg/m^3\right)$	fa $\left(kg/m^3\right)$	$ca-I$ $\left(kg/m^3\right)$	$ca-II$ $\left(kg/m^3\right)$	$ca-III$ $\left(kg/m^3\right)$	c $\left(kg/m^3\right)$	w/c
0.90	30	2765.82	46.18	180.00	575.21	376.34	576.30	275.33	350.00	0.514
	35	2765.82	46.18	180.00	575.21	376.34	576.30	275.33	350.00	0.514
	40	2853.59	49.48	180.00	568.95	372.99	573.97	271.07	369.41	0.487
	45	2966.54	53.26	180.00	560.53	368.84	571.33	265.46	394.39	0.456
	50	3093.38	57.17	180.00	542.75	367.48	575.97	257.23	422.31	0.426
	55	3209.25	61.24	188.51	416.93	426.37	626.03	236.08	448.84	0.420
0.95	30	2765.82	46.18	180.00	575.21	376.34	576.30	275.33	350.00	0.514
	35	2821.81	48.31	180.22	571.17	374.00	574.56	272.47	362.46	0.497
	40	2918.69	51.71	180.00	564.32	370.54	572.32	267.81	383.81	0.469
	45	3029.52	55.25	180.00	552.84	367.98	573.22	260.76	408.29	0.441
	50	3141.17	58.96	182.40	501.31	378.31	605.11	245.62	433.12	0.421
	55	3265.62	62.70	197.95	416.93	625.13	626.03	0.00	471.30	0.420
0.99	30	2858.45	49.65	180.00	568.81	372.77	573.80	270.71	370.49	0.486
	35	2942.43	52.51	180.00	561.93	370.05	572.66	266.02	389.06	0.463
	40	3036.93	55.52	180.00	550.60	368.71	575.45	258.82	409.93	0.439
	45	3115.71	58.79	180.00	490.14	387.83	623.07	242.10	426.54	0.422
	50	3295.92	61.99	196.92	416.93	343.31	600.18	303.19	468.86	0.420

Table 4.21 Reliability based design optimization results for concrete without fly ash for 91 days curing age using QOLSR model

Target Reliability R	Target $st91$ (MPa)	$cost$ $(Rs.)$	Predicted $st91$ (MPa)	w $\left(kg/m^3\right)$	fa $\left(kg/m^3\right)$	$ca-I$ $\left(kg/m^3\right)$	$ca-II$ $\left(kg/m^3\right)$	$ca-III$ $\left(kg/m^3\right)$	c $\left(kg/m^3\right)$	w/c
0.90	30	2765.82	50.89	180.00	575.21	376.34	576.30	275.33	350.00	0.514
	35	2770.94	51.41	180.00	578.90	374.08	576.16	272.82	351.27	0.512
	40	2859.64	54.97	180.00	581.34	366.33	572.28	265.03	371.15	0.485
	45	2930.70	58.85	180.00	599.39	352.18	569.42	249.32	387.64	0.464
	50	3014.43	62.77	180.00	616.45	337.93	565.87	233.06	406.93	0.442
	55	3141.25	66.80	183.67	641.92	306.90	558.52	209.34	437.32	0.420
0.95	30	2785.12	51.64	180.00	575.13	374.96	575.44	274.00	354.31	0.508
	35	2863.20	54.88	180.00	578.49	367.54	572.06	266.42	371.85	0.484
	40	2924.17	58.48	180.00	597.37	353.78	569.61	250.92	386.12	0.466
	45	2999.16	62.09	180.00	613.58	340.61	566.35	235.85	403.42	0.446
	50	3063.08	65.99	180.00	642.18	322.77	563.13	214.28	418.70	0.430
	55	-	-	-	-	-	-	-	-	-
0.99	30	2918.83	58.15	180.00	595.52	355.27	569.76	252.28	384.86	0.468
	35	2981.83	61.18	180.00	608.55	344.56	566.98	239.93	399.38	0.451
	40	3072.27	64.07	180.00	609.85	337.55	562.92	232.48	419.62	0.429
	45	3103.74	67.90	180.00	642.18	300.46	595.22	197.00	428.04	0.421
	50	-	-	-	-	-	-	-	-	-

Table 4.22 Reliability based design optimization results for concrete without fly ash for 91 days curing age using LGRR model

Target Reliability R	Target $st91$ (MPa)	$cost$ $(Rs.)$	Predicted $st91$ (MPa)	w $\left(kg/m^3\right)$	fa $\left(kg/m^3\right)$	$ca-I$ $\left(kg/m^3\right)$	$ca-II$ $\left(kg/m^3\right)$	$ca-III$ $\left(kg/m^3\right)$	c $\left(kg/m^3\right)$	w/c
0.90	30	2765.82	50.29	180.00	575.21	376.34	576.30	275.33	350.00	0.514
	35	2765.82	50.29	180.00	575.21	376.34	576.30	275.33	350.00	0.514
	40	2808.29	51.97	180.16	573.28	374.05	574.40	273.04	359.48	0.501
	45	2908.12	55.85	180.00	571.50	368.06	571.07	265.88	381.66	0.472
	50	3020.41	59.81	180.00	573.32	359.33	568.50	253.96	406.86	0.442
	55	3258.22	63.95	196.90	642.18	259.04	596.59	157.95	468.81	0.420
0.95	30	2765.82	50.29	180.00	575.21	376.34	576.30	275.33	350.00	0.514
	35	2789.88	51.22	180.16	574.07	375.00	575.17	273.98	355.39	0.507
	40	2879.81	54.78	180.00	570.77	370.37	571.63	269.15	375.30	0.480
	45	2975.47	58.33	184.55	642.18	327.97	589.05	186.57	401.53	0.460
	50	3095.49	62.16	180.00	570.43	355.38	565.43	249.83	423.53	0.425
	55	-	-	-	-	-	-	-	-	-
0.99	30	2839.92	53.27	180.00	572.21	372.53	573.22	271.41	366.44	0.491
	35	2921.55	56.35	180.00	571.68	367.17	570.66	264.42	384.68	0.468
	40	3012.48	59.53	180.00	572.59	360.50	568.31	255.25	405.06	0.444
	45	3117.39	62.80	180.00	568.82	354.76	564.18	249.27	428.36	0.420
	50	-	-	-	-	-	-	-	-	-

Table 4.23 Reliability based design optimization results for concrete without fly ash for 91 days curing age using LTRR/LOLSR model

Target Reliability R	Target $st91$ (MPa)	$cost$ $(Rs.)$	Predicted $st91$ (MPa)	w $\left(kg/m^3\right)$	fa $\left(kg/m^3\right)$	$ca-I$ $\left(kg/m^3\right)$	$ca-II$ $\left(kg/m^3\right)$	$ca-III$ $\left(kg/m^3\right)$	c $\left(kg/m^3\right)$	w/c
0.90	30	2765.82	52.41	180.00	575.21	376.34	576.30	275.33	350.00	0.514
	35	2765.82	52.41	180.00	575.21	376.34	576.30	275.33	350.00	0.514
	40	2815.44	54.67	180.00	574.08	373.47	573.85	272.45	361.04	0.499
	45	2898.98	58.47	180.00	578.47	366.27	568.95	264.04	379.83	0.474
	50	2985.54	62.37	180.00	590.67	355.85	562.86	251.11	399.58	0.450
	55	3089.89	66.28	180.00	597.64	345.74	556.44	240.42	423.09	0.425
0.95	30	2765.82	52.41	180.00	575.21	376.34	576.30	275.33	350.00	0.514
	35	2812.53	54.53	180.01	574.04	373.67	574.00	272.66	360.389	0.499
	40	2889.24	58.02	180.00	577.27	367.41	569.62	265.36	377.62	0.477
	45	2967.60	61.61	180.00	588.73	357.89	564.07	253.34	395.51	0.455
	50	3065.39	65.21	180.00	591.22	350.35	558.62	245.13	417.42	0.431
	55	3139.01	69.29	180.00	642.18	19.20	626.03	439.54	428.57	0.420
0.99	30	2837.24	58.09	180.00	642.18	347.59	507.46	287.36	366.91	0.491
	35	2910.13	61.73	180.06	642.18	342.18	559.91	226.84	384.58	0.468
	40	3022.83	63.62	180.00	588.50	354.47	561.23	249.38	407.83	0.441
	45	3114.08	66.74	180.00	589.26	348.05	556.35	242.57	428.22	0.420
	50	-	-	-	-	-	-	-	-	-

Table 4.24 Reliability based design optimization results for concrete without fly ash for 91 days curing age using LPCR model

Target Reliability R	Target $st91$ (MPa)	$cost$ $(Rs.)$	Predicted $st91$ (MPa)	w $\left(kg/m^3\right)$	fa $\left(kg/m^3\right)$	$ca-I$ $\left(kg/m^3\right)$	$ca-II$ $\left(kg/m^3\right)$	$ca-III$ $\left(kg/m^3\right)$	c $\left(kg/m^3\right)$	w/c
0.90	30	2765.82	45.72	180.00	575.21	376.34	576.30	275.33	350.00	0.514
	35	2765.82	45.72	180.00	575.21	376.34	576.30	275.33	350.00	0.514
	40	2847.32	48.65	180.22	568.85	373.09	573.94	271.65	368.08	0.490
	45	2872.67	53.04	180.00	416.93	468.72	626.03	282.52	370.36	0.486
	50	3053.23	57.08	180.00	479.15	393.87	623.00	259.66	412.03	0.437
	55	3293.44	61.21	198.32	497.96	350.29	565.67	240.51	472.20	0.420
0.95	30	2765.82	45.72	180.00	575.21	376.34	576.30	275.33	350.00	0.514
	35	2802.35	47.04	180.29	572.25	374.73	575.08	273.54	358.17	0.503
	40	2909.81	50.80	180.00	563.97	370.99	572.67	269.04	381.81	0.471
	45	3030.69	54.74	180.00	550.13	368.15	573.23	263.28	408.42	0.441
	50	3117.43	58.88	180.00	474.34	391.59	620.94	257.00	426.21	0.422
	55	3310.23	63.15	199.20	416.93	370.66	617.42	249.49	474.27	0.420
0.99	30	2821.18	47.70	180.54	570.75	373.80	574.31	272.54	362.42	0.498
	35	2918.04	51.07	180.00	563.53	370.65	572.35	268.64	383.62	0.469
	40	3024.88	54.57	180.00	550.49	368.45	573.57	263.32	407.15	0.442
	45	3063.01	58.50	180.00	416.93	443.45	626.03	271.73	412.72	0.436
	50	3234.49	62.04	191.05	416.93	401.45	626.03	248.64	454.87	0.420

Table 4.25 Reliability based design optimization results for concrete with fly ash for 28 days curing age using QGRR model

Target Reliability R	Target $st28$ (MPa)	$cost$ $(Rs.)$	Predicted $st28$ (MPa)	w $\left(kg/m^3\right)$	fa $\left(kg/m^3\right)$	$ca-I$ $\left(kg/m^3\right)$	$ca-II$ $\left(kg/m^3\right)$	$ca-III$ $\left(kg/m^3\right)$	cm $\left(kg/m^3\right)$	w/cm
0.90	25	2643.69	35.95	203.56	626.85	429.02	464.69	148.34	400.00	0.509
	30	2663.88	40.40	191.00	626.85	440.35	475.75	159.26	400.00	0.477
	35	2751.55	43.80	180.00	588.93	431.61	478.42	218.17	415.92	0.433
	40	2918.02	47.31	196.86	625.82	375.96	440.53	179.73	468.57	0.420
	45	-	-	-	-	-	-	-	-	-
0.95	25	2656.96	38.95	195.20	626.85	437.81	472.08	154.37	400.00	0.488
	30	2677.83	43.22	182.54	626.85	447.56	480.52	169.65	400.00	0.456
	35	2764.48	46.30	180.00	626.85	413.07	463.58	208.67	420.39	0.428
	40	-	-	-	-	-	-	-	-	-
0.99	25	2687.63	44.03	180.00	626.85	406.36	481.82	214.95	400.00	0.450
	30	2775.95	46.61	180.00	626.85	408.05	456.44	217.24	423.24	0.425
	35	2955.00	47.60	196.88	626.73	77.86	458.26	450.56	468.76	0.420
	40	-	-	-	-	-	-	-	-	-

Table 4.26 Reliability based design optimization results for concrete with fly ash for 28 days curing age using QTRR model

Target Reliability R	Target $st28$ (MPa)	$cost$ $(Rs.)$	Predicted $st28$ (MPa)	w $\left(kg/m^3\right)$	fa $\left(kg/m^3\right)$	$ca-I$ $\left(kg/m^3\right)$	$ca-II$ $\left(kg/m^3\right)$	$ca-III$ $\left(kg/m^3\right)$	cm $\left(kg/m^3\right)$	w/cm
0.90	25	2678.08	36.83	180.50	626.85	446.82	513.13	144.03	400.00	0.451
	30	2879.11	40.69	191.70	601.82	402.36	471.34	173.67	455.88	0.420
	35	2910.85	50.59	198.55	626.85	378.00	614.22	0.00	472.74	0.420
	40	-	-	-	-	-	-	-	-	-
	45	-	-	-	-	-	-	-	-	-
0.95	25	2717.52	41.45	180.00	626.85	459.56	555.38	80.97	412.17	0.437
	30	2849.49	49.59	190.45	626.85	417.64	614.25	0.00	453.46	0.420
	35	-	-	-	-	-	-	-	-	-
	40	-	-	-	-	-	-	-	-	-
0.99	25	2854.27	49.66	191.08	626.85	414.55	614.25	0.00	454.97	0.420
	30	-	-	-	-	-	-	-	-	-
	35	-	-	-	-	-	-	-	-	-
	40	-	-	-	-	-	-	-	-	-

Table 4.27 Reliability based design optimization results for concrete with fly ash for 28 days curing age using QPCR model

Target Reliability R	Target $st28$ (MPa)	$cost$ $(Rs.)$	Predicted $st28$ (MPa)	w $\left(kg/m^3\right)$	fa $\left(kg/m^3\right)$	$ca-I$ $\left(kg/m^3\right)$	$ca-II$ $\left(kg/m^3\right)$	$ca-III$ $\left(kg/m^3\right)$	cm $\left(kg/m^3\right)$	w/cm
0.90	25	2661.81	32.47	190.37	624.43	455.63	492.26	132.51	400.01	0.476
	30	2710.96	36.88	192.71	522.26	442.75	495.48	232.99	408.16	0.472
	35	2724.30	41.42	180.00	438.71	492.66	568.28	235.91	404.48	0.445
	40	2817.41	45.76	180.00	416.93	490.27	570.85	236.28	428.49	0.420
	45	-	-	-	-	-	-	-	-	-
0.95	25	2700.62	34.36	191.27	624.42	450.81	486.64	130.65	410.67	0.466
	30	2733.99	38.71	185.90	522.22	448.11	501.59	236.65	411.42	0.452
	35	2746.46	43.09	180.00	416.93	503.70	589.19	221.98	410.23	0.439
	40	2873.89	47.17	187.72	416.93	477.53	562.47	220.00	446.96	0.420
0.99	25	2747.36	37.87	180.00	621.39	460.05	497.54	136.69	418.25	0.430
	30	2778.21	41.96	180.00	499.44	460.60	519.66	237.82	420.14	0.428
	35	2889.78	45.69	190.63	487.97	444.15	503.04	223.37	453.97	0.420
	40	-	-	-	-	-	-	-	-	-

Table 4.28 Reliability based design optimization results for concrete with fly ash for 28 days curing age using LGRR model

Target Reliability R	Target $st28$ (MPa)	$cost$ $(Rs.)$	Predicted $st28$ (MPa)	w $\left(kg/m^3\right)$	fa $\left(kg/m^3\right)$	$ca-I$ $\left(kg/m^3\right)$	$ca-II$ $\left(kg/m^3\right)$	$ca-III$ $\left(kg/m^3\right)$	cm $\left(kg/m^3\right)$	w/cm
0.90	25	2658.27	34.45	199.85	626.81	443.81	477.14	128.84	403.02	0.496
	30	2691.16	39.20	186.97	594.46	440.34	491.09	184.38	403.98	0.463
	35	2742.76	43.78	180.00	590.10	432.18	497.00	200.02	414.16	0.435
	40	2927.17	47.69	197.17	558.56	409.01	475.41	181.07	469.45	0.420
	45	-	-	-	-	-	-	-	-	-
0.95	25	2672.86	37.09	193.48	626.78	449.23	482.81	133.55	404.20	0.479
	30	2705.15	41.76	180.90	598.96	443.83	494.76	187.39	405.28	0.446
	35	2794.97	45.97	180.00	565.87	433.94	492.46	216.00	426.86	0.422
	40	-	-	-	-	-	-	-	-	-
0.99	25	2693.41	42.08	180.00	626.85	461.80	495.99	143.85	403.94	0.446
	30	2770.27	45.97	180.00	626.85	435.43	499.24	148.16	423.99	0.425
	35	-	-	-	-	-	-	-	-	-
	40	-	-	-	-	-	-	-	-	-

Table 4.29 Reliability based design optimization results for concrete with fly ash for 28 days curing age using LTRR model

Target Reliability R	Target $st28$ (MPa)	$cost$ $(Rs.)$	Predicted $st28$ (MPa)	w $\left(kg/m^3\right)$	fa $\left(kg/m^3\right)$	$ca-I$ $\left(kg/m^3\right)$	$ca-II$ $\left(kg/m^3\right)$	$ca-III$ $\left(kg/m^3\right)$	cm $\left(kg/m^3\right)$	w/cm
0.90	25	2660.27	34.43	199.07	626.80	444.51	478.55	128.61	403.24	0.494
	30	2701.84	39.18	184.39	571.84	441.01	495.10	209.31	404.41	0.456
	35	2709.75	43.80	180.00	626.85	483.76	614.25	0.00	412.64	0.436
	40	2864.04	47.85	192.19	604.44	455.07	591.94	0.00	457.61	0.420
	45	-	-	-	-	-	-	-	-	-
0.95	25	2676.28	37.05	192.18	626.77	450.38	484.90	133.43	404.59	0.475
	30	2716.04	41.68	180.00	599.67	437.74	507.41	180.29	407.98	0.441
	35	2756.33	45.99	180.00	626.85	491.88	594.56	0.00	425.01	0.424
	40	-	-	-	-	-	-	-	-	-
0.99	25	2708.08	41.90	180.00	626.85	461.06	499.53	137.47	408.00	0.441
	30	2782.98	45.82	180.00	626.85	417.06	529.04	133.73	427.68	0.421
	35	-	-	-	-	-	-	-	-	-
	40	-	-	-	-	-	-	-	-	-

Table 4.30 Reliability based design optimization results for concrete with fly ash for 28 days curing age using LPCR model

Target Reliability R	Target $st28$ (MPa)	$cost$ $(Rs.)$	Predicted $st28$ (MPa)	w $\left(kg/m^3\right)$	fa $\left(kg/m^3\right)$	$ca-I$ $\left(kg/m^3\right)$	$ca-II$ $\left(kg/m^3\right)$	$ca-III$ $\left(kg/m^3\right)$	cm $\left(kg/m^3\right)$	w/cm
0.90	25	2656.97	31.86	193.51	621.91	453.98	490.79	129.97	400.00	0.484
	30	2694.65	36.46	189.29	578.73	523.59	569.94	31.41	410.40	0.461
	35	2710.17	41.30	180.24	417.79	499.77	575.46	246.85	400.00	0.451
	40	2817.54	45.80	180.00	416.93	489.78	565.04	242.54	428.34	0.420
	45	-	-	-	-	-	-	-	-	-
0.95	25	2696.65	33.61	194.96	623.06	447.89	483.83	127.59	411.15	0.474
	30	2718.29	38.23	182.73	577.95	528.89	576.06	35.00	413.90	0.441
	35	2759.04	42.91	180.00	434.16	490.34	561.94	240.89	413.39	0.435
	40	2872.20	47.24	187.38	416.93	477.60	556.04	227.80	446.14	0.420
0.99	25	2676.95	37.32	187.54	503.53	513.72	572.86	128.97	400.05	0.469
	30	2744.70	41.50	180.00	519.84	555.73	614.25	34.48	418.37	0.430
	35	2809.09	45.90	180.00	419.67	487.64	614.25	194.74	427.59	0.421
	40	2955.67	49.83	199.49	416.93	438.88	608.35	157.02	475.00	0.420

Table 4.31 Reliability based design optimization results for concrete with fly ash for 28 days curing age using LOLSR model

Target Reliability R	Target $st28$ (MPa)	$cost$ $(Rs.)$	Predicted $st28$ (MPa)	w $\left(kg/m^3\right)$	fa $\left(kg/m^3\right)$	$ca-I$ $\left(kg/m^3\right)$	$ca-II$ $\left(kg/m^3\right)$	$ca-III$ $\left(kg/m^3\right)$	cm $\left(kg/m^3\right)$	w/cm
0.90	25	2684.92	35.12	197.03	552.55	431.45	482.94	217.44	404.23	0.487
	30	2676.01	39.94	187.55	626.80	428.66	520.79	133.60	402.52	0.466
	35	2736.36	44.50	180.00	602.97	432.67	496.89	187.30	413.20	0.436
	40	2919.81	48.98	197.71	626.85	371.97	479.35	140.87	470.55	0.420
	45	-	-	-	-	-	-	-	-	-
0.95	25	2699.38	37.94	190.84	557.37	434.88	486.65	220.35	405.63	0.470
	30	2690.07	42.73	181.08	626.78	434.18	526.70	138.40	403.52	0.449
	35	2792.30	46.83	180.00	582.59	432.80	491.49	200.76	427.05	0.421
	40	-	-	-	-	-	-	-	-	-
0.99	25	2719.54	43.20	180.00	589.96	434.66	494.58	205.75	407.87	0.441
	30	2741.69	47.30	180.00	626.85	475.87	614.25	0.00	421.05	0.428
	35	-	-	-	-	-	-	-	-	-
	40	-	-	-	-	-	-	-	-	-

Table 4.32 Reliability based design optimization results for concrete with fly ash for 56 days curing age using QGRR model

Target Reliability R	Target $st56$ (MPa)	$cost$ $(Rs.)$	Predicted $st56$ (MPa)	w $\left(kg/m^3\right)$	fa $\left(kg/m^3\right)$	$ca-I$ $\left(kg/m^3\right)$	$ca-II$ $\left(kg/m^3\right)$	$ca-III$ $\left(kg/m^3\right)$	cm $\left(kg/m^3\right)$	w/cm
0.90	25	2635.83	36.08	206.82	626.85	438.06	471.80	124.16	400.01	0.517
	30	2661.99	40.34	198.53	626.73	444.20	478.53	130.20	403.43	0.492
	35	2692.75	44.72	189.72	552.05	440.86	496.04	215.77	403.45	0.470
	40	2709.63	49.09	180.00	542.50	446.67	542.35	199.64	404.22	0.445
	45	2820.13	53.01	182.62	490.06	427.91	553.28	228.90	432.12	0.423
	50	-	-	-	-	-	-	-	-	-
0.95	25	2655.80	38.91	201.85	626.75	441.37	475.41	127.54	403.20	0.501
	30	2675.84	43.03	192.46	626.67	449.14	484.01	134.84	404.54	0.476
	35	2705.73	47.24	183.59	555.91	444.54	500.19	219.18	404.44	0.454
	40	2736.71	51.44	180.00	518.09	452.47	614.25	141.78	412.48	0.436
	45	2958.66	54.48	199.02	424.43	398.58	583.11	215.20	473.86	0.420
0.99	25	2666.89	44.22	187.39	626.85	455.25	490.72	139.66	400.00	0.468
	30	2695.57	47.89	180.00	626.22	459.99	497.71	144.11	404.47	0.445
	35	2750.11	51.64	180.00	522.64	438.75	597.50	164.03	415.41	0.433
	40	2952.02	54.01	198.82	458.97	403.24	557.00	201.60	473.37	0.420
	45	-	-	-	-	-	-	-	-	-

Table 4.33 Reliability based design optimization results for concrete with fly ash for 56 days curing age using QTRR model

Target Reliability R	Target $st56$ (MPa)	$cost$ $(Rs.)$	Predicted $st56$ (MPa)	w $\left(kg/m^3\right)$	fa $\left(kg/m^3\right)$	$ca-I$ $\left(kg/m^3\right)$	$ca-II$ $\left(kg/m^3\right)$	$ca-III$ $\left(kg/m^3\right)$	cm $\left(kg/m^3\right)$	w/cm
0.90	25	2739.91	55.30	180.00	626.85	435.41	614.25	40.97	419.15	0.429
	30	2896.16	63.88	196.62	626.85	387.46	614.25	0.00	468.13	0.420
	35	-	-	-	-	-	-	-	-	-
	40	-	-	-	-	-	-	-	-	-
	45	-	-	-	-	-	-	-	-	-
	50	-	-	-	-	-	-	-	-	-
0.95	25	2918.03	64.37	199.50	626.85	373.32	614.25	0.00	475.00	0.420
	30	-	-	-	-	-	-	-	-	-
	35	-	-	-	-	-	-	-	-	-
	40	-	-	-	-	-	-	-	-	-
	45	-	-	-	-	-	-	-	-	-
0.99	25	-	-	-	-	-	-	-	-	-
	30	-	-	-	-	-	-	-	-	-
	35	-	-	-	-	-	-	-	-	-
	40	-	-	-	-	-	-	-	-	-
	45	-	-	-	-	-	-	-	-	-

Table 4.34 Reliability based design optimization results for concrete with fly ash for 56 days curing age using QPCR model

Target Reliability R	Target $st56$ (MPa)	$cost$ $(Rs.)$	Predicted $st56$ (MPa)	w $\left(kg/m^3\right)$	fa $\left(kg/m^3\right)$	$ca-I$ $\left(kg/m^3\right)$	$ca-II$ $\left(kg/m^3\right)$	$ca-III$ $\left(kg/m^3\right)$	cm $\left(kg/m^3\right)$	w/cm
0.90	25	2615.50	32.84	219.54	626.30	427.15	459.88	113.83	400.00	0.549
	30	2650.26	37.35	197.76	623.42	448.93	484.71	128.15	400.01	0.494
	35	2700.94	41.75	193.43	562.75	445.10	491.19	191.59	408.13	0.474
	40	2723.38	46.28	183.47	483.31	471.94	538.31	228.07	406.97	0.451
	45	2762.19	50.71	180.00	416.93	502.19	614.25	194.68	415.19	0.434
	50	2957.30	54.81	199.44	416.93	453.93	571.42	178.53	474.85	0.420
0.95	25	2630.62	34.98	210.18	621.27	438.83	473.79	118.48	400.01	0.525
	30	2684.92	39.21	196.02	623.33	447.50	483.17	127.98	408.47	0.480
	35	2723.82	43.55	186.75	561.93	450.63	497.57	195.25	411.39	0.454
	40	2707.74	48.08	180.02	424.63	502.68	585.42	227.81	400.05	0.450
	45	2817.52	52.12	180.00	416.93	489.76	574.56	233.13	428.60	0.420
0.99	25	2630.29	38.82	220.00	472.89	491.64	544.77	124.74	400.00	0.550
	30	2683.75	43.00	180.00	569.85	487.98	536.50	141.00	400.08	0.450
	35	2762.48	46.76	180.00	536.55	465.48	518.55	197.96	418.18	0.430
	40	2777.77	50.89	180.00	416.93	498.02	585.93	223.22	418.44	0.430
	45	2934.94	54.36	196.34	416.93	463.92	565.93	188.93	467.43	0.420

Table 4.35 Reliability based design optimization results for concrete with fly ash for 56 days curing age using QOLSR model

Target Reliability R	Target $st56$ (MPa)	$cost$ $(Rs.)$	Predicted $st56$ (MPa)	w $\left(kg/m^3\right)$	fa $\left(kg/m^3\right)$	$ca-I$ $\left(kg/m^3\right)$	$ca-II$ $\left(kg/m^3\right)$	$ca-III$ $\left(kg/m^3\right)$	cm $\left(kg/m^3\right)$	w/cm
0.90	25	2691.60	59.10	214.49	541.97	428.46	454.58	205.30	413.10	0.519
	30	2703.79	60.48	212.98	519.67	429.17	453.31	231.47	414.35	0.514
	35	2651.74	64.43	215.12	499.55	429.50	450.18	262.20	400.00	0.538
	40	2647.69	66.77	220.03	481.85	426.44	445.99	274.52	400.06	0.550
	45	2654.17	65.87	220.00	471.20	417.50	416.89	322.46	400.00	0.550
	50	-	-	-	-	-	-	-	-	-
0.95	25	2660.51	62.95	212.90	503.50	410.42	421.50	310.24	400.00	0.532
	30	2660.51	62.95	212.90	503.50	410.42	421.50	310.24	400.00	0.532
	35	2651.31	66.60	220.06	463.95	451.35	420.09	293.67	400.11	0.550
	40	-	-	-	-	-	-	-	-	-
	45	-	-	-	-	-	-	-	-	-
0.99	25	2888.80	69.23	201.21	537.95	419.86	404.18	260.50	458.08	0.439
	30	2963.37	73.89	199.45	496.04	420.28	399.38	296.95	474.89	0.420
	35	-	-	-	-	-	-	-	-	-
	40	-	-	-	-	-	-	-	-	-
	45	-	-	-	-	-	-	-	-	-

Table 4.36 Reliability based design optimization results for concrete with fly ash for 56 days curing age using LGRR model

Target Reliability R	Target $st56$ (MPa)	$cost$ $(Rs.)$	Predicted $st56$ (MPa)	w $\left(kg/m^3\right)$	fa $\left(kg/m^3\right)$	$ca-I$ $\left(kg/m^3\right)$	$ca-II$ $\left(kg/m^3\right)$	$ca-III$ $\left(kg/m^3\right)$	cm $\left(kg/m^3\right)$	w/cm
0.90	25	2613.76	36.04	211.44	624.82	499.96	527.64	0.00	400.00	0.529
	30	2643.57	40.83	201.86	626.85	417.52	507.80	122.08	400.00	0.505
	35	2690.85	45.56	190.35	549.44	435.85	487.12	231.09	402.64	0.473
	40	2702.96	50.37	180.73	560.60	441.55	493.12	233.72	402.21	0.449
	45	2772.89	54.72	180.00	587.68	424.01	489.10	211.31	421.68	0.427
	50	-	-	-	-	-	-	-	-	-
0.95	25	2638.76	39.17	204.81	626.85	441.29	474.65	123.48	400.01	0.512
	30	2660.41	43.82	196.77	626.81	421.20	511.65	125.88	402.32	0.489
	35	2702.74	48.51	184.83	553.66	438.95	490.43	233.96	403.61	0.458
	40	2724.44	53.06	180.00	611.29	422.75	493.56	194.54	410.01	0.439
	45	2801.25	57.20	181.20	626.85	303.96	602.71	165.46	431.45	0.420
0.99	25	2667.28	44.89	194.51	626.79	448.08	481.89	133.75	403.14	0.482
	30	2672.19	49.65	183.98	626.85	433.55	524.63	136.68	400.00	0.460
	35	2737.17	53.67	180.00	612.25	419.96	491.12	195.61	413.35	0.435
	40	2934.72	56.02	199.48	626.85	291.33	558.57	133.60	475.00	0.420
	45	-	-	-	-	-	-	-	-	-

Table 4.37 Reliability based design optimization results for concrete with fly ash for 56 days curing age using LTRR/LOLSR model

Target Reliability R	Target $st56$ (MPa)	$cost$ $(Rs.)$	Predicted $st56$ (MPa)	w $\left(kg/m^3\right)$	fa $\left(kg/m^3\right)$	$ca-I$ $\left(kg/m^3\right)$	$ca-II$ $\left(kg/m^3\right)$	$ca-III$ $\left(kg/m^3\right)$	cm $\left(kg/m^3\right)$	w/cm
0.90	25	2614.73	62.69	220.00	626.85	426.39	458.96	113.70	400.00	0.550
	30	2614.73	62.69	220.00	626.85	426.39	458.96	113.70	400.00	0.550
	35	2614.73	62.69	220.00	626.85	426.39	458.96	113.70	400.00	0.550
	40	2614.73	62.69	220.00	626.85	426.39	458.96	113.70	400.00	0.550
	45	2614.73	62.69	220.00	626.85	426.39	458.96	113.70	400.00	0.550
	50	2614.73	62.69	220.00	626.85	426.39	458.96	113.70	400.00	0.550
	55	2635.30	67.29	211.60	626.84	433.33	466.42	119.87	401.90	0.526
	60	2655.04	72.01	202.53	626.82	441.13	474.60	126.67	403.29	0.502
0.95	25	2614.73	62.69	220.00	626.85	426.39	458.96	113.70	400.00	0.550
	30	2614.73	62.69	220.00	626.85	426.39	458.96	113.70	400.00	0.550
	35	2614.73	62.69	220.00	626.85	426.39	458.96	113.70	400.00	0.550
	40	2614.73	62.69	220.00	626.85	426.39	458.96	113.70	400.00	0.550
	45	2614.73	62.69	220.00	626.85	426.39	458.96	113.70	400.00	0.550
	50	2625.85	66.12	212.81	625.35	435.88	468.74	115.23	400.00	0.532
0.99	25	2614.73	62.69	220.00	626.85	426.39	458.96	113.70	400.00	0.550
	30	2614.73	62.69	220.00	626.85	426.39	458.96	113.70	400.00	0.550
	35	2614.73	62.69	220.00	626.85	426.39	458.96	113.70	400.00	0.550
	40	2617.31	63.64	218.00	624.86	431.76	466.25	108.65	400.00	0.545
	45	2632.91	68.17	208.56	626.85	437.22	470.56	121.66	400.01	0.521

Table 4.38 Reliability based design optimization results for concrete with fly ash for 56 days curing age using LPCR model

Target Reliability R	Target $st56$ (MPa)	$cost$ $(Rs.)$	Predicted $st56$ (MPa)	w $\left(kg/m^3\right)$	fa $\left(kg/m^3\right)$	$ca-I$ $\left(kg/m^3\right)$	$ca-II$ $\left(kg/m^3\right)$	$ca-III$ $\left(kg/m^3\right)$	cm $\left(kg/m^3\right)$	w/cm
0.90	25	2614.73	33.27	220.00	626.85	426.39	458.96	113.70	400.00	0.550
	30	2643.25	36.66	202.07	623.78	445.11	480.62	124.28	400.00	0.505
	35	2702.16	41.28	194.60	572.30	444.86	489.31	179.57	409.53	0.475
	40	2719.15	46.04	191.21	454.03	482.40	546.44	218.51	408.53	0.468
	45	2763.22	50.73	180.00	416.93	507.24	614.25	189.36	415.65	0.433
	50	2951.39	55.00	198.80	416.93	462.76	574.62	169.89	473.33	0.420
0.95	25	2619.67	33.88	216.91	625.92	429.85	463.06	115.36	400.00	0.542
	30	2659.22	38.54	192.07	622.09	455.20	492.44	130.75	400.00	0.480
	35	2724.94	43.00	187.89	571.59	450.36	495.70	183.25	412.76	0.455
	40	2740.83	47.70	184.32	453.47	488.09	553.03	222.44	411.38	0.448
	45	2815.25	52.44	181.40	416.94	495.45	614.25	184.10	430.06	0.422
0.99	25	2650.28	37.51	197.75	622.24	449.67	486.48	126.90	400.03	0.494
	30	2721.11	41.70	187.60	622.32	453.97	491.07	131.44	414.54	0.453
	35	2765.39	46.14	180.00	552.77	463.39	513.55	186.85	419.71	0.429
	40	2775.27	50.73	180.00	416.93	505.29	577.92	224.54	417.78	0.431
	45	2920.57	54.55	194.81	416.93	471.51	592.81	162.71	463.83	0.420

Table 4.39 Reliability based design optimization results for concrete with fly ash for 91 days curing age using QGRR model

Target Reliability R	Target $st91$ (MPa)	$cost$ $(Rs.)$	Predicted $st91$ (MPa)	w $\left(kg/m^3\right)$	fa $\left(kg/m^3\right)$	$ca-I$ $\left(kg/m^3\right)$	$ca-II$ $\left(kg/m^3\right)$	$ca-III$ $\left(kg/m^3\right)$	cm $\left(kg/m^3\right)$	w/cm
0.90	30	2614.73	41.39	220.00	626.85	426.39	458.96	113.70	400.00	0.550
	35	2614.73	41.39	220.00	626.85	426.39	458.96	113.70	400.00	0.550
	40	2644.67	46.02	201.35	626.18	443.32	477.36	128.49	400.03	0.503
	45	2712.31	51.81	184.93	554.31	441.43	492.82	225.74	406.45	0.455
	50	2810.82	57.01	180.82	547.84	435.26	491.39	228.78	430.52	0.420
	55	-	-	-	-	-	-	-	-	-
0.95	30	2614.73	41.39	220.00	626.85	426.39	458.96	113.70	400.00	0.550
	35	2614.73	41.39	220.00	626.85	426.39	458.96	113.70	400.00	0.550
	40	2655.87	48.03	194.21	626.85	449.51	484.77	133.28	400.00	0.486
	45	2731.22	53.91	180.00	558.51	442.36	495.97	227.66	409.51	0.440
	50	2903.66	58.16	197.60	626.85	382.61	614.25	0.00	470.49	0.420
0.99	30	2614.73	41.39	220.00	626.85	426.39	458.96	113.70	400.00	0.550
	35	2630.70	44.95	205.77	626.69	457.19	513.92	67.65	400.00	0.514
	40	2676.67	52.16	180.86	626.85	461.92	502.18	139.07	400.00	0.452
	45	2827.11	57.17	183.46	558.79	423.32	502.47	205.84	436.81	0.420
	50	-	-	-	-	-	-	-	-	-

Table 4.40 Reliability based design optimization results for concrete with fly ash for 91 days curing age using QTRR model

Target Reliability R	Target $st91$ (MPa)	$cost$ $(Rs.)$	Predicted $st91$ (MPa)	w $\left(kg/m^3\right)$	fa $\left(kg/m^3\right)$	$ca-I$ $\left(kg/m^3\right)$	$ca-II$ $\left(kg/m^3\right)$	$ca-III$ $\left(kg/m^3\right)$	cm $\left(kg/m^3\right)$	w/cm
0.90	30	2795.75	53.66	197.87	610.07	397.49	614.25	28.88	440.83	0.449
	35	2898.85	59.12	207.29	614.03	385.67	596.60	0.00	472.80	0.438
	40	-	-	-	-	-	-	-	-	-
	45	-	-	-	-	-	-	-	-	-
	50	-	-	-	-	-	-	-	-	-
	55	-	-	-	-	-	-	-	-	-
0.95	30	2932.30	51.96	199.70	564.87	393.53	568.60	87.81	474.70	0.421
	35	-	-	-	-	-	-	-	-	-
	40	-	-	-	-	-	-	-	-	-
	45	-	-	-	-	-	-	-	-	-
	50	-	-	-	-	-	-	-	-	-
0.99	30	-	-	-	-	-	-	-	-	-
	35	-	-	-	-	-	-	-	-	-
	40	-	-	-	-	-	-	-	-	-
	45	-	-	-	-	-	-	-	-	-
	50	-	-	-	-	-	-	-	-	-

Table 4.41 Reliability based design optimization results for concrete with fly ash for 91 days curing age using QPCR model

Target Reliability R	Target $st91$ (MPa)	$cost$ $(Rs.)$	Predicted $st91$ (MPa)	w $\left(kg/m^3\right)$	fa $\left(kg/m^3\right)$	$ca-I$ $\left(kg/m^3\right)$	$ca-II$ $\left(kg/m^3\right)$	$ca-III$ $\left(kg/m^3\right)$	cm $\left(kg/m^3\right)$	w/cm
0.90	30	2614.73	39.83	220.00	626.85	426.39	458.96	113.70	400.00	0.550
	35	2629.35	41.63	211.11	620.15	438.44	472.35	118.98	400.00	0.528
	40	2691.83	46.03	193.67	617.61	449.67	485.21	135.39	408.99	0.474
	45	2715.54	50.54	188.91	486.93	467.56	523.08	229.11	407.14	0.464
	50	2751.03	55.00	180.00	416.93	526.87	614.25	172.69	413.02	0.436
	55	2954.54	59.15	199.49	416.93	442.71	614.25	147.59	475.00	0.420
0.95	30	2614.73	39.83	220.00	626.85	426.39	458.96	113.70	400.00	0.550
	35	2647.01	43.44	199.92	622.54	447.53	481.91	127.52	400.01	0.500
	40	2716.08	47.63	187.39	616.07	454.96	491.02	139.10	412.74	0.454
	45	2737.42	52.02	181.95	486.55	473.33	529.44	233.19	410.01	0.444
	50	2793.41	56.25	180.00	416.93	521.54	604.48	177.32	424.06	0.424
0.99	30	2639.47	42.63	204.63	622.90	442.95	477.01	124.10	400.01	0.512
	35	2701.66	46.51	192.15	620.89	451.53	486.40	131.00	411.20	0.467
	40	2757.44	50.45	180.43	594.23	468.19	507.66	143.92	420.19	0.429
	45	2756.63	54.70	180.00	416.93	506.22	572.58	233.51	412.59	0.436
	50	2872.37	58.29	191.25	416.93	635.24	614.25	0.00	455.35	0.420

Table 4.42 Reliability based design optimization results for concrete with fly ash for 91 days curing age using LGRR model

Target Reliability R	Target $st91$ (MPa)	$cost$ $(Rs.)$	Predicted $st91$ (MPa)	w $\left(kg/m^3\right)$	fa $\left(kg/m^3\right)$	$ca-I$ $\left(kg/m^3\right)$	$ca-II$ $\left(kg/m^3\right)$	$ca-III$ $\left(kg/m^3\right)$	cm $\left(kg/m^3\right)$	w/cm
0.90	30	2614.73	39.58	220.00	626.85	426.39	458.96	113.70	400.00	0.550
	35	2635.75	42.83	210.84	626.84	434.18	466.96	120.69	401.69	0.525
	40	2685.23	47.56	197.03	543.21	433.75	483.01	225.01	403.86	0.488
	45	2706.50	52.34	181.67	552.39	443.53	493.67	236.30	403.24	0.451
	50	2809.28	56.71	180.63	548.67	436.01	491.15	228.32	430.08	0.420
	55	-	-	-	-	-	-	-	-	-
0.95	30	2618.80	40.40	217.44	626.85	428.86	461.44	115.55	400.00	0.544
	35	2642.15	45.08	202.84	626.85	442.27	475.23	127.10	400.01	0.507
	40	2699.00	49.66	191.07	547.36	437.30	486.62	228.13	405.13	0.472
	45	2728.35	54.24	180.00	602.78	440.07	507.24	171.74	411.58	0.437
	50	2966.47	57.86	199.39	626.59	0.00	614.25	362.72	475.00	0.420
0.99	30	2640.19	44.69	204.06	626.85	441.18	474.07	126.09	400.01	0.510
	35	2676.08	49.09	192.87	626.77	449.71	482.62	134.29	404.79	0.476
	40	2723.59	53.58	180.00	562.34	443.45	495.09	225.20	407.67	0.442
	45	2815.77	57.20	185.99	625.35	441.11	614.25	0.00	442.83	0.420
	50	-	-	-	-	-	-	-	-	-

Table 4.43 Reliability based design optimization results for concrete with fly ash for 91 days curing age using LTRR/LOLSR model

Target Reliability R	Target $st91$ (MPa)	$cost$ $(Rs.)$	Predicted $st91$ (MPa)	w $\left(kg/m^3\right)$	fa $\left(kg/m^3\right)$	$ca-I$ $\left(kg/m^3\right)$	$ca-II$ $\left(kg/m^3\right)$	$ca-III$ $\left(kg/m^3\right)$	cm $\left(kg/m^3\right)$	w/cm
0.90	30	2614.73	39.71	220.00	626.85	426.39	458.96	113.70	400.00	0.550
	35	2634.21	42.41	211.78	626.82	433.28	466.33	119.74	401.68	0.527
	40	2666.16	47.13	196.73	626.80	445.88	479.74	131.72	403.77	0.487
	45	2701.89	51.94	180.00	553.14	447.46	499.72	231.86	401.50	0.448
	50	2824.65	56.25	182.57	529.83	439.25	507.20	219.67	434.69	0.420
	55	-	-	-	-	-	-	-	-	-
0.95	30	2615.51	39.86	219.48	626.85	427.10	459.74	113.61	400.00	0.549
	35	2641.13	44.54	203.46	626.68	441.67	475.30	126.18	400.01	0.509
	40	2680.89	49.12	190.58	626.77	451.04	485.19	136.21	405.08	0.470
	45	2733.09	53.70	180.00	552.28	456.16	546.17	170.03	411.62	0.437
	50	2897.69	57.66	191.79	416.93	468.76	613.66	159.50	456.65	0.420
0.99	30	2637.82	43.93	205.55	626.60	439.81	473.28	124.59	400.01	0.514
	35	2676.98	48.32	193.52	626.77	448.78	482.63	133.006	405.32	0.477
	40	2710.37	52.79	180.00	620.96	463.12	507.10	133.63	408.57	0.441
	45	2811.02	56.79	181.00	477.18	458.05	614.13	159.08	430.94	0.420
	50	-	-	-	-	-	-	-	-	-

Table 4.44 Reliability based design optimization results for concrete with fly ash for 91 days curing age using LPCR model

Target Reliability R	Target $st91$ (MPa)	$cost$ $(Rs.)$	Predicted $st91$ (MPa)	w $\left(kg/m^3\right)$	fa $\left(kg/m^3\right)$	$ca-I$ $\left(kg/m^3\right)$	$ca-II$ $\left(kg/m^3\right)$	$ca-III$ $\left(kg/m^3\right)$	cm $\left(kg/m^3\right)$	w/cm
0.90	30	2614.73	40.32	220.00	626.85	426.39	458.96	113.70	400.00	0.550
	35	2620.47	40.91	216.42	625.76	430.44	463.42	115.85	400.00	0.541
	40	2688.32	45.54	195.93	623.10	447.67	482.48	128.22	409.31	0.479
	45	2715.14	50.30	194.12	472.62	468.53	524.17	226.70	408.83	0.475
	50	2743.39	55.02	180.00	416.93	579.29	609.75	126.50	412.66	0.436
	55	2948.61	59.32	199.24	416.93	498.13	586.08	122.38	474.37	0.420
0.95	30	2614.73	40.32	220.00	626.85	426.39	458.96	113.70	400.00	0.550
	35	2631.97	42.58	210.43	603.57	446.68	482.86	119.54	400.00	0.526
	40	2711.64	47.06	189.22	622.12	453.31	488.72	132.07	412.66	0.459
	45	2737.41	51.75	187.29	471.84	474.26	530.51	230.78	411.85	0.455
	50	2797.42	56.74	180.00	417.30	564.71	614.17	123.02	426.98	0.422
0.99	30	2599.97	41.18	220.00	593.66	693.62	343.95	0.00	400.00	0.550
	35	2688.65	45.48	196.98	622.48	446.90	481.67	127.16	409.84	0.481
	40	2680.21	50.20	187.24	481.74	521.19	581.10	136.94	400.00	0.468
	45	2752.16	54.53	180.00	416.93	504.14	570.10	239.17	411.23	0.438
	50	2884.65	58.43	191.22	416.93	540.28	611.95	94.51	455.28	0.420

Table 4.45 Assumed standard deviation

Grade of concrete	Assumed standard deviation (MPa)
M10 M15	3.5
M20 M25	4.0
M30 M35 M40 M45 M50 M55	5.0

Table 4.46 Safety factor based DDO results for concrete without fly ash for 28 days curing age using QGRR model

Target $st28$ (MPa)	Safety margin (MPa)	$cost$ $(Rs.)$	Predicted $st28$ (MPa)	w $\left(kg/m^3\right)$	fa $\left(kg/m^3\right)$	$ca-I$ $\left(kg/m^3\right)$	$ca-II$ $\left(kg/m^3\right)$	$ca-III$ $\left(kg/m^3\right)$	c $\left(kg/m^3\right)$	w/c	Reliability
25	6.60	2704.28	37.12	192.46	641.13	614.77	518.58	0.00	350.00	0.550	0.818
30	8.25	2707.16	38.35	191.11	642.18	579.00	557.22	0.00	350.00	0.546	0.739
35	8.25	2720.44	43.27	182.51	638.02	586.18	577.25	0.00	350.00	0.521	0.756
40	8.25	2785.44	48.31	180.02	641.58	530.41	625.12	0.00	363.32	0.495	0.788
45	8.25	2919.15	53.96	180.00	642.13	503.33	625.88	0.00	392.90	0.458	0.857
50	8.25	3075.25	58.26	180.00	640.23	239.29	614.60	246.11	420.19	0.428	0.883

Table 4.47 Safety factor based DDO results for concrete without fly ash for 28 days curing age using QTRR/QOLSR model

Target $st28$ (MPa)	Safety margin (MPa)	$cost$ $(Rs.)$	Predicted $st28$ (MPa)	w $\left(kg/m^3\right)$	fa $\left(kg/m^3\right)$	$ca-I$ $\left(kg/m^3\right)$	$ca-II$ $\left(kg/m^3\right)$	$ca-III$ $\left(kg/m^3\right)$	c $\left(kg/m^3\right)$	w/c	Reliability
25	6.60	2706.79	37.79	192.12	632.91	575.43	565.06	2.52	350.00	0.549	0.824
30	8.25	2708.57	38.45	192.64	640.84	573.08	544.18	15.52	350.38	0.550	0.735
35	8.25	2722.88	43.25	183.68	642.06	532.54	589.76	32.57	350.00	0.525	0.757
40	8.25	2760.44	48.25	180.00	642.18	581.38	456.43	120.06	355.08	0.507	0.796
45	8.25	2892.21	53.27	180.01	619.41	570.42	380.12	205.91	381.60	0.472	0.877
50	8.25	3086.41	58.28	180.01	416.94	520.11	413.52	402.45	414.89	0.434	0.936

Table 4.48 Safety factor based DDO results for concrete without fly ash for 28 days curing age using QPCR model

Target $st28$ (MPa)	Safety margin (MPa)	$cost$ $(Rs.)$	Predicted $st28$ (MPa)	w $\left(kg/m^3\right)$	fa $\left(kg/m^3\right)$	$ca-I$ $\left(kg/m^3\right)$	$ca-II$ $\left(kg/m^3\right)$	$ca-III$ $\left(kg/m^3\right)$	c $\left(kg/m^3\right)$	w/c	Reliability
25	6.60	2711.50	33.69	192.59	641.19	500.53	603.84	27.79	350.39	0.550	0.843
30	8.25	2737.00	38.25	180.11	550.57	617.55	613.89	29.45	350.31	0.514	0.850
35	8.25	2806.97	43.24	180.00	416.93	721.73	622.26	47.37	362.74	0.496	0.876
40	8.25	2993.76	48.28	180.01	432.18	445.61	624.63	268.40	397.73	0.453	0.912
45	8.25	3115.58	53.28	181.77	416.93	699.83	626.02	0.760	432.97	0.420	0.942
50	8.25	-	-	-	-	-	-	-	-	-	-

Table 4.49 Safety factor based DDO results for concrete without fly ash for 28 days curing age using LGRR model

Target $st28$ (MPa)	Safety margin (MPa)	$cost$ $(Rs.)$	Predicted $st28$ (MPa)	w $\left(kg/m^3\right)$	fa $\left(kg/m^3\right)$	$ca-I$ $\left(kg/m^3\right)$	$ca-II$ $\left(kg/m^3\right)$	$ca-III$ $\left(kg/m^3\right)$	c $\left(kg/m^3\right)$	w/c	Reliability
25	6.60	2706.77	38.08	192.50	641.07	543.62	579.49	9.90	350.00	0.550	0.874
30	8.25	2707.87	38.49	192.54	641.41	496.27	625.30	11.05	350.01	0.550	0.772
35	8.25	2774.39	43.34	180.65	599.41	323.65	556.20	318.33	351.36	0.514	0.777
40	8.25	2841.70	48.30	180.00	640.28	266.14	557.77	320.18	366.63	0.491	0.793
45	8.25	2970.98	53.30	180.17	627.08	239.62	549.96	342.96	394.42	0.457	0.818
50	8.25	3064.59	58.32	180.00	642.16	223.87	622.74	253.49	417.59	0.431	0.839

Table 4.50 Safety factor based DDO results for concrete without fly ash for 28 days curing age using LTRR/LOLSR model

Target $st28$ (MPa)	Safety margin (MPa)	$cost$ $(Rs.)$	Predicted $st28$ (MPa)	w $\left(kg/m^3\right)$	fa $\left(kg/m^3\right)$	$ca-I$ $\left(kg/m^3\right)$	$ca-II$ $\left(kg/m^3\right)$	$ca-III$ $\left(kg/m^3\right)$	c $\left(kg/m^3\right)$	w/c	Reliability
25	6.60	2706.77	38.51	192.50	641.07	543.62	579.49	9.90	350.00	0.550	0.876
30	8.25	2706.97	39.08	192.40	642.18	503.24	626.03	3.23	350.00	0.550	0.782
35	8.25	2745.18	43.26	184.29	641.53	336.52	609.64	202.60	350.00	0.527	0.768
40	8.25	2857.80	48.25	180.00	617.95	271.49	536.08	356.59	368.86	0.488	0.786
45	8.25	2965.85	53.26	180.07	624.96	259.62	527.01	349.05	393.17	0.458	0.809
50	8.25	3074.06	58.31	180.00	642.14	233.83	535.58	328.19	417.88	0.431	0.832

Table 4.51 Safety factor based DDO results for concrete without fly ash for 28 days curing age using LPCR model

Target $st28$ (MPa)	Safety margin (MPa)	$cost$ $(Rs.)$	Predicted $st28$ (MPa)	w $\left(kg/m^3\right)$	fa $\left(kg/m^3\right)$	$ca-I$ $\left(kg/m^3\right)$	$ca-II$ $\left(kg/m^3\right)$	$ca-III$ $\left(kg/m^3\right)$	c $\left(kg/m^3\right)$	w/c	Reliability
25	6.60	2706.55	33.42	192.36	642.18	526.30	604.98	1.65	350.00	0.550	0.858
30	8.25	2722.23	38.29	192.04	481.51	669.95	624.76	7.34	350.35	0.548	0.870
35	8.25	2846.69	43.26	180.00	416.93	455.58	608.00	318.10	363.69	0.495	0.889
40	8.25	2945.42	48.27	180.00	416.93	717.33	574.44	72.61	392.83	0.458	0.912
45	8.25	3078.66	53.23	180.00	416.93	713.01	626.02	1.32	424.06	0.424	0.932
50	8.25	-	-	-	-	-	-	-	-	-	

Table 4.52 Safety factor based DDO results for concrete with fly ash for 28 days curing age using QGRR model

Target $st28$ (MPa)	Safety margin (MPa)	$cost$ $(Rs.)$	Predicted $st28$ (MPa)	w $\left(kg/m^3\right)$	fa $\left(kg/m^3\right)$	$ca-I$ $\left(kg/m^3\right)$	$ca-II$ $\left(kg/m^3\right)$	$ca-III$ $\left(kg/m^3\right)$	cm $\left(kg/m^3\right)$	w/cm	Reliability
25	6.60	2637.02	31.60	214.17	626.05	309.73	491.78	211.03	400.00	0.535	0.796
30	8.25	2655.54	42.58	185.69	624.80	490.58	587.25	18.34	400.03	0.464	0.926
35	8.25	2667.10	44.15	180.54	626.80	602.18	430.09	73.87	400.01	0.451	0.868
40	8.25	2765.38	48.27	180.00	626.64	635.13	442.12	6.51	427.95	0.421	0.860
45	8.25	2889.11	48.95	190.41	510.91	204.58	453.09	306.40	474.82	0.401	0.793

Table 4.53 Safety factor based DDO results for concrete with fly ash for 28 days curing age using QTRR model

Target $st28$ (MPa)	Safety margin (MPa)	$cost$ $(Rs.)$	Predicted $st28$ (MPa)	w $\left(kg/m^3\right)$	fa $\left(kg/m^3\right)$	$ca-I$ $\left(kg/m^3\right)$	$ca-II$ $\left(kg/m^3\right)$	$ca-III$ $\left(kg/m^3\right)$	cm $\left(kg/m^3\right)$	w/cm	Reliability
25	6.60	2681.98	33.37	192.03	625.69	225.61	550.41	293.86	400.00	0.480	0.815
30	8.25	2710.45	38.28	183.49	604.91	149.47	566.28	395.59	400.11	0.459	0.774
35	8.25	2715.66	43.31	183.16	626.35	55.32	589.18	443.57	400.03	0.458	0.738
40	8.25	2882.54	44.56	191.59	508.57	193.83	454.49	305.27	474.94	0.403	0.708
45	8.25	-	-	-	-	-	-	-	-	-	-

Table 4.54 Safety factor based DDO results for concrete with fly ash for 28 days curing age using QPCR model

Target $st28$ (MPa)	Safety margin (MPa)	$cost$ $(Rs.)$	Predicted $st28$ (MPa)	w $\left(kg/m^3\right)$	fa $\left(kg/m^3\right)$	$ca-I$ $\left(kg/m^3\right)$	$ca-II$ $\left(kg/m^3\right)$	$ca-III$ $\left(kg/m^3\right)$	cm $\left(kg/m^3\right)$	w/cm	Reliability
25	6.60	2628.30	31.60	217.96	503.60	462.63	569.31	102.79	400.00	0.545	0.886
30	8.25	2682.23	38.26	197.57	416.93	450.53	604.16	222.62	400.04	0.494	**0.952**
35	8.25	2772.39	43.28	180.00	417.60	431.93	556.13	319.60	413.84	0.435	**0.967**
40	8.25	2876.65	48.26	191.85	416.93	630.43	614.23	1.29	456.75	0.420	**0.982**
45	8.25	-	-	-	-	-	-	-	-	-	-

Table 4.55 Safety factor based DDO results for concrete with fly ash for 28 days curing age using QOLSR model

Target $st28$ (MPa)	Safety margin (MPa)	$cost$ $(Rs.)$	Predicted $st28$ (MPa)	w $\left(kg/m^3\right)$	fa $\left(kg/m^3\right)$	$ca-I$ $\left(kg/m^3\right)$	$ca-II$ $\left(kg/m^3\right)$	$ca-III$ $\left(kg/m^3\right)$	cm $\left(kg/m^3\right)$	w/cm	Reliability
25	6.60	2677.70	35.37	210.05	626.83	39.16	614.25	361.52	403.24	0.521	0.603
30	8.25	2789.28	47.20	186.90	625.05	38.12	612.42	409.44	421.91	0.443	0.671
35	8.25	2679.87	44.03	207.71	626.85	0.00	570.90	450.60	400.00	0.519	0.578
40	8.25	2692.91	48.60	198.30	625.78	1.00	609.15	438.08	400.00	0.496	0.575
45	8.25	-	-	-	-	-	-	-	-	-	-

Table 4.56 Safety factor based DDO results for concrete with fly ash for 28 days curing age using LGRR model

Target $st28$ (MPa)	Safety margin (MPa)	$cost$ $(Rs.)$	Predicted $st28$ (MPa)	w $\left(kg/m^3\right)$	fa $\left(kg/m^3\right)$	$ca-I$ $\left(kg/m^3\right)$	$ca-II$ $\left(kg/m^3\right)$	$ca-III$ $\left(kg/m^3\right)$	cm $\left(kg/m^3\right)$	w/cm	Reliability
25	6.60	2652.74	31.61	205.97	623.99	283.69	518.42	233.72	400.00	0.515	0.821
30	8.25	2686.58	38.26	188.16	626.85	268.15	517.66	292.86	400.00	0.470	0.882
35	8.25	2744.44	43.25	180.03	601.41	252.61	539.88	324.27	410.31	0.439	0.893
40	8.25	2903.13	48.26	195.25	625.43	262.88	581.89	161.07	463.93	0.421	0.922
45	8.25	-	-	-	-	-	-	-	-	-	-

Table 4.57 Safety factor based DDO results for concrete with fly ash for 28 days curing age using LTRR model

Target $st28$ (MPa)	Safety margin (MPa)	$cost$ $(Rs.)$	Predicted $st28$ (MPa)	w $\left(kg/m^3\right)$	fa $\left(kg/m^3\right)$	$ca-I$ $\left(kg/m^3\right)$	$ca-II$ $\left(kg/m^3\right)$	$ca-III$ $\left(kg/m^3\right)$	cm $\left(kg/m^3\right)$	w/cm	Reliability
25	6.60	2648.28	31.67	206.53	626.85	281.07	562.42	189.10	400.40	0.516	0.824
30	8.25	2648.87	38.25	189.07	626.85	465.44	614.25	4.85	400.08	0.473	0.882
35	8.25	2737.52	43.27	180.01	626.85	261.22	612.40	217.80	412.35	0.437	0.894
40	8.25	2874.98	48.28	193.76	626.85	401.89	613.63	0.20	461.43	0.420	0.921
45	8.25	-	-	-	-	-	-	-	-	-	-

Table 4.58 Safety factor based DDO results for concrete with fly ash for 28 days curing age using LPCR model

Target $st28$ (MPa)	Safety margin (MPa)	$cost$ $(Rs.)$	Predicted $st28$ (MPa)	w $\left(kg/m^3\right)$	fa $\left(kg/m^3\right)$	$ca-I$ $\left(kg/m^3\right)$	$ca-II$ $\left(kg/m^3\right)$	$ca-III$ $\left(kg/m^3\right)$	cm $\left(kg/m^3\right)$	w/cm	Reliability
25	6.60	2625.27	31.61	220.00	511.79	407.89	612.46	100.48	400.00	0.550	0.902
30	8.25	2649.03	38.31	201.73	416.93	657.54	614.25	0.28	400.69	0.503	**0.957**
35	8.25	2777.80	43.25	180.81	419.45	358.37	581.45	362.32	413.98	0.437	**0.965**
40	8.25	2859.82	48.23	189.46	416.93	647.45	612.03	0.00	451.18	0.420	**0.977**
45	8.25	-	-	-	-	-	-	-	-	-	-

Table 4.59 Safety factor based DDO results for concrete with fly ash for 28 days curing age using LOLSR model

Target $st28$ (MPa)	Safety margin (MPa)	$cost$ $(Rs.)$	Predicted $st28$ (MPa)	w $\left(kg/m^3\right)$	fa $\left(kg/m^3\right)$	$ca-I$ $\left(kg/m^3\right)$	$ca-II$ $\left(kg/m^3\right)$	$ca-III$ $\left(kg/m^3\right)$	cm $\left(kg/m^3\right)$	w/cm	Reliability
25	6.60	2620.35	31.68	209.02	626.85	426.27	603.80	1.39	400.40	0.522	0.806
30	8.25	2645.74	38.32	192.38	626.85	457.00	614.25	5.02	400.40	0.480	0.865
35	8.25	2729.82	43.32	180.03	612.70	249.34	526.36	332.84	406.42	0.443	0.874
40	8.25	2800.63	48.30	180.20	626.85	219.67	612.79	243.23	428.10	0.421	0.889
45	8.25	-	-	-	-	-	-	-	-	-	-

Table 4.60 Percentage rise in cost with reliability level for concrete without fly ash for 28 days curing age

28 days compressive strength Model	Percentage rise in cost to raise the reliability level from 0.90 to 0.95	Percentage rise in cost to raise the reliability level from 0.90 to 0.95
QGRR model	2.50-3.59	4.68-4.75
QTRR/OLSR model	0.00-4.20	5.61-7.61
QPCR model	2.20-4.50	4.05-4.72
LGRR model	1.54-2.65	4.57-4.94
LTRR/LOLSR model	1.58-3.53	4.60-4.77
LPCR model	1.99-5.89	0.97-4.61

Table 4.61 Percentage rise in cost with reliability level for concrete without fly ash for 56 days curing age

56 days compressive strength Model	Percentage rise in cost to raise the reliability level from 0.90 to 0.95	Percentage rise in cost to raise the reliability level from 0.90 to 0.95
QGRR model	0.31-2.48	3.02-5.15
QPCR model	1.01-2.32	4.10-4.61
LGRR model	0.00-6.70	4.41-7.24
LTRR model	0.94-4.75	4.48-6.81
LPCR model	0.00-2.17	3.72-6.15

Table 4.62 Percentage rise in cost with reliability level for concrete without fly ash for 91 days curing age

91 days compressive strength Model	Percentage rise in cost to raise the reliability level from 0.90 to 0.95	Percentage rise in cost to raise the reliability level from 0.90 to 0.95
QGRR model	0.00-4.04	3.70-6.17
QTRR model	0.16-2.83	-0.53-7.56
QPCR model	0.00-2.28	2.85-4.27
QOLSR model	0.70-3.33	3.49-5.06
LGRR model	0.00-2.55	2.68-4.77
LTRR model	0.00-2.67	2.58-4.94
LPCR model	0.00-5.50	1.07-4.13

Table 4.63 Percentage of various types of coarse aggregates in total coarse aggregate component for concrete without fly ash for 28 days curing age

Model	Percentage of $ca-I$ in total coarse aggregate component	Percentage of $ca-II$ in total coarse aggregate component	Percentage of $ca-III$ in total coarse aggregate component
QGRR model	29-31	46-50	20-25
QTRR/QOLSR model	31-45	28-47	15-23
QPCR model	30-31	47-50	19-22
LGRR model	27-31	47-54	19-23
LTRR/LOLSR model	29-31	47-50	20-22
LPCR model	30-42	46-50	0.07-22

Table 4.64 Percentage of various types of coarse aggregates in total coarse aggregate component for concrete without fly ash for 56 days curing age

Model	Percentage of $ca-I$ in total coarse aggregate component	Percentage of $ca-II$ in total coarse aggregate component	Percentage of $ca-III$ in total coarse aggregate component
QGRR model	27-31	47-50	22-26
QPCR model	30-31	47-52	18-22
LGRR model	27-31	47-57	13-22
LTRR model	28-31	47-58	16-22
LPCR model	30-50	47-51	19-22

Table 4.65 Percentage of various types of coarse aggregates in total coarse aggregate component for concrete without fly ash for 91 days curing age

Model	Percentage of $ca-I$ in total coarse aggregate component	Percentage of $ca-II$ in total coarse aggregate component	Percentage of $ca-III$ in total coarse aggregate component
QGRR model	24-35	42-48	22-33
QTRR model	31-63	33-47	10-22
QPCR model	31-50	47-50	0-22
QOLSR model	27-31	47-54	18-22
LGRR model	26-31	47-59	16-22
LTRR/LOLSR model	0.02-31	47-58	20-41
LPCR model	30-34	47-50	19-22

Table 4.66 Percentage rise in cost with reliability level for concrete with fly ash for 28 days curing age

28 days compressive strength Model	Percentage rise in cost to raise the reliability level from 0.90 to 0.95	Percentage rise in cost to raise the reliability level from 0.90 to 0.95
QGRR model	0.47-0.52	1.15-6.89
QTRR model	-1.03-1.47	5.03
QPCR model	0.81-2.00	1.62-5.22
LGRR model	0.52-1.90	0.77-2.41
LTRR model	0.53-1.72	1.19-2.46
LPCR model	0.88-1.94	-0.73-2.91
LOLSR model	0.53-2.04	0.7-1.92

Table 4.67 Percentage rise in cost with reliability level for concrete with fly ash for 56 days curing age

56 days compressive strength Model	Percentage rise in cost to raise the reliability level from 0.90 to 0.95	Percentage rise in cost to raise the reliability level from 0.90 to 0.95
QGRR model	0.48-4.91	0.42-7.87
QPCR model	-0.57-2.00	-0.04-4.17
LGRR model	0.44-1.02	0.44-7.72
LPCR model	0.19-1.88	1.17-3.74

Table 4.68 Percentage rise in cost with reliability level for concrete with fly ash for 91 days curing age

91 days compressive strength Model	Percentage rise in cost to raise the reliability level from 0.90 to 0.95	Percentage rise in cost to raise the reliability level from 0.90 to 0.95
QGRR model	0.00-3.00	0.00-3.51
QPCR model	0.00-1.54	0.70-2.83
LGRR model	0.16-5.60	0.82-3.20
LTRR/LOLSR model	0.03-2.59	0.85-2.85
LPCR model	0.00-1.97	-0.56-3.12

Table 4.69 Percentage of various types of coarse aggregates in total coarse aggregate component for concrete with fly ash for 28 days curing age

Model	Percentage of $ca-I$ in total coarse aggregate component	Percentage of $ca-II$ in total coarse aggregate component	Percentage of $ca-III$ in total coarse aggregate component
QGRR model	8-41	42-46	14-46
QTRR model	38-40	45-60	0-17
QPCR model	38-42	42-46	12-20
LGRR model	38-42	43-46	12-19
LTRR model	39-45	43-57	0-18
LPCR model	38-47	43-51	3-19
LOLSR model	37-44	43-56	0-19

Table 4.70 Percentage of various types of coarse aggregates in total coarse aggregate component for concrete with fly ash for 56 days curing age

Model	Percentage of $ca-I$ in total coarse aggregate component	Percentage of $ca-II$ in total coarse aggregate component	Percentage of $ca-III$ in total coarse aggregate component
QGRR model	33-42	43-51	12-19
QPCR model	38-43	43-47	11-18
LGRR model	28-49	42-51	0-20
LPCR model	38-43	44-48	11-18

Table 4.71 Percentage of various types of coarse aggregates in total coarse aggregate component for concrete with fly ash for 91 days curing age

Model	Percentage of $ca-I$ in total coarse aggregate component	Percentage of $ca-II$ in total coarse aggregate component	Percentage of $ca-III$ in total coarse aggregate component
QGRR model	37-44	42-62	0-18
QPCR model	37-43	43-51	11-19
LGRR model	38-43	42-63	11-37
LTRR/LOLSR model	37-43	42-50	11-20
LPCR model	38-67	33-49	0-19

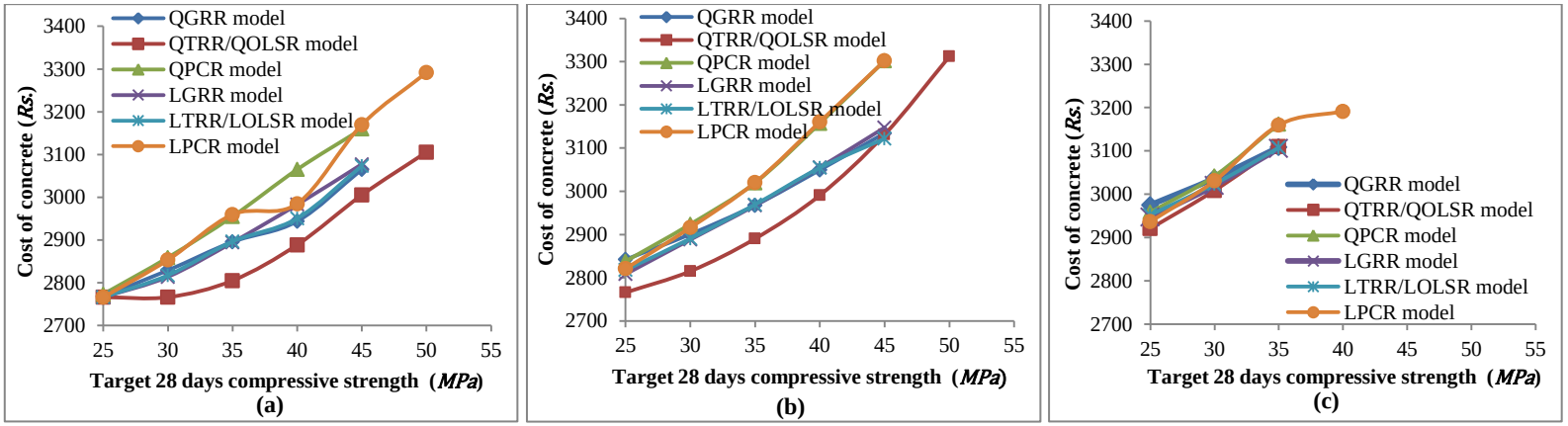

Figure 4.1 Variation of cost of concrete with target 28 days compressive strength for different compressive strength models with (a) R = 0.90 (b) R = 0.95 and (c) R = 0.99 for concrete without fly ash

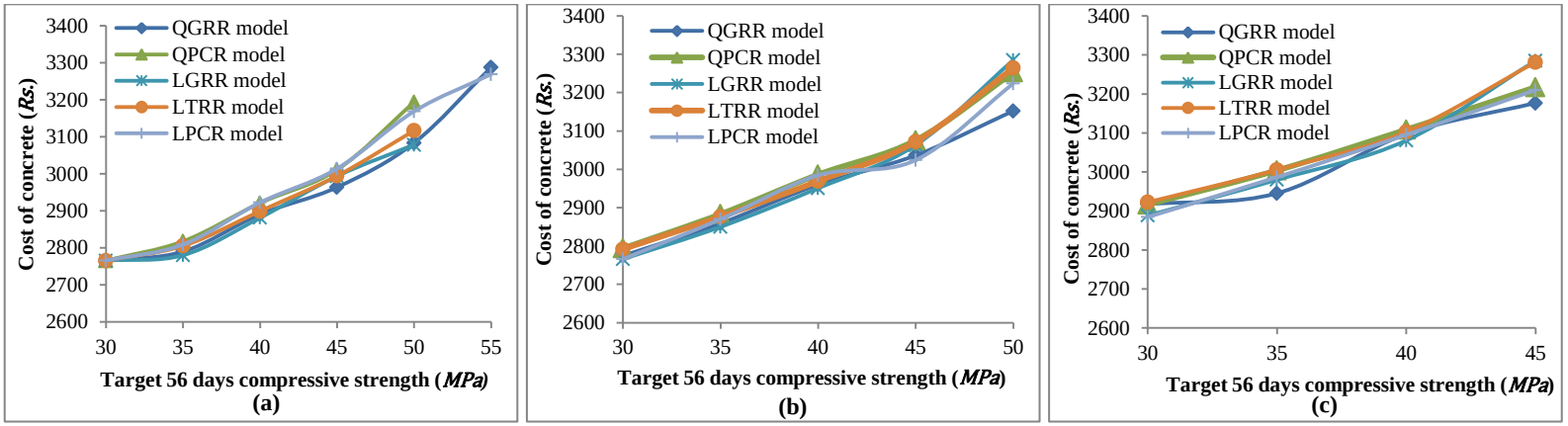

Figure 4.2 Variation of cost of concrete with target 56 days compressive strength for different compressive strength models with (a) R = 0.90 (b) R = 0.95 and (c) R = 0.99 for concrete without fly ash

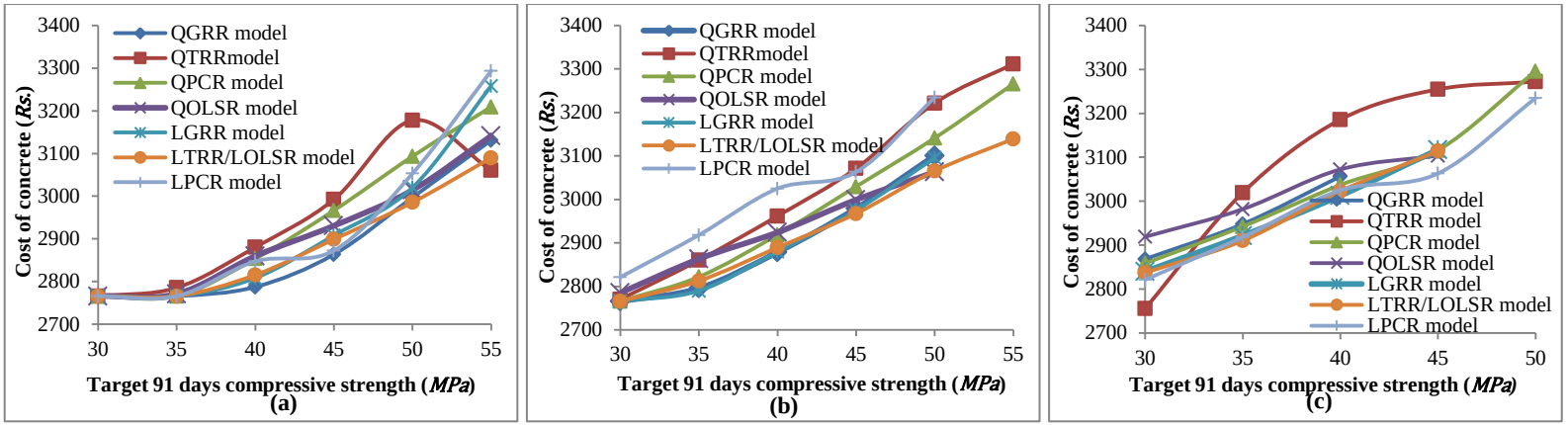

Figure 4.3 Variation of cost of concrete with target 91 days compressive strength for different compressive strength models with (a) R = 0.90 (b) R = 0.95 and (c) R = 0.99 for concrete without fly ash

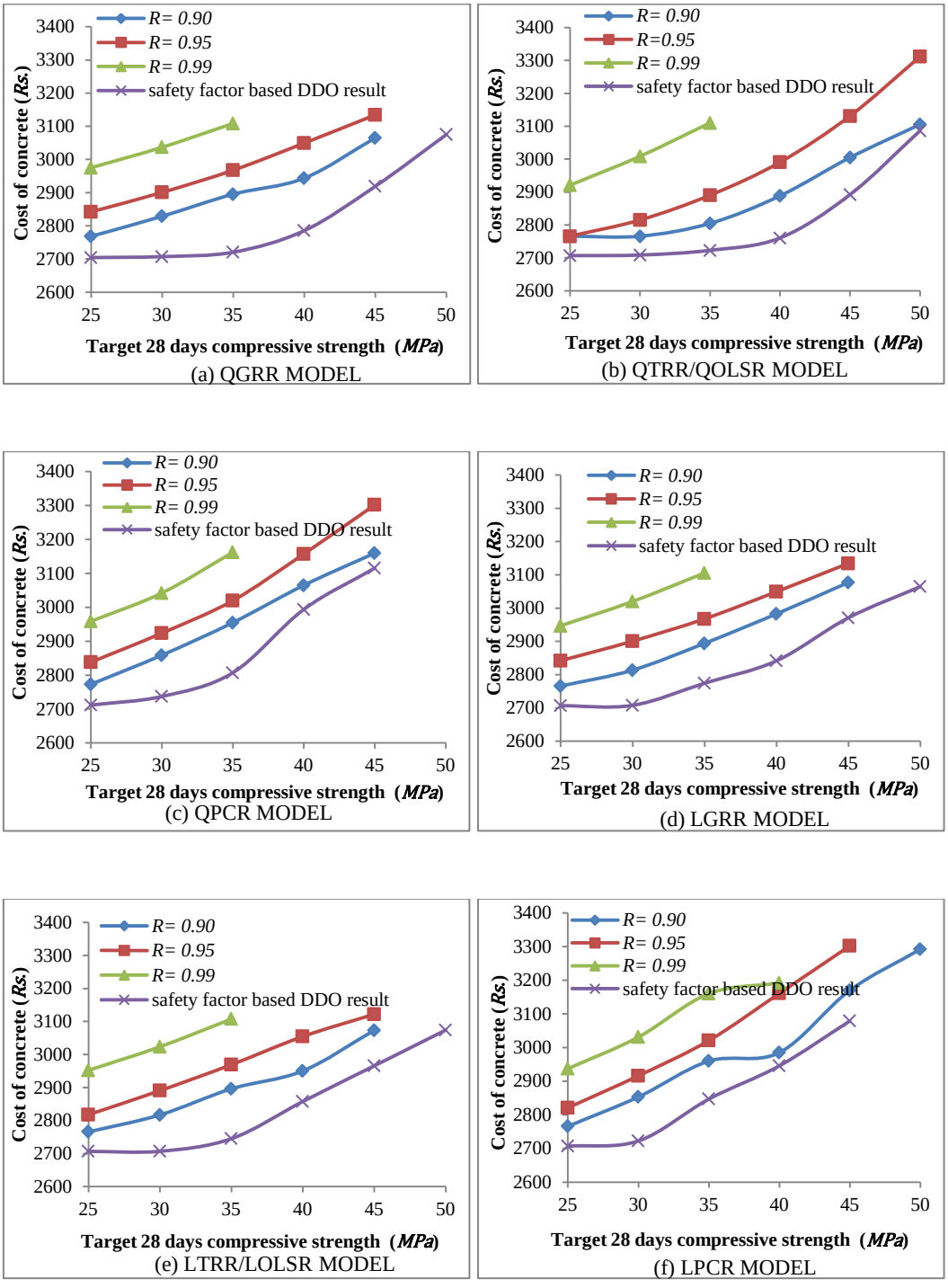

Figure 4.4 Variation of cost of concrete with target 28 days compressive strength for different reliability levels for concrete without fly ash using different compressive strength models

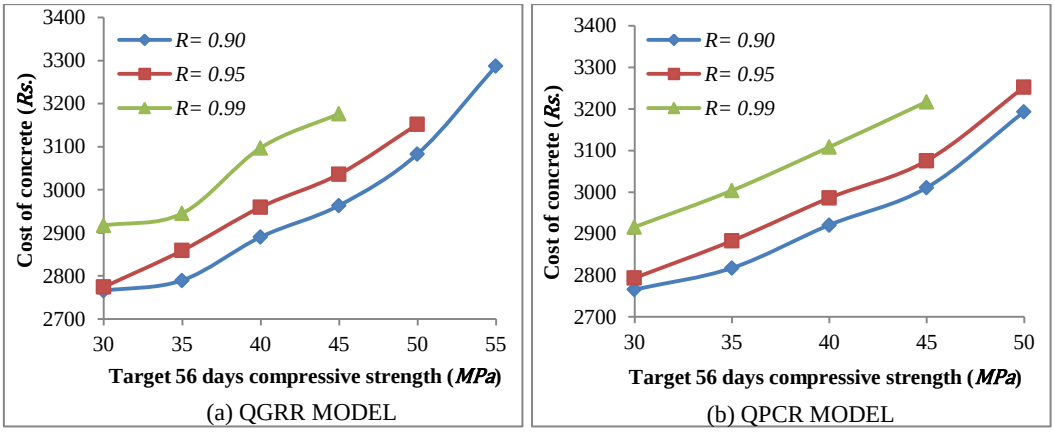

(a) QGRR MODEL

(b) QPCR MODEL

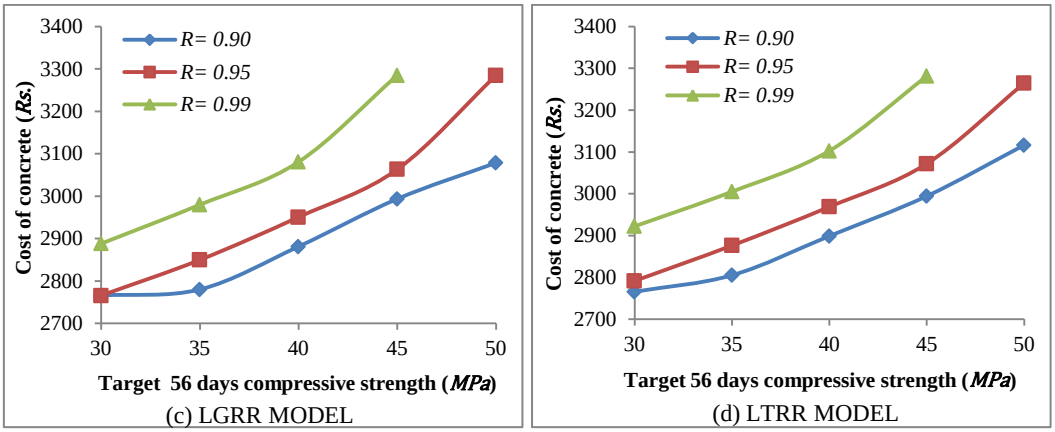

(c) LGRR MODEL

(d) LTRR MODEL

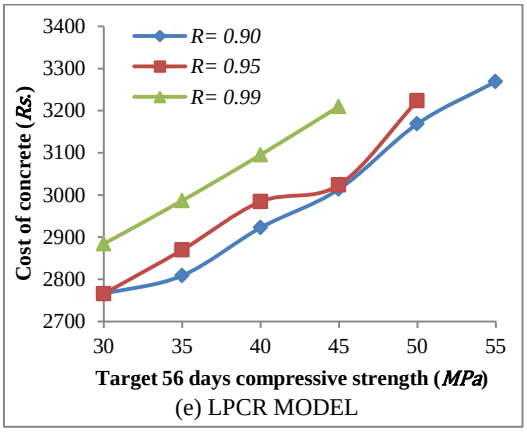

(e) LPCR MODEL

Figure 4.5 Variation of cost of concrete with target 56 days compressive strength for different reliability levels for concrete without fly ash using different compressive strength models

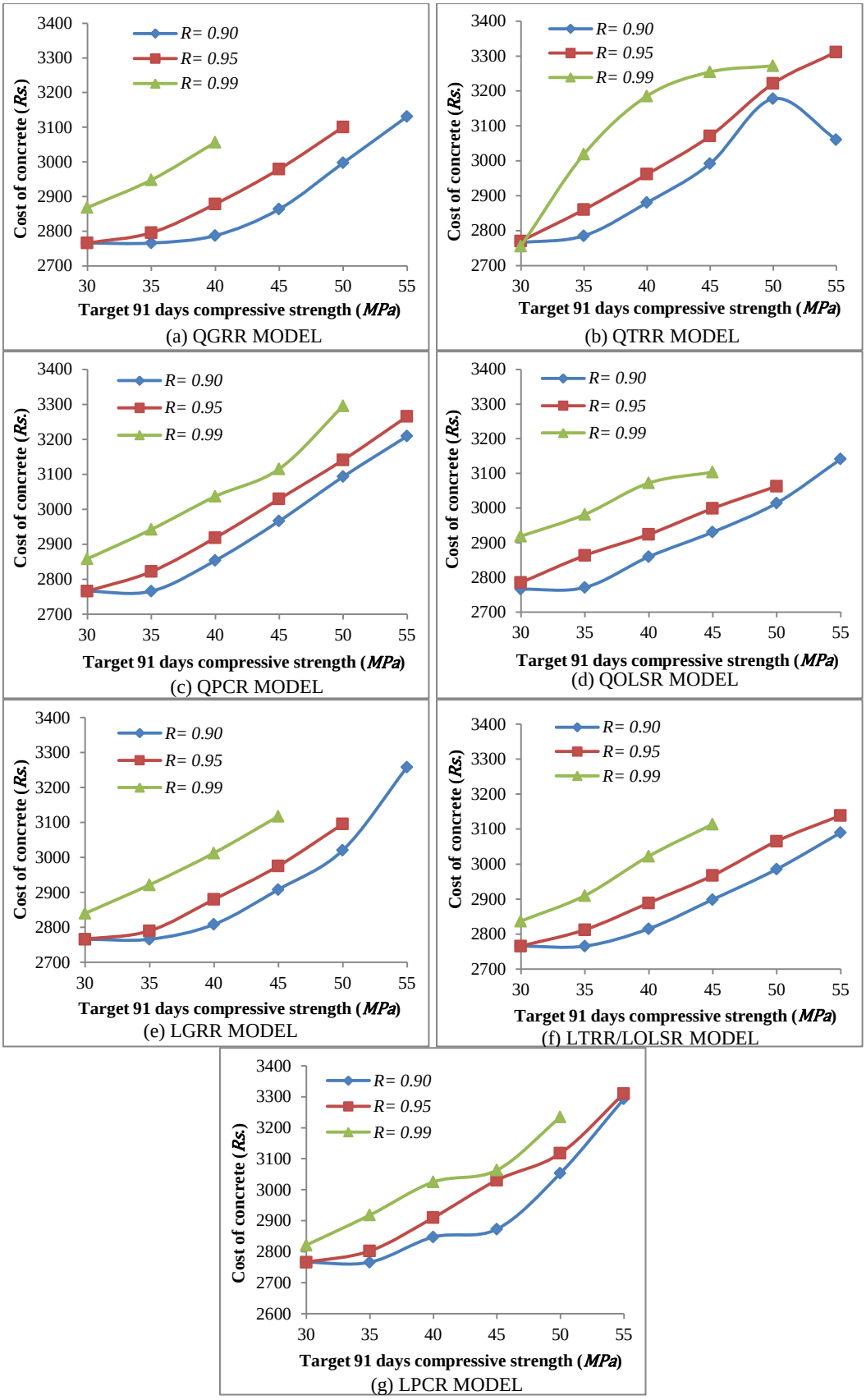

Figure 4.6 Variation of cost of concrete with target 91 days compressive strength for different reliability levels for concrete without fly ash using different compressive strength models

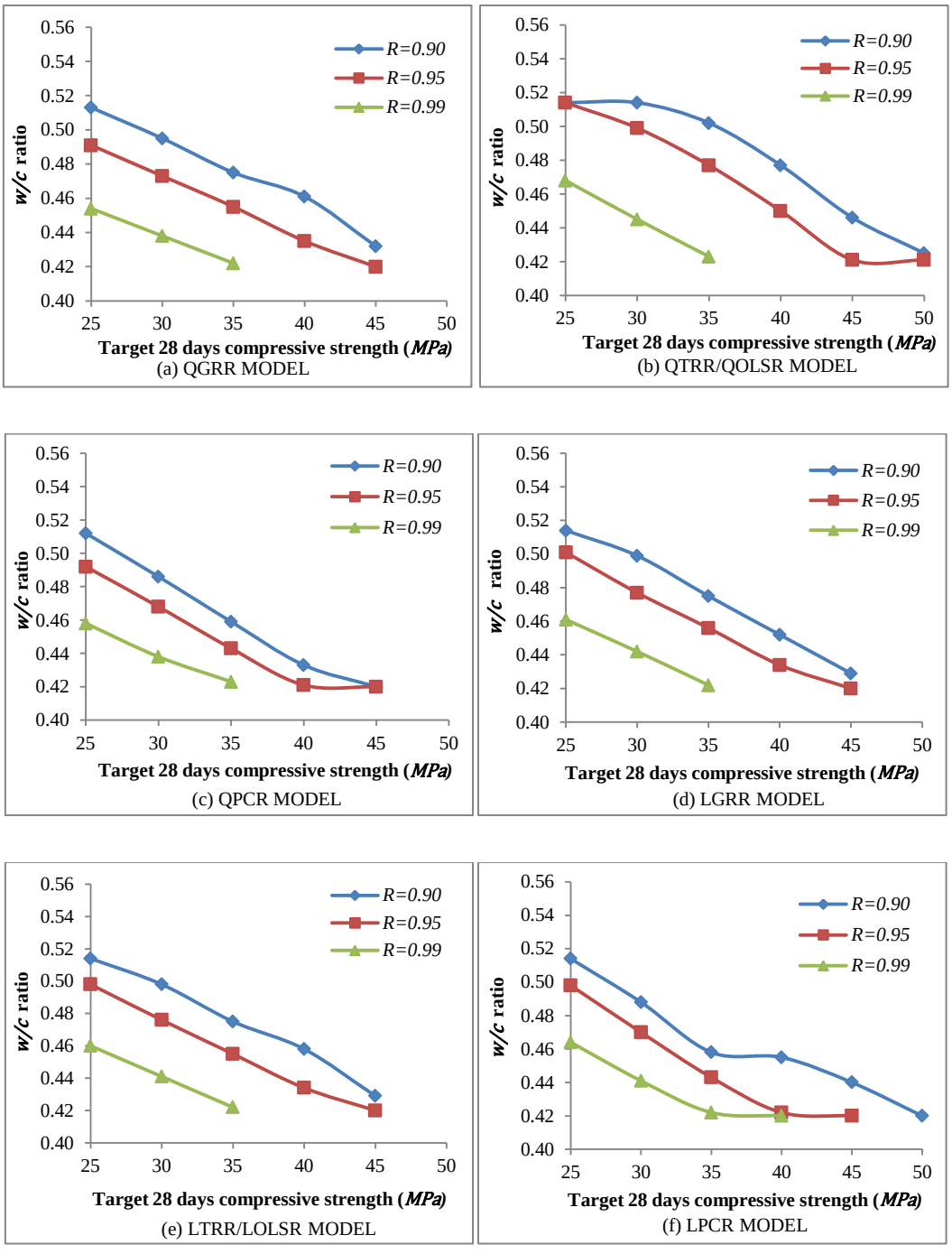

Figure 4.7 Variation of optimal w/c ratio with target 28 days compressive strength for different reliability levels for concrete without fly ash using different compressive strength models

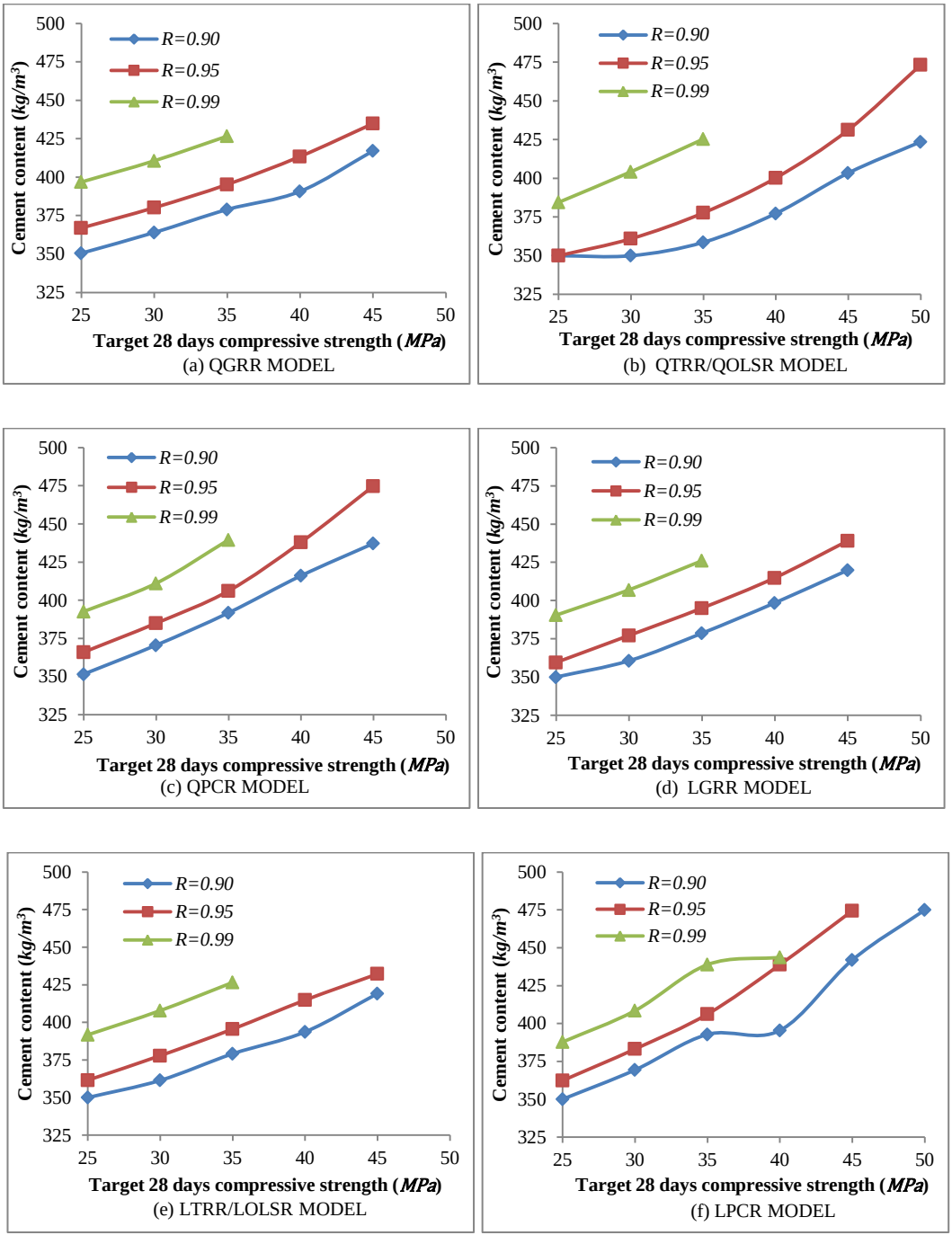

Figure 4.8 Variation of optimal cement content with target 28 days compressive strength for different reliability levels for concrete without fly ash using different compressive strength models

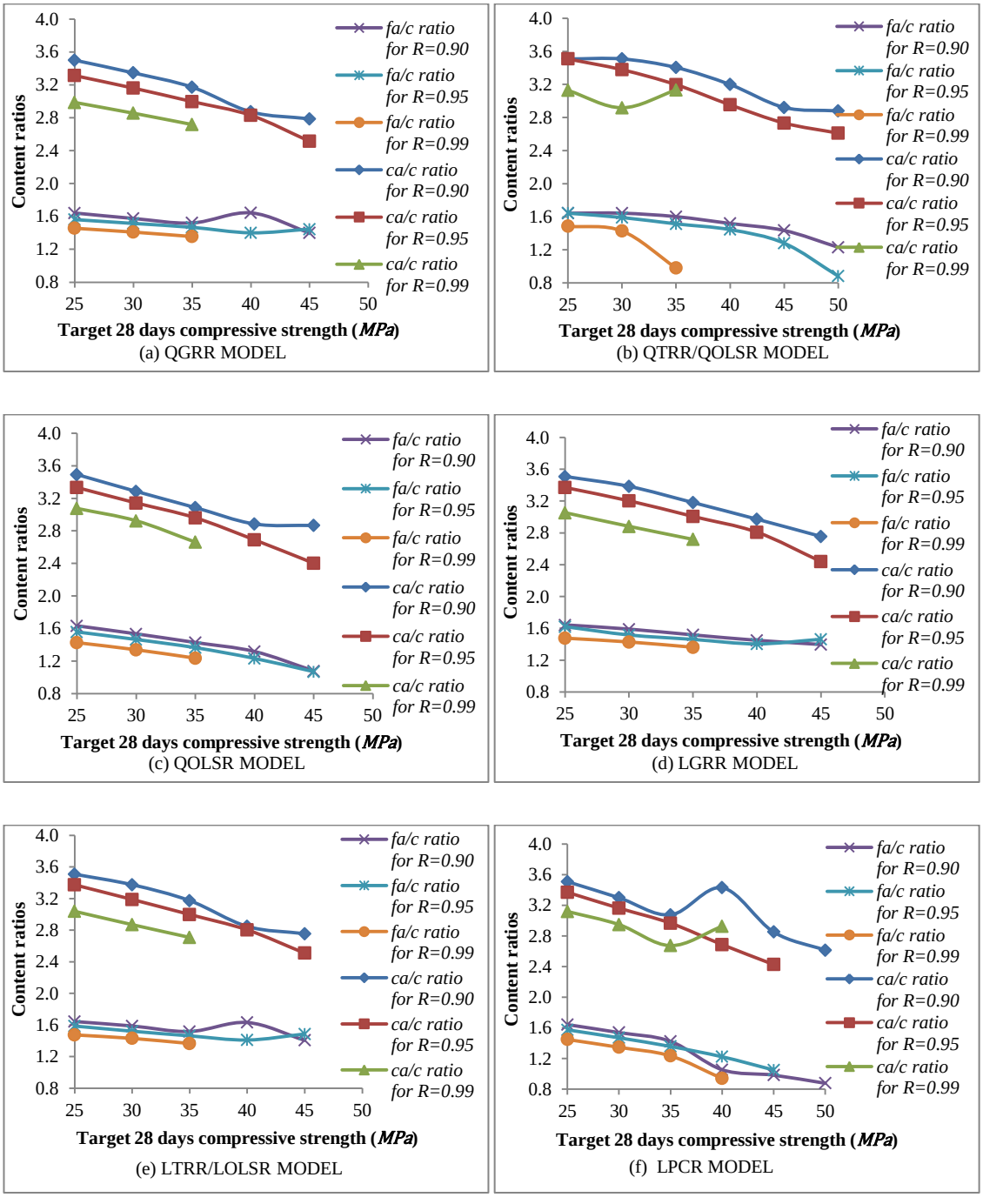

Figure 4.9 Variation of optimal fa/c ratio and ca/c ratio with target 28 days compressive strength for different reliability levels for concrete without fly ash using different compressive strength models

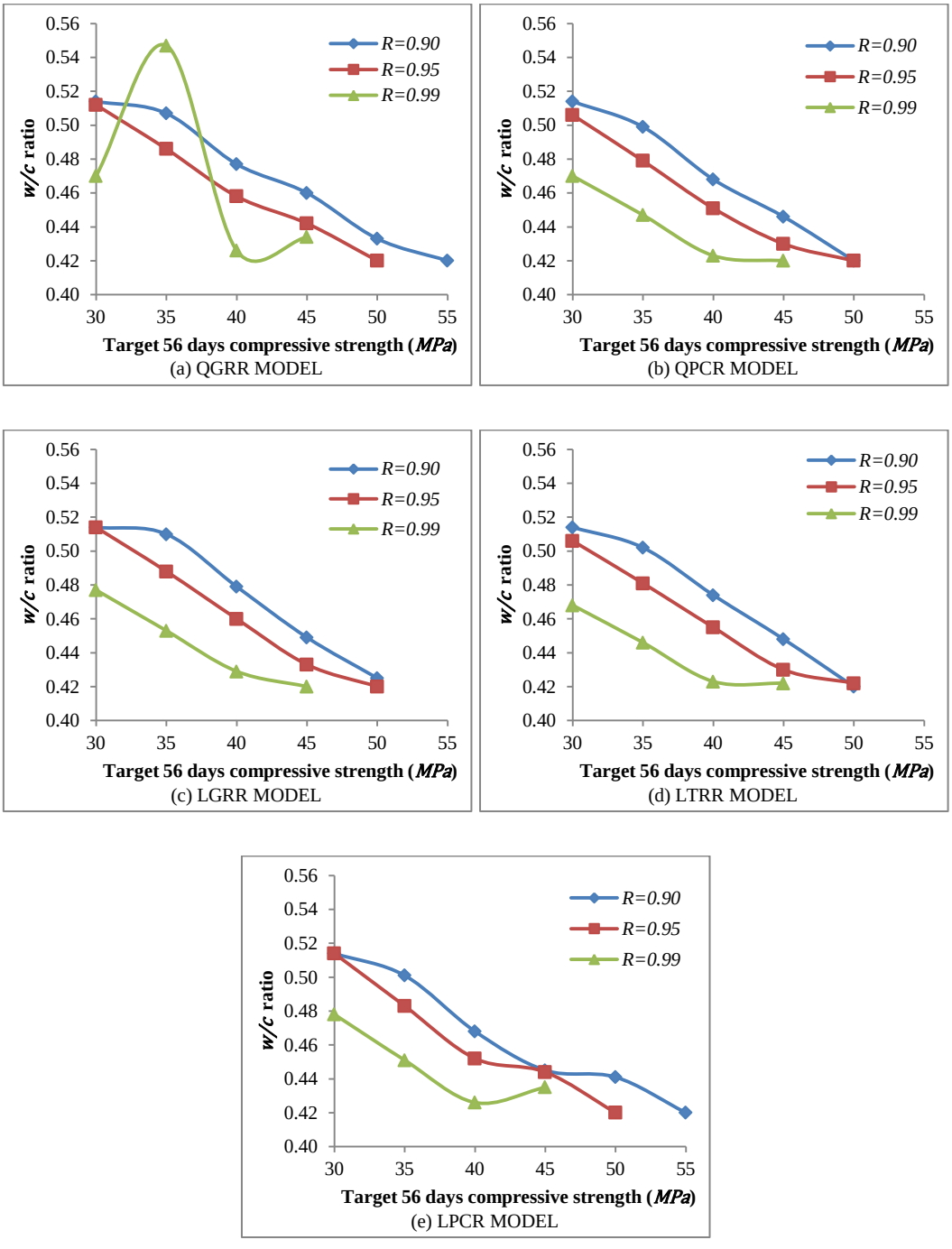

Figure 4.10 Variation of optimal w/c ratio with target 56 days compressive strength for different reliability levels for concrete without fly ash using different compressive strength models

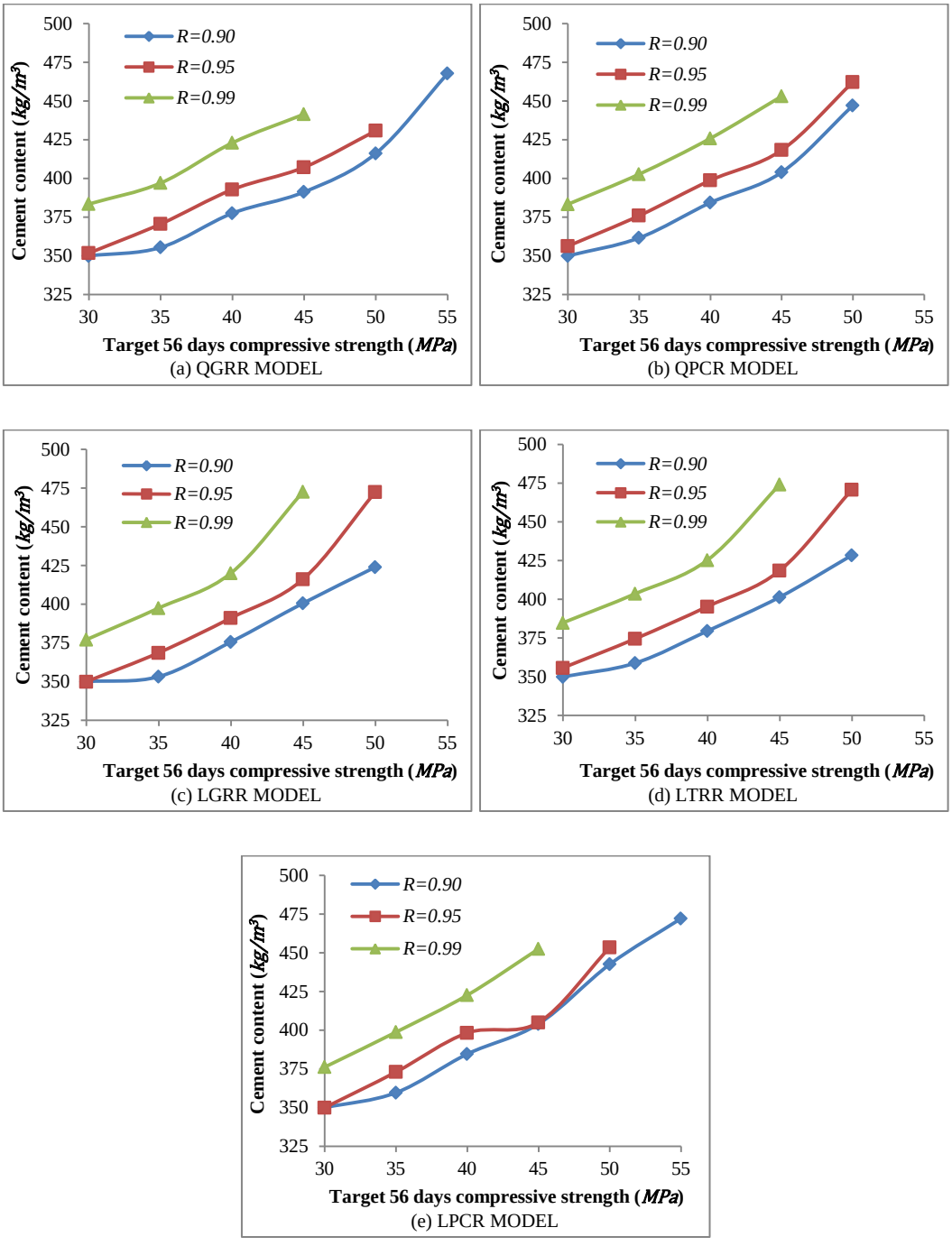

Figure 4.11 Variation of optimal cement content with target 56 days compressive strength for different reliability levels for concrete without fly ash using different compressive strength models

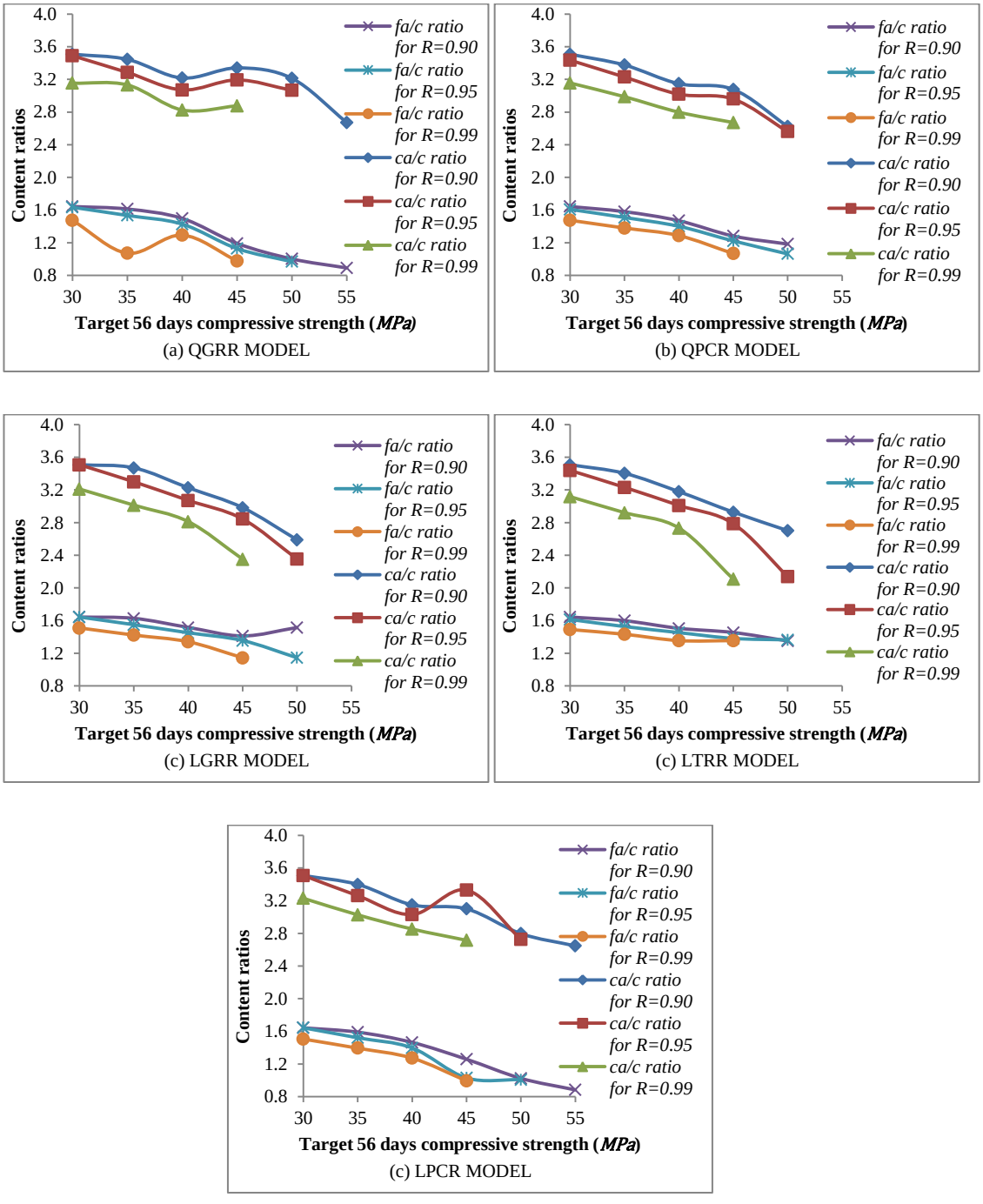

Figure 4.12 Variation of optimal fa/c ratio and ca/c ratio with target 56 days compressive strength for different reliability levels for concrete without fly ash using different compressive strength models

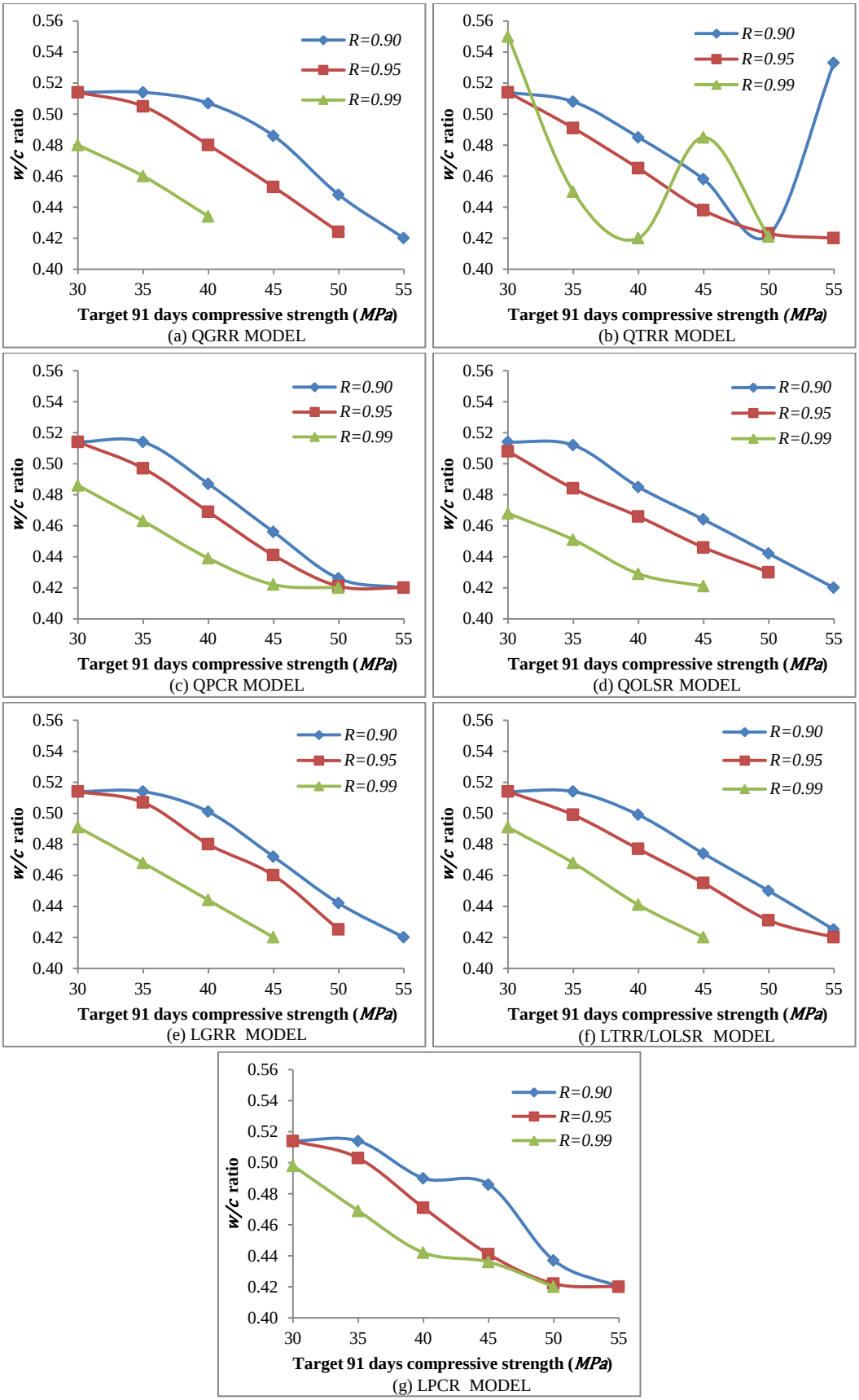

Figure 4.13 Variation of optimal w/c ratio with target 91 days compressive strength for different reliability levels for concrete without fly ash using different compressive strength models

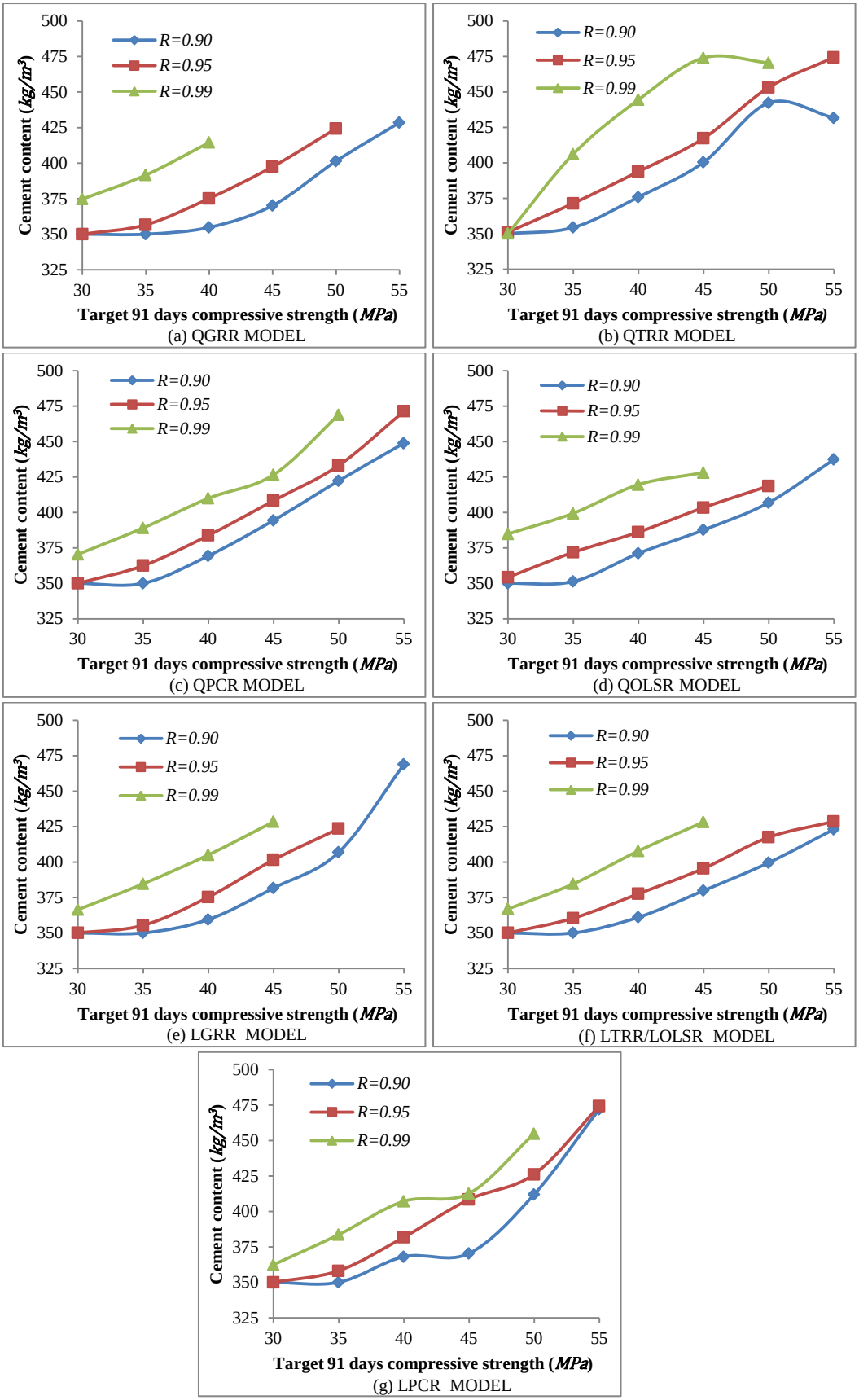

Figure 4.14 Variation of optimal cement content with target 91 days compressive strength for different reliability levels for concrete without fly ash using different compressive strength models

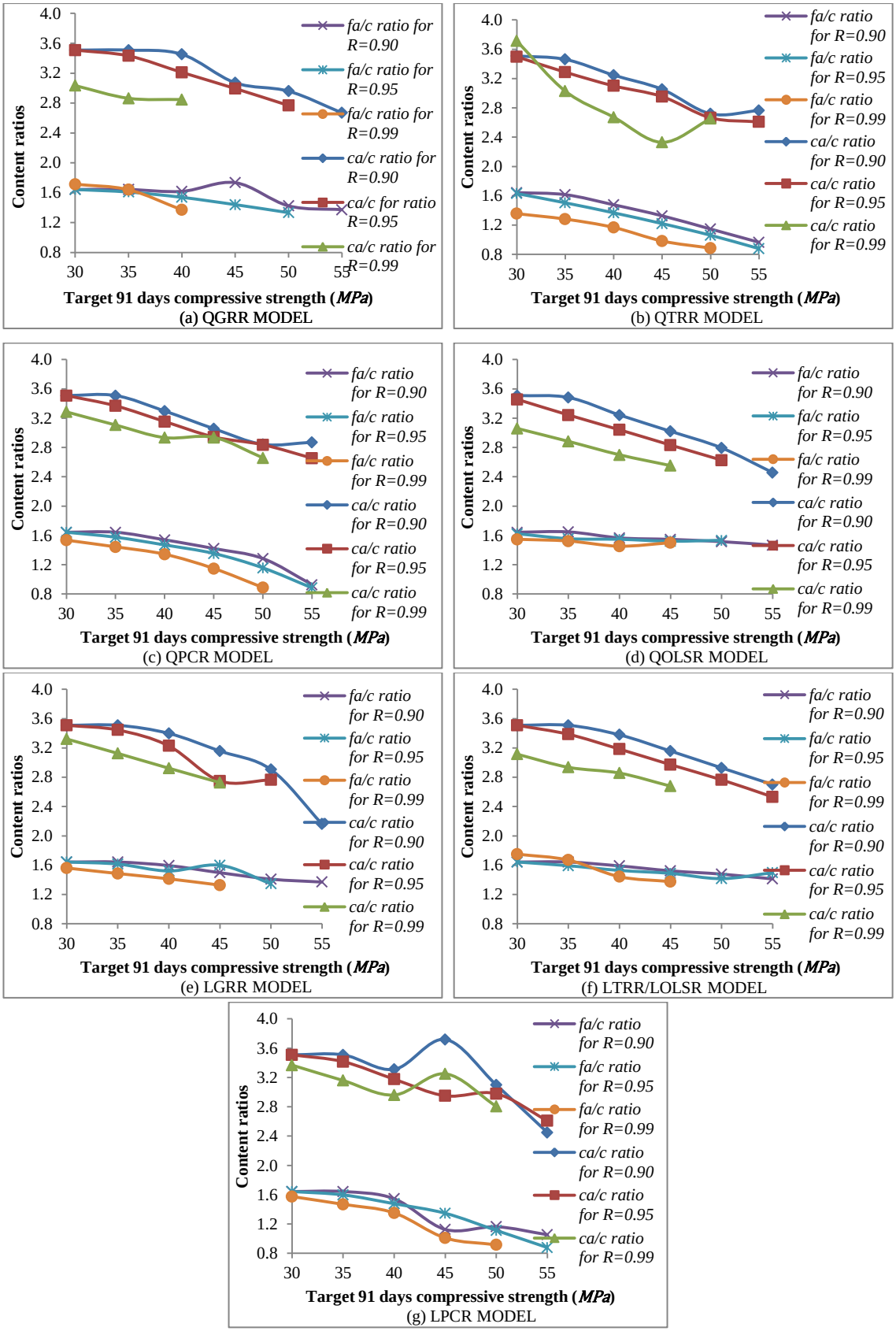

Figure 4.15 Variation of optimal fa/c ratio and ca/c ratio with target 91 days compressive strength for different reliability levels for concrete without fly ash using different compressive strength models

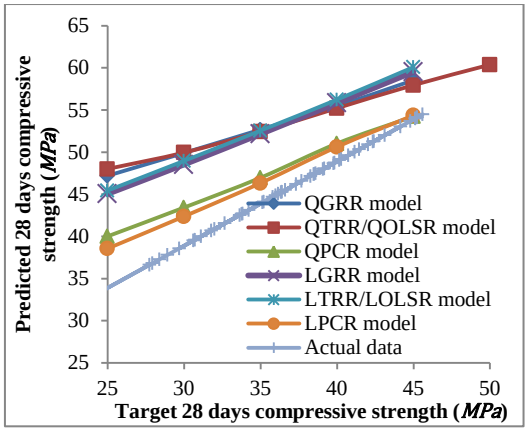

Figure 4.16 Variation of Target 28 days strength with Predicted 28 days strength for *R* = 0.95 for concrete without fly ash

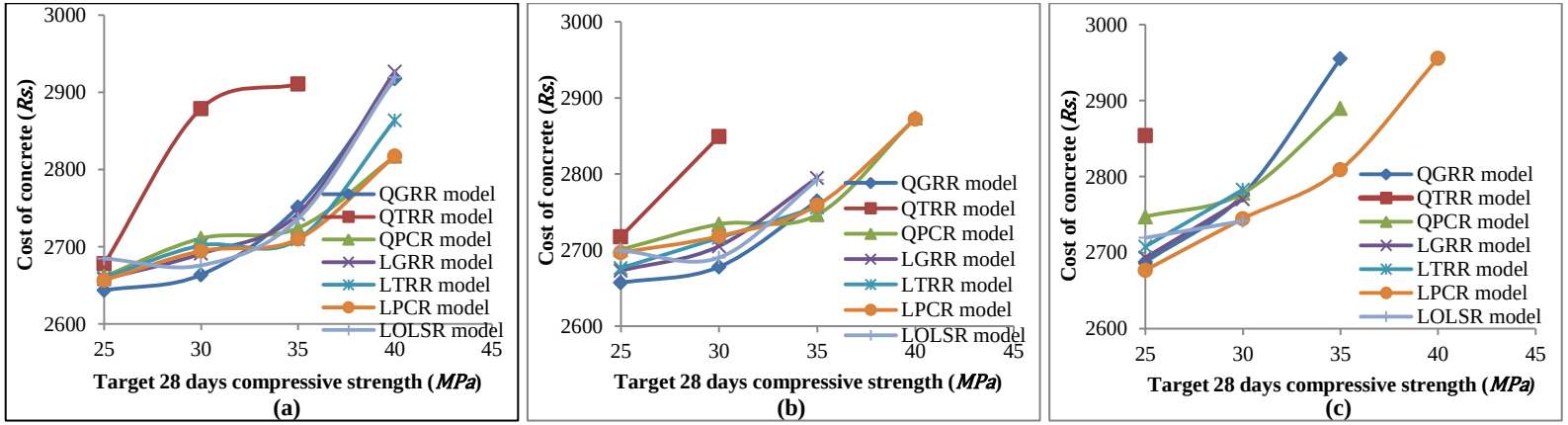

Figure 4.17 Variation of cost of concrete with target 28 days compressive strength for different compressive strength models with (a) *R* = 0.90 (b) *R* = 0.95 and (c) *R* = 0.99 for concrete with fly ash

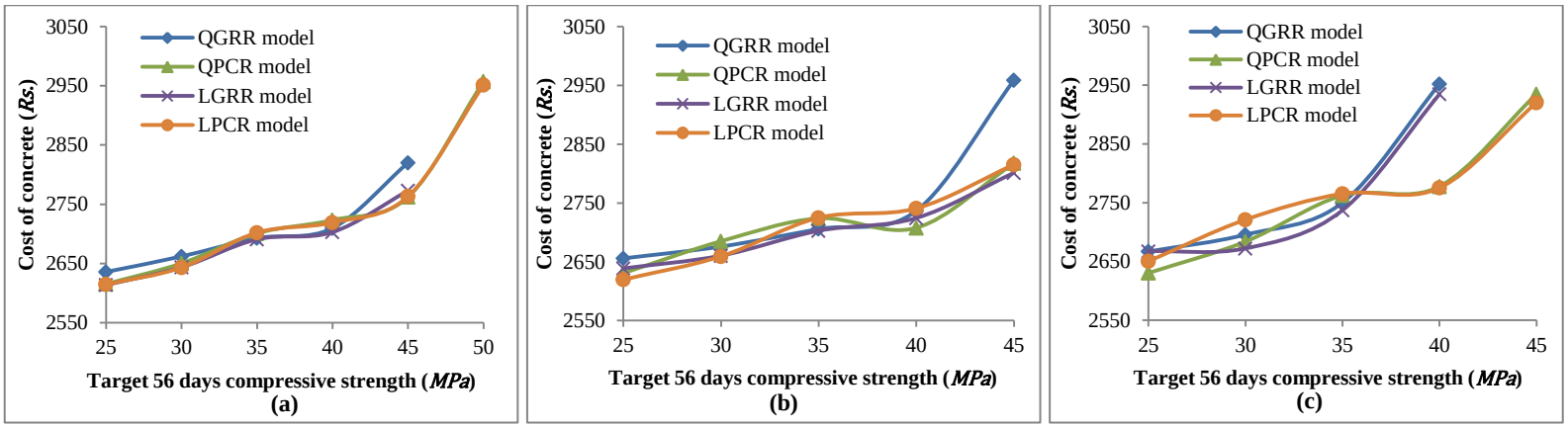

Figure 4.18 Variation of cost of concrete with target 56 days compressive strength for different compressive strength models with (a) R = 0.90 (b) R = 0.95 and (c) R = 0.99 for concrete with fly ash

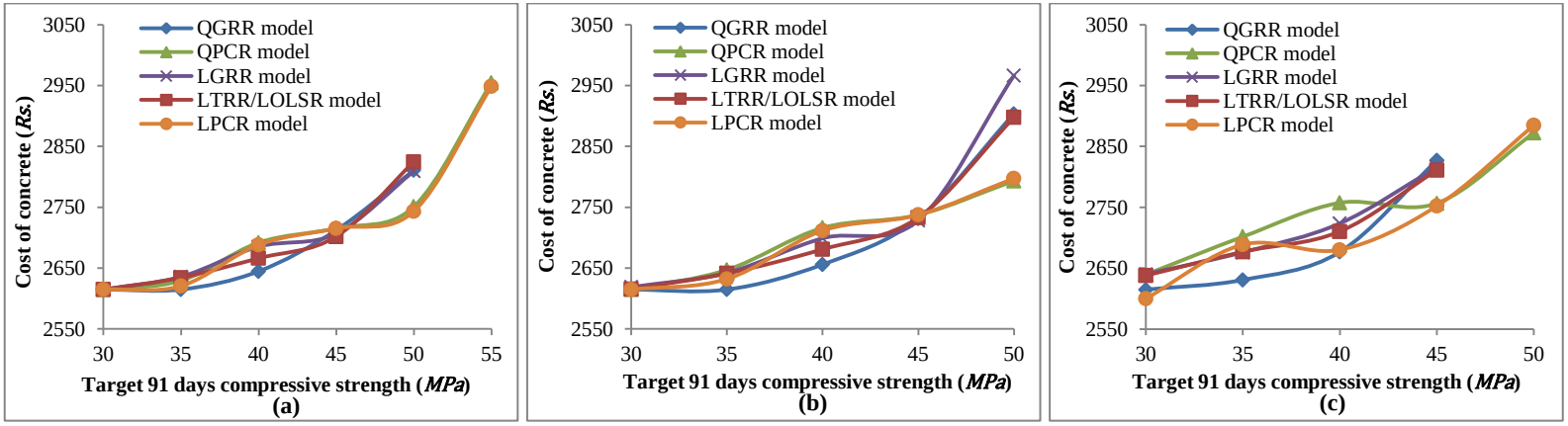

Figure 4.19 Variation of cost of concrete with target 91 days compressive strength for different compressive strength models with (a) R = 0.90 (b) R = 0.95 and (c) R = 0.99 for concrete with fly ash

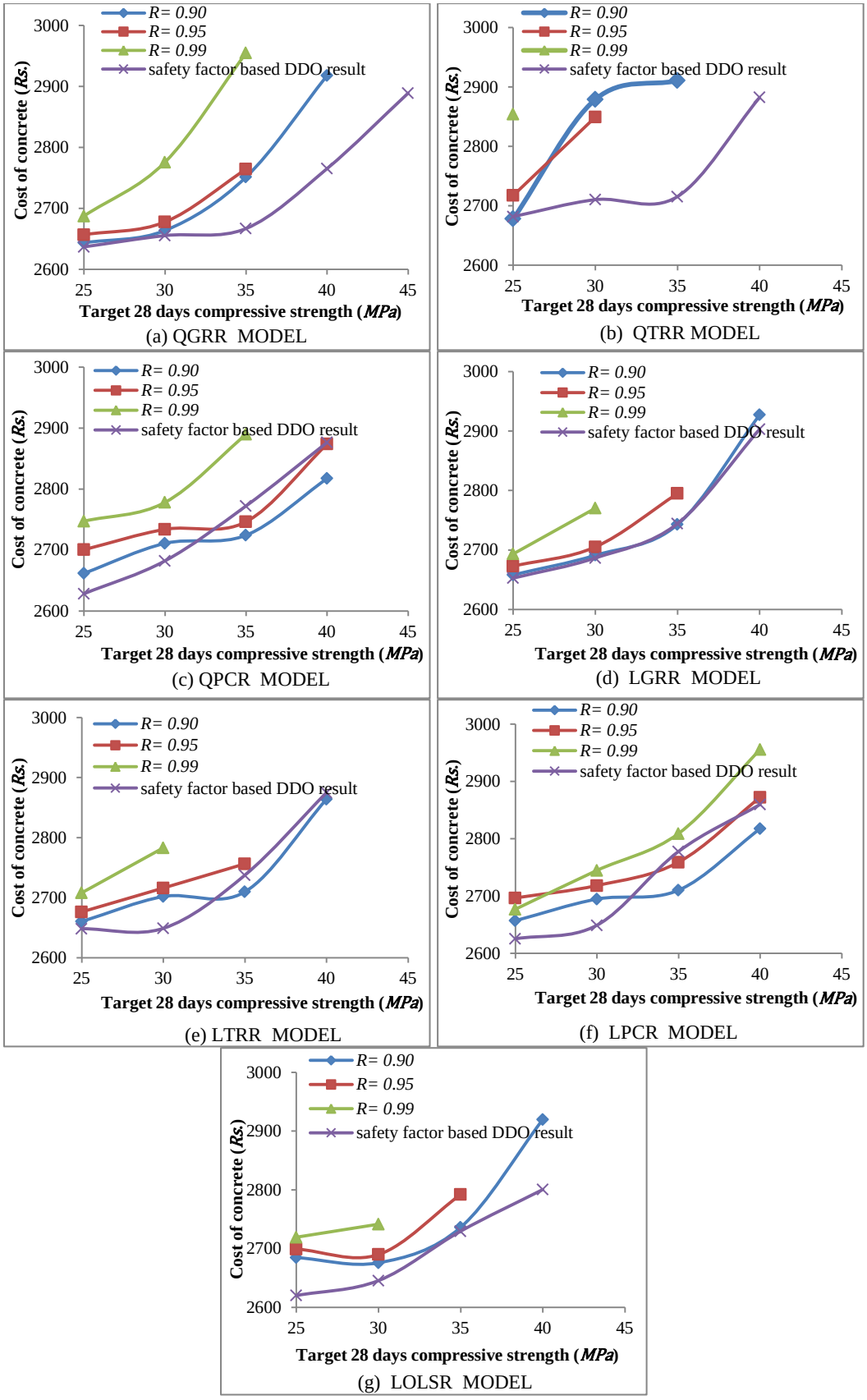

Figure 4.20 Variation of cost of concrete with target 28 days compressive strength for different reliability levels for concrete with fly ash using different compressive strength models

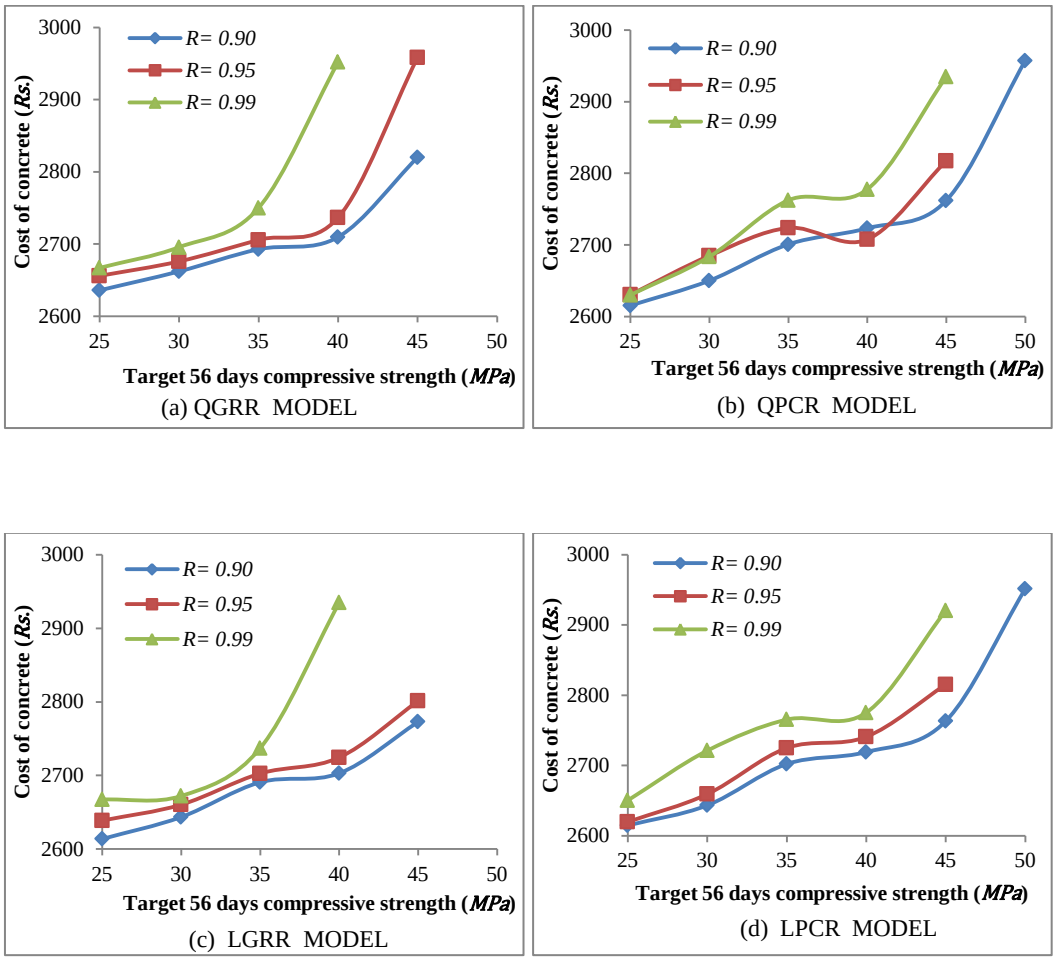

Figure 4.21 Variation of cost of concrete with target 56 days compressive strength for different reliability levels for concrete with fly ash using different compressive strength models

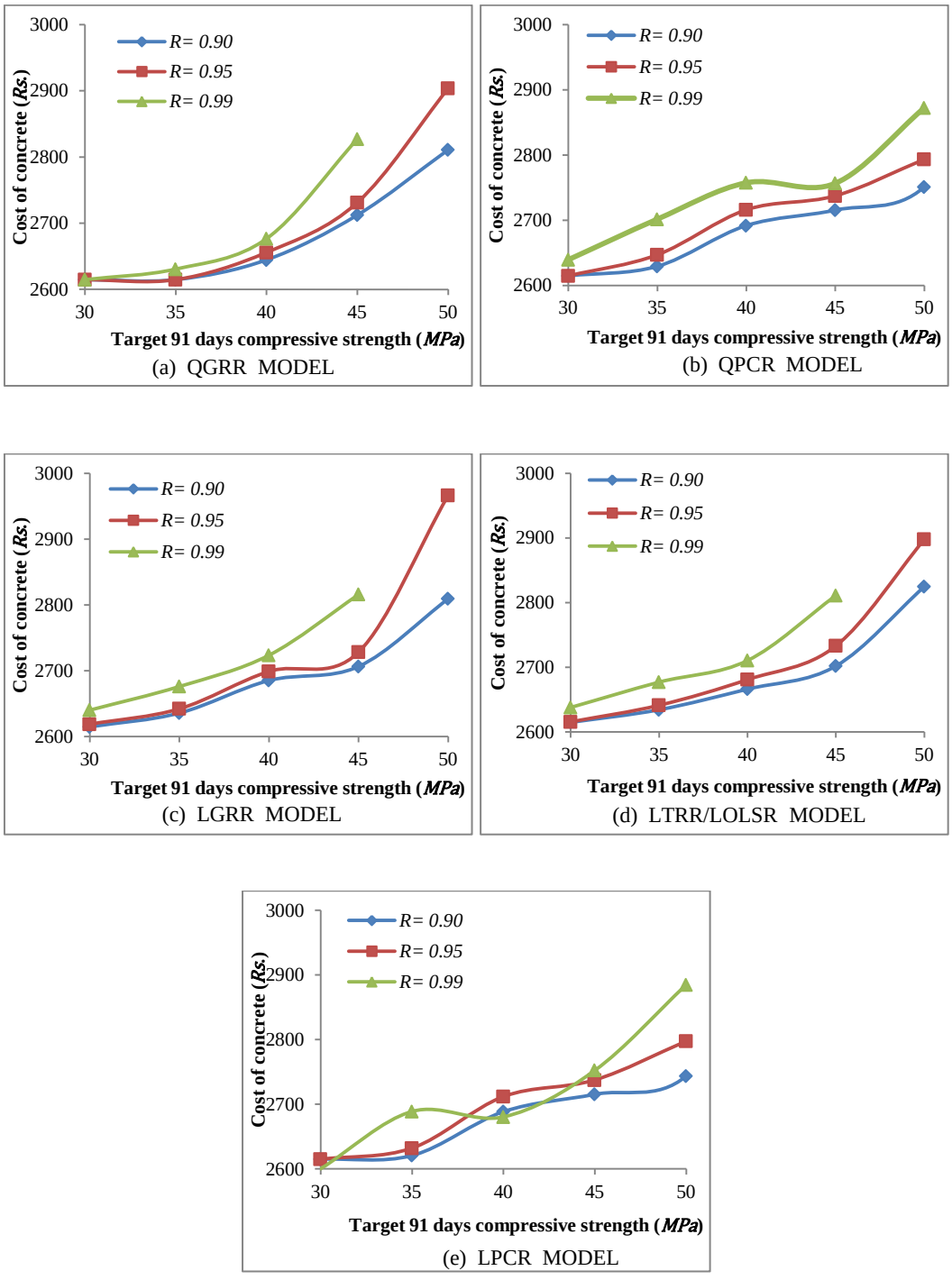

Figure 4.22 Variation of cost of concrete with target 91 days compressive strength for different reliability levels for concrete with fly ash using different compressive strength models

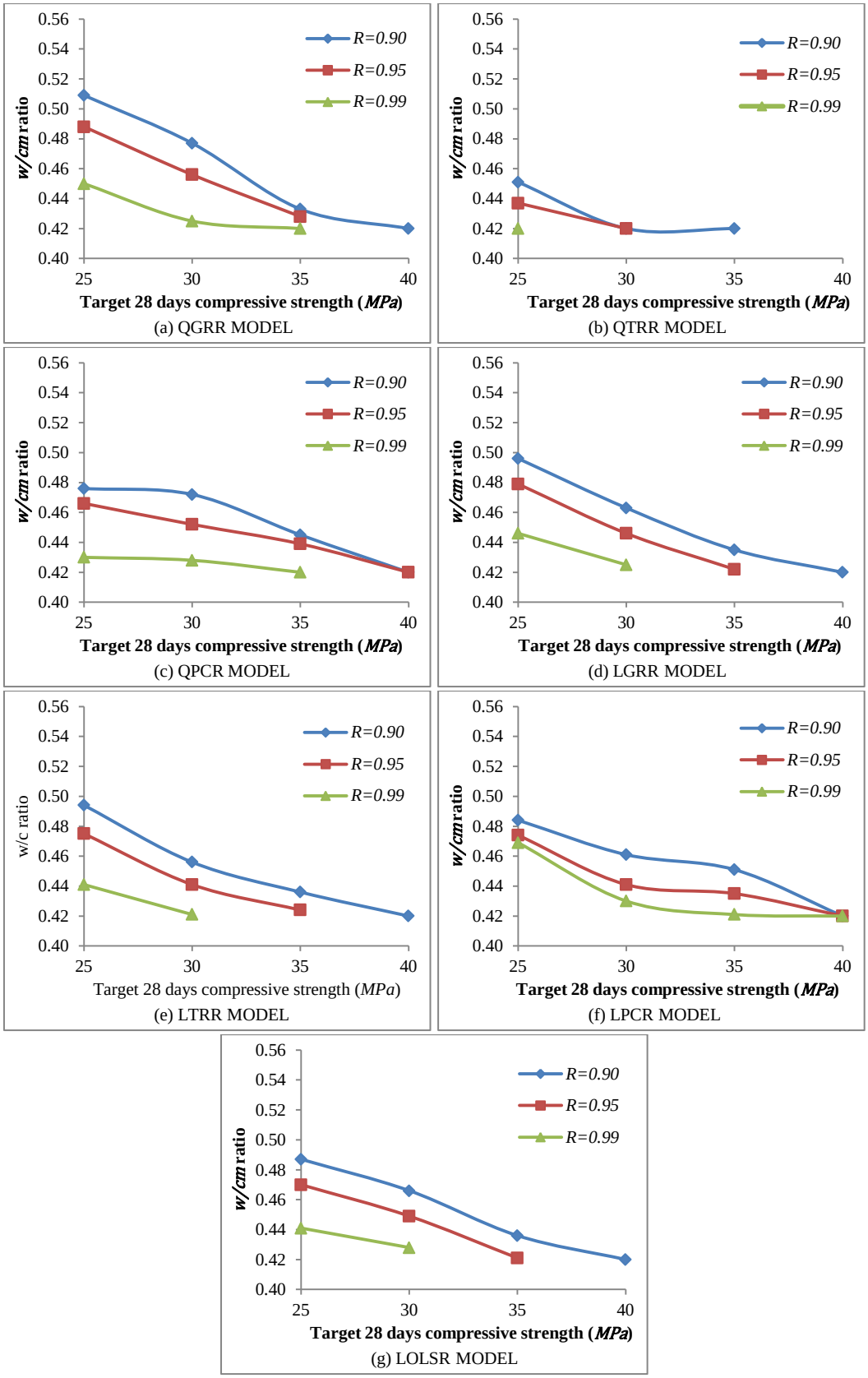

Figure 4.23 Variation of optimal w/cm ratio with target 28 days compressive strength for different reliability levels for concrete with fly ash using different compressive strength models

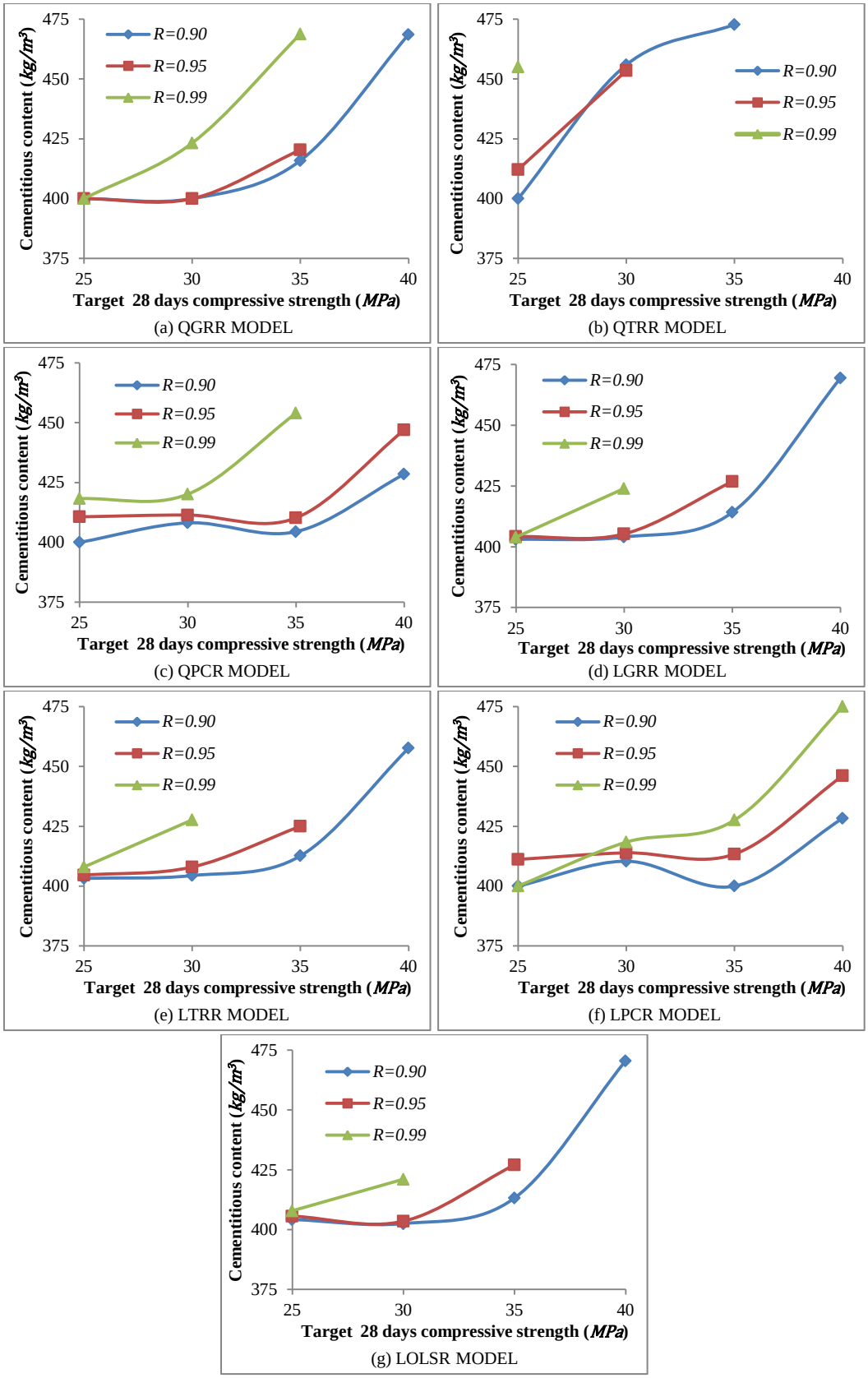

Figure 4.24 Variation of optimal cementitious content with target 28 days compressive strength for different reliability levels for concrete with fly ash using different compressive strength models

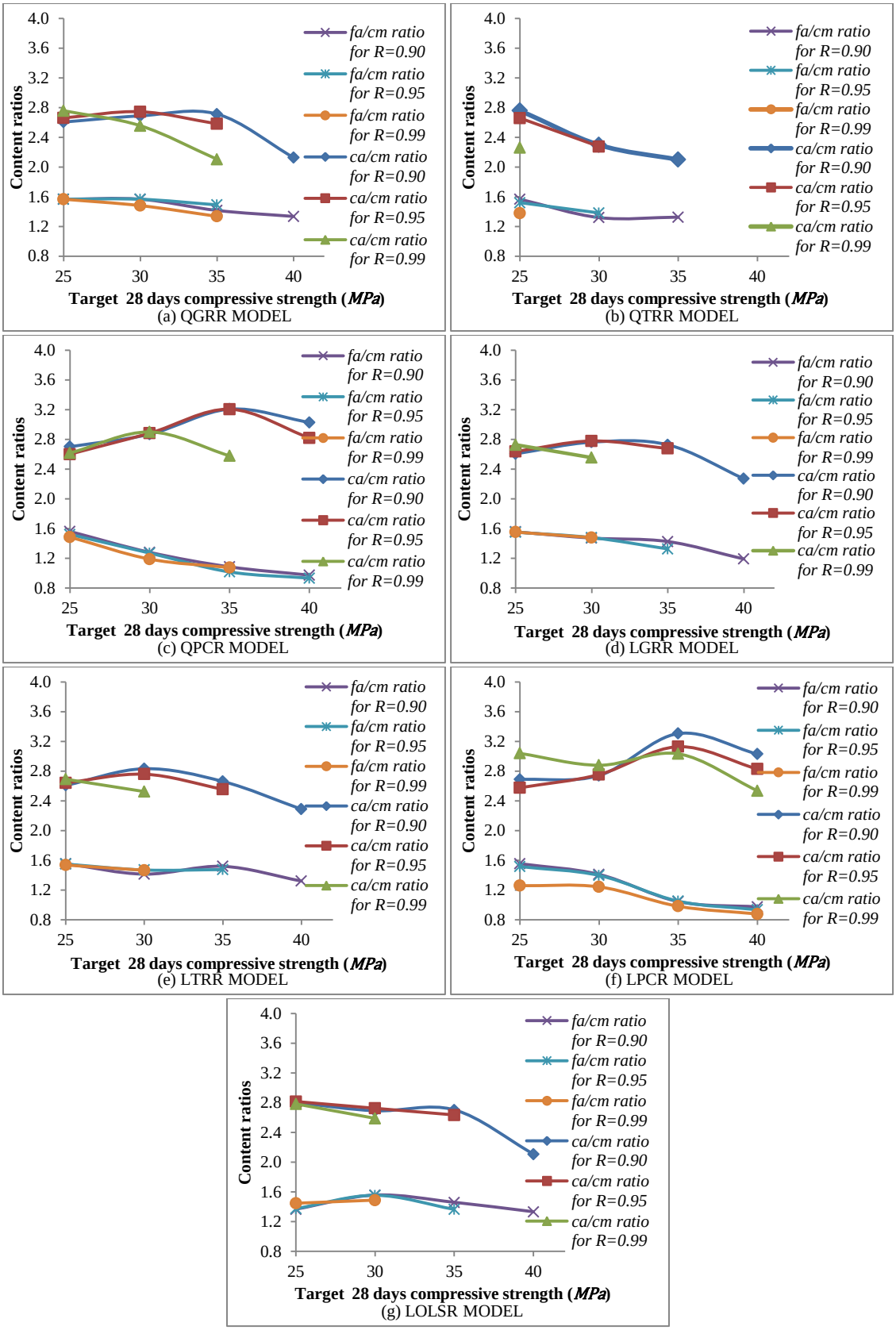

Figure 4.25 Variation of optimal fa/cm ratio and ca/cm ratio with target 28 days compressive strength for different reliability levels for concrete with fly ash using different compressive strength models

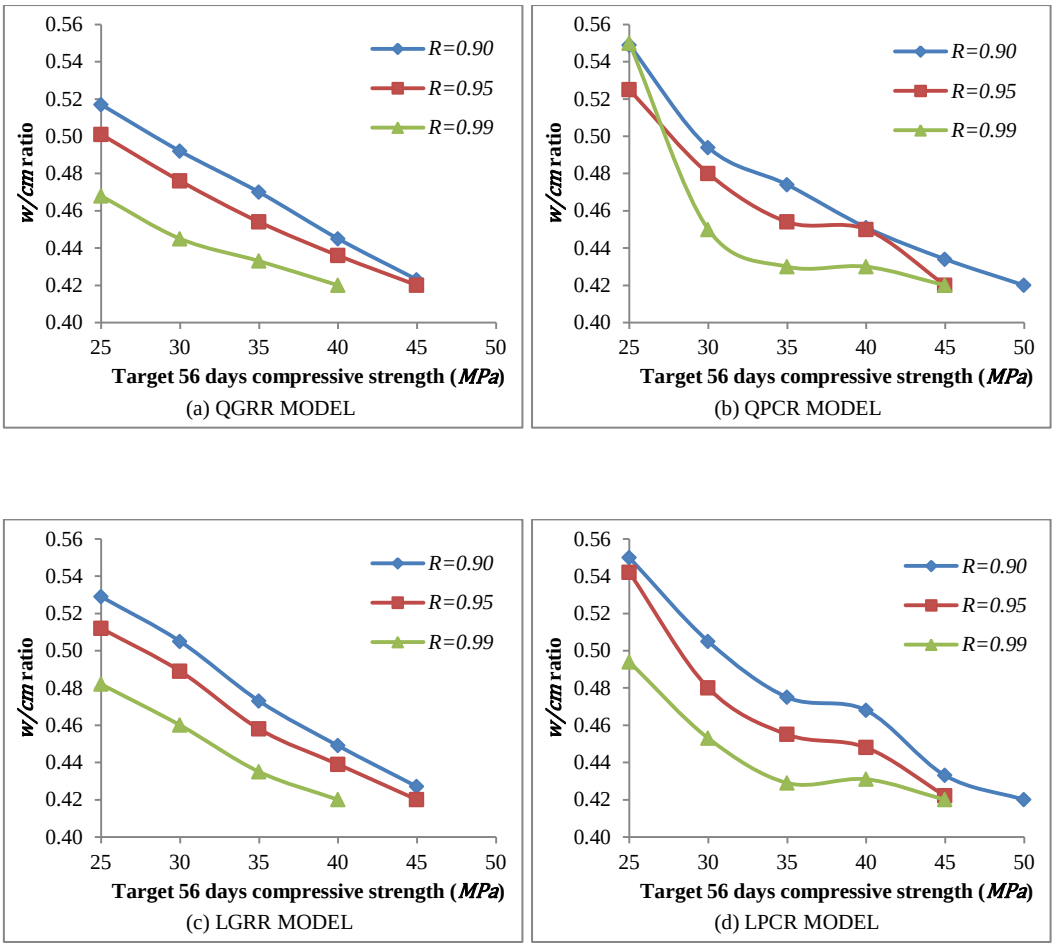

(a) QGRR MODEL

(b) QPCR MODEL

(c) LGRR MODEL

(d) LPCR MODEL

Figure 4.26 Variation of optimal *w/cm* ratio with target 56 days compressive strength for different reliability levels for concrete with fly ash using different compressive strength models

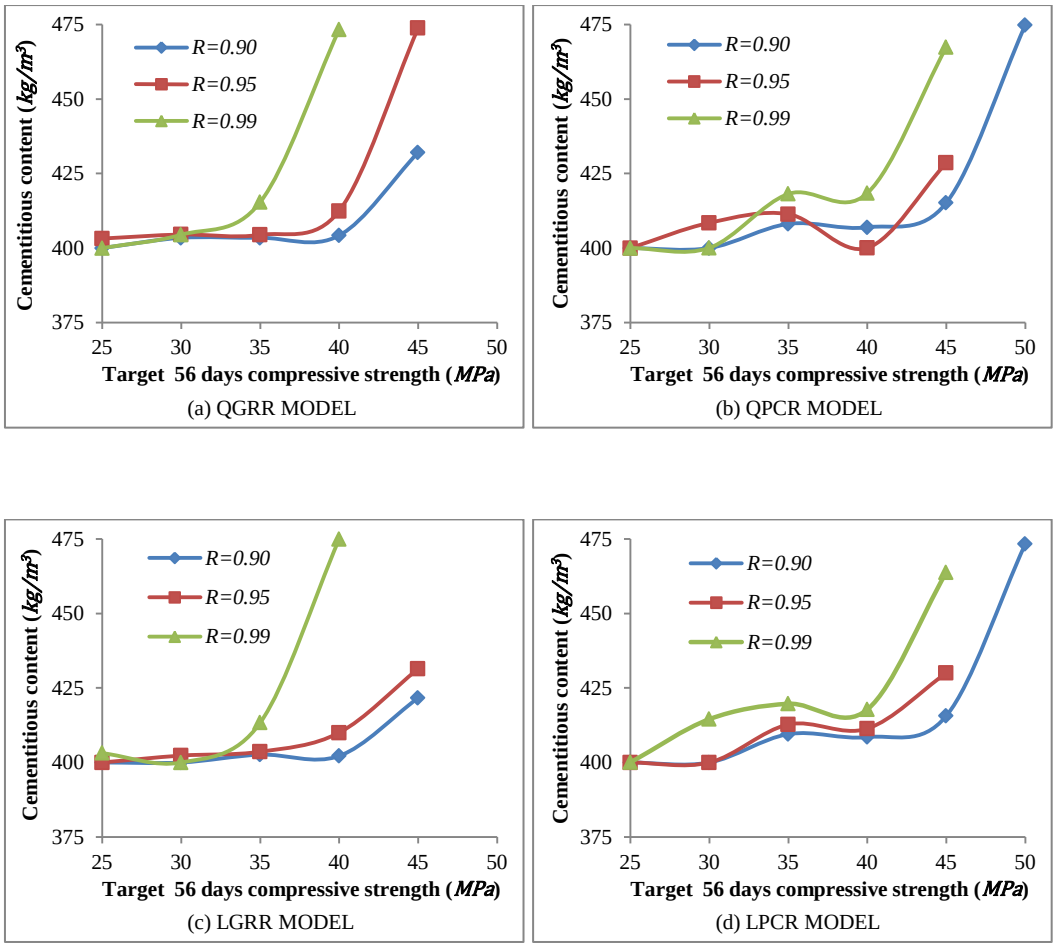

Figure 4.27 Variation of optimal cementitious content with target 56 days compressive strength for different reliability levels for concrete with fly ash using different compressive strength models

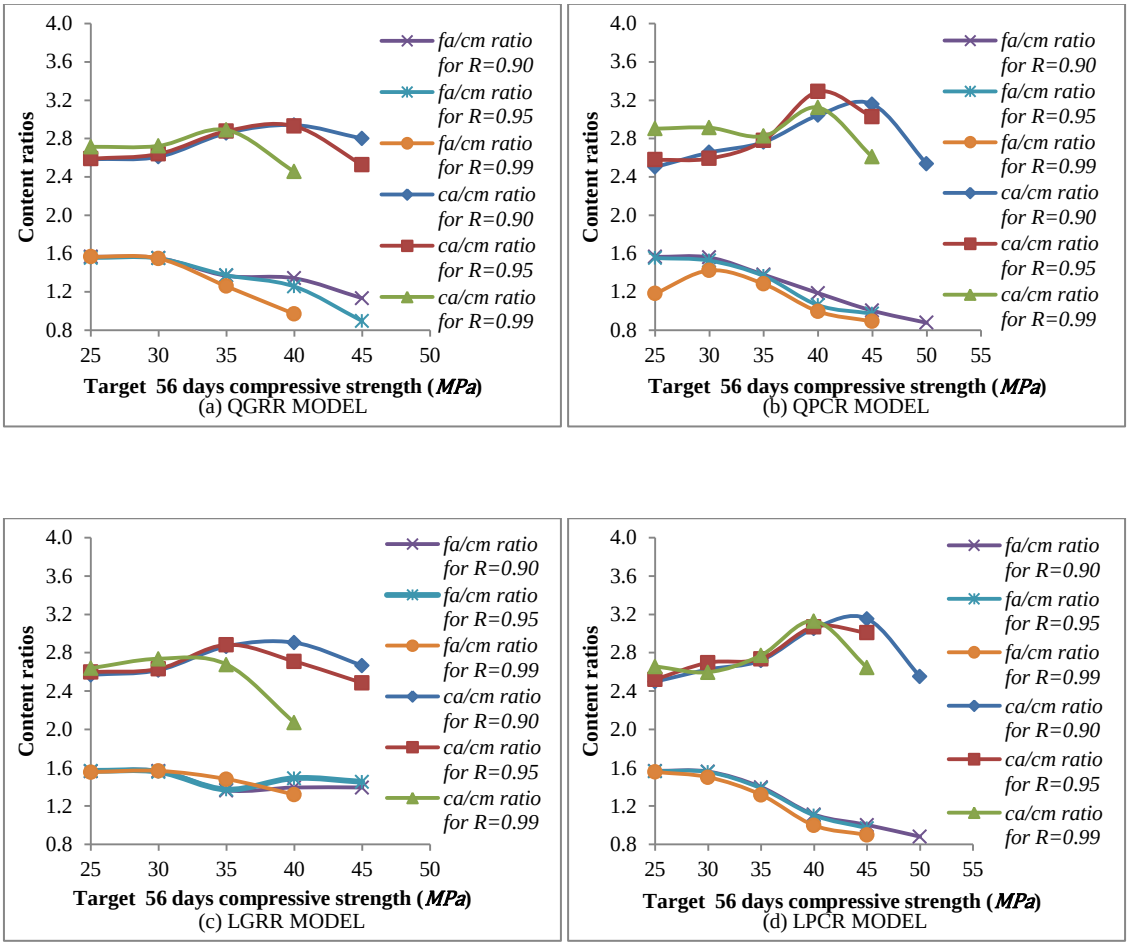

Figure 4.28 Variation of optimal fa/cm ratio and ca/cm ratio with target 56 days compressive strength for different reliability levels for concrete with fly ash using different compressive strength models

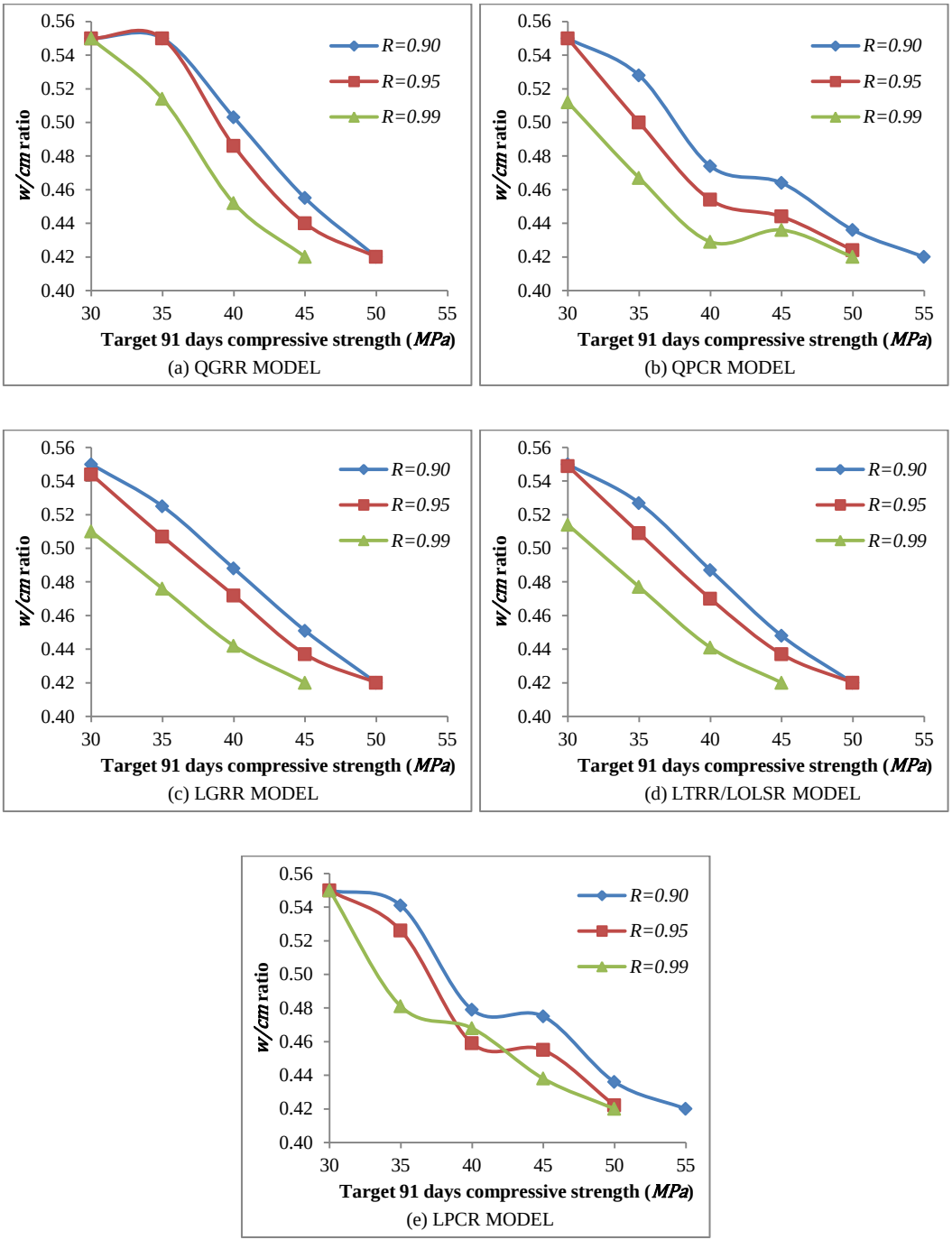

(a) QGRR MODEL

(b) QPCR MODEL

(c) LGRR MODEL

(d) LTRR/LOLSR MODEL

(e) LPCR MODEL

Figure 4.29 Variation of optimal w/cm ratio with target 91 days compressive strength for different reliability levels for concrete with fly ash using different compressive strength models

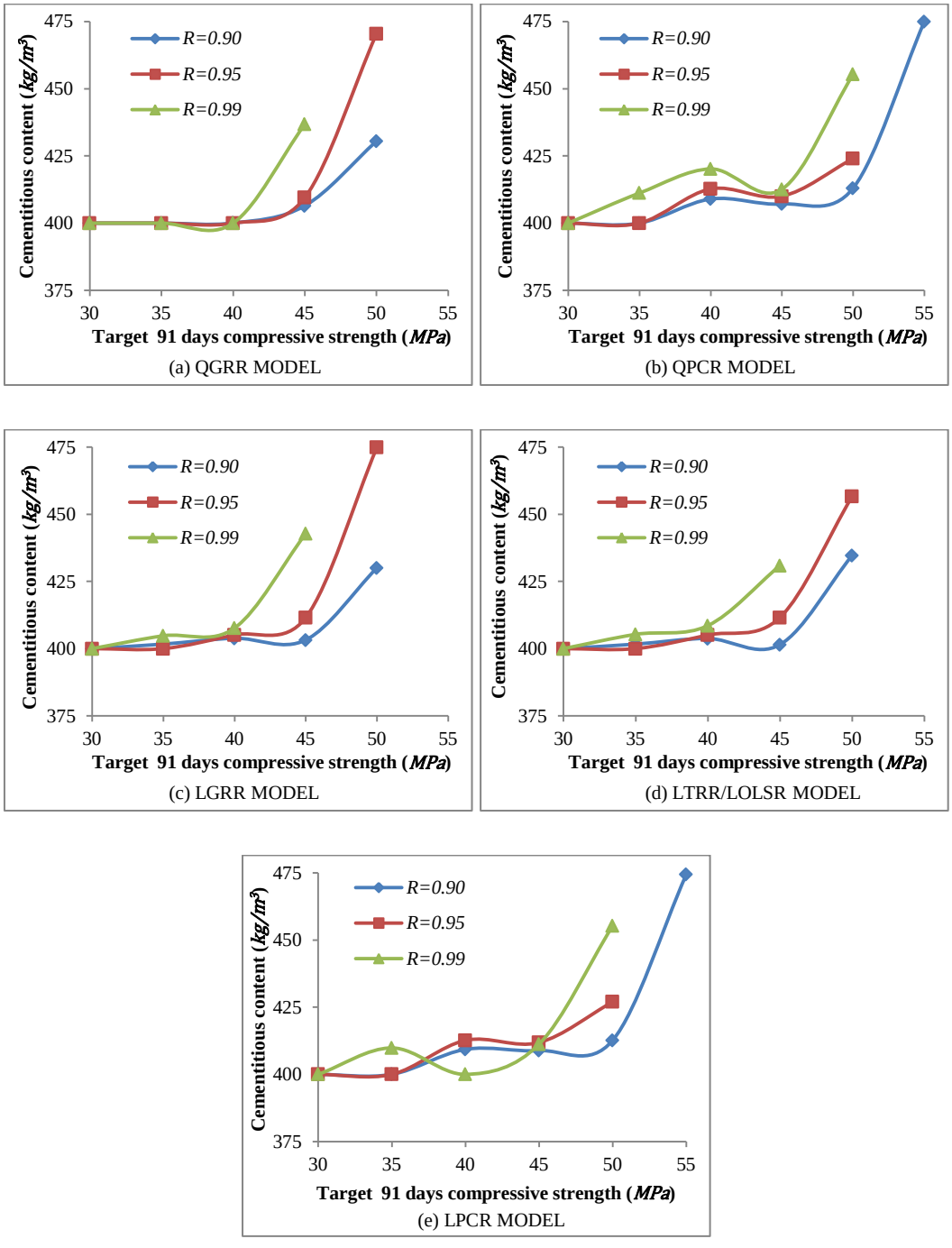

Figure 4.30 Variation of optimal cementitious content with target 91 days compressive strength for different reliability levels for concrete with fly ash using different compressive strength models

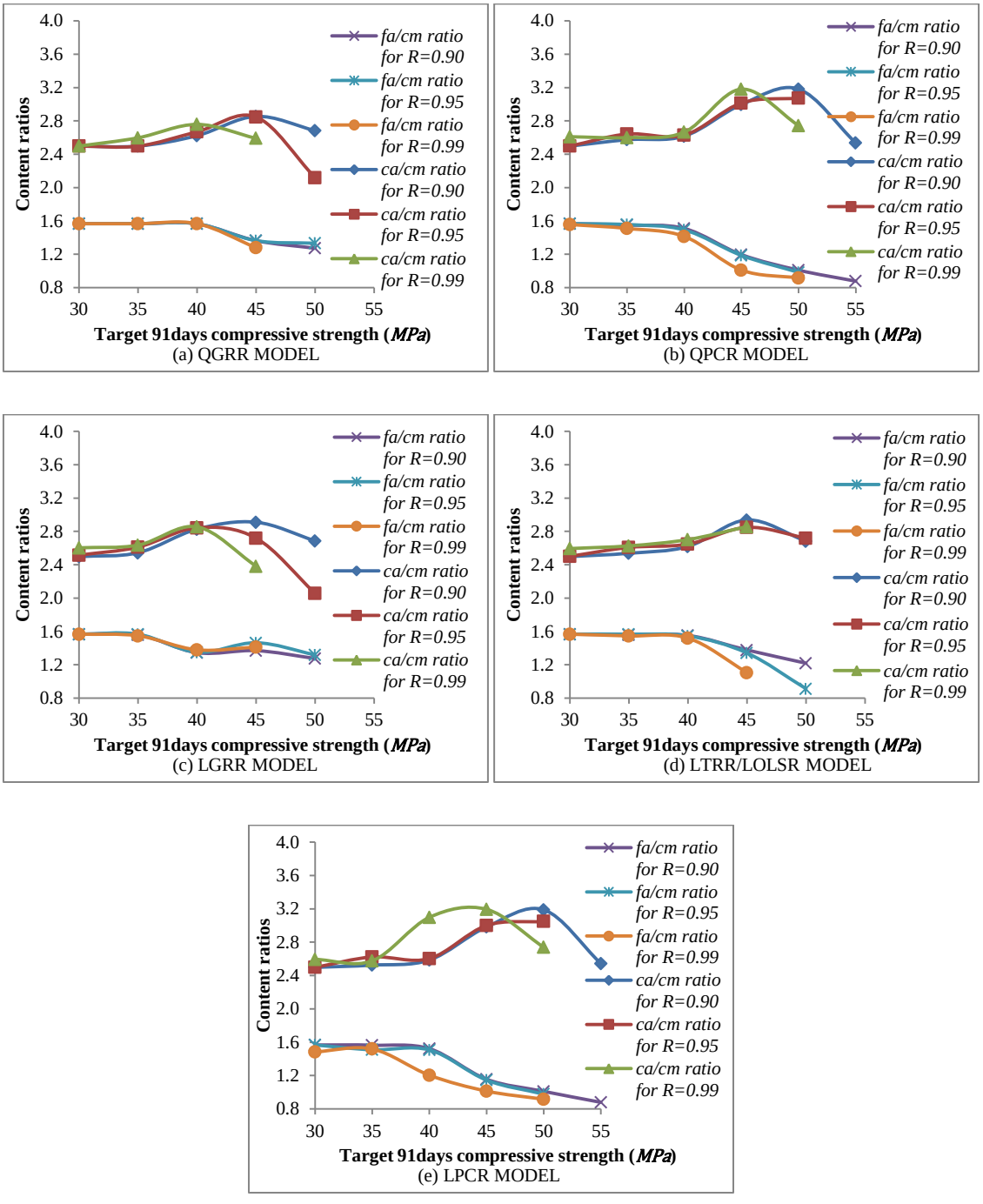

Figure 4.31 Variation of optimal fa/cm ratio and ca/cm ratio with target 91 days compressive strength for different reliability levels for concrete with fly ash using different compressive strength models

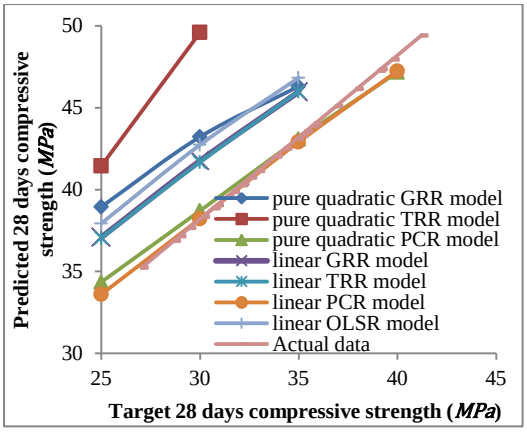

Figure 4.32 Variation of Target 28 days strength with Predicted 28 days strength for R = 0.95 for concrete with fly ash

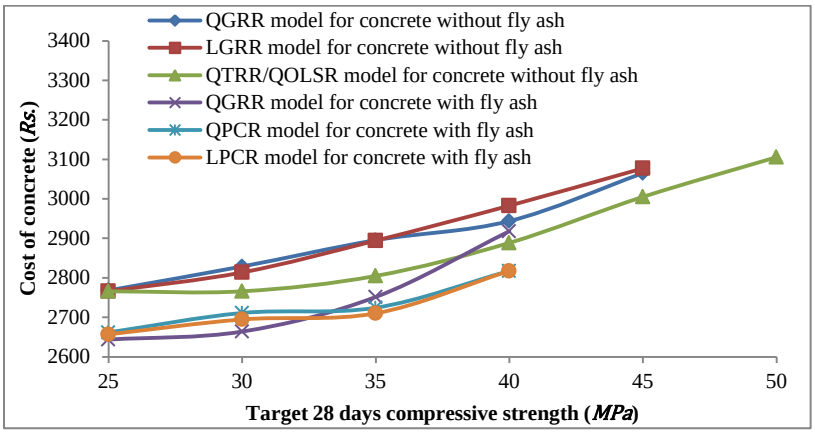

Figure 4.33(a) Variation of optimal cost with target 28 days compressive strength for concrete with and without fly ash for reliability level of 0.90

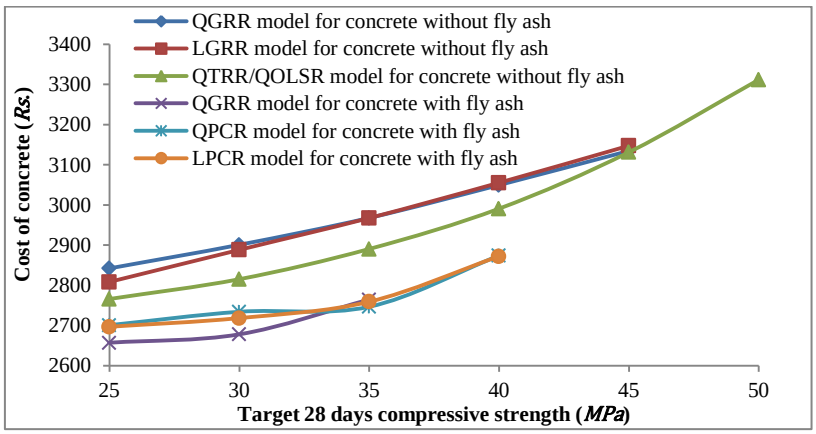

Figure 4.33(b) Variation of optimal cost with target 28 days compressive strength for concrete with and without fly ash for reliability level of 0.95

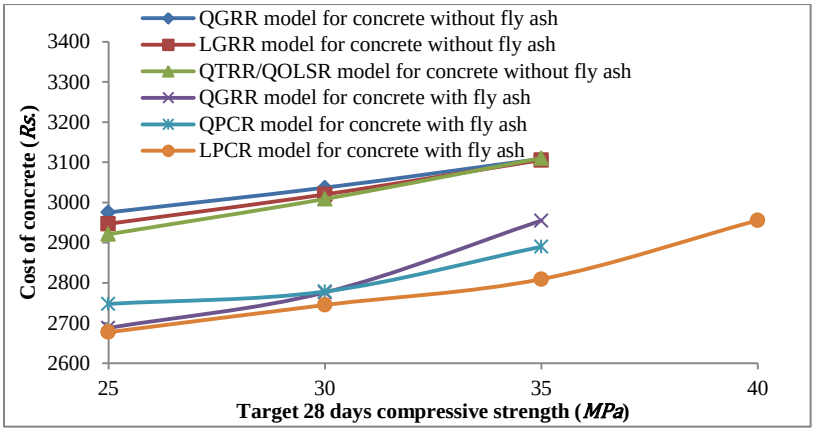

Figure 4.33(c) Variation of optimal cost with target 28 days compressive strength for concrete with and without fly ash for reliability level of 0.99

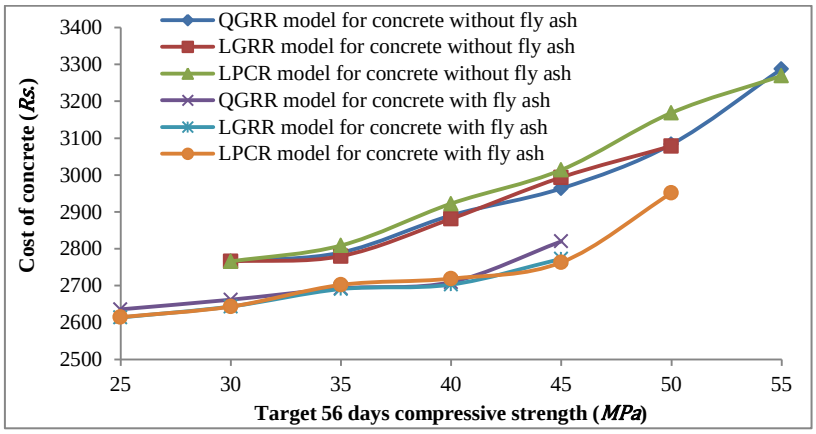

Figure 4.34(a) Variation of optimal cost with target 56 days compressive strength for concrete with and without fly ash for reliability level of 0.90

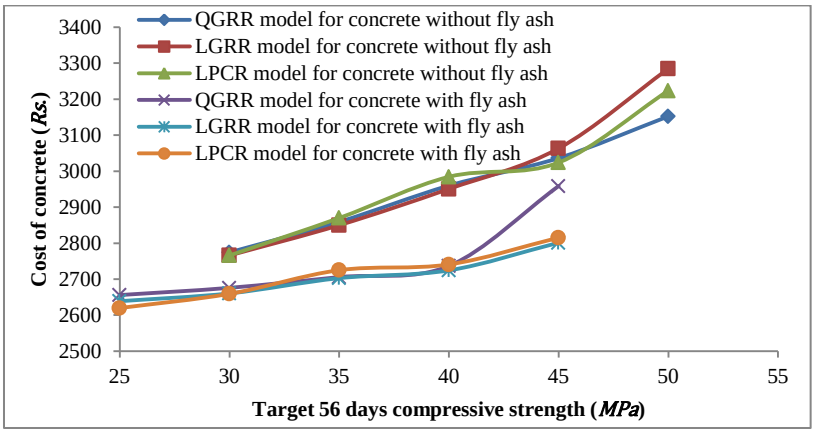

Figure 4.34(b) Variation of optimal cost with target 56 days compressive strength for concrete with and without fly ash for reliability level of 0.95

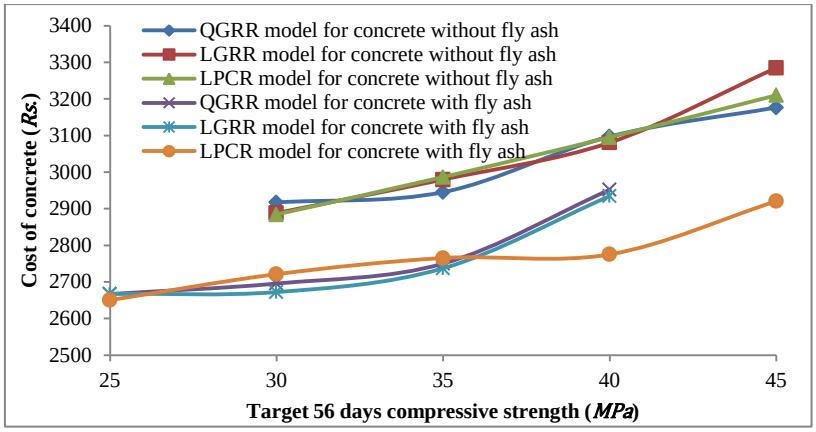

Figure 4.34(c) Variation of optimal cost with target 56 days compressive strength for concrete with and without fly ash for reliability level of 0.99

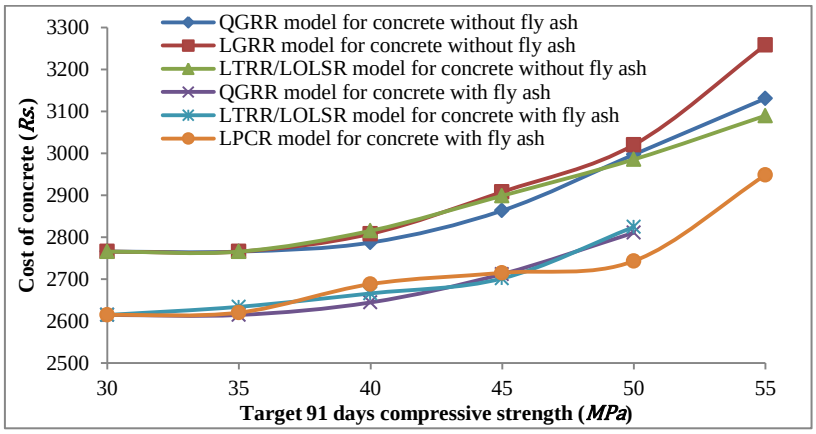

Figure 4.35(a) Variation of optimal cost with target 91 days compressive strength for concrete with and without fly ash for reliability level of 0.90

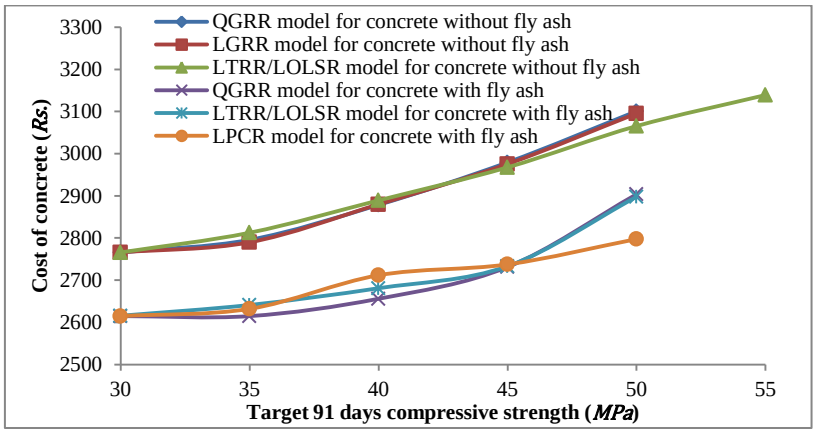

Figure 4.35(b) Variation of optimal cost with target 91 days compressive strength for concrete with and without fly ash for reliability level of 0.95

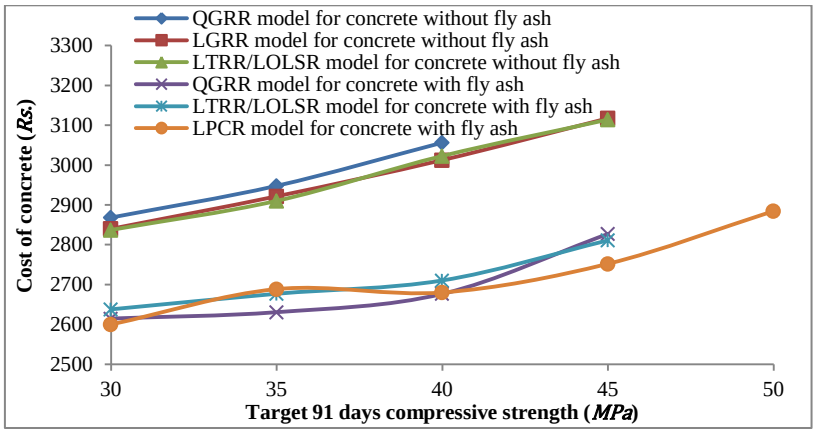

Figure 4.35(c) Variation of optimal cost with target 91 days compressive strength for concrete with and without fly ash for reliability level of 0.99

CHAPTER 5

RELIABILITY BASED MULTI-OBJECTIVE OPTIMIZATION OF CONCRETE MIX PARAMETERS

==========

5.0 GENERAL

Studying the impact of reliability on optimal solutions can be of a great practical importance as it gives an idea regarding how the design variables change so as to make corresponding solution more and more reliable. This can be realized by making optimization problem multi-objective by considering minimization of probability of failure of one or more constraints as additional objectives and obtaining a set of non-dominated solutions, *i.e.*, a Pareto-optimal front. The present chapter describes the optimal concrete mix proportions meeting the requirements of two objectives, namely, cost and reliability, under certain restrictions. Pareto-optimal fronts have been obtained considering various factors like compressive strength requirements, regression modeling technique, reliability level, curing age and percentage replacement of cement by fly ash. Performance of compressive strength models has been assessed on the basis of cost and reliability. Variation in parameters of optimized concrete mix proportions has also been studied. The proposed reliability based design procedure has been demonstrated with the help of a concrete mix design example.

5.1 FORMULATION OF MULTI-OBJECTIVE RBDO MODEL FOR CONCRETE MIX PARAMETERS

The formulation of the multi-objective RBDO model for the problem in hand requires satisfying two main objectives. The first objective is to minimize the cost of concrete and the second objective is to design a mix having compressive strength for a given curing age above a specified level with minimum probability of failure. These objectives are minimized satisfying a ratio constraint, an absolute volume constraint,

boundary constraints on input variables and a reliability constraint on compressive strength requirement. Input variables are the same as taken in single-objective RBDO problem discussed in Chapter 4. These variables are $w, fa, ca-I, ca-II, ca-III$ and b. It is presumed that all the six input variables are random in nature and follow normal distribution with their respective means and standard deviations listed in Tables 4.1 and 4.2.

Multi-objective RBDO problem for evaluating optimized concrete mix proportions is formulated as follows:

$$\left.\begin{array}{c} \underset{\mu_w,\,\mu_{fa},\,\mu_{ca-I},\mu_{ca-II},\mu_{ca-III},\mu_b}{Minimize} \quad cost\,(fa, ca-I, ca-II, ca-III, b) \\ \underset{\mu_w,\,\mu_{fa},\,\mu_{ca-I},\mu_{ca-II},\mu_{ca-III},\mu_b}{Minimize} \quad st\_pof = 1 - \text{Prob}\left(cst_t(\text{w}, fa, ca-I, ca-II, ca-III, b) \geq f_{c,t}\right) \\ Subject\ to: \quad st\_pof \leq P_f \\ 0.42 \leq {}^{w}/_{b} \leq 0.55 \\ v = 1.00 \\ w_l \leq w \leq w_u \\ fa_l \leq fa \leq fa_u \\ ca-I_l \leq ca-I \leq ca-I_u \\ ca-II_l \leq ca-II \leq ca-II_u \\ ca-III_l \leq ca-III \leq ca-III_u \\ b_l \leq b \leq b_u \end{array}\right\} \quad (5.1)$$

In (5.1), all the notations have already been explained in Chapter 4 except the following two notations:

st_pof - Probability of failure of compressive strength constraint

P_f - Upper bound on probability of failure of compressive strength constraint

All the constraints in (5.1) are the same as taken in single-objective RBDO problem given in (4.1) except the first constraint. First constraint in (5.1) is the reliability constraint on compressive strength of concrete that has been posed as a constraint on failure probability. This constraint ensures that compressive strength of concrete for a given curing period is more than a specified value of compressive strength $f_{c,t}$ with reliability not less than 1- P_f. Lesser is the value of st_pof, more is the reliability of the obtained concrete mix design. So, these two terms will be interchangeably used in discussion of optimization results.

The multi-objective RBDO problem given in (5.1) has been solved using NSGA-II technique. This technique has been implemented using VisualDoc 7.2 developed by Vanderplaats Research & Development Inc. It can further be noted from (5.1) that there is one equality constraint on absolute volume of concrete in the proposed model.

NSGA-II cannot handle equality constraint as such and hence, penalty function method is used to convert the equality constraint into inequality constraint. Using this method, the equality constraint is replaced by the inequality constraint given in (5.2).

$$|v - 1| - \varepsilon \leq 0 \tag{5.2}$$

Herein, ε is a small positive number and is called penalty parameter. In the present work, ε is taken as 1 percent of total volume of concrete, *i.e.*, 0.01.

Three best performing models of compressive strength of concrete with or without fly ash have been selected for each curing age on the basis of their performance in case of single-objective optimizations discussed in Chapter 4. Table 5.1 gives a comprehensive list of selected models.

The multi-objective RBDO models based on the selected models have been solved using NSGA-II technique. Optimizations have been performed for concrete without fly ash and for concrete with 15% replacement of cement by fly ash by varying the parameters of curing age, target compressive strength and probability of failure. The variation in parameters is listed in Table 5.2. The optimizations have been performed for target compressive strength ranging from 25 MPa to 55 MPa as this represents a fairly representative group covering all the ranges of practical use of concrete. The minimum value has been taken as 25 MPa for 28 days and 30 MPa for 91 days curing age for concrete with or without fly ash. This value has been taken as 30 MPa and 25 MPa for 56 days curing age for concrete without and with fly ash, respectively.

5.2 SELECTION OF NSGA-II PARAMETERS

The aim of the study is to locate global Pareto-optimal fronts in each of the cases taken up for finding optimized concrete mix proportions. However, the Pareto-optimal solutions obtained can be dependent upon chosen NSGA-II parameters and, if NSGA-II parameters are not suitably chosen, the optimization results may correspond to a local Pareto-optimal front rather than the global Pareto-optimal front. There are four main parameters in NSGA-II, namely, population size, number of generations, mutation probability and cross over probability. Firstly, experimentation is done to select the optimal values of population size keeping cross over probability as 0.8, mutation probability as 0.9 and number of generations as100. Here, cross over probability of 0.8 signifies that 80% strings in the population are used in the cross over operation to generate new and probably better strings and mutation probability of 0.9 means that

once a bit is mutated in a string, the next mutated bit is determined by an exponential distribution with mean equal to (1/0.9). It is worth mentioning here that cross over helps in converging towards a good solution, probably, global optimum , while mutation helps in exploring whole search space.

Population size is taken as 16, 18, 20, 22 in each of the cases under study. The Pareto-optimal fronts obtained for different population sizes for minimum value of target compressive strength for a given curing age and P_f = 0.1 using selected models for concrete without and with fly ash are shown in Figures 5.1-5.6. The population size corresponding to which best Pareto-optimal front is obtained is selected and has been shown in Figures for each case.

Next, keeping population size and number of generations fixed, mutation probability and crossover probability is varied randomly between 0 and 1. However, on analysis, it is observed that Pareto-fronts do not show any significant variation corresponding to changes in these two probabilities. So, mutation probability and crossover probability are taken as 0.9 and 0.8 in the remaining cases as well. Further, keeping population size, mutation probability and crossover probability fixed, Pareto-optimal fronts are obtained for number of generaions as 50, 75 and 100. It is seen that best Pareto-optimal fronts are obtained corresponding to number of generations as 100. Thus, number of generations is fixed as 100 in the present study.

5.3 DISCUSSION OF RESULTS FOR CONCRETE WITHOUT FLY ASH

In this section, Pareto-optimal fronts obtained corresponding to various factors like compressive strength requirements, regression modeling technique, reliability level, and curing age for concrete without fly ash have been analyzed to identify the best model that produces concrete mixes with minimum cost and minimum probability of failure.

5.3.1 Variation of cost of concrete with probability of failure for 28 days curing age

Figures 5.7(a)-(c) depict the locations of Pareto-optimal fronts based on QGRR model for 28 days compressive strength with P_f = 0.1, 0.05 and 0.01, respectively. It can be noted from Figure 5.7(a) that Pareto-optimal front for target $st28$ of 25 MPa does not cover entire range of allowed probability of failure. Also, Figure 5.7(b) shows that no

pareto-optimal solution is obtained for probability of failure beyond 0.03 for target $st28$ of 25 MPa. These observations can be attributed to the fact that 25 MPa is a very small value of compressive strength and can be attained with a very high level of reliability for range of parameters under study. Figure 5.7(c) reveals that no solution is obtained for $st28$ of 45 MPa and P_f of 0.01. This observation is also indicated from Pareto-optimal front obtained for $st28$ of 45 MPa and P_f of 0.1 and 0.05 as shown in Figures 5.7 (a) and (b). It can be seen from the curves that no optimal solution is obtained for probability of failure below 0.019 for this value of target strength. This indicates that target strength of 45 MPa cannot be achieved for reliability greater than 0.981 within the predefined range of the concrete mix parameters. In all the remaining cases, Pareto-optimal solutions are uniformly spread over the entire range of allowed probability of failure. Thus, the decision maker is provided with a wide range of options within the desired limits of probability of failure.

Further, it can also be observed from Figures 5.7(a)-(c) that the Pareto-optimal fronts move parallel to each other in upward direction as the specified compressive strength increases from 25 MPa to 45 MPa. However, the gap between the Pareto curves does increase with rise in target compressive strength. This indicates that the fronts are not uniformly sensitive to a change in compressive strength requirements. Hence, rise in optimal cost for a unit rise in compressive strength of concrete for a given probability of failure is more in higher strength regions.

Figures 5.8(a)-(c) show the Pareto-optimal fronts based on LGRR model for 28 days compressive strength with target P_f = 0.1, 0.05 and 0.01, respectively. It can be seen from the figures that Pareto-optimal fronts obtained for every value of target $st28$ cover almost the entire range of allowed probability of failure except for $st28$ = 40 MPa with P_f = 0.01 and $st28$ = 45 MPa with P_f = 0.1and 0.05. In the cases mentioned above, Pareto fronts are very narrow and the gap of these curves from the curves lying immediately below them is very wide. These observations suggest that only a few concrete mix designs can achieve target strength of 40 MPa with reliability greater than 0.99 or achieve target strength of 45 MPa with reliability greater than 0.95. Also, these designs are not cost effective. Figure 5.8 (c) reveals that no solution is obtained for $st28$ = 45 MPa with P_f = 0.01. This means that 28 days compressive strength of 45 MPa is not achievable with reliability greater than 0.99 in this case, within the predefined ranges of the considered parameters.

Pareto-optimal fronts based on QTRR/QOLSR model are shown in figures 5.9(a)-(c). Curves are achieved for 28 days compressive strength requirements ranging from 25 MPa - 45 MPa and all the three reliability levels. It can be seen from the figures that for very low values of P_f (10^{-4}or below for $st28$ = 25 MPa - 35 MPa and 10^{-3} or below for $st28$ = 40 MPa and 45 MPa), the drop in optimal cost is rapid, but thereafter it is slow. This means larger sacrifice in optimal cost is needed as compared to the decrease in probability of failure for achieving a solution that have such a low probability of failure requirements. So, lowering probability of failure below a certain level may not be cost effective and the decision maker should assess the required reliability level properly to get reliable economic design. Figures also reveal that target $st28$ of 25 MPa, 30 MPa and 35 MPa can be achieved with high reliability. Also, curves for these values of compressive strengths are very close to each other for P_f = 0.1 and 0.05. It suggests that strength upto 35 MPa can be achieved with a nominal rise in optimal cost for a given reliability.

Figures 5.10(a)-(c), 5.11(a)-(c), 5.12(a)-(c), 5.13(a)-(c) and 5.14(a)-(c) divulge the comparative performance of all the three models for different compressive strength requirements and different probabilities of failure. It can be noted from the figures that QTRR/QOLSR performs best in all the cases related to 28 days compressive strength. Pareto-curves for QTRR/QOLSR model lie much below the curves for QGRR and LGRR model suggesting that QTRR/QOLSR model offers significant improvement in optimal costs for a given reliability. Performance of QGRR and LGRR models are comparable with QGRR model giving Pareto-optimal fronts slightly better than LGRR model except only for one case of target $st28$ = 25 MPa and P_f = 0.05.

Further, it can be noted from Figure 5.14(b) that for target $st28$ = 45 MPa and P_f = 0.05, LGRR model performs worst with only 5 Pareto-optimal solutions that lie much above the solutions obtained from QGRR model. Figure 5.14(c) shows that for target $st28$ = 45 MPa and P_f = 0.01, QGRR and LGRR models do not yield any solution. But, QTRR/QOLSR model give Pareto front covering a wide range of allowed failure probability.

It is seen that QTRR/QOLSR model gives best Pareto-optimal fronts for each probability level and each 28 days compressive strength requirement.

5.3.2 Variation of cost of concrete with probability of failure for 56 days curing age

The Figures 5.15(a)-(c) describe the locations of Pareto-optimal fronts based on QGRR model for 56 days compressive strength with P_f = 0.1, 0.05 and 0.01, respectively. Pareto-optimal fronts are obtained for target 56 days compressive strength ranging from 30 MPa-55 MPa corresponding to all the three reliability levels. However for target $st56$ = 55 MPa, a small Pareto-optimal front is obtained only for one value of P_f, *i.e.*, 0.1. It can be observed from the figures that for probability of failure 10^{-3} or below, the optimal cost falls more swiftly than the rise in probability of failure for target $st56$ of 30 MPa, 35 MPa, 40 MPa and 45 MPa. This means that achieving highly reliable concrete mix proportions is not economical. Further, the gap between the curves widens as the target strength increases. This observation is same as obtained for 28 days strength cases. Pareto-optimal solutions are evenly distributed along the curves covering approximately entire range of allowed failure probability, except for target $st56$ of 30 MPa and 35 MPa with P_f = 0.1.

Pareto-optimal fronts obtained for LGRR model are shown in Figures 5.16(a)-(c). Fronts are obtained upto target 56 days strength of 50 MPa with P_f = 0.1 and 0.05. However, for P_f = 0.01, Pareto-optimal fronts are obtained upto target strength of 45 MPa. Also, for target strength of 50 MPa, only 9 and 6 optimal solutions are obtained for P_f = 0.1 and 0.05, respectively. These solutions are confined to a narrow region of allowed failure probability. These observations indicate that 56 days compressive strength of 50 MPa cannot be attained with a reliability greater than 0.97 within the specified ranges of concrete mix parameters.

Figures 5.17(a)-(c) show the Pareto-optimal fronts obtained using LPCR model for 56 days strength. Pareto-optimal fronts are achieved for target strength ranging from 30 MPa-50 MPa and for all reliability levels. However, for target strength of 50 MPa and P_f = 0.01, only 4 pareto-optimal points are found resulting into a narrow Pareto-optimal front. It can be seen from the figures that for very low values of P_f (10^{-4}or below for $st56$ = 30 MPa, 35 MPa and 10^{-3} or below for $st56$ = 40 MPa), the fall in optimal cost is rapid, but thereafter it is slow. This means that to raise the reliability level above a particular limit may not be cost effective. Further, for target $st56$ = 30 MPa, Pareto-optimal solutions are obtained upto 0.016 probability of failure. In a similar manner, maximum value of probability of failure achieved for target strength of 35 MPa is

0.049. This means that concrete mix designs attained for these target strengths are highly reliable.

Comparative performance of all the three models for different compressive strength requirements and different probabilities of failure is shown in Figures 5.18(a)-(c), 5.19(a)-(c), 5.20(a)-(c), 5.21(a)-(c), 5.22(a)-(c) and 5.23. It can be noted from Figures 5.18(a)-(b) that Pareto-optimal curves for all the three models for target $st56$ = 30 MPa are placed very close to each other for P_f = 0.1 and 0.05 with curve for LPCR model slightly below the curves for other two models. However, for P_f = 0.01, QGRR model gives the most optimized results closely followed by LPCR model.

Figures 5.19(a)-(c) reveal that for target 56 days strength of 35 MPa, QGRR and LPCR models give similar results that are better than that for LGRR model. It can be seen from Figures 5.20(a)-(c), 5.21(a)-(c), 5.22(a)-(c) that for target strength requirements of 40 MPa, 45 MPa and 50 MPa, LGRR model performs worst and QGRR model give best results. However, LPCR model yield Pareto-optimal curve overlapping the curve corresponding to QGRR model for $st56$ = 40 MPa, 45 MPa with P_f = 0.1. Further, Figure 5.22(c) shows that for target $st56$ = 50 MPa and P_f = 0.01, only QGRR model produces a Pareto-optimal front covering a significant range of probability of failure. LPCR gives a very narrow front made up of only four points and LGRR model does not give any solution. Also, for target $st56$ = 55 MPa and P_f = 0.1, only QGRR model yields a Pareto-optimal front (Figure 5.23).

Hence, it was seen that performance of QGRR model and LPCR model are similar and better than LGRR model when all the 56 days compressive strength requirements and all the three reliability levels are considered.

5.3.3 Variation of cost of concrete with probability of failure for 91 days curing age

Pareto-optimal fronts obtained using all the three models selected for 91 days compressive strength with different probabilities of failure are shown in Figures 5.24(a)-(c), 5.25(a)-(c) and 5.26(a)-(c). It can be seen from the figures that irrespective of the compressive strength model used, there are two common observations in the results obtained. Firstly, for very low values of P_f (10^{-3}or below) for $st91$ = 30 MPa - 40 MPa, the drop in optimal cost is sharp, but subsequently the drop rate slows down. This means rise in optimal cost is sharp as compared to the decrease in probability of

failure for achieving a solution that have such a low probability of failure requirements. So, lowering probability of failure below a certain level may not be cost effective. Secondly, Pareto-optimal curves go upwards as strength requirement increases for a given reliability level. This is justified as to get higher strength more cost is to be paid. However, this rise is not uniform in the sense that as one move upwards, the gap between the curves widens implying that to raise the strength by one unit in higher strength region is costlier than in lower strength regions. The observations other than the above two observations for different models are summarized below.

For target $st91$ of of 55 MPa, QGRR model based solutions are obtained for probability of failure above 0.7 (Figure 5.24(a)). This means that compressive strength of 55 MPa cannot be achieved with reliability greater than 93 percent. This limit for strength requirement of 50 MPa is 98 percent. However, upto target strength of 45 MPa, strengths can be achieved with very high reliabilities.

It can be seen for Figures 5.25(a)-(c) that results obtained using LGRR model are almost similar to results obtained using QGRR model. However, it can be seen from Figure 5.25(a) that for target $st91$ = 30 MPa and P_f = 0.1, Pareto-optimal front goes upto probability of failure of 0.011. But, when the optimization was run for target st91 = 30 MPa and P_f = 0.05, solutions are obtained upto probability of failure 0.048 (Figure 5.25(b)). This indicates that in former case, NSGA-II optimizer is not able to explore the entire search space to yield widely spread solutions.

Figures 5.26(a)-(c) reveal that when LTRR/LOLSR model for 91 days compressive strength is used, solutions are obtained upto target $st91$ of 50 MPa with each reliability level and for $st91$ = 55 MPa with P_f = 0.1 and 0.05. It can be seen from Figures 5.26(b) and 5.26(c) that for $st91$ = 55 MPa with P_f = 0.05 and $st91$ = 50 MPa with P_f = 0.01, only 4 Pareto-optimal points are obtained in each case that result in very narrow Pareto-optimal fronts. It can be said that compressive strength of 55 MPa and 50 MPa can be realized with maximum reliability of 0.95 and 0.99, respectively. Further, for target $st91$ of 30 MPa, Figures 5.26(a) and 5.26 (b) show that Pareto fronts go upto probability of failure 0.0094 and 0.033, respectively. This observation is similar to the one made in case of LGRR model based results for 91 days strength. Again, this might be due to the local convergence of optimizer. It can be noted from Figure 5.26(a) that for target $st91$ = 35 MPa with P_f = 0.1, there is only one solution with probability of failure 0.096 while all the other solutions have probability of failure below 0.03. So, in

between 0.03 and 0.096, no solution is obtained. This indicates that the solutions are not uniformly distributed in this case.

Comparative performance of all the three models for different compressive strength requirements and different probabilities of failure is shown in Figures 5.27(a)-(c), 5.28(a)-(c), 5.29(a)-(c), 5.30(a)-(c), 5.31(a)-(c), 5.32(a)-(b). It can be seen from Figures 5.27(a)-(c) that for target $st91$ = 30 MPa, initially all the curves are overlapping. But, as probability of failure increases curves based on QGRR model lies above the LGRR and LTRR/LOLSR models based curves. LTRR/LOLSR and LGRR models perform slightly better than QGRR model. Figures 5.28(a)-(c) show that for $st91$ = 35 MPa, all the three curves are very close to each other with QGRR model based curve lying uppermost for all reliability levels. It can be noted from Figures 5.29(a)-(c) that for target $st91$ = 40 MPa, LTRR/LOLSR model performs best for each reliability level followed by LGRR model. For target $st91$ of 45 MPa, 50 MPa and 55 MPa, LTRR/LOLSR model performs best and LGRR model gives worst results(Figures 5.30(a)-5.32(b)).

Hence, it can be seen that all the three selected models perform fairly well upto target $st91$ of 40 MPa for each reliability level under consideration. However, afterwards LTRR/LOLSR model performs better than other two models.

5.4 DISCUSSION OF RESULTS FOR CONCRETE WITH 15 % REPLACEMENT OF CEMENT BY FLY ASH

In this section, Pareto-optimal fronts obtained corresponding to various factors like compressive strength requirements, regression modeling technique, reliability level, and curing age for concrete with 15% replacement of cement by fly ash have been analyzed to identify the best model that produces concrete mixes with minimum cost and minimum probability of failure.

5.4.1 Variation of cost of concrete with probability of failure for 28 days curing age

Pareto-optimal fronts achieved using all the three selected models for 28 days compressive strength for concrete with fly ash for different probabilities of failure are shown in Figures 5.33(a)-(c), 5.34(a)-(c) and 5.35(a)-(c). Figures 5.33(a)-(c) depict that using QGRR model, Pareto-optimal fronts are obtained upto target $st28$ of 35 MPa for

P_f = 0.1 and 0.05 and upto 30 MPa for P_f = 0.01. As strength requirement increases, the widening gap between the curves implies that for concrete with fly ash, it is much costlier to raise the required strength level from 30 MPa to 35 MPa than 25 MPa to 30 MPa. Figure 5.33(a) shows that for target $st28$ of 25 MPa and 30 MPa, only one Pareto point is obtained for probability of failure above 0.06 and 0.04 respectively. Also, Figure 5.33(b) reveals that target $st28$ of 25 MPa, only two solutions are obtained for probability of failure above 0.02. These observations suggest that spread of solutions is not uniform in these cases.

Pareto-optimal fronts obtained using QPCR model are demonstrated in Figures 5.34(a)-(c). It can be seen from the figures that optimal solutions are achieved upto target strength of 40 MPa with P_f = 0.1 and 0.05. However, for P_f = 0.01, results are obtained upto target strength of 35 MPa. Pareto-optimal fronts for $st28$ of 25 MPa and 30 MPa are very close to each other in each case. Further, Figure 5.34(a) shows that for target $st28$ of 40 MPa, no solution is obtained for probability of failure below 0.03. It suggests that this strength can be attained with reliability not more than 0.97. Further, for probability of failure 10^{-3} or below and $st28$ of 25 MPa and 30 MPa, the Pareto fronts are almost parallel to cost axis implying that lowering of probability of failure below a certain level is not economical.

Investigation of Pareto-optimal fronts obtained using LPCR model (Figures 5.35(a)-(c)) conveys that the results obtained using LPCR model are similar to the results obtained using QPCR model.

Further, performance of all the three models for different compressive strength requirements and different probabilities of failure have been compared and the results have been presented in Figures 5.36(a)-(c), 5.37(a)-(c), 5.38(a)-(c), 5.39(a)-(b). Figures 5.36(a)-(c) show that Pareto fronts for all the three models are very close to each other with LPCR model performing slightly better than other two models. It can be noted from Figures 5.37(a)-(c), 5.38(a)-(c) that for target st28 of 30 MPa and 35 MPa, fronts for both PCR models are almost overlapping and lie below the front obtained using QGRR model indicating that they perform better than QGRR model. Figures 5.39(a)-(b) depict that no solution is obtained using QGRR model for target $st28$ = 40 MPa. LPCR model performs better than QPCR model in these cases.

Hence, it can be inferred that upto target 28 days strength of 35 MPa, performance of both the PCR models are more or less same irrespective of the reliability level.

Subsequently, LPCR model achieves better Pareto-optimal front than QPCR model. However, performance of both the PCR models is better than QGRR model in each case under consideration.

5.4.2 Variation of cost of concrete with probability of failure for 56 days curing age

Pareto-optimal fronts obtained using all the three models selected for 56 days compressive strength with different probabilities of failure are shown in Figures 5.40(a)-(c), 5.41(a)-(c) and 5.42(a)-(c). It can be seen from the figures that irrespective of the compressive strength model used, there are two common observations in the results obtained. Firstly, for very low values of probability of failure (10^{-4}or below for $st56$ = 25 MPa and 10^{-3}or below for $st56$ = 30 MPa), optimal cost falls sharply, but thereafter the decrease in optimal cost with rise in probability of failure is nominal. Secondly, Pareto-optimal curves go upwards with widening gap between the curves as strength requirement increases for a given reliability level. The implications of these observations have already been discussed in earlier cases. The observations other than the above two observations for different models are given below.

It can be seen from Figures 5.40(a)-(c) that Pareto-optimal fronts based on QGRR model are obtained for target $st56$ of 30 MPa, 35 MPa and 40 MPa with P_f = 0.1 and 0.05 and for target $st56$ of 30 MPa and 35 MPa with P_f = 0.01. Target strength of 40 MPa can be realized with reliability not more than 0.98.

It can be noted from Figures 5.41(a) that for target strength of 25 MPa, LGRR model based Pareto curve extends upto upper level of probability of failure, *i.e.*, 0.1. However, for this target strength, the Pareto curves go only upto failure probability of 0.02 when P_f = 0.05 (Figure 5.41(b)) and upto failure probability of 0.0003 when P_f = 0.01 (Figure 5.41(c)). The curves in latter two cases do not cover entire range. It indicates that NSGA II fails to give widely spread solutions in these cases. Also, it can be seen from Figure 5.41 (b) that for target $st56$ = 30 MPa with P_f = 0.05, Pareto-optimal curve falls sharply upto failure probability of 0.003 and above this value the curve becomes almost parallel to probability of failure axis. This means that variation in cost with probability of failure is negligibly small for failure probability greater than 0.003. But, this observation seems to be unreliable as over a very wide region, cost appears to be least dependent on probability of failure.

Figures 5.42(a)-(c) summarize all the Pareto-optimal fronts obtained using LPCR model. It can be noted from Figures that for target strength of 25 MPa, same front is obtained for all the three reliability levels. This front is confined to a region below failure probability of 0.0004. Pareto-optimal curves for 30 MPa and 35 MPa, also offer solutions having high reliabilities. It can be seen from Figure 5.42(b) that for target $st56$ of 30 MPa with P_f = 0.05; only two Pareto-optimal solutions having almost same cost are found beyond failure probability of 0.006. This observation also points towards the problem of lack of spread among the solutions.

Comparison of performances of various compressive strength models for different 56 days compressive strength requirements and probability of failure levels are presented in Figures 5.43(a)-(c), 5.44(a)-(c), 5.45(a)-(c), 5.46(a)-(c), 5.47(a)-(c). Figures 5.43(a)-(c) show that for target $st56$ = 25 MPa, Pareto-optimal curves based on QGRR and LGRR model are overlapping each other and cover almost entire range of allowed failure probability. Pareto curve based on LPCR model also coincide with these two curves but is confined to probability of failure below 0.0004. It can be noted from Figures 5.44(a)-(c) that for target $st56$ = 30 MPa, all three Pareto curve lie close to each other with curve based on QGRR model uppermost and that based on LPCR model lowermost. This means that LPCR model performs best while QGRR model performs worst. In all the remaining cases also, it is observed that performance of LPCR model is better than the other two models.

So, 56 days LPCR compressive strength model produced better Pareto-optimal fronts in comparison to other two models.

5.4.3 Variation of cost of concrete with probability of failure for 91 days curing age

Pareto-optimal fronts obtained using QGRR, LPCR and LTRR/LOLSR model for 91 days compressive strength has been demonstrated in figures 5.48(a)-(c), 5.49(a)-(c)and 5.50(a)-(c).

It can be seen from Figures 5.48(a)-(c) that QGRR model yielded Pareto-optimal solutions upto target strength of 50 MPa with P_f = 0.1 and upto target strength of 45 MPa with P_f = 0.05 and 0.01. It can be noted from Figures 5.48(a)-(b) that for target strength of 30 MPa, same Pareto-optimal front is obtained for P_f = 0.1 and 0.05 and this front is restricted to failure probability below 0.01. This might be due to the fact

that 30 MPa is a very small value of target strength for 91 days curing age and can be attained with very high reliability. Figure 5.48(b) shows that Pareto curve corresponding to 35 MPa target strength is restricted below failure probability of 0.007 while Figure 5.48(a) reveals that the Pareto curve for this strength goes upto failure probability of 0.1. This indicates that NSGA-II is not able to explore entire search space to find global optimal solutions for P_f = 0.05 case. However, Pareto-curves for target strength of 40 MPa and 45 MPa cover an acceptable range of probability of failure with the widening gap between the curves with increasing target strength.

Figures 5.49(a)-(c) reveal that for LPCR model Pareto-optimal solutions upto target strength of 50 MPa with P_f = 0.1, 0.05 and upto target strength of 45 MPa with P_f = 0.01 are obtained. Pareto curves for target $st91$ of 30 MPa and 35 MPa are independent of reliability level. This means that these strengths can be realized with very high reliability. Also, for target $st91$ of 40 MPa, Pareto-optimal solutions are obtained upto probability of failure 0.033.

5.50(a)-(c) demonstrate that LTRR/LOLSR model give Pareto-optimal solutions upto target strength of 50 MPa with P_f = 0.1 and upto target strength of 45 MPa with P_f = 0.05, 0.01. For target $st91$ of 50 MPa with P_f = 0.1, a narrow Pareto-optimal front is obtained which lies much above the curve for 45 MPa. Similarly, for target $st91$ of 45 MPa with P_f = 0.01, only 7 closely packed solutions are found that form a front lying much above the front for target strength of 40 MPa. Figures 5.50(a)-(b) that for target strength of 30 MPa, same Pareto-optimal front is obtained for P_f = 0.1 and 0.05 and this front is restricted to failure probability below 0.03.

Figures 5.51(a)-(c), 5.52(a)-(c), 5.53(a)-(c), 5.54(a)-(c), 5.55(a)-(b) reveal the comparative performance of all the three models for different compressive strength requirements and different probabilities of failure. It can be noted from Figures 5.51(a)-(c) and 5.52(a)-(c) that for target $st91$ of 30 MPa and 35 MPa, initially all the curves are overlapping, thereafter performance of LPCR is best followed by QGRR model. The only drawback of LPCR based curve is that it does not cover the entire range of allowed failure probability. In all the remaining cases also, LPCR performs best and LTRR/LOLSR is worst.

Hence, LPCR model for 91 days concrete compressive strength performs best when all the compressive strength requirements and all the three reliability levels are considered.

Considering the observations for all the three curing ages for concrete with fly ash, linear regression model based on PCR technique yields concrete mix proportions characterized by lowest cost and lowest probability of failure.

5.5 VARIATION IN CONCRETE MIX PARAMETERS

In this section, variation of water-binder ratio with probability of failure has been demonstrated for concrete with or without fly ash and different curing ages. The cases with upper bound 0.1 on allowed probability of failure has been discussed as this covers a fairly large range of allowed failure probability. Further, the variation of binder content, fine aggregate-binder content and total aggregate-binder content with water-binder ratio has also been studied.

5.5.1 Variation of water-binder ratio with probability of failure

Figures 5.56(a)-(c), 5.60(a)-(c), 5.64(a)-(c), 5.68(a)-(c), 5.72(a)-(c) and 5.76(a)-(c) show the variation of w/b ratio with probability of failure for different compressive strength models and curing ages of 28 days, 56 days and 91 days for concrete without and with fly ash. It can be seen from the figures that w/b ratio falls as target strength rises for a given reliability level except for two cases. These cases are of QTRR/QOLSR model based results for target 28 days compressive strength of 25 MPa and 30 MPa for concrete without fly ash and QGRR model based results for target 56 days compressive strength of 30 MPa and 35 MPa for concrete without fly ash (Figs. 5.56(c) and 5.60 (a)). It is also observed that w/b ratio rises as probability of failure rises for a given target strength, in general. The relationship between these two variables can be expressed as:

$$w/b = A(st\_pof)^B \tag{5.3}$$

where A and B are constants.

Tables 5.3-5.8 summarizes the parameters of (5.3) obtained in each case under study. Also, the value of coefficient of determination R^2 which is a measure of variation in dependent variable explained by the predictor variable has also been given in Tables for each case. Value of R^2 is greater than 0.9 in most of the cases indicating that the (5.3) demonstrates the relationship between w/c ratio and probability of failure efficiently. The cases where (5.3) does not fit the data adequately for concrete without fly ash are that of target $st28$ of 45 MPa using LGRR model, target $st56$ of 45 MPa using

QGRR model, target $st56$ of 45 MPa using LGRR model, target $st56$ of 35 MPa using LPCR model. Such cases for concrete with fly ash are that of target $st28$ of 35 MPa and 40 MPa using QPCR model, target $st28$ of 30 MPa and 35 MPa using LPCR model, target $st56$ of 40 MPa using LPCR model and target $st91$ of 30 MPa and 45 MPa using LGRR model. It is also seen from the figures that variation of w/c or w/cm ratio with st_pof does not follow any particular trend for certain target strength requirements. The cases for concrete without fly ash where no particular trend is observed are that of target $st56$ of 50 MPa for all the models, target $st56$ of 55 MPa for QGRR model and target $st91$ of 55 MPa for QGRR model and LGRR model. Such cases for concrete with fly ash are that of target $st28$ of 40 MPa for LPCR model, target $st56$ of 45 MPa for LGRR model and LPCR model and target $st91$ of 50 MPa for all the models. It can be said that for high compressive strength requirements for a given curing age, w/b ratio vary randomly with probability of failure.

5.5.2 Variation of binder content with water-binder ratio

Figures 5.57(a)-(c), 5.61(a)-(c), 5.65(a)-(c), 5.69(a)-(c), 5.73(a)-(c) and 5.77(a)-(c) depict the variation of b with w/b ratio for different compressive strength models and curing ages of 28 days, 56 days and 91 days for concrete without and with fly ash. It can be seen from the figures 5.57(a)-(c), 5.61(a)-(c) and 5.65(a)-(c) that cement content decreases with increase in w/c ratio and curves for different compressive strength requirements for a given curing age appear to follow either a linear or a quadratic curve expressed as:

$$b = a_0 + a_1\left(w/b\right) \tag{5.4}$$

or

$$b = a_0 + a_1\left(w/b\right) + a_2\left(w/b\right)^2 \tag{5.5}$$

Coefficients of best fitted curve in each case and corresponding value of R^2 is given in Tables 5.9(a)-(c). So, Eqs. (5.4) and (5.5) can be used to find cement content corresponding to a given w/c ratio depending upon the curing age and the compressive strength model used for concrete without fly ash. Figures 5.69(a)-(c), 5.73(a)-(c) and 5.77(a)-(c) reveal that for concrete with fly ash, variation of cm content with w/cm ratio is not uniform for a given curing age. It can be seen from Figures 5.69(a)-(c) and 5.73 (a)-(c) that for curing age of 28 days and 56 days, fall of cm content with rise in

w/cm ratio for w/cm ratio less than 0.46 is sharper than that for w/cm ratio greater than 0.46. Similar observation was made for curing age of 91 days and w/cm ratio of 0.45. Neither linear nor quadratic curves are able to represent the relationship between cm content and w/cm ratio. However, cubic curves are capable to characterize this relationship to some extent. Coefficients of best fitted cubic curve in each case and corresponding value of R^2 for concrete with fly ash is given in Tables 5.10(a)-(c).

5.5.3 Variation of fine aggregate-binder ratio with water-binder ratio

Figures 5.58(a)-(c), 5.62(a)-(c), 5.66(a)-(c), 5.70(a)-(c), 5.74(a)-(c) and 5.78(a)-(c) depict the variation of fa/b ratio with w/b ratio for different compressive strength models and curing ages of 28 days, 56 days and 91 days for concrete without and with fly ash. It can be seen from the figures that fa/b ratio varies randomly with w/b ratio in all the cases except three cases. These cases are that of QGRR and LGRR models for 28 days curing age for concrete without fly ash and that of LTRR/LOLSR model for 91 days curing age for concrete without fly ash. In these three cases fa/c ratio rises linearly with w/c ratio for a given curing age. However, in all the cases, overall trend indicates towards a positive correlation between the two ratios.

5.5.4 Variation of coarse aggregate-binder ratio with water-binder ratio

Figures 5.59(a)-(c), 5.63(a)-(c), 5.67(a)-(c), 5.71(a)-(c), 5.75(a)-(c) and 5.79(a)-(c) show the variation of total coarse aggregate-binder (ca/b) ratio with w/b ratio for different compressive strength models and curing ages of 28 days, 56 days and 91 days for concrete without and with fly ash. It can be noted from Figures 5.59(a)-(c), 5.63(a)-(c) and 5.67(a)-(c) that for concrete without fly ash ca/c ratio rises as w/c ratio rises. For both GRR models for curing age of 28 days and for all the three models for curing age of 91 days, this rise is linear. However, in remaining cases for concrete without fly ash, the variation of ca/c ratio with w/c ratio is random. 5.71(a)-(c), 5.75(a)-(c) and 5.79(a)-(c) suggest that for concrete with fly ash, variation of ca/cm ratio with w/cm ratio does not follow any trend. This means that dependency between these two ratios is very less for concrete with fly ash.

5.6 CONCRETE MIX DESIGN EXAMPLE

The proposed reliability based mix design procedure uses the optimized concrete mix proportions obtained in the present study. The optimal concrete mix proportions for a given curing age depends upon the model used and specified reliability level. The method gives proportions in terms of quantity of materials required per unit volume of concrete. The method is equally applicable to concrete mixes using 15% replacement of cement by fly ash.

The method is suitable for the design of normal concrete mixes having cube compressive strength ranging from 25 MPa-55 MPa, for non-air-entertained concrete and for curing ages of 28, 56 and 91 days. The proposed reliability based design procedure of mix proportioning is illustrated for a mixture with the following design stipulations.

5.6.1 Design stipulations

- Target compressive cube strength at 28 days — 35 MPa
- Target reliability — 0.98
- Maximum size of aggregate zone — 20 mm
- Zone of Aggregates — A
- Degree of workability — Medium
- Degree of quality control — Very Good
- Type of exposure — Mild
- Assumed probability distribution for strength variation — Normal
- Cement replacement by fly ash, percent — Nil

5.6.2 Characteristics of materials

(i) Cement

Type of cement used	Ordinary Portland cement
Specific gravity of cement	3.10
7 days compressive strength of 70.4 mm cubes	33.5 MPa
28 days compressive strength of 70.4 mm cubes	44.6 MP

(ii) Aggregates

For the coarse aggregates belonging to zone A, the fractions of coarse aggregates of types $CA-I$, $CA-II$, $CA-III$ are 0.67, 0.33 and 0, respectively.

a) Specific gravity	
$CA-I$	2.61
$CA-II$	2.68
Fine Aggregate	2.66
b) Fineness modulus	
Fine aggregate	2.41
c) Water absorption	
$CA-I$	1.5 percent
$CA-II$	1.3 percent
Fine Aggregate	1.2 percent
d) Grading of fine aggregates	
Percentage passing 600-micron sieve	71.8 percent
Grading zone	III

5.6.3 Step by step procedure for proportioning of concrete mix

It is worth mentioning here that for 28 days compressive strength of concrete without fly ash, best performance was obtained for QTRR/QOLSR model. So, the optimal results based on this model have been used to find the required concrete mix proportions.

(i) Water-cement material ratio

For the target compressive strength of 35 MPa, the optimized water-cement ratio for the concrete mix corresponding to reliability of 0.98, calculated from Figure 5.56(c), is 0.500.

(ii) Cement content

For the water-cement ratio of 0.500, the cement content obtained from Figure 5.57(c) is 360.5 kg/m^3.

(iii) Fine aggregate-cement content ratio

For the water-cement ratio of 0.500, the fine aggregate-cement content ratio as obtained from Figure 5.58(c) is 1.78.

(iv) Coarse aggregate-cement content ratio

For the water-cement ratio of 0.500, the coarse aggregate-cement content ratio as obtained from Figure 5.59(c) is 3.18.

As per concrete mix design requirement, coarse aggregates belong to zone A, therefore,

$ca - I/c$ ratio = 3.18×0.67 = 2.131

$ca - II/c$ ratio = 3.18×0.33 = 1.177

(v) Revision of values of cement content and aggregate-cement content ratio

The revised values of the aggregate to cement content ratios are calculated as given below:

Revised cement content = (3.10×360.5)/3.12 = 358.19 kg/m^3

Revised fa/c ratio = (2.66×1.78)/2.54 = 1.864

Revised $ca - I/c$ ratio = (2.61×2.131)/2.68 = 2.075

Revised $ca - II/c$ ratio = (2.68×1.177)/2.68 = 1.177

(vi) water content

w/c remains same as grading of fine aggregates used is the same as used in the present study. So, revised value of water content is

0.500×358.19 = 179.10 kg/m^3

(vii) Aggregate contents

fa content = 1.864×358.19 = 667.67 kg/m^3

$ca - I$ content = 2.075×358.19 = 743.24 kg/m^3

$ca - II$ content = 1.177 ×358.19 = 421.59 kg/m^3

(viii) **Mix proportions**

Thus, the trial mix proportion is:

w	c	fa	$ca - I$	$ca - II$
179.10	358.19	667.67	743.24	421.59

herein, each of the content values is measured in kg/m^3.

5.7 SUMMARY

In this chapter, an extensive has been carried out to obtain reliable optimal concrete mix proportions characterized by minimum cost and minimum probability of failure. Optimal concrete mix proportions has been achieved considering factors of compressive strength requirements, regression modeling technique, curing age, percentage replacement of cement by fly ash and reliability levels. The optimal concrete mix proportions obtained forms a base for proposed reliability based design methodology for concrete mix design. This methodology could be a valuable tool for

minimizing the number of trial batches required to identify the optimal concrete mix proportions having desired properties and reliability.

Table 5.1 List of selected compressive strength models

Curing age	Selected compressive strength models	
	For concrete without fly ash	For concrete with 15% replacement of cement by fly ash
28 days	QGRR model, LGRR model, QTRR/QOLSR model	QGRR model, QPCR model, LPCR model
56 days	QGRR model, LGRR model, LPCR model	QGRR model, LGRR model, LPCR model
91 days	QGRR model, LGRR model, LTRR/LOLSR model	QGRR model, LPCR model, LTRR/LOLSR model

Table 5.2 Variation in parameters

Parameter	For concrete without fly ash	For concrete with 15% replacement of concrete by fly ash
Curing age	28, 56, 91 days	28, 56, 91 days
Maximum allowed failure probability (P_f)	0.1, 0.05, 0.01	0.1, 0.05, 0.01
Target compressive strength	25, 30, 35,40, 45, 50, 55 MPa	25, 30, 35,40, 45, 50, 55 MPa

Table 5.3 Parameters for relationship between w/c ratio and probability of failure for concrete without fly ash and 28 days curing age

f_c	QGRR MODEL			LGRR MODEL			QTRR/QOLSR MODEL		
(MPa)	A	B	R^2	A	B	R^2	A	B	R^2
25	0.548	0.024	0.992	0.560	0.029	0.971	0.536	0.008	0.951
30	0.533	0.023	0.968	0.550	0.033	0.961	0.542	0.012	0.975
35	0.936	0.017	0.936	0.526	0.034	0.974	0.539	0.017	0.948
40	0.499	0.020	0.980	0.505	0.040	0.986	0.526	0.020	0.965
45	0.483	0.036	0.947	0.463	0.028	0.797	0.514	0.030	0.981

Table 5.4 Parameters for relationship between w/c ratio and probability of failure for concrete without fly ash and 56 days curing age

f_c	QGRR MODEL			LGRR MODEL			LPCR MODEL		
(MPa)	A	B	R^2	A	B	R^2	A	B	R^2
30	0.548	0.008	0.916	0.560	0.023	0.963	0.583	0.019	0.961
35	0.543	0.012	0.915	0.543	0.027	0.974	0.537	0.015	0.871
40	0.558	0.023	0.943	0.516	0.029	0.968	0.533	0.025	0.921
45	0.493	0.015	0.899	0.481	0.027	0.826	0.505	0.033	0.960
50	-	-	-	-	-	-	-	-	-
55	-	-	-	No optimization results			No optimization results		

Table 5.5 Parameters for relationship between w/c ratio and probability of failure for concrete without fly ash and 91 days curing age

f_c	QGRR MODEL			LGRR MODEL			LTRR/LOLSR MODEL		
(MPa)	A	B	R^2	A	B	R^2	A	B	R^2
30	0.576	0.026	0.974	0.553	0.018	0.977	0.560	0.021	0.979
35	0.571	0.032	0.985	0.544	0.021	0.926	0.557	0.025	0.965
40	0.565	0.041	0.981	0.537	0.029	0.974	0.553	0.033	0.964
45	0.540	0.047	0.970	0.515	0.033	0.980	0.536	0.037	0.980
50	0.536	0.064	0.970	0.481	0.036	0.939	0.509	0.043	0.978
55	-	-	-	-	-	-	0.494	0.052	0.985

Table 5.6 Parameters for relationship between w/cm ratio and probability of failure for concrete with fly ash and 28 days curing age

f_c	QGRR MODEL			QPCR MODEL			LPCR MODEL		
(MPa)	A	B	R^2	A	B	R^2	A	B	R^2
25	0.537	0.030	0.952	0.567	0.022	0.933	0.575	0.026	0.913
30	0.505	0.033	0.983	0.526	0.025	0.943	0.541	0.030	0.876
35	0.469	0.031	0.936	0.469	0.020	0.830	0.464	0.017	0.788
40	No optimization results			0.470	0.034	0.848	-	-	-

Table 5.7 Parameters for relationship between w/cm ratio and probability of failure for concrete with fly ash and 56 days curing age

f_c	QGRR MODEL			LGRR MODEL			LPCR MODEL		
(MPa)	A	B	R^2	A	B	R^2	A	B	R^2
25	0.552	0.024	0.981	0.560	0.026	0.994	0.610	0.016	0.964
30	0.516	0.024	0.970	0.540	0.031	0.998	0.591	0.023	0.947
35	0.516	0.036	0.983	0.513	0.031	0.989	0.532	0.024	0.936
40	0.504	0.046	0.982	0.514	0.040	0.978	0.503	0.030	0.888
45	No optimization results			-	-	-	-	-	-

Table 5.8 Parameters for relationship between w/cm ratio and probability of failure for concrete with fly ash and 91 days curing age

f_c	QGRR MODEL			LGRR MODEL			LTRR/LOLSR MODEL		
(MPa)	A	B	R^2	A	B	R^2	A	B	R^2
30	0.587	0.020	0.982	0.622	0.015	0.897	0.578	0.019	0.994
35	0.563	0.024	0.966	0.613	0.021	0.943	0.562	0.026	0.990
40	0.526	0.028	0.977	0.541	0.021	0.907	0.513	0.027	0.976
45	0.493	0.032	0.988	0.514	0.029	0.889	0.487	0.032	0.962
50	-	-	-	-	-	-	-	-	-

Table 5.9(a) Parameters for relationship between c and w/c ratio for concrete without fly ash and 28 days curing age

Compressive strength model	a_0	a_1	a_2	R^2
QGRR MODEL	791.2	-864.8	-	0.991
LGRR MODEL	773.0	-823.1	-	0.963
QTRR/QOLSR MODEL	1541.0	4116.0	3512.0	0.992

Table 5.9(b) Parameters for relationship between c and w/c ratio for concrete without fly ash and 56 days curing age

Compressive strength model	a_0	a_1	a_2	R^2
QGRR MODEL	2045.0	-6061.0	5424.0	0.877
LGRR MODEL	2188.0	-6779.0	6243.0	0.934
LPCR MODEL	2037.0	-6116.0	5541.0	0.899

Table 5.9(c) Parameters for relationship between c and w/c ratio for concrete without fly ash and 91 days curing age

Compressive strength model	a_0	a_1	a_2	R^2
QGRR MODEL	1503.0	-3974.0	3383.0	0.990
LGRR MODEL	1951.0	-5793.0	5221.0	0.948
LTRR/LOLSR MODEL	777.4	-833.3	-	0.975

Table 5.10(a) Parameters for relationship between cm and w/cm ratio for concrete with fly ash and 28 days curing age

Compressive strength model	a_0	a_1	a_2	a_3	R^2
QGRR MODEL	15834	-94730	19352	-13159	0.926
QPCR MODEL	17386	-10206	20397	-13557	0.780
LPCR MODEL	20684	-12265	24665	-16491	0.735

Table 5.10(b) Parameters for relationship between cm and w/cm ratio for concrete with fly ash and 56 days curing age

Compressive strength model	a_0	a_1	a_2	a_3	R^2
QGRR MODEL	12422	-73560	14983	-10160	0.957
LGRR MODEL	11140	-65234	13187	-88730	0.967
LPCR MODEL	17461	-10364	20932	-14064	0.748

Table 5.10(c) Parameters for relationship between cm and w/cm ratio for concrete with fly ash and 91 days curing age

Compressive strength model	a_0	a_1	a_2	a_3	R^2
QGRR MODEL	20113	-11998	24280	-16334	0.832
LPCR MODEL	15067	-88067	17591	-11687	0.729
LTRR/LOLSR MODEL	24416	-14638	29659	-19978	0.864

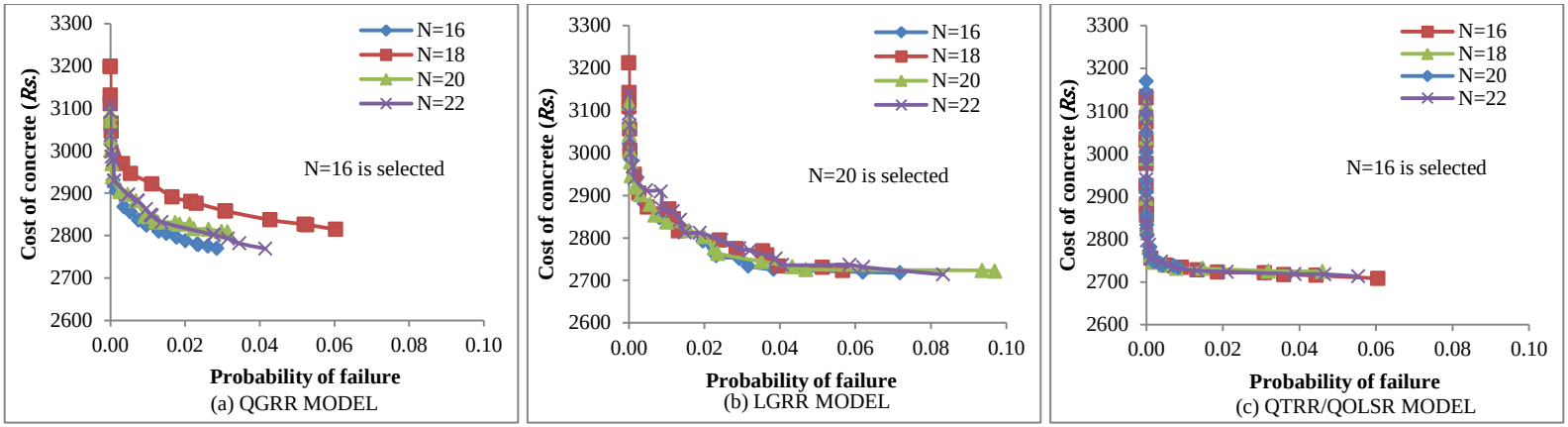

Figure 5.1 Pareto-optimal fronts for different population sizes for target 28 days compressive strength of 25 MPa with P_f = 0.1 for concrete without fly ash

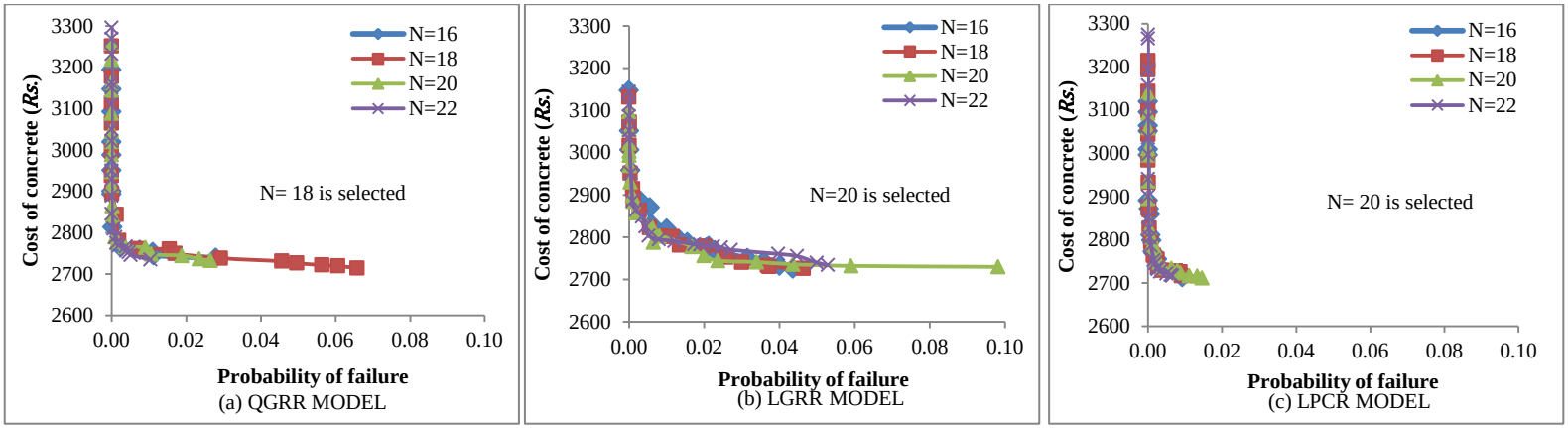

Figure 5.2 Pareto-optimal fronts for different population sizes for target 56 days compressive strength of 30 MPa with P_f = 0.1 for concrete without fly ash

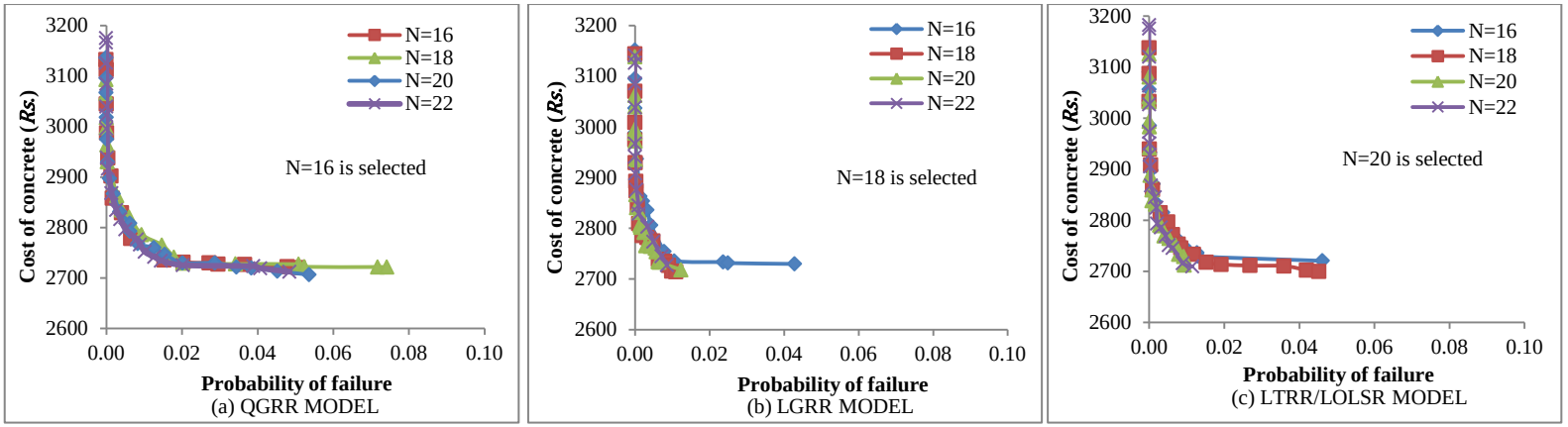

Figure 5.3 Pareto-optimal fronts for different population sizes for target 91 days compressive strength of 30 MPa with P_f=0.1 for concrete without fly ash

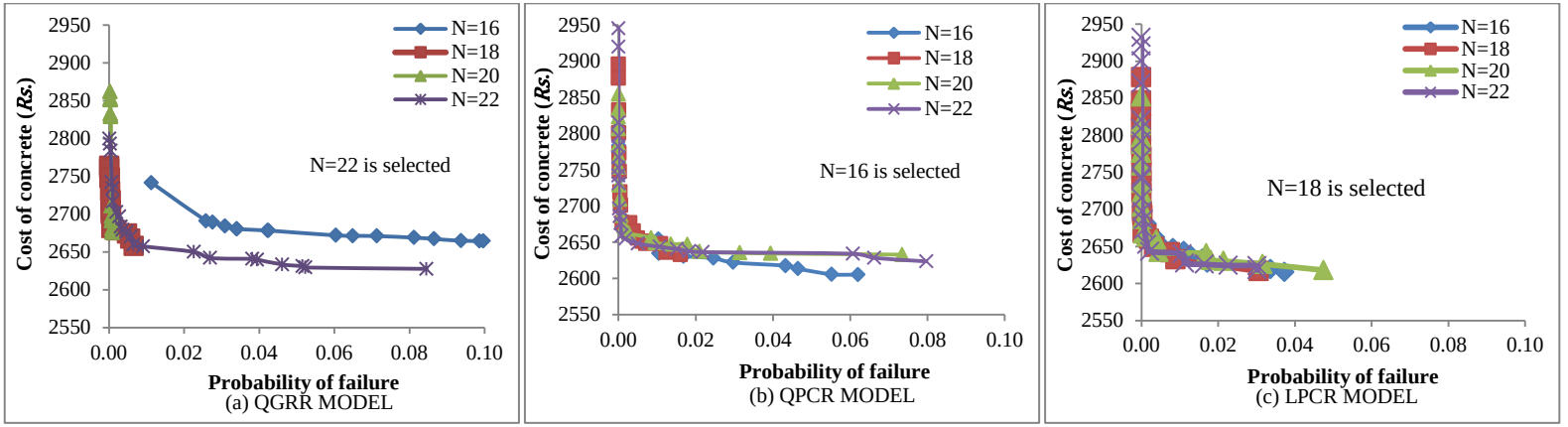

Figure 5.4 Pareto-optimal fronts for different population sizes for target 28 days compressive strength of 25 MPa with P_f = 0.1 for concrete with fly ash

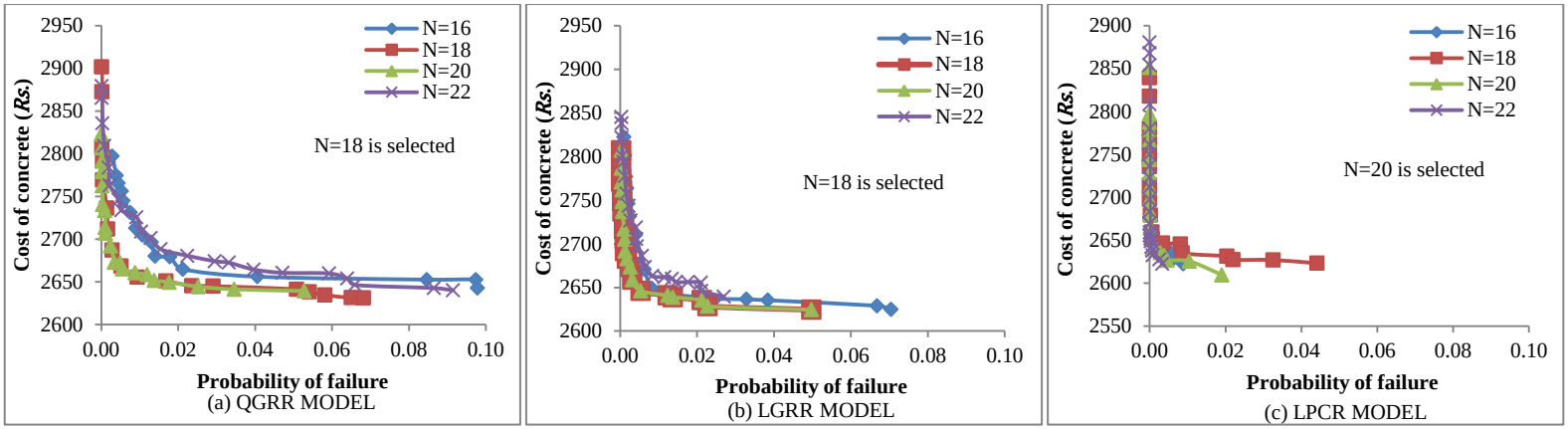

Figure 5.5 Pareto-optimal fronts for different population sizes for target 56 days compressive strength of 30 MPa with P_f = 0.1 for concrete with fly ash

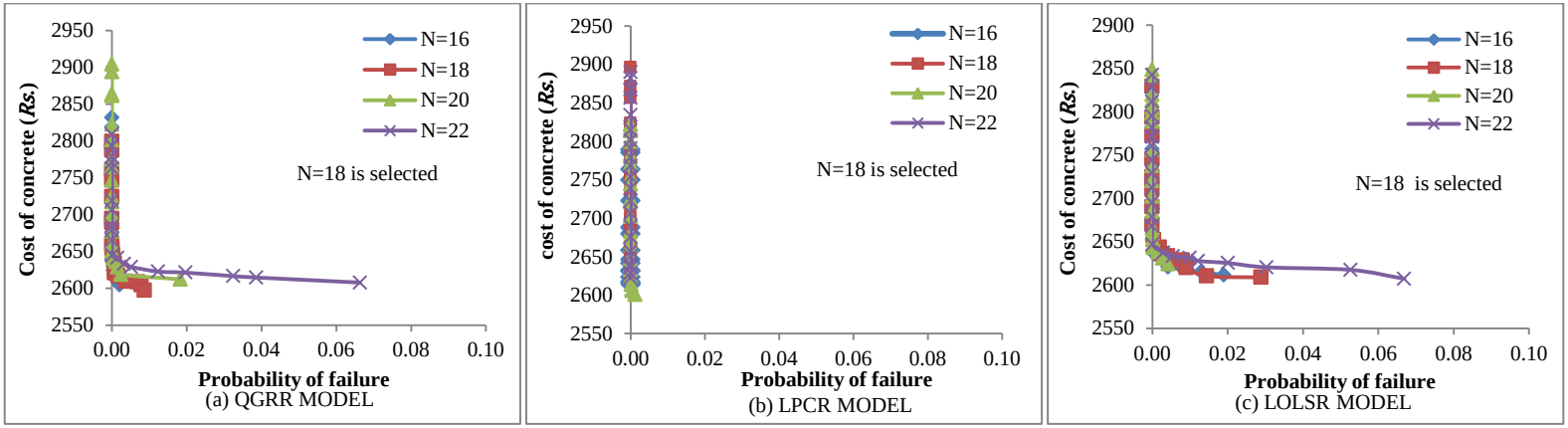

Figure 5.6 Pareto-optimal fronts for different population sizes for target 91 days compressive strength of 30 MPa with P_f = 0.1 for concrete with fly ash

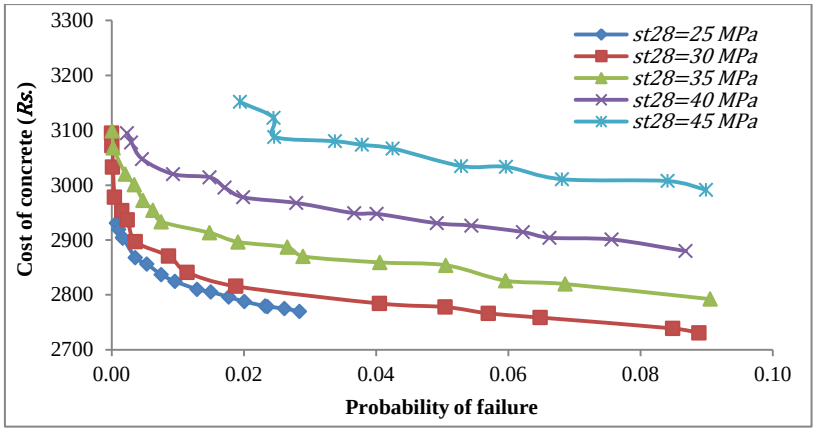

Figure 5.7(a) Pareto-optimal fronts based on QGRR model of 28 days compressive strength with P_f = 0.1 for concrete without fly ash

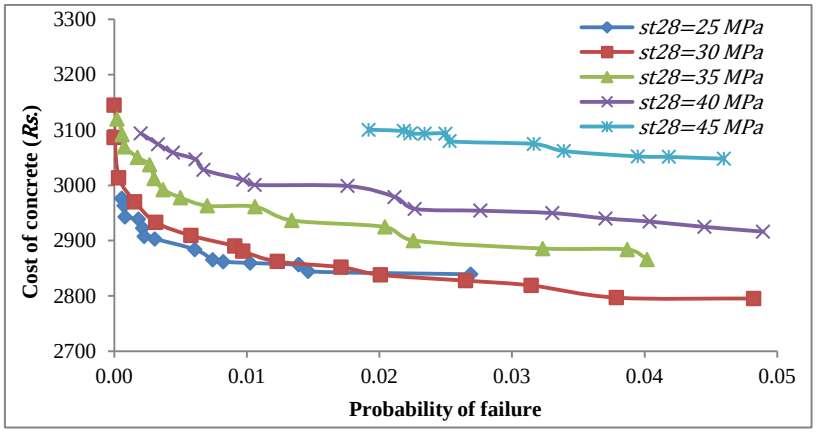

Figure 5.7(b) Pareto-optimal fronts based on QGRR model of 28 days compressive strength with P_f = 0.05 for concrete without fly ash

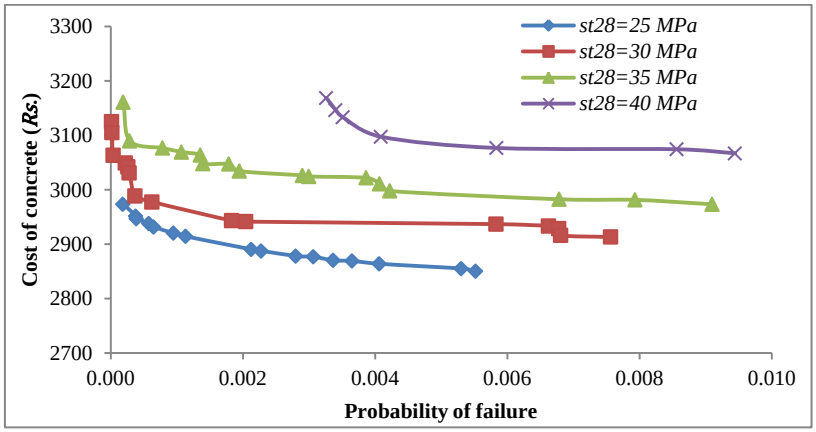

Figure 5.7(c) Pareto-optimal fronts based on QGRR model of 28 days compressive strength with P_f = 0.01 for concrete without fly ash

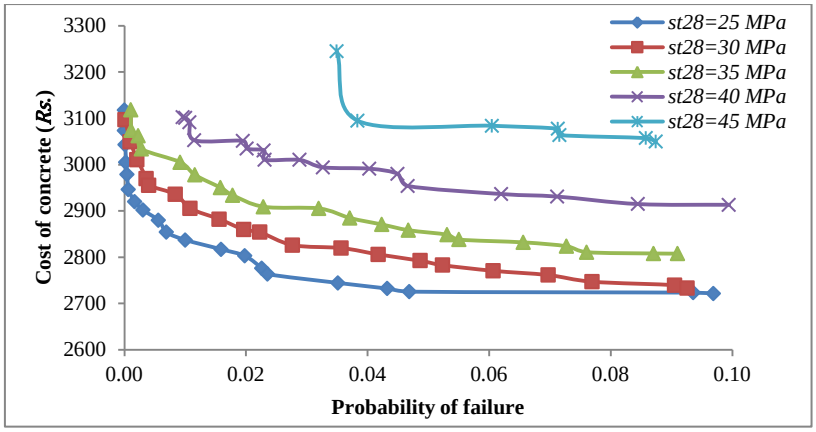

Figure 5.8(a) Pareto-optimal fronts based on LGRR model of 28 days compressive strength with P_f = 0.1 for concrete without fly ash

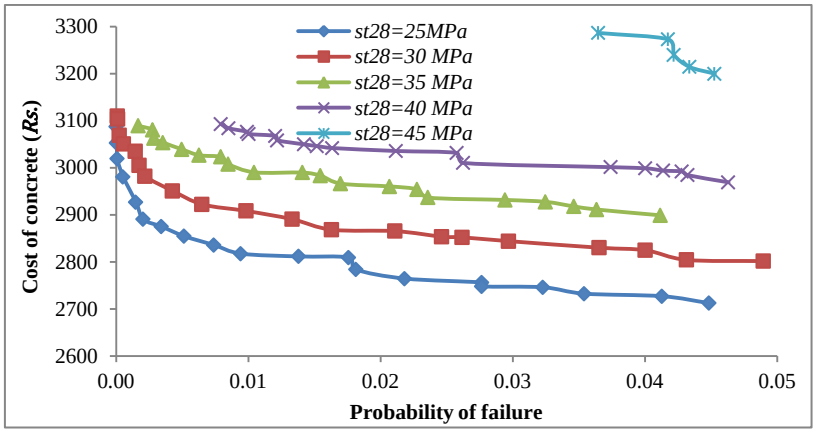

Figure 5.8(b) Pareto-optimal fronts based on LGRR model of 28 days compressive strength with P_f = 0.05 for concrete without fly ash

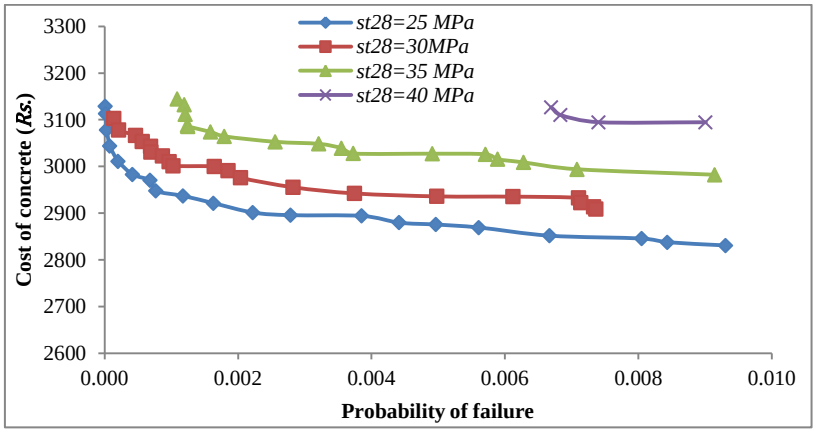

Figure 5.8(c) Pareto-optimal fronts based on LGRR model of 28 days compressive strength with P_f = 0.01 for concrete without fly ash

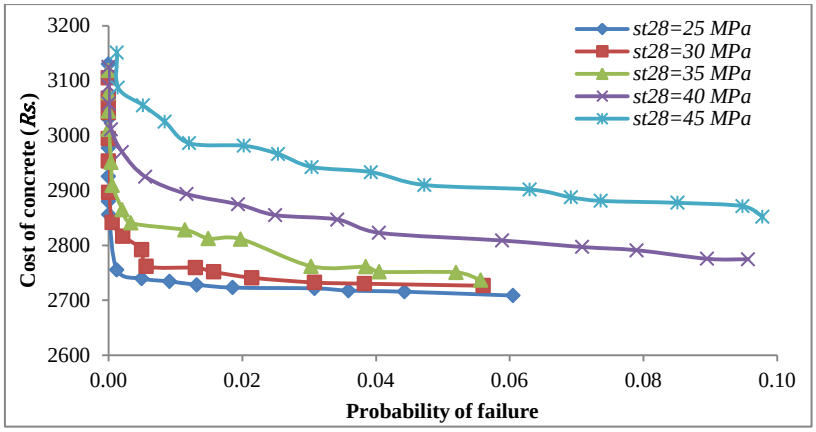

Figure 5.9(a) Pareto-optimal fronts based on QTRR/QOLSR model of 28 days compressive strength with P_f = 0.1 for concrete without fly ash

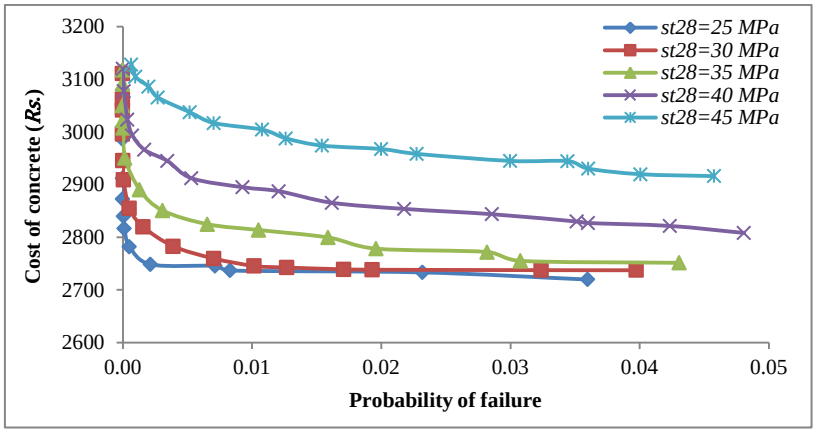

Figure 5.9(b) Pareto-optimal fronts based on QTRR/QOLSR model of 28 days compressive strength with P_f = 0.05 for concrete without fly ash

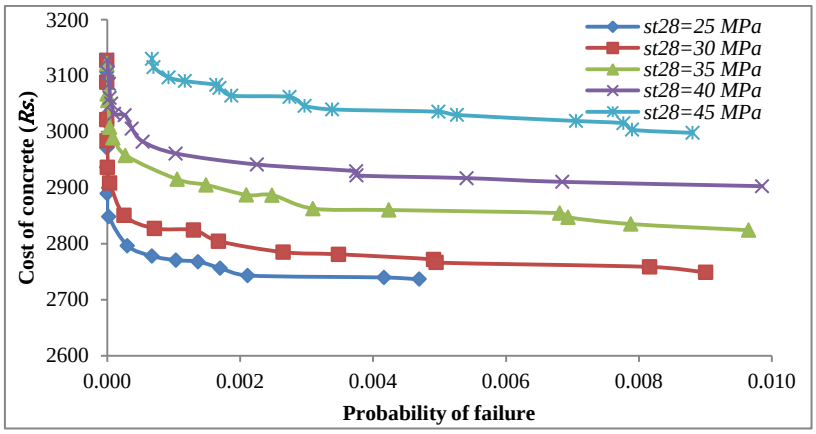

Figure 5.9(c) Pareto-optimal fronts based on QTRR/QOLSR model of 28 days compressive strength with P_f = 0.01 for concrete without fly ash

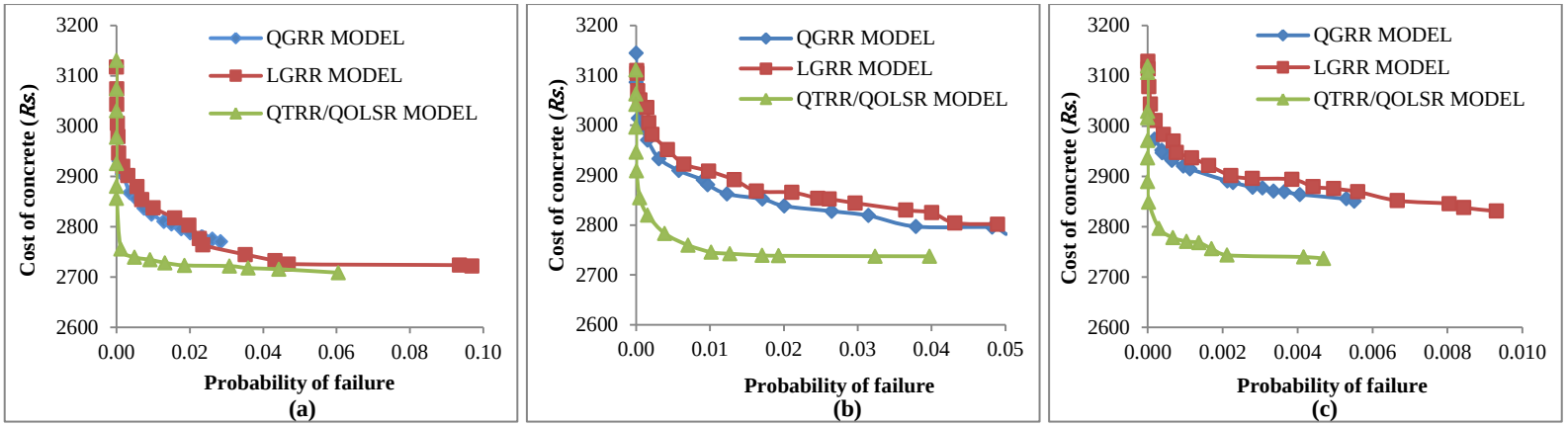

Figure 5.10 Pareto-optimal fronts obtained for different models of 28 days compressive strength for target $st28$ = 25 MPa with (a) P_f = 0.1 (b) P_f = 0.05 and (c) P_f = 0.01, for concrete without fly ash

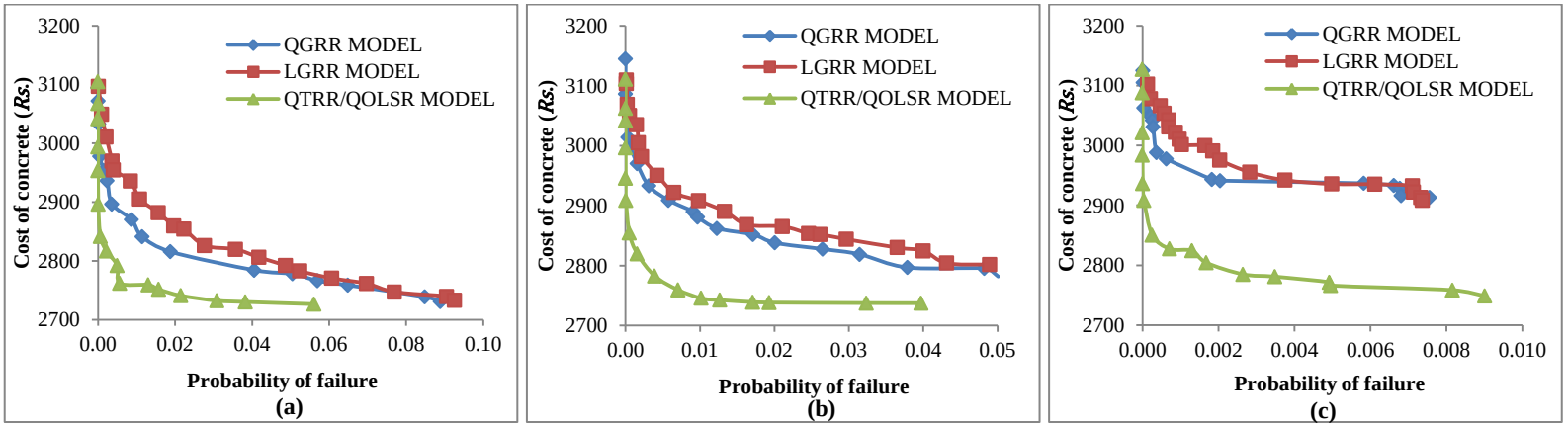

Figure 5.11 Pareto-optimal fronts obtained for different models of 28 days compressive strength for target $st28$ = 30 MPa with (a) P_f = 0.1 (b) P_f = 0.05 and (c) P_f = 0.01, for concrete without fly ash

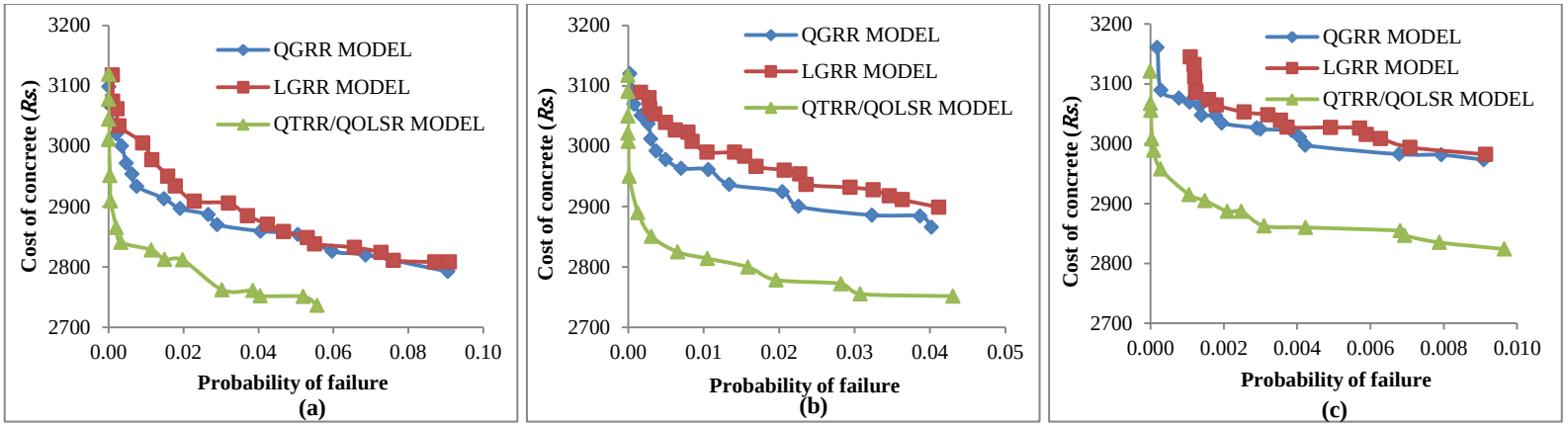

Figure 5.12 Pareto-optimal fronts obtained for different models of 28 days compressive strength for target $st28$ = 35 MPa with (a) P_f = 0.1 (b) P_f = 0.05 and (c) P_f = 0.01, for concrete without fly ash

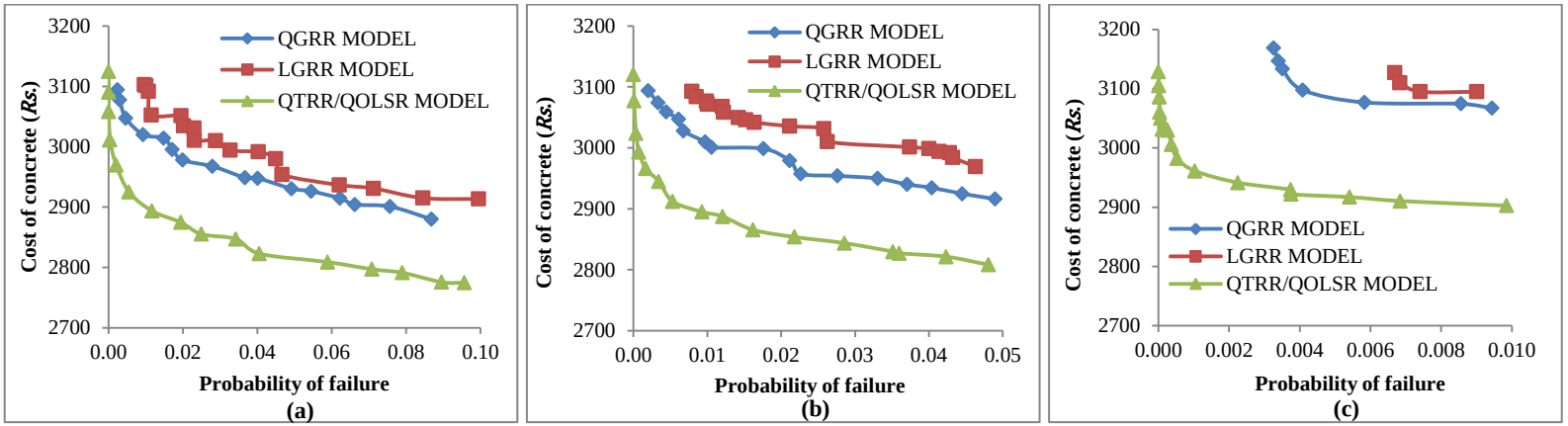

Figure 5.13 Pareto-optimal fronts obtained for different models of 28 days compressive strength for target $st28$ = 40 MPa with (a) P_f = 0.1 (b) P_f = 0.05 and (c) P_f = 0.01, for concrete without fly ash

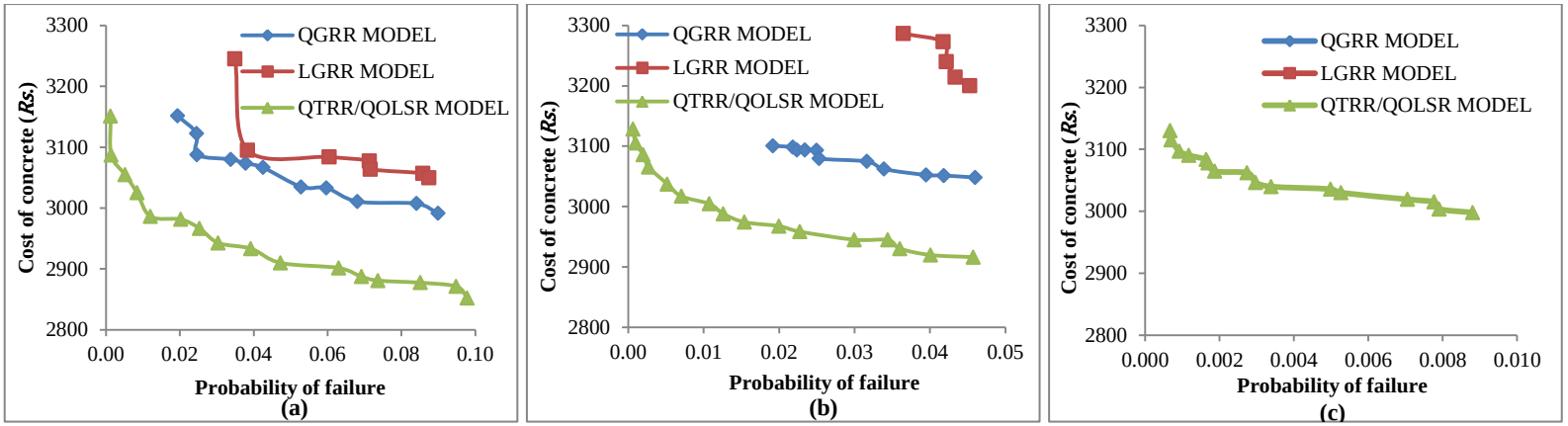

Figure 5.14 Pareto-optimal fronts obtained for different models of 28 days compressive strength for target $st28$ = 45 MPa with (a) P_f = 0.1 (b) P_f = 0.05 and (c) P_f = 0.01, for concrete without fly ash

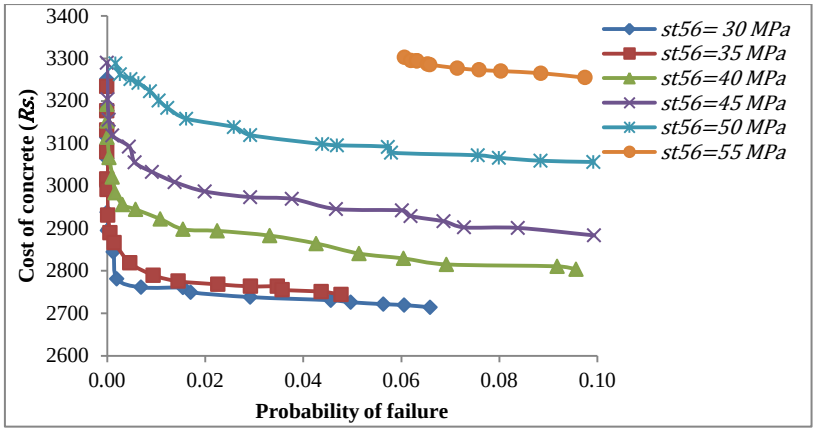

Figure 5.15(a) Pareto-optimal fronts based on QGRR model of 56 days compressive strength with P_f = 0.1 for concrete without fly ash

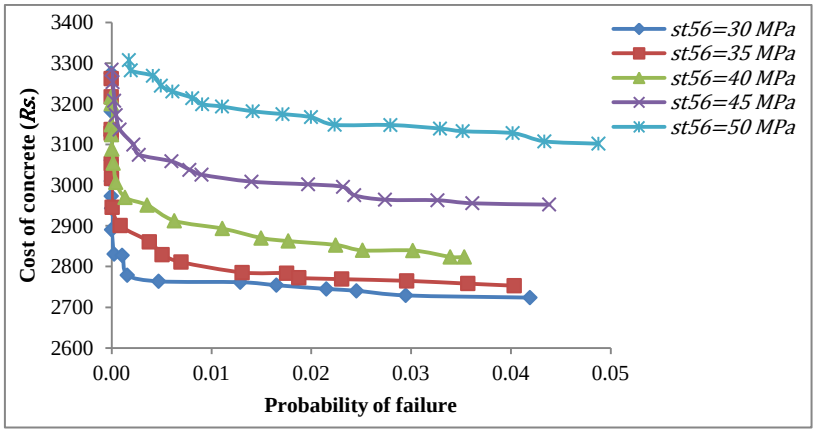

Figure 5.15(b) Pareto-optimal fronts based on QGRR model of 56 days compressive strength with P_f = 0.05 for concrete without fly ash

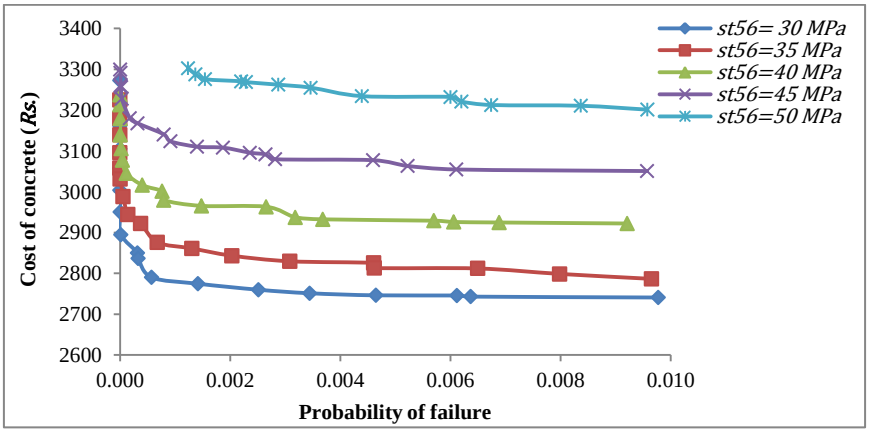

Figure 5.15(c) Pareto-optimal fronts based on QGRR model of 56 days compressive strength with P_f = 0.01 for concrete without fly ash

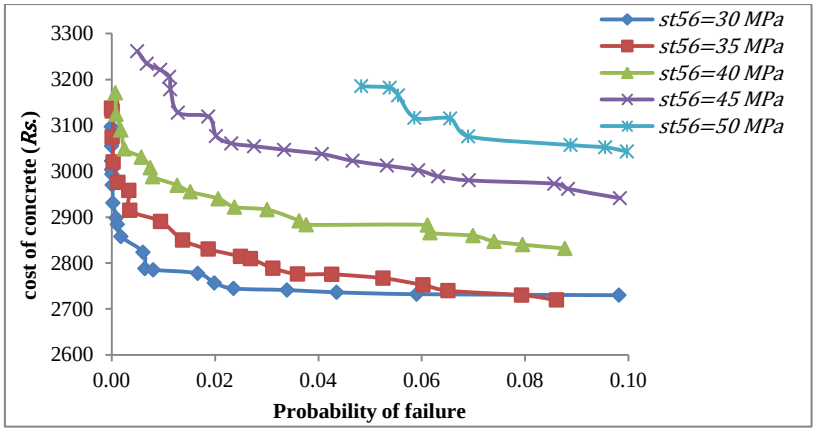

Figure 5.16(a) Pareto-optimal fronts based on LGRR model of 56 days compressive strength with P_f = 0.1 for concrete without fly ash

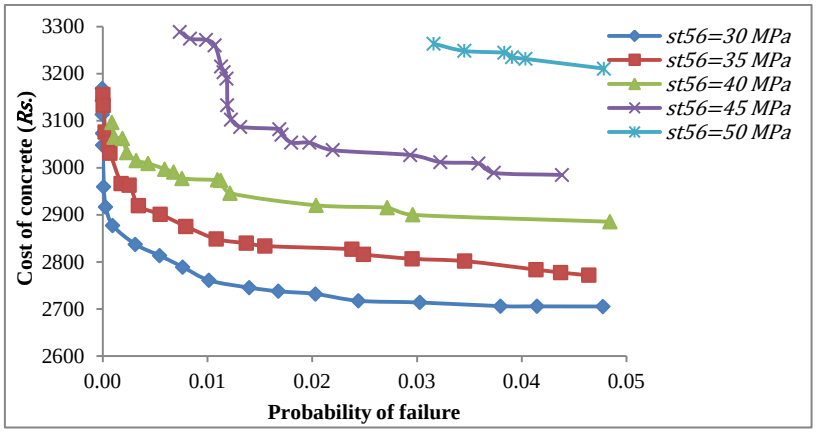

Figure 5.16(b) Pareto-optimal fronts based on LGRR model of 56 days compressive strength with P_f = 0.05 for concrete without fly ash

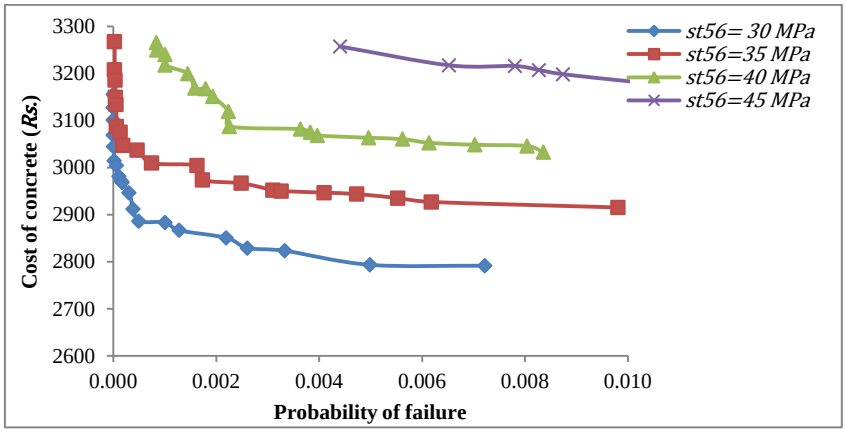

Figure 5.16(c) Pareto-optimal fronts based on LGRR model of 56 days compressive strength with P_f = 0.01 for concrete without fly ash

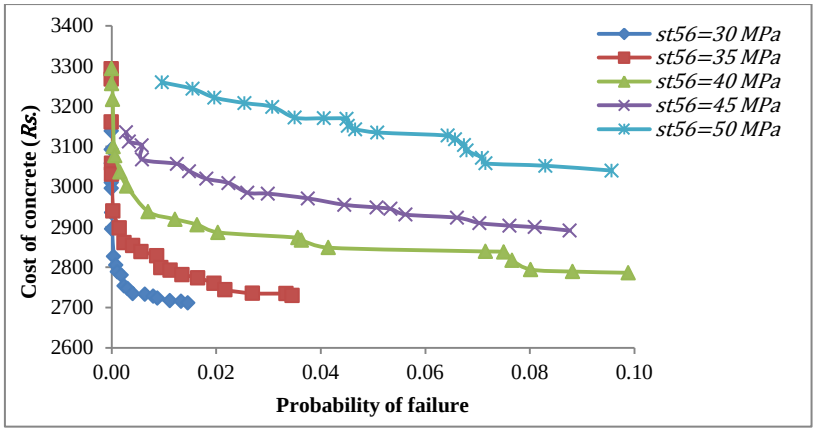

Figure 5.17(a) Pareto-optimal fronts based on LPCR model of 56 days compressive strength with P_f = 0.1 for concrete without fly ash

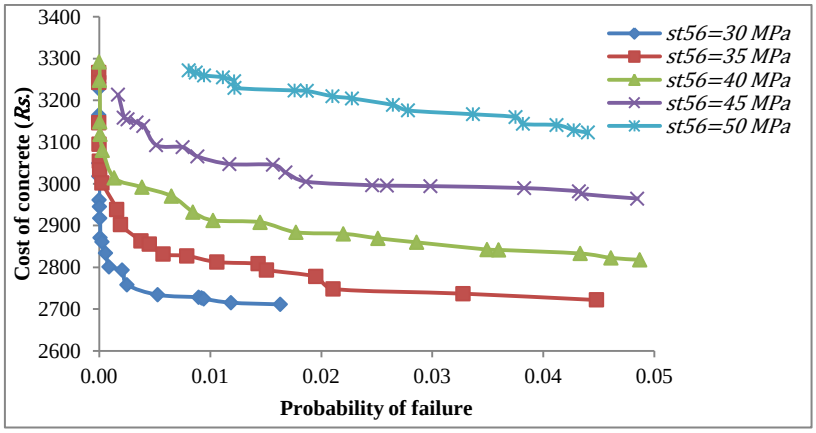

Figure 5.17(b) Pareto-optimal fronts based on LPCR model of 56 days compressive strength with P_f = 0.05 for concrete without fly ash

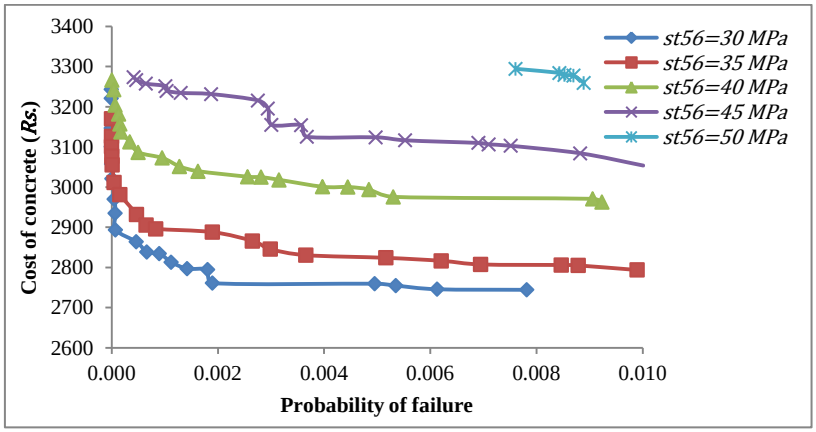

Figure 5.17(c) Pareto-optimal fronts based on LPCR model of 56 days compressive strength with P_f = 0.01 for concrete without fly ash

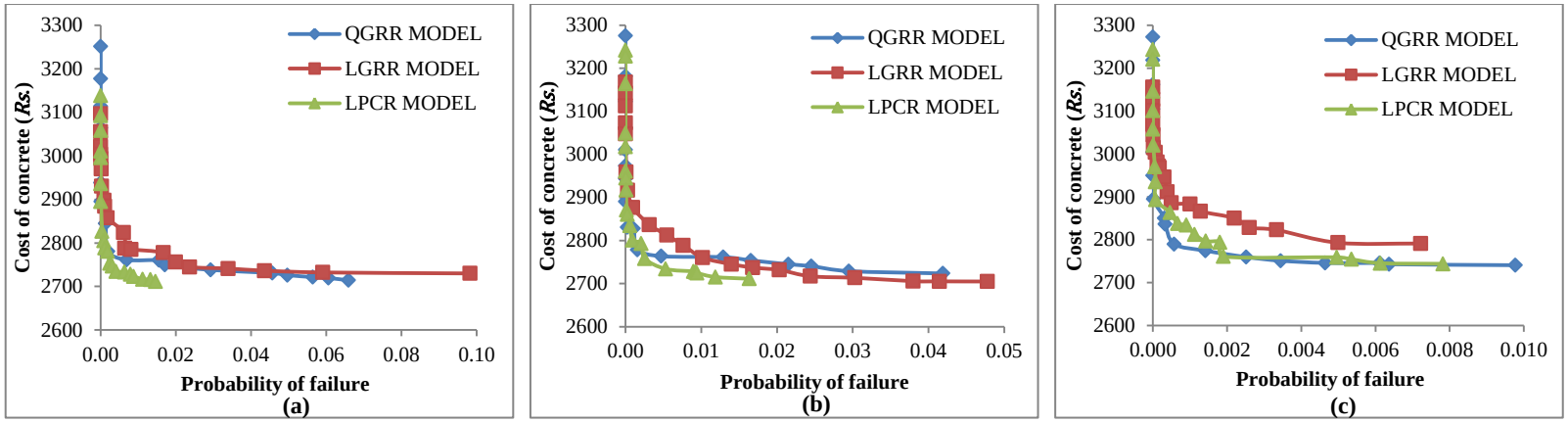

Figure 5.18 Pareto-optimal fronts obtained for different models of 56 days compressive strength for target $st56$ = 30 MPa with (a) P_f = 0.1 (b) P_f = 0.05 and (c) P_f = 0.01, for concrete without fly ash

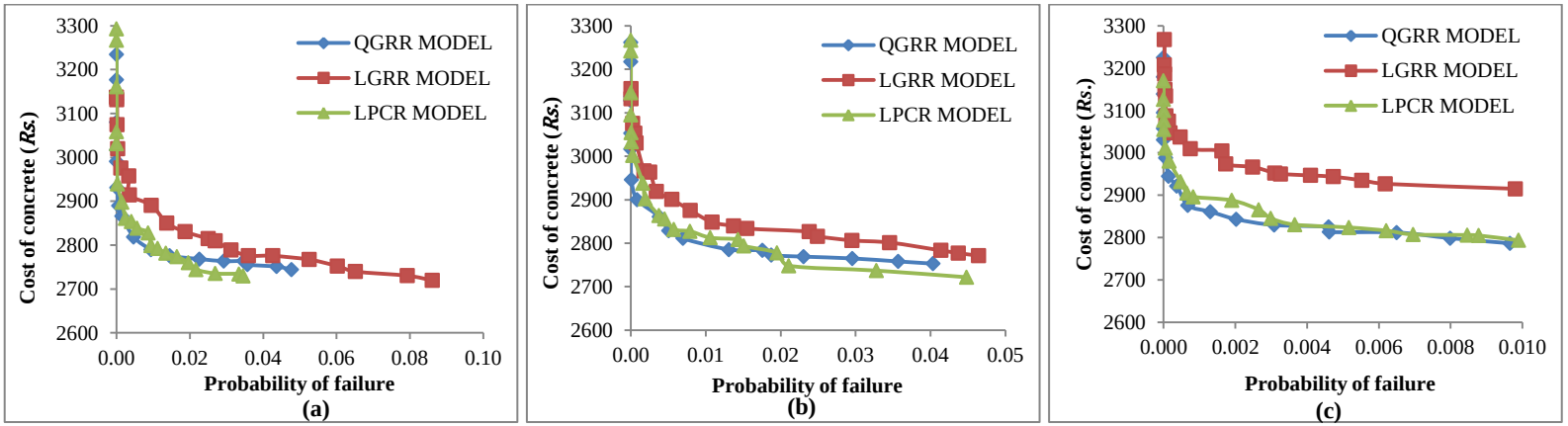

Figure 5.19 Pareto-optimal fronts obtained for different models of 56 days compressive strength for target $st56$ = 35 MPa with (a) P_f = 0.1 (b) P_f = 0.05 and (c) P_f = 0.01, for concrete without fly ash

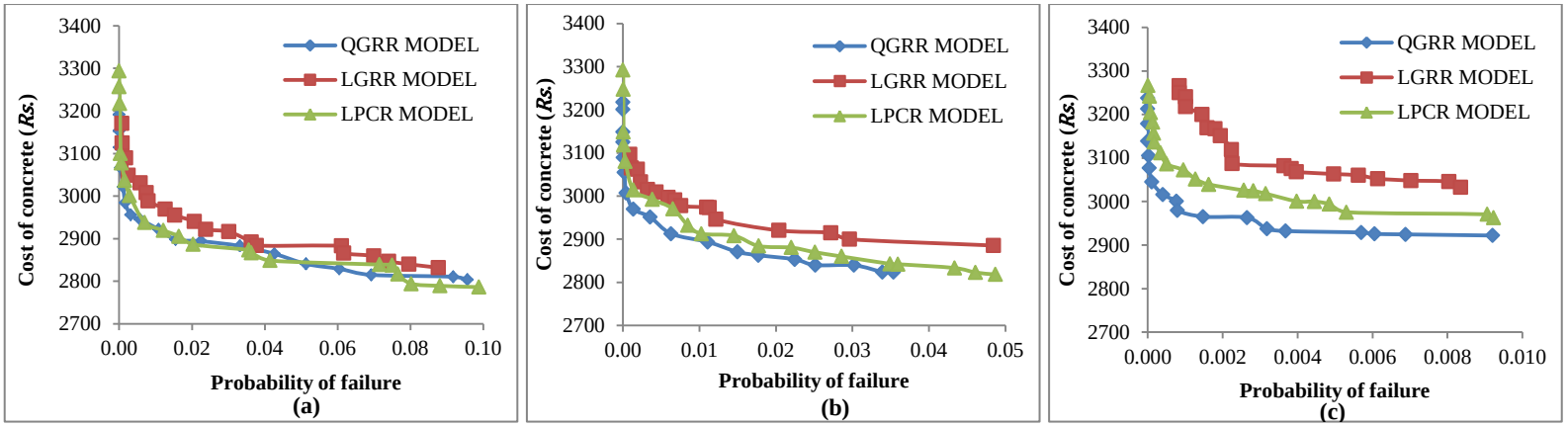

Figure 5.20 Pareto-optimal fronts obtained for different models of 56 days compressive strength for target $st56$ = 40 MPa with (a) P_f = 0.1 (b) P_f = 0.05 and (c) P_f = 0.01, for concrete without fly ash

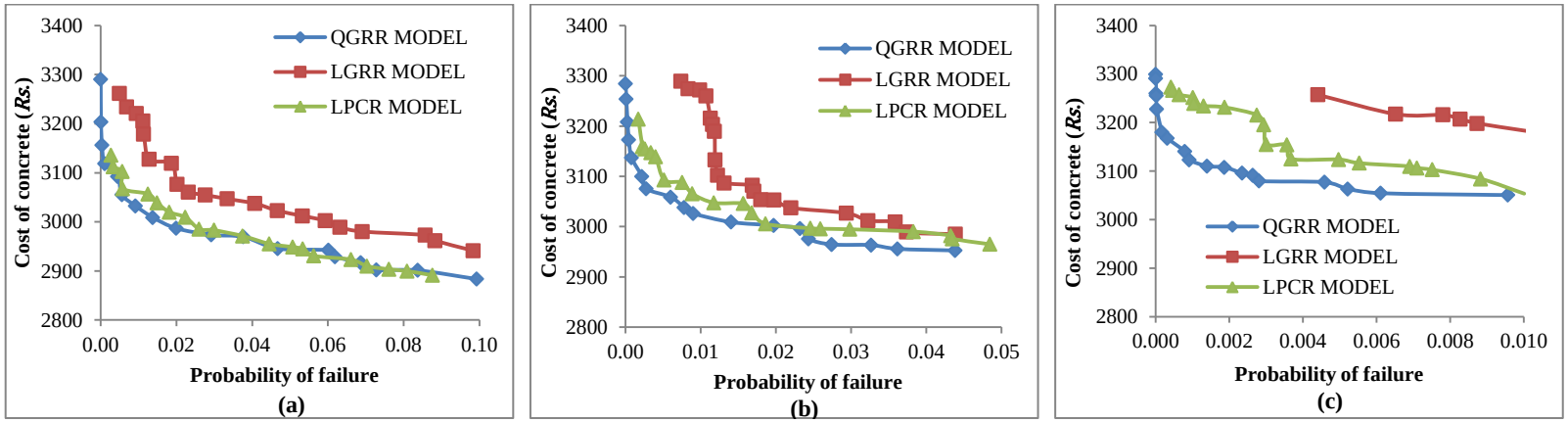

Figure 5.21 Pareto-optimal fronts obtained for different models of 56 days compressive strength for target $st56$ = 45 MPa with (a) P_f = 0.1 (b) P_f = 0.05 and (c) P_f = 0.01, for concrete without fly ash

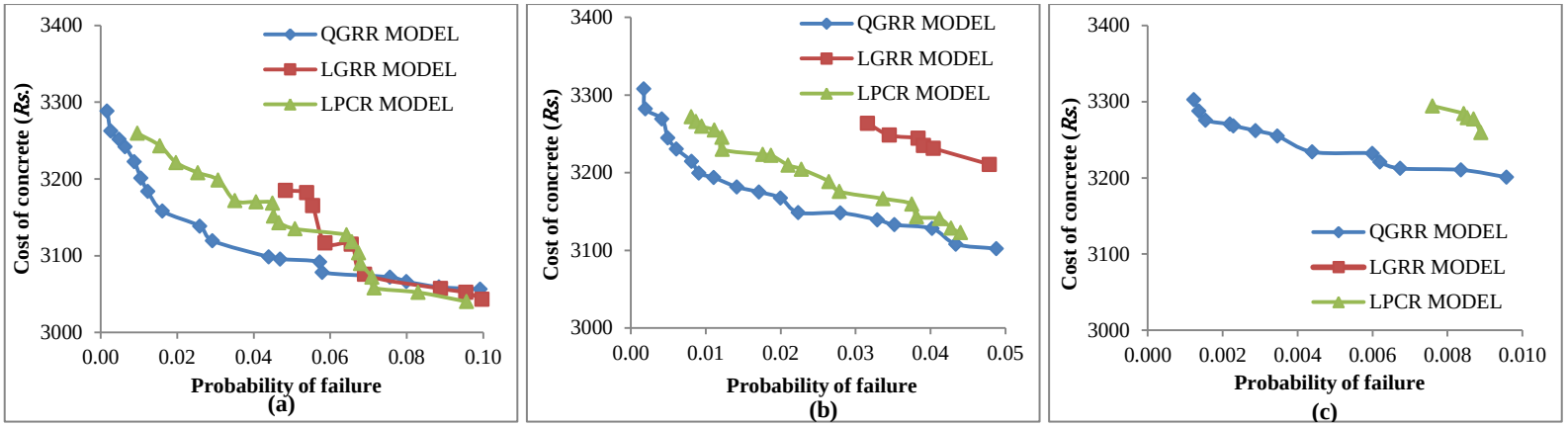

Figure 5.22 Pareto-optimal fronts obtained for different models of 56 days compressive strength for target $st56$ = 50 MPa with (a) P_f = 0.1 (b) P_f = 0.05 and (c) P_f = 0.01, for concrete without fly ash

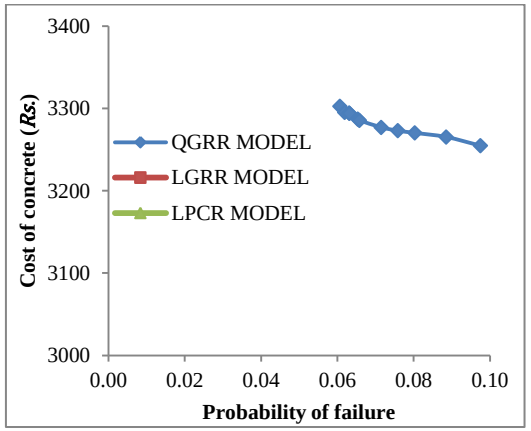

Figure 5.23 Pareto-optimal fronts obtained for different models of 56 days compressive strength for target $st56$ = 55 MPa with P_f = 0.1 for concrete without fly ash

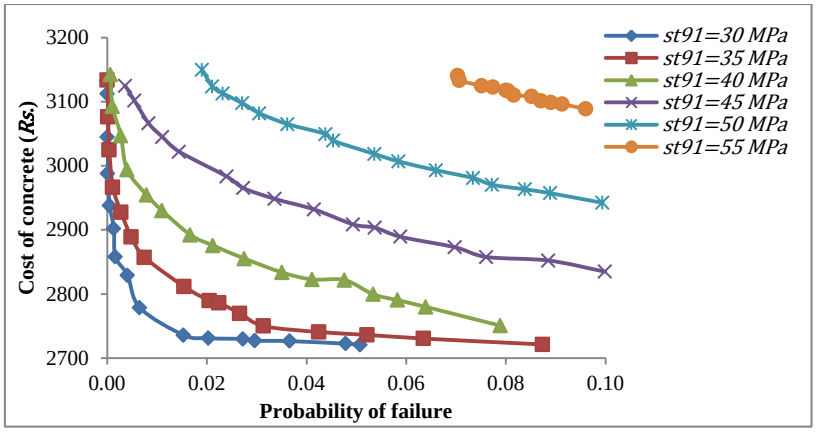

Figure 5.24(a) Pareto-optimal fronts based on QGRR model of 91 days compressive strength with P_f = 0.1 for concrete without fly ash

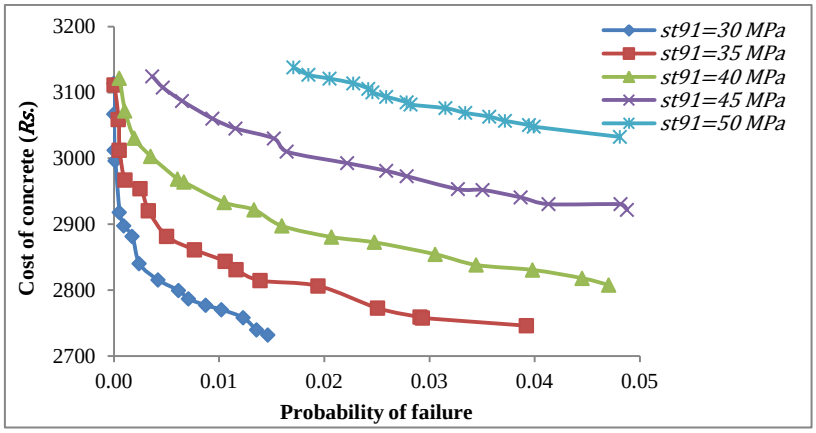

Figure 5.24(b) Pareto-optimal fronts based on QGRR model of 91 days compressive strength with P_f = 0.05 for concrete without fly ash

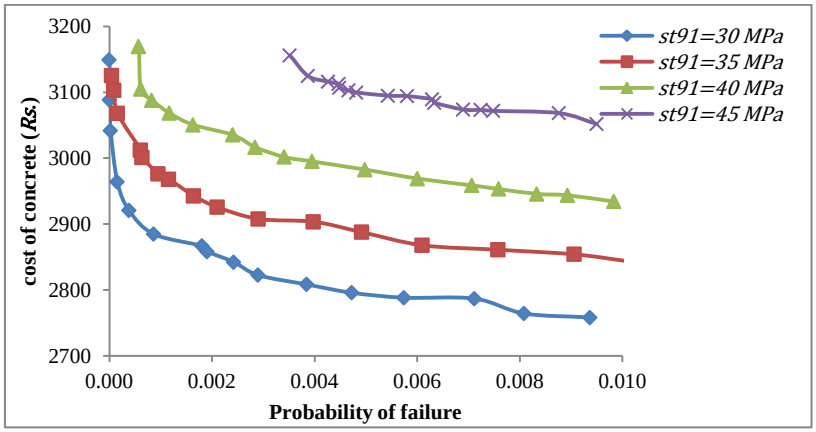

Figure 5.24(c) Pareto-optimal fronts based on QGRR model of 91 days compressive strength with P_f = 0.01 for concrete without fly ash

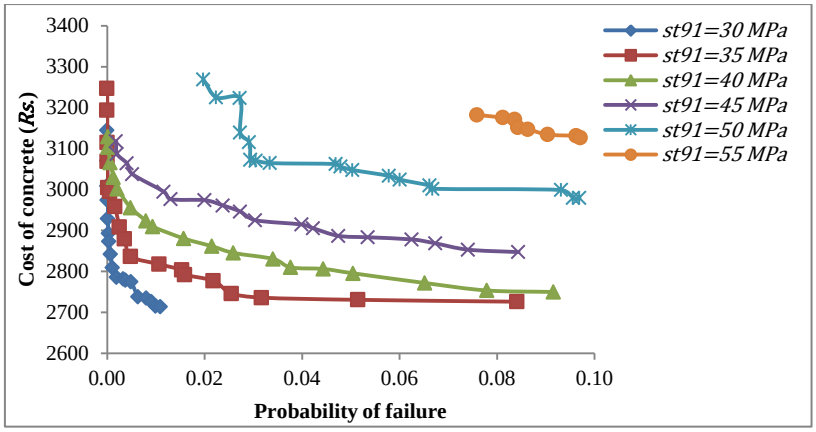

Figure 5.25(a) Pareto-optimal fronts based on LGRR model of 91 days compressive strength with P_f = 0.1 for concrete without fly ash

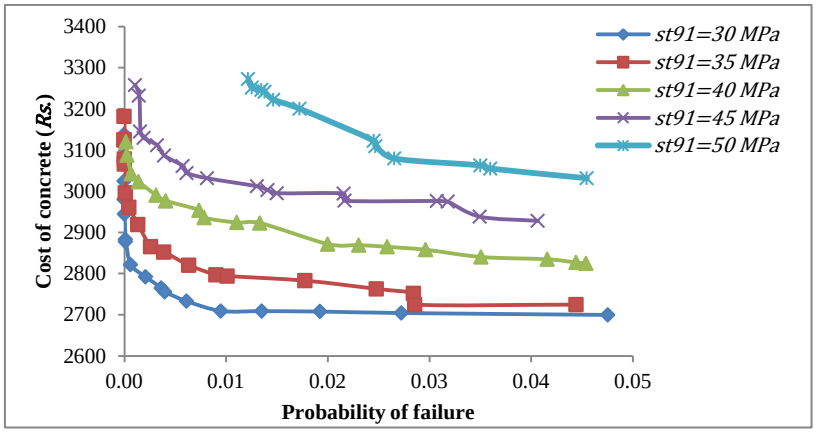

Figure 5.25(b) Pareto-optimal fronts based on LGRR model of 91 days compressive strength with P_f = 0.05 for concrete without fly ash

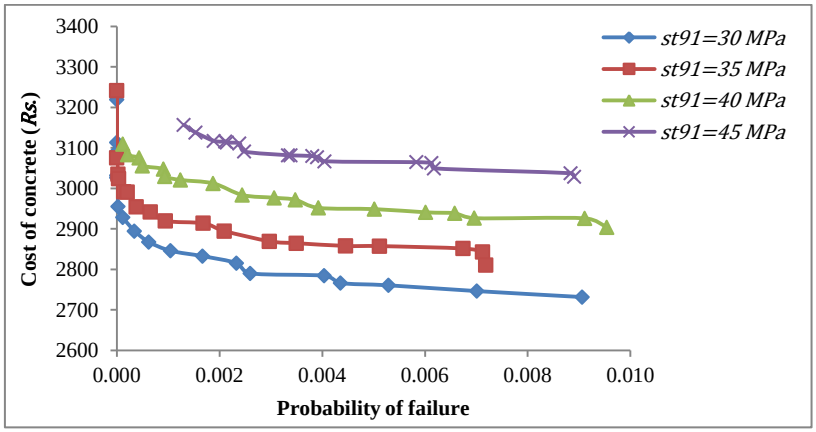

Figure 5.25(c) Pareto-optimal fronts based on LGRR model of 91 days compressive strength with P_f = 0.01 for concrete without fly ash

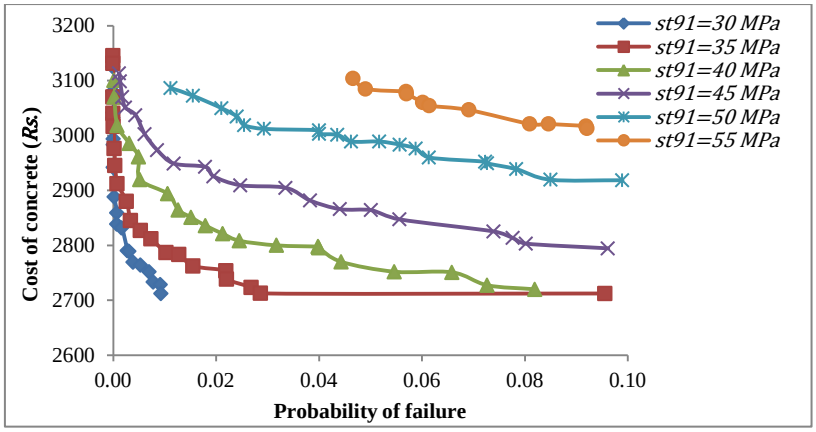

Figure 5.26(a) Pareto-optimal fronts based on LTRR/LOLSR model of 91 days compressive strength with P_f = 0.1 for concrete without fly ash

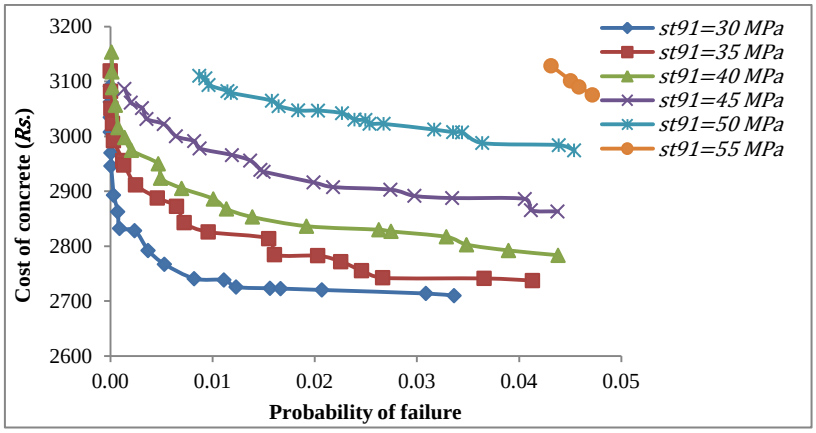

Figure 5.26(b) Pareto-optimal fronts based on LTRR/LOLSR model of 91 days compressive strength with P_f = 0.05 for concrete without fly ash

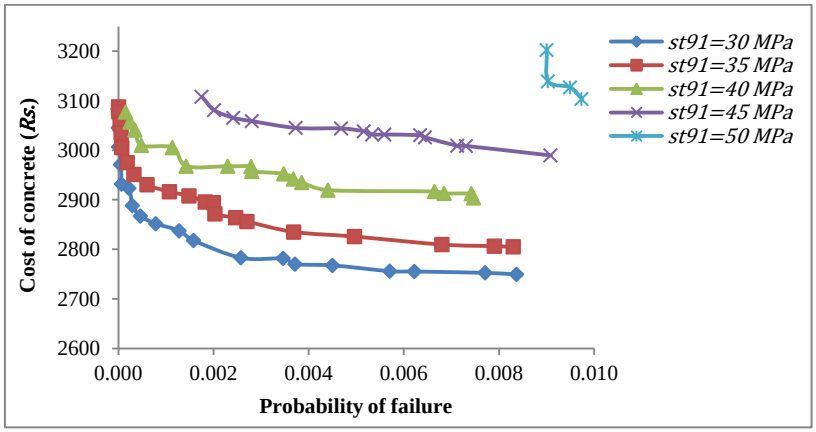

Figure 5.26(c) Pareto-optimal fronts based on LTRR/LOLSR model of 91 days compressive strength with P_f = 0.01 for concrete without fly ash

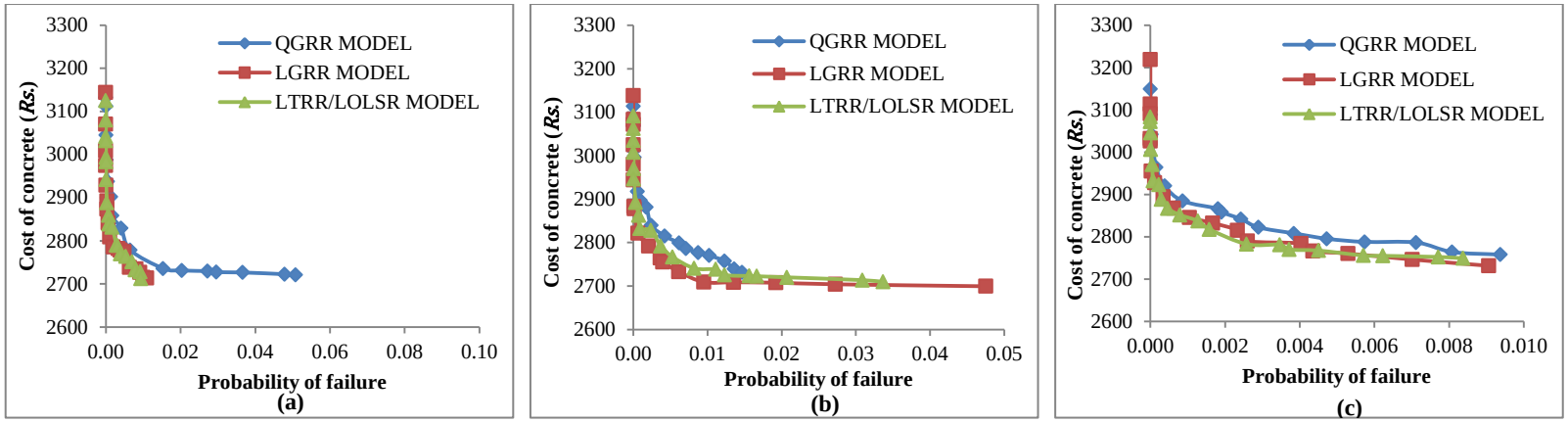

Figure 5.27 Pareto-optimal fronts obtained for different models of 91 days compressive strength for target $st91$ = 30 MPa with (a) P_f = 0.1 (b) P_f = 0.05 and (c) P_f = 0.01, for concrete without fly ash

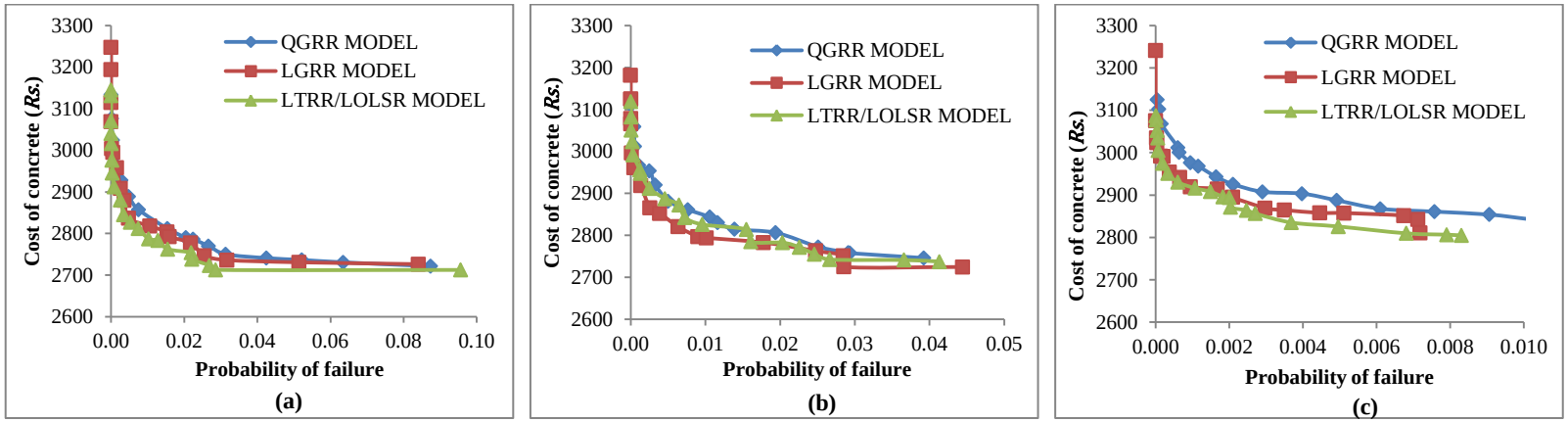

Figure 5.28 Pareto-optimal fronts obtained for different models of 91 days compressive strength for target $st91$ = 35 MPa with (a) P_f = 0.1 (b) P_f = 0.05 and (c) P_f = 0.01, for concrete without fly ash

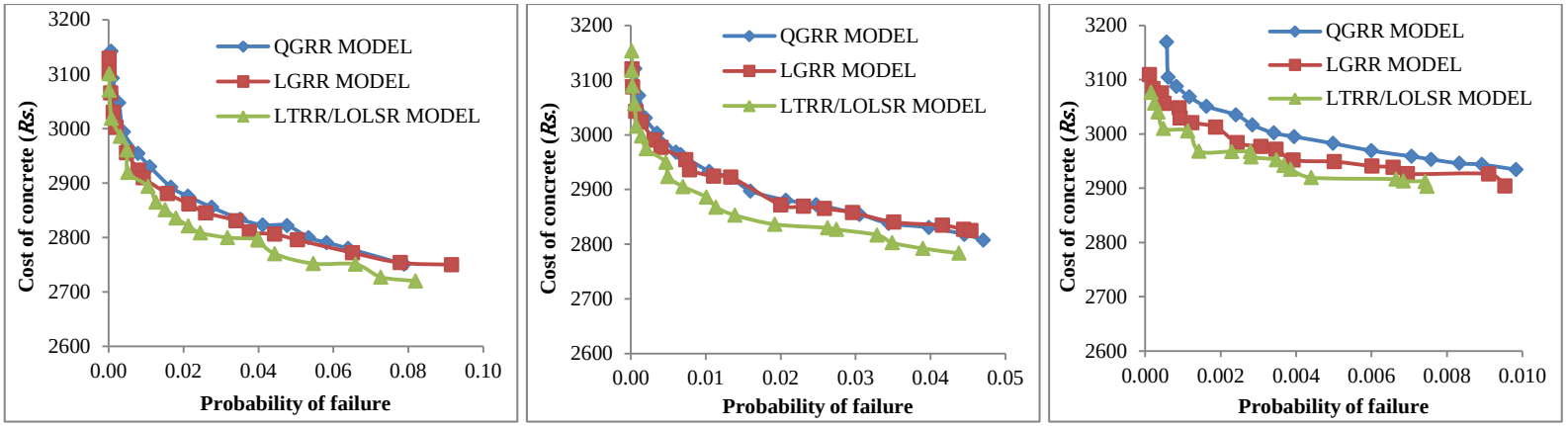

Figure 5.29 Pareto-optimal fronts obtained for different models of 91 days compressive strength for target $st91 = 40\ MPa$ with (a) $P_f = 0.1$ (b) $P_f = 0.05$ and (c) $P_f = 0.01$, for concrete without fly ash

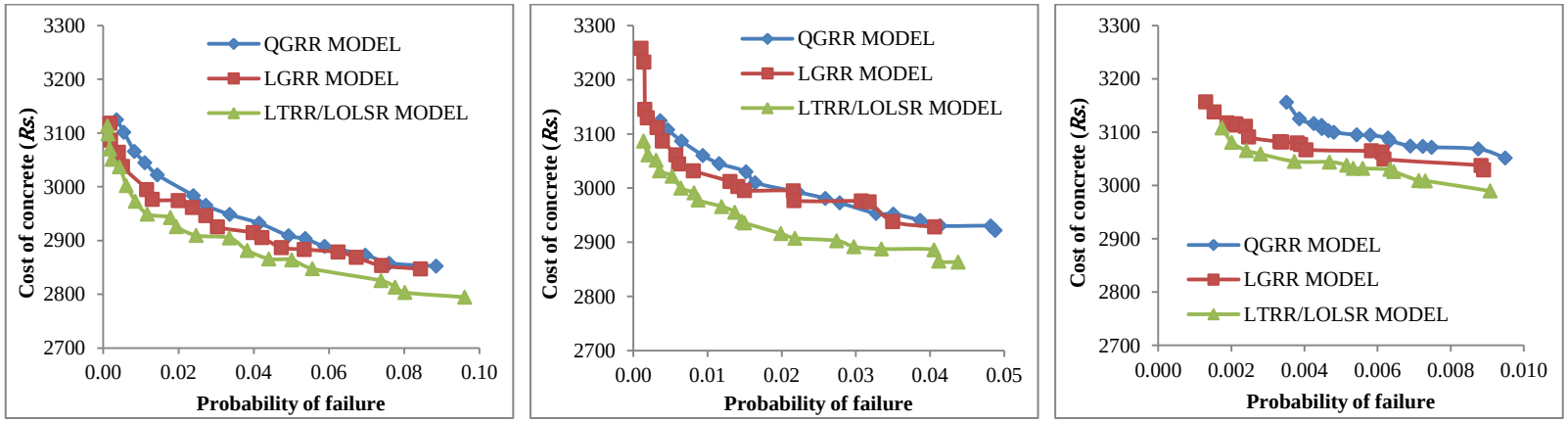

Figure 5.30 Pareto-optimal fronts obtained for different models of 91 days compressive strength for target $st91 = 45\ MPa$ with (a) $P_f = 0.1$ (b) $P_f = 0.05$ and (c) $P_f = 0.01$, for concrete without fly ash

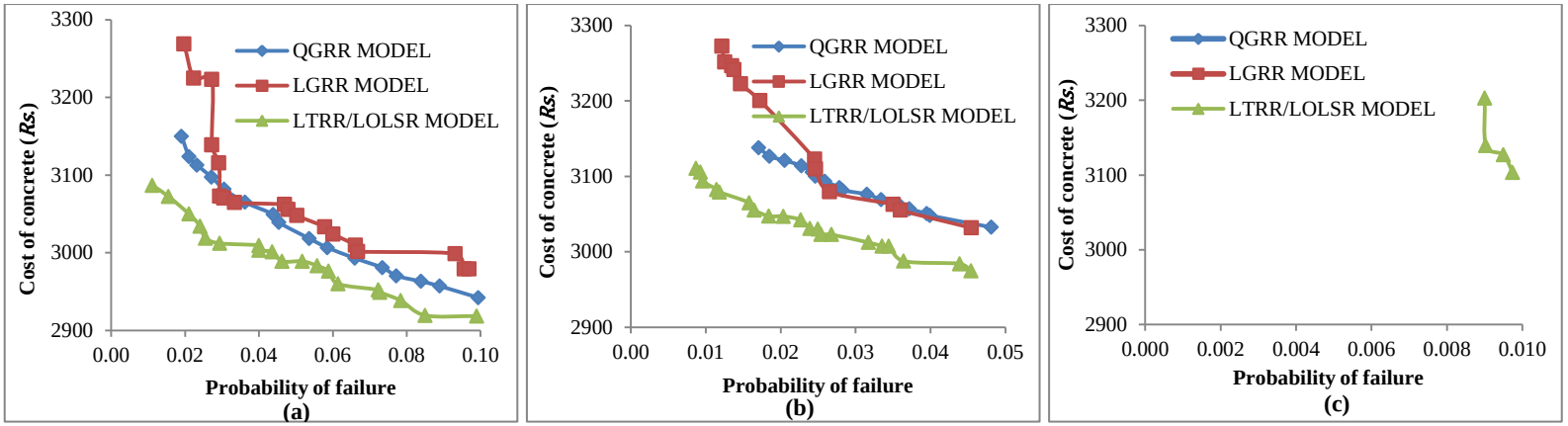

Figure 5.31 Pareto-optimal fronts obtained for different models of 91 days compressive strength for target $st91 = 50\ MPa$ with (a) $P_f = 0.1$ (b) $P_f = 0.05$ and (c) $P_f = 0.01$, for concrete without fly ash

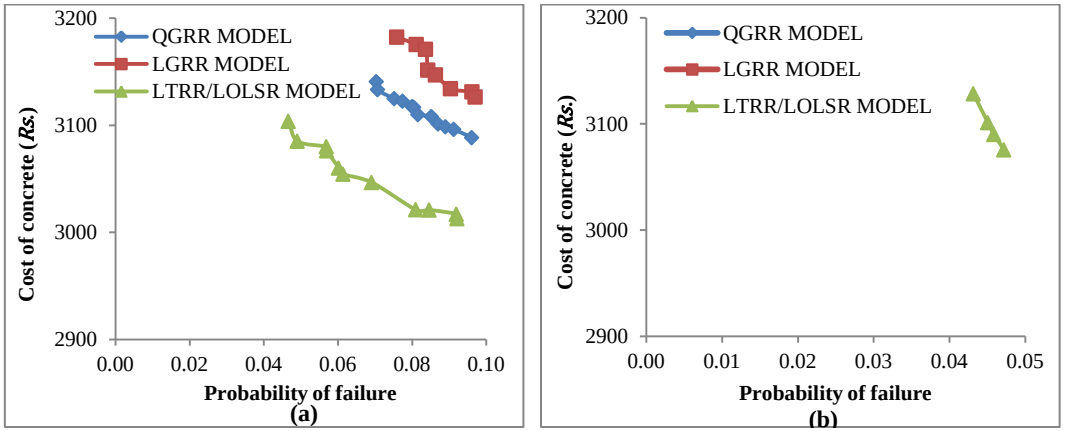

Figure 5.32 Pareto-optimal fronts obtained for different models of 91 days compressive strength for target $st91 = 55\ MPa$ with (a) $P_f = 0.1$ and (b) $P_f = 0.05$, for concrete without fly ash

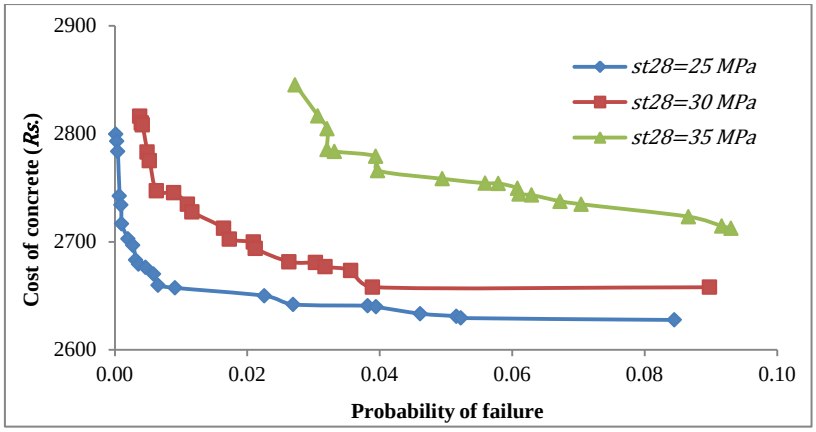

Figure 5.33(a) Pareto-optimal fronts based on QGRR model of 28 days compressive strength with P_f = 0.1 for concrete with fly ash

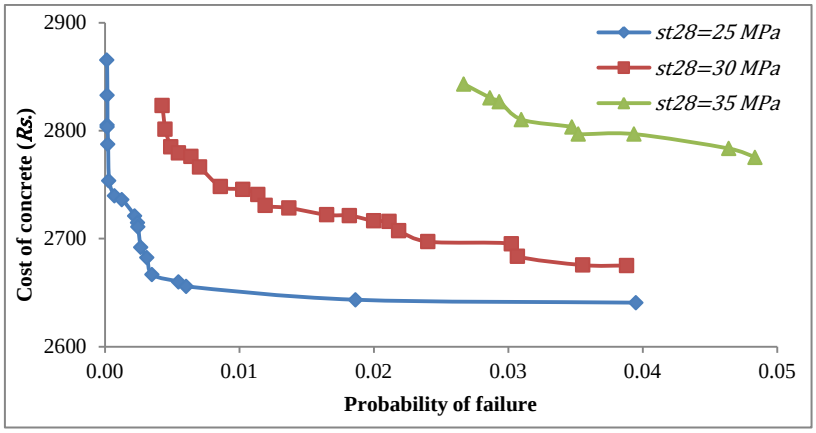

Figure 5.33(b) Pareto-optimal fronts based on QGRR model of 28 days compressive strength with P_f = 0.05 for concrete with fly ash

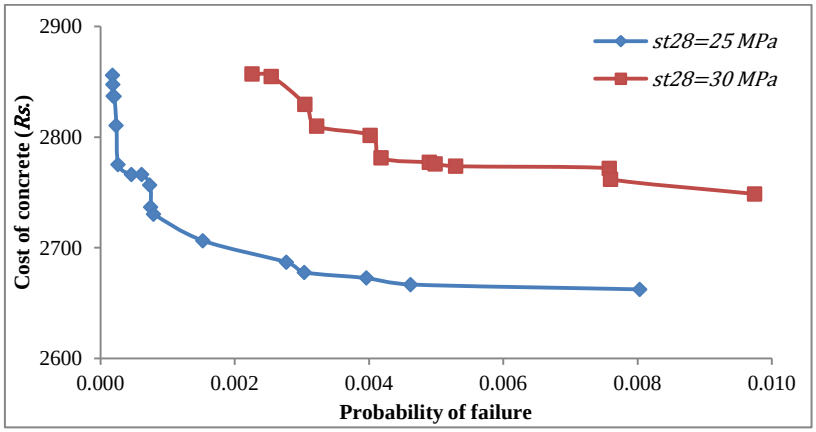

Figure 5.33(c) Pareto-optimal fronts based on QGRR model of 28 days compressive strength with P_f = 0.01 for concrete with fly ash

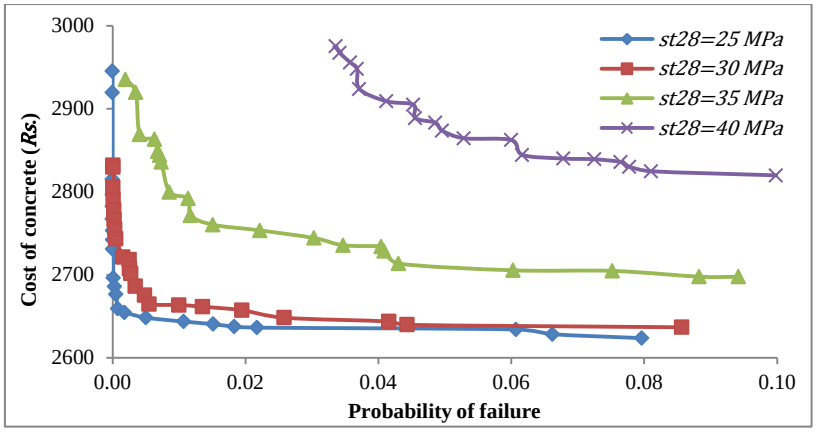

Figure 5.34(a) Pareto-optimal fronts based on QPCR model of 28 days compressive strength with P_f = 0.1 for concrete with fly ash

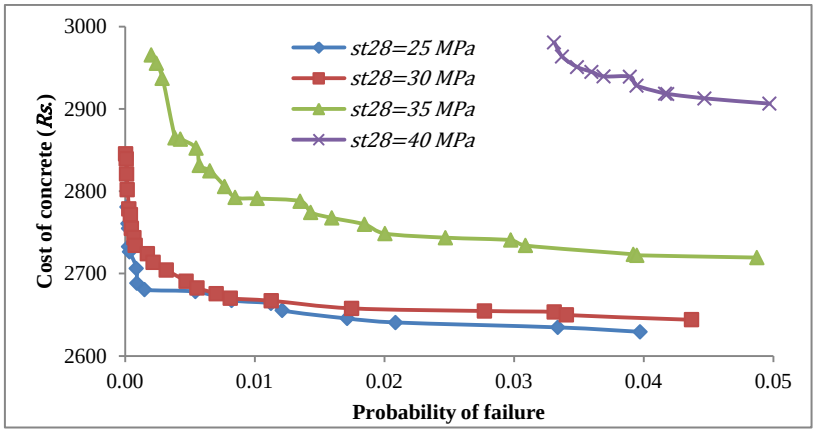

Figure 5.34(b) Pareto-optimal fronts based on QPCR model of 28 days compressive strength with P_f = 0.05 for concrete with fly ash

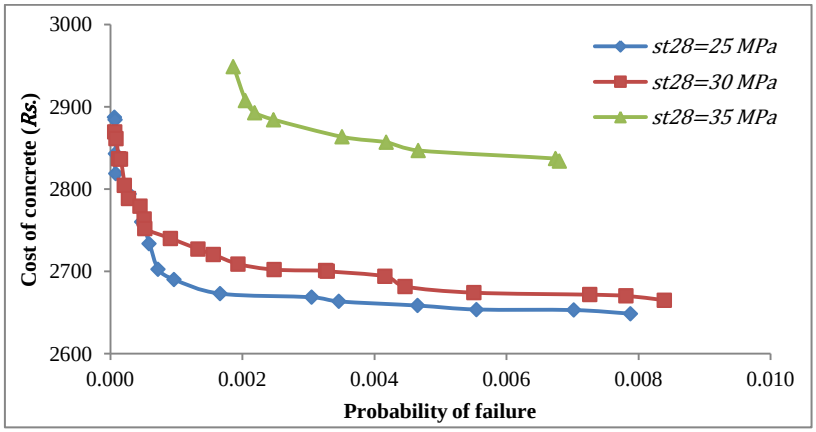

Figure 5.34(c) Pareto-optimal fronts based on QPCR model of 28 days compressive strength with P_f = 0.01 for concrete with fly ash

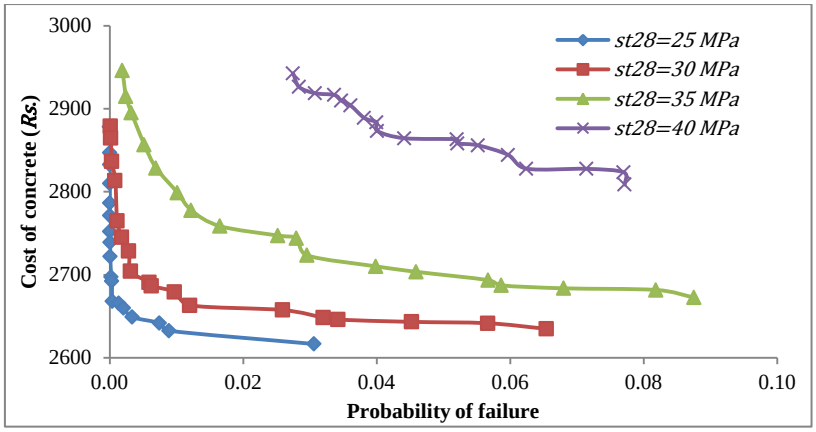

Figure 5.35(a) Pareto-optimal fronts based on LPCR model of 28 days compressive strength with P_f = 0.1 for concrete with fly ash

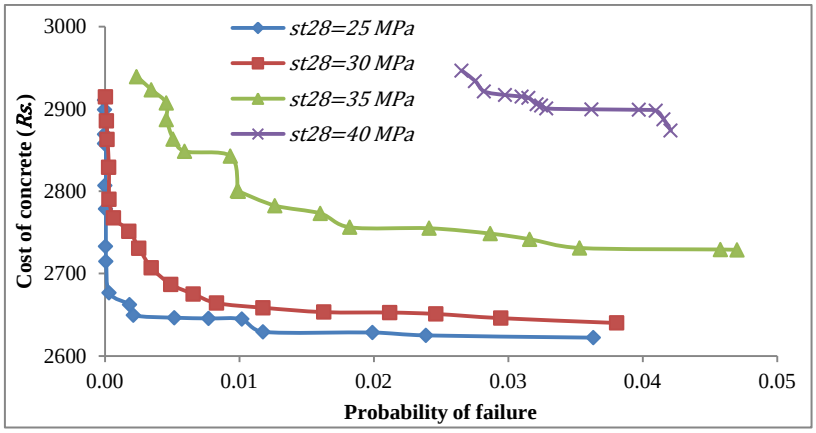

Figure 5.35(b) Pareto-optimal fronts based on LPCR model of 28 days compressive strength with P_f = 0.05 for concrete with fly ash

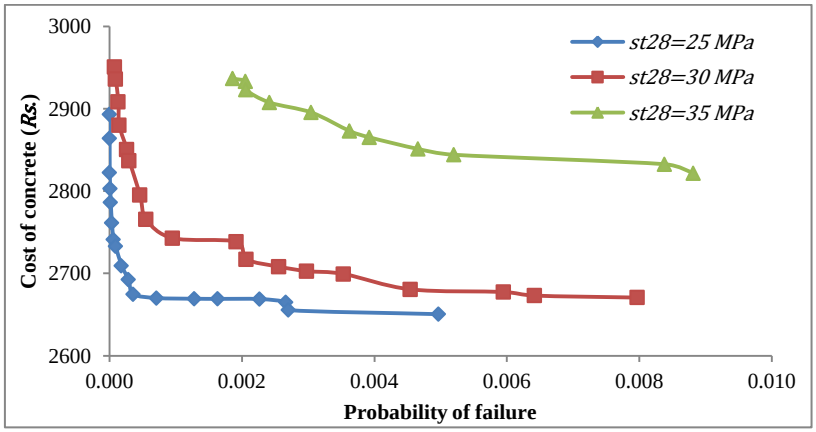

Figure 5.35(c) Pareto-optimal fronts based on LPCR model of 28 days compressive strength with P_f = 0.01 for concrete with fly ash

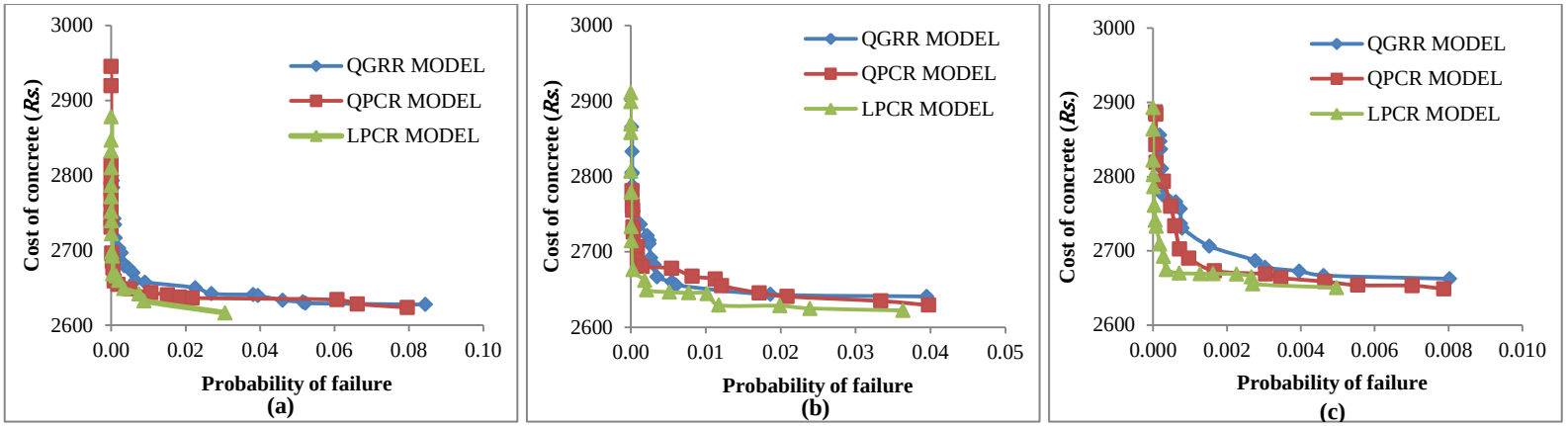

Figure 5.36 Pareto-optimal fronts obtained for different models of 28 days compressive strength for target $st28$ = 25 MPa with (a) P_f = 0.1 (b) P_f = 0.05 and (c) P_f = 0.01, for concrete with fly ash

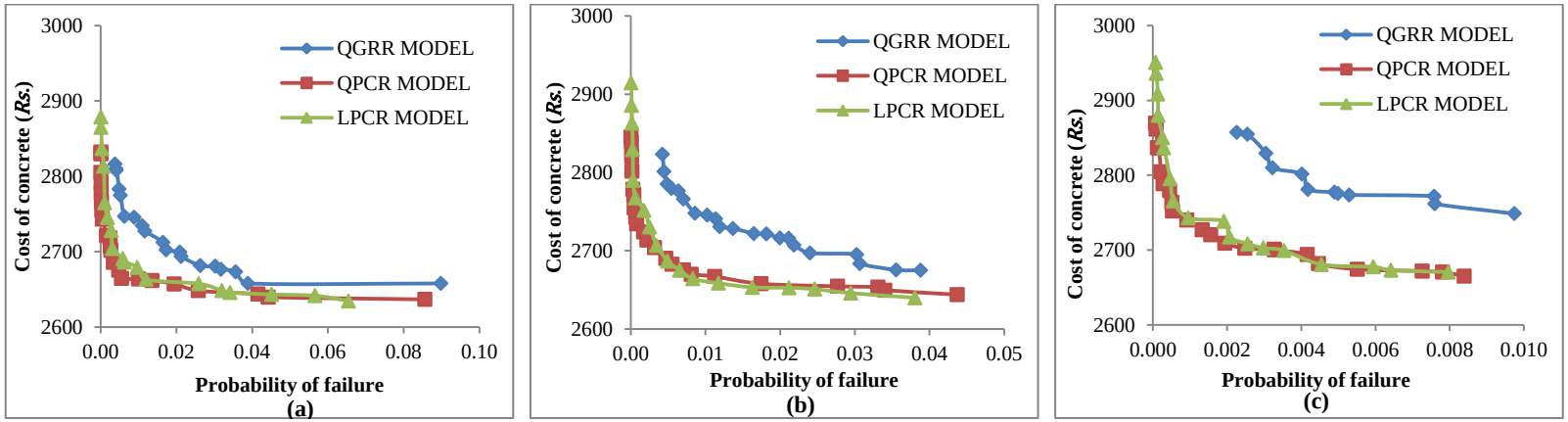

Figure 5.37 Pareto-optimal fronts obtained for different models of 28 days compressive strength for target $st28$ = 30 MPa with (a) P_f = 0.1 (b) P_f = 0.05 and (c) P_f = 0.01, for concrete with fly ash

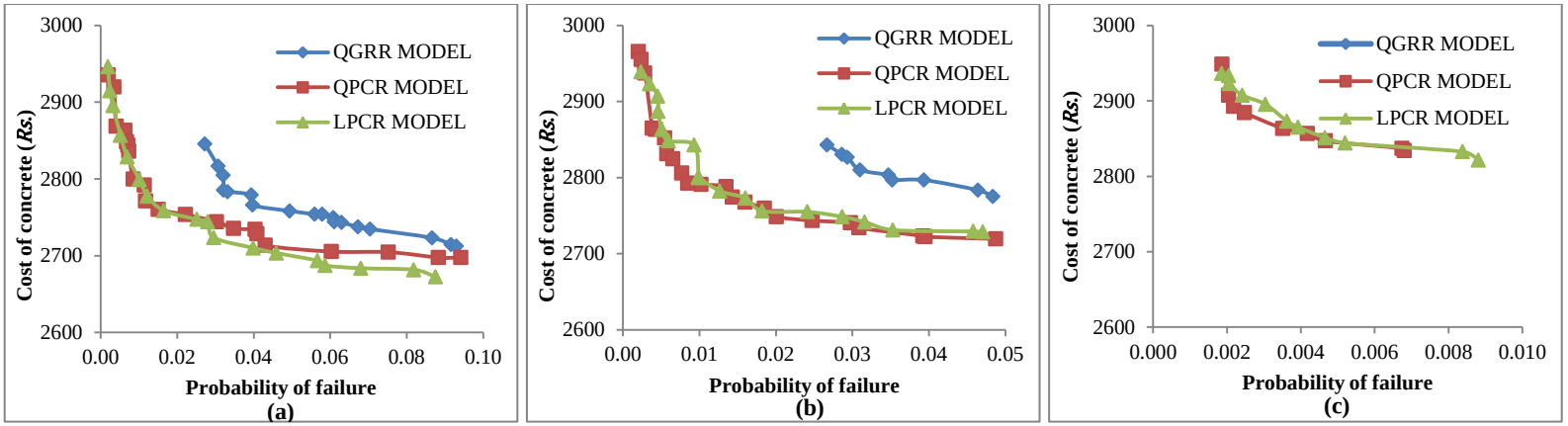

Figure 5.38 Pareto-optimal fronts obtained for different models of 28 days compressive strength with target $st28$ = 35 MPa with (a) P_f = 0.1 (b) P_f = 0.05 and (c) P_f = 0.01, for concrete with fly ash

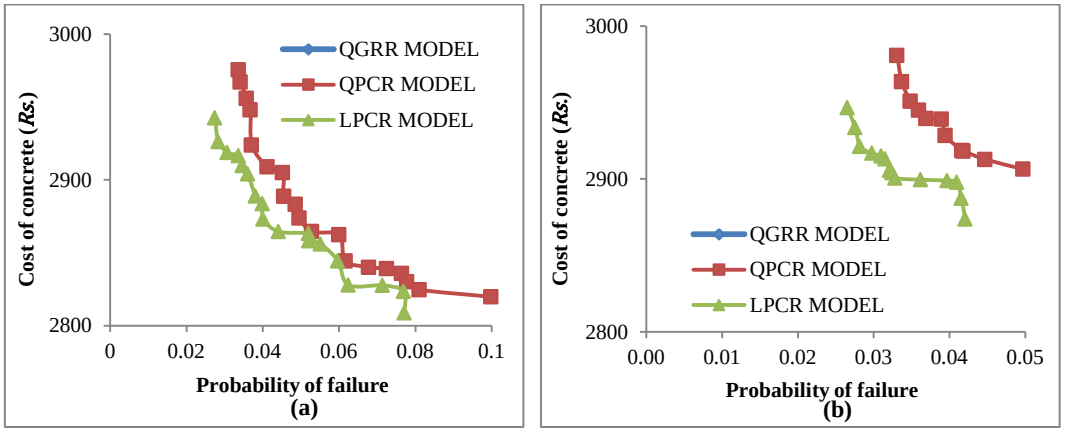

Figure 5.39 Pareto-optimal fronts obtained for different models of 28 days compressive strength for target $st28$ = 45 MPa with (a) P_f = 0.1 and (b) P_f = 0.05, for concrete with fly ash

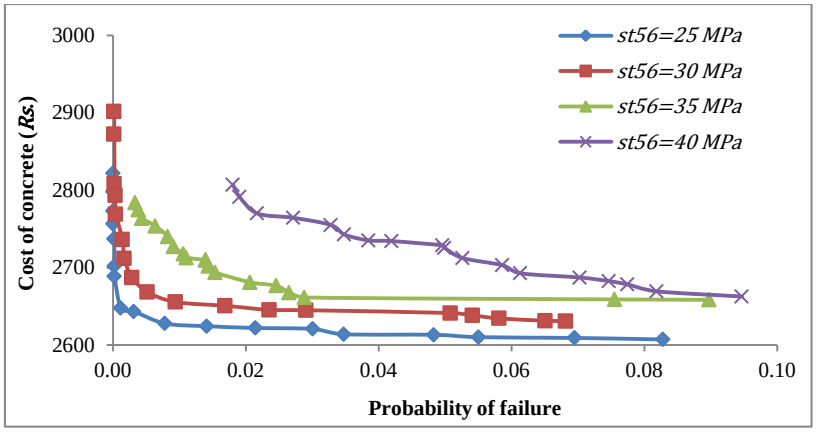

Figure 5.40(a) Pareto-optimal fronts based on QGRR model of 56 days compressive strength with P_f = 0.1 for concrete with fly ash

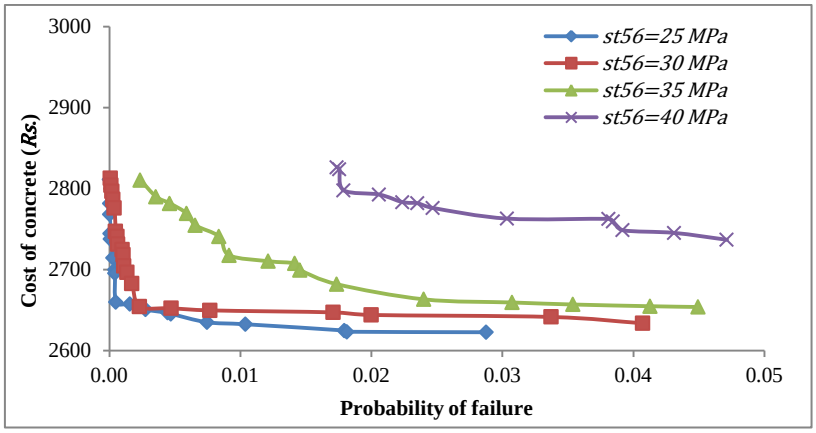

Figure 5.40(b) Pareto-optimal fronts based on QGRR model of 56 days compressive strength with P_f = 0.05 for concrete with fly ash

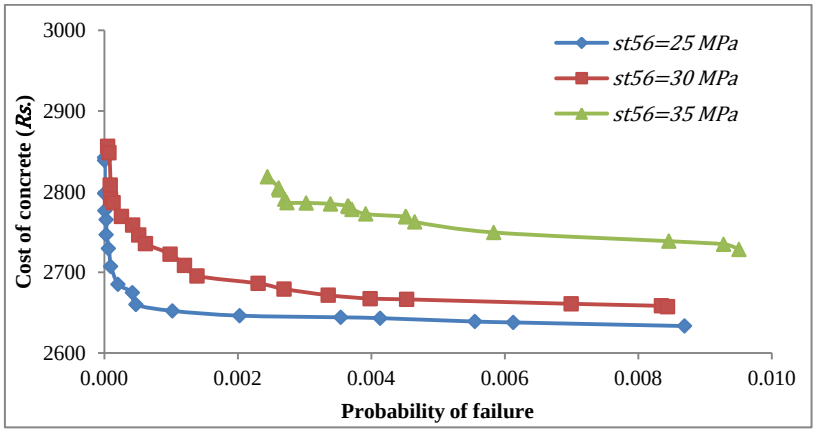

Figure 5.40(c) Pareto-optimal fronts based on QGRR model of 56 days compressive strength with P_f = 0.01 for concrete with fly ash

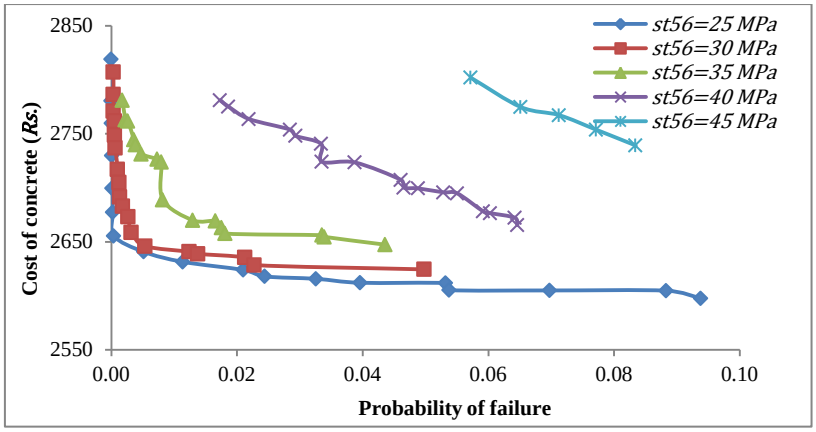

Figure 5.41(a) Pareto-optimal fronts based on LGRR model of 56 days compressive strength with P_f = 0.1 for concrete with fly ash

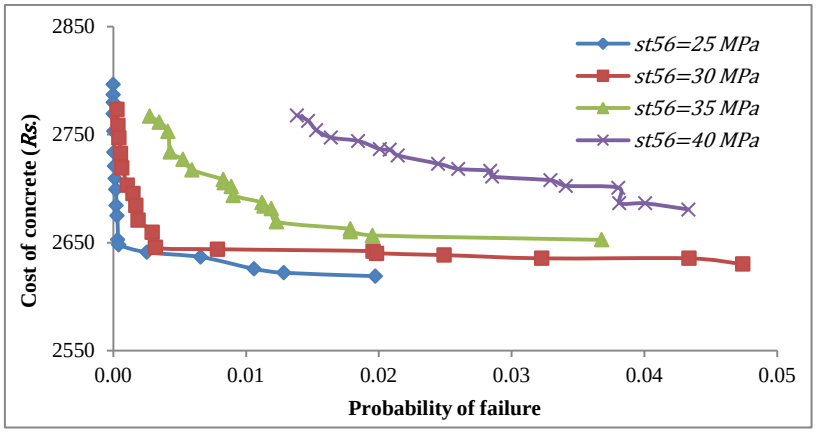

Figure 5.41(b) Pareto-optimal fronts based on LGRR model of 56 days compressive strength with P_f = 0.05 for concrete with fly ash

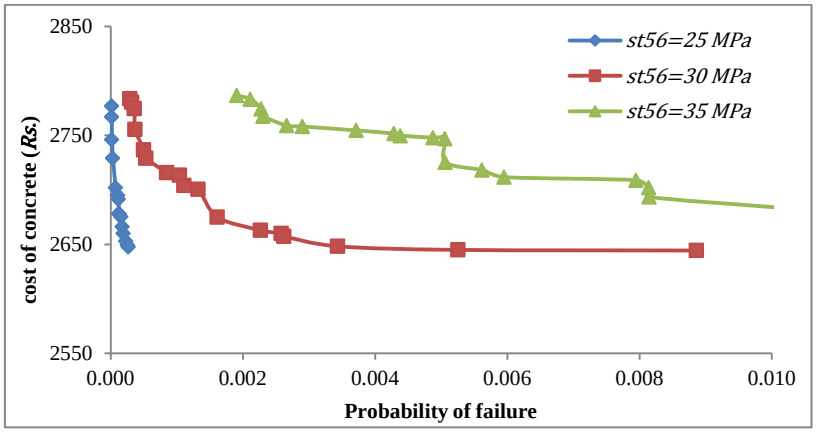

Figure 5.41(c) Pareto-optimal fronts based on LGRR model of 56 days compressive strength with P_f = 0.01 for concrete with fly ash

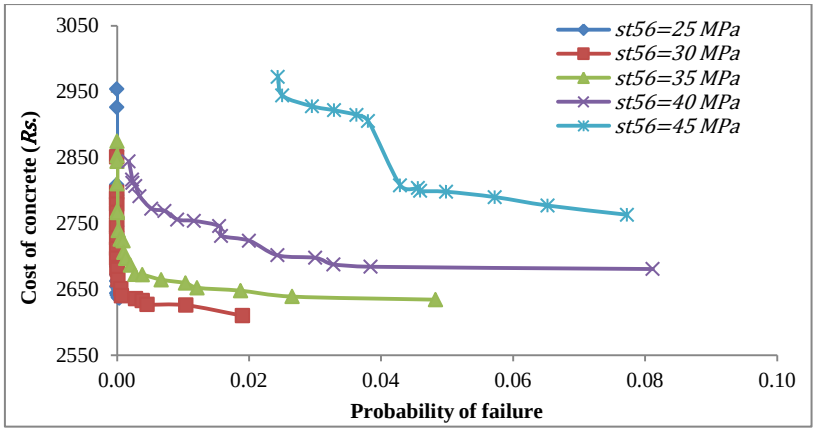

Figure 5.42(a) Pareto-optimal fronts based on LPCR model of 56 days compressive strength with P_f = 0.1 for concrete with fly ash

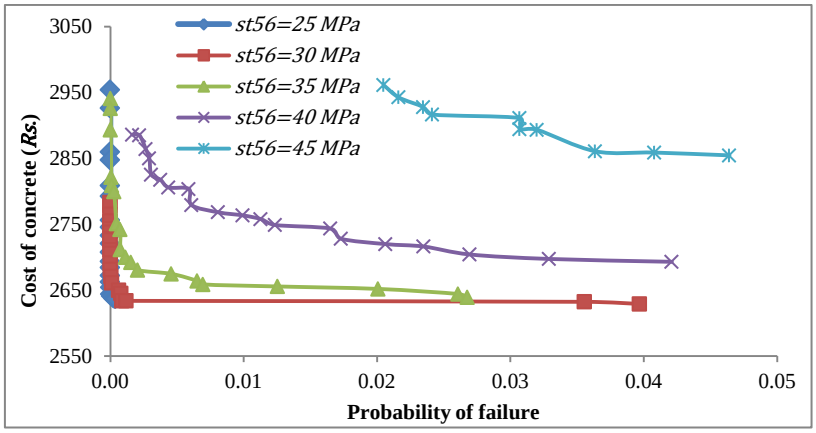

Figure 5.42(b) Pareto-optimal fronts based on LPCR model of 56 days compressive strength with P_f = 0.05 for concrete with fly ash

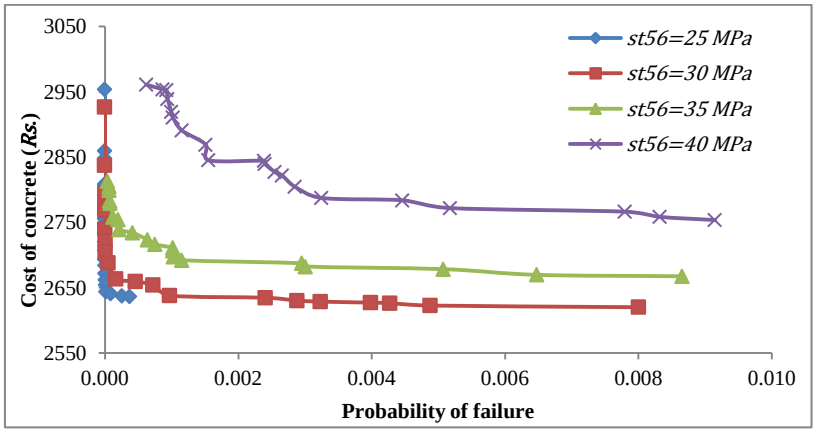

Figure 5.42(c) Pareto-optimal fronts based on LPCR model of 56 days compressive strength with P_f = 0.01 for concrete with fly ash

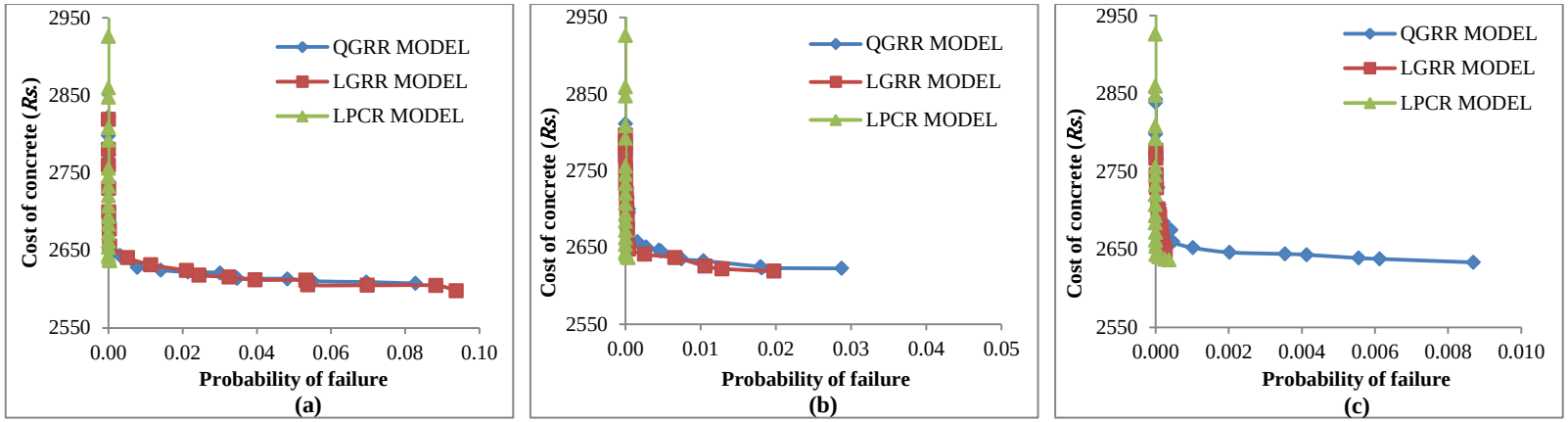

Figure 5.43 Pareto-optimal fronts obtained for different models of 56 days compressive strength for target $st56$ = 25 MPa with (a) P_f = 0.1 (b) P_f = 0.05 and (c) P_f = 0.01, for concrete with fly ash

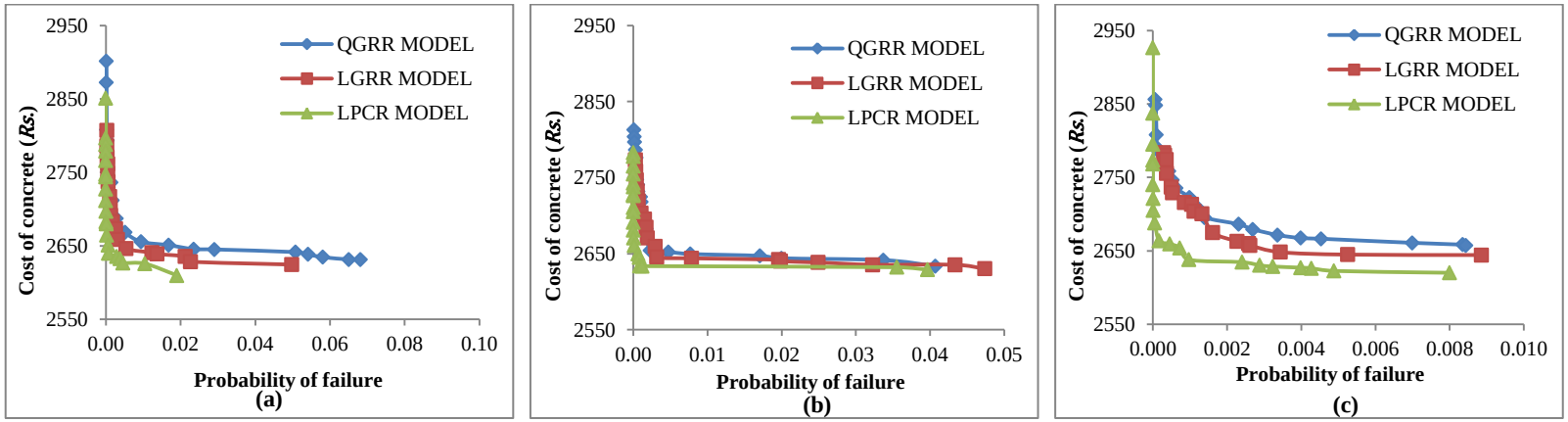

Figure 5.44 Pareto-optimal fronts obtained for different models of 56 days compressive strength for target $st56$ = 30 MPa with (a) P_f = 0.1 (b) P_f = 0.05 and (c) P_f = 0.01, for concrete with fly ash

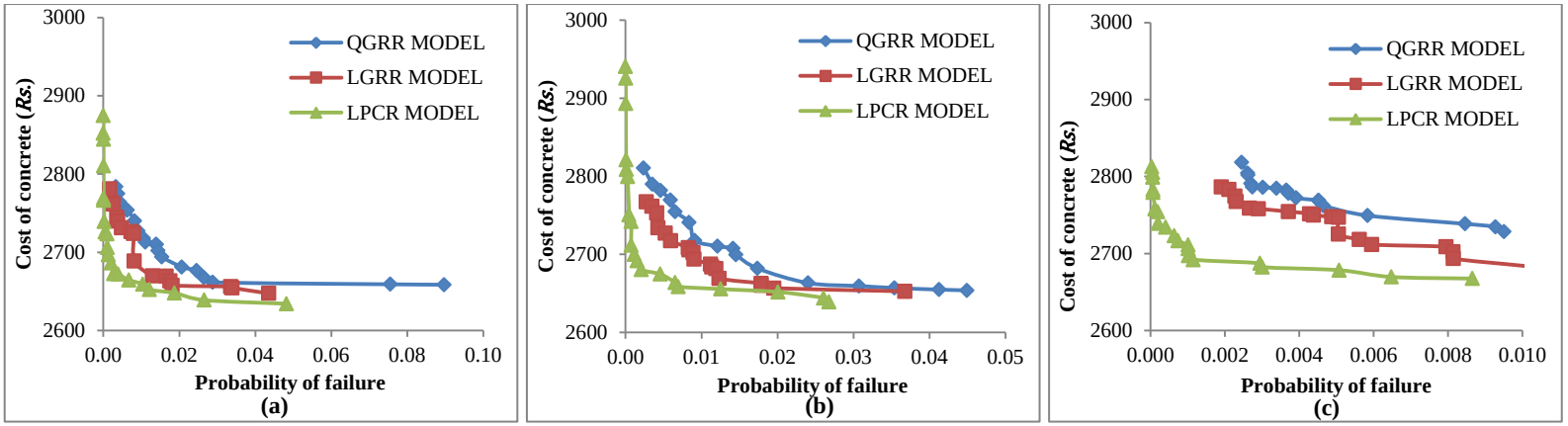

Figure 5.45 Pareto-optimal fronts obtained for different models of 56 days compressive strength for target $st56$ = 35 MPa with (a) P_f = 0.1 (b) P_f = 0.05 and (c) P_f = 0.01, for concrete with fly ash

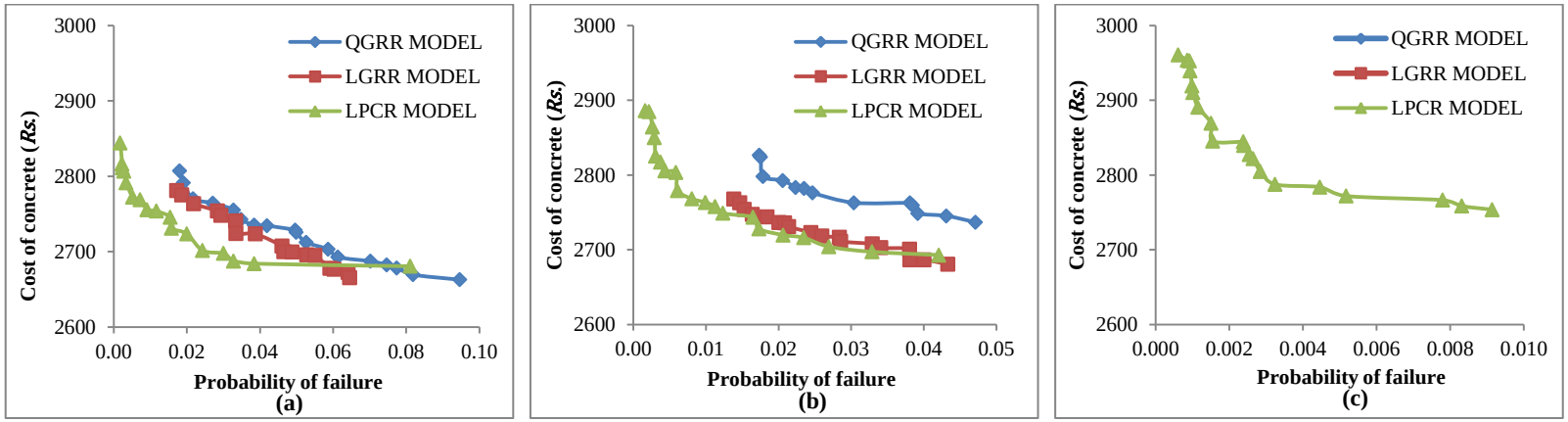

Figure 5.46 Pareto-optimal fronts obtained for different models of 56 days compressive strength for target $st56$ = 40 MPa with (a) P_f = 0.1 (b) P_f = 0.05 and (c) P_f = 0.01, for concrete with fly ash

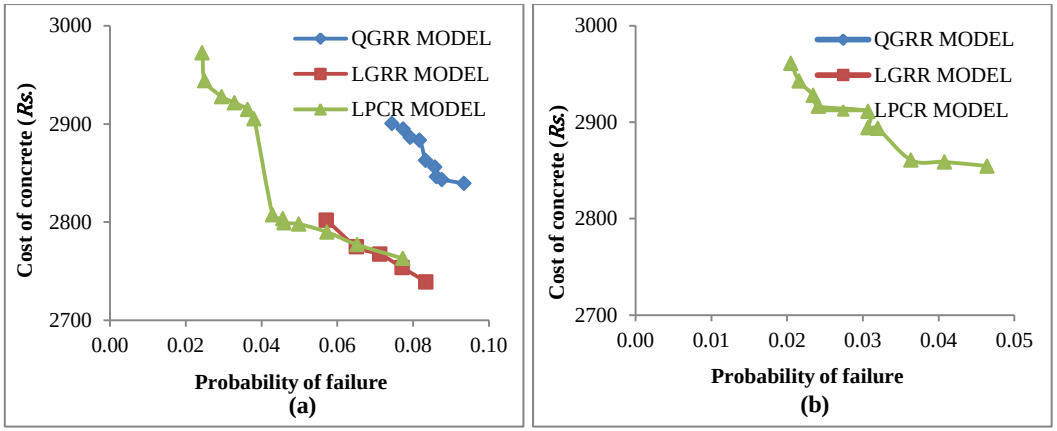

Figure 5.47 Pareto-optimal fronts obtained for different models of 56 days compressive strength with target $st56 = 45\ MPa$ with (a) $P_f = 0.1$ (b) $P_f = 0.05$; for concrete with fly ash

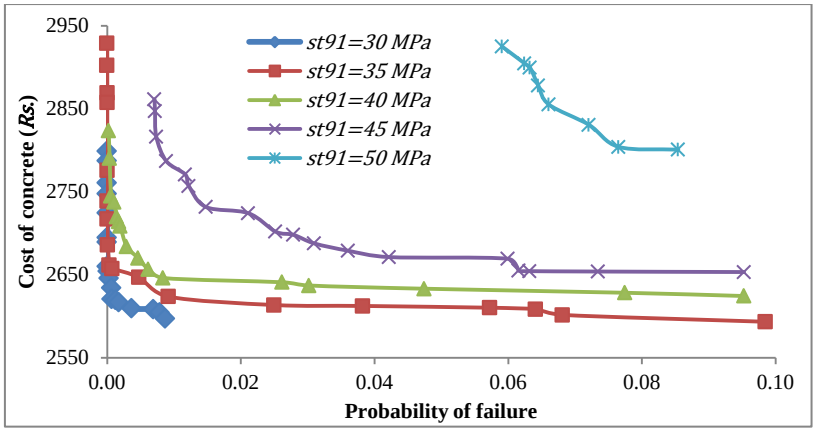

Figure 5.48(a) Pareto-optimal fronts based on QGRR model of 91 days compressive strength with P_f = 0.1 for concrete with fly ash

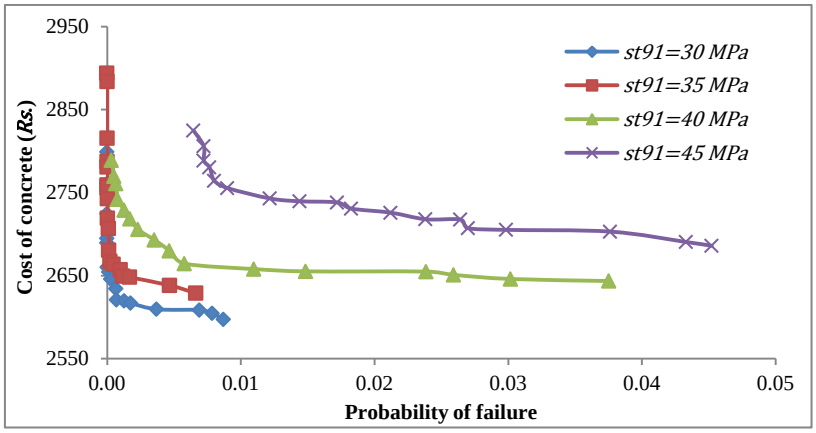

Figure 5.48(b) Pareto-optimal fronts based on QGRR model of 91 days compressive strength with P_f = 0.05 for concrete with fly ash

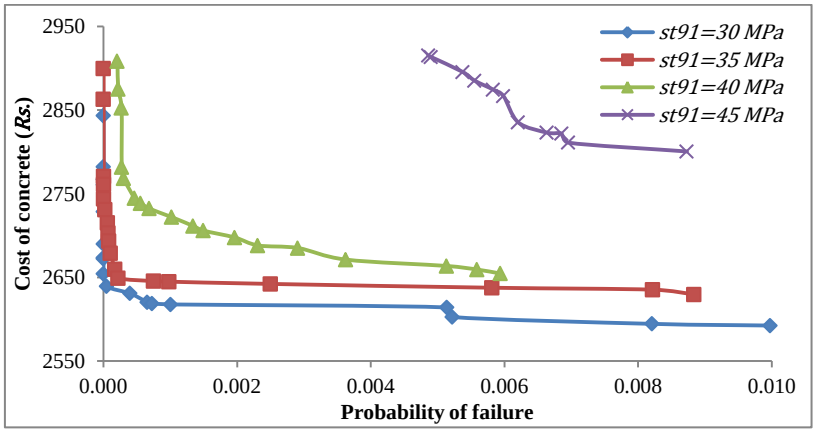

Figure 5.48(c) Pareto-optimal fronts based on QGRR model of 91 days compressive strength with P_f = 0.01 for concrete with fly ash

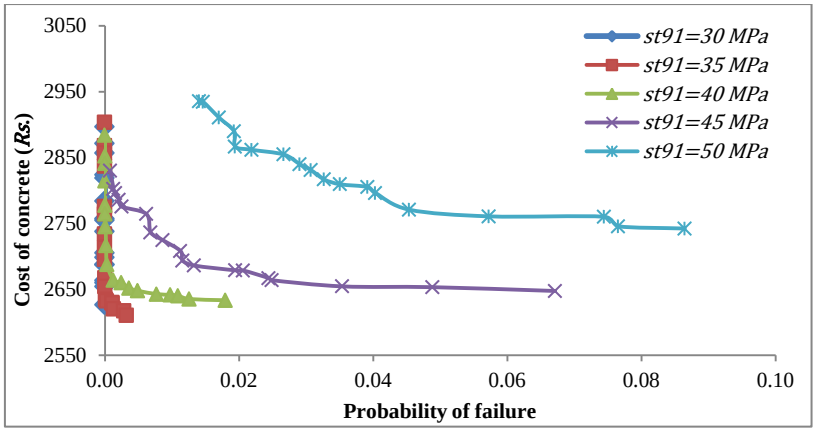

Figure 5.49(a) Pareto-optimal fronts based on LPCR model of 91 days compressive strength with P_f = 0.1 for concrete with fly ash

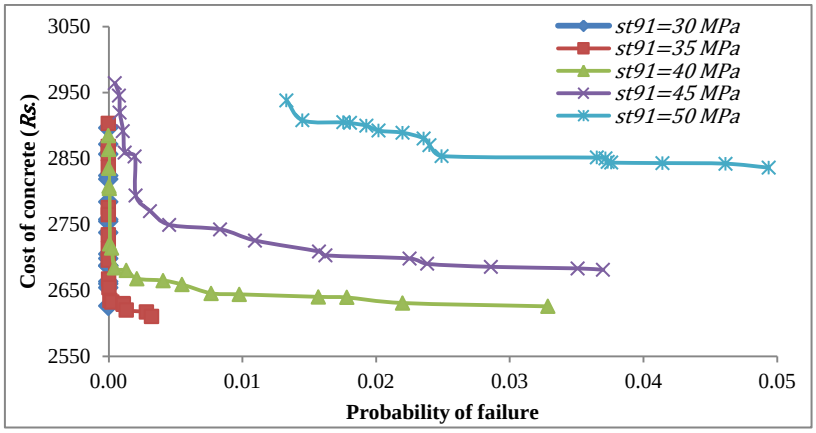

Figure 5.49(b) Pareto-optimal fronts based on LPCR model of 91 days compressive strength with P_f = 0.05 for concrete with fly ash

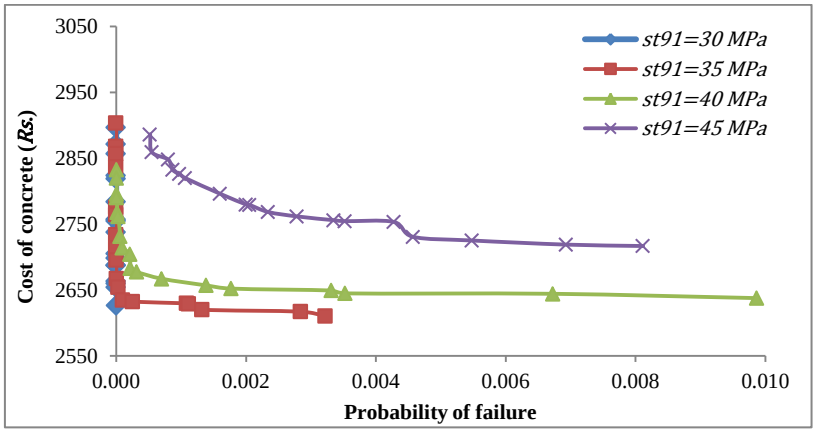

Figure 5.49(c) Pareto-optimal fronts based on LPCR model of 91 days compressive strength with P_f = 0.01 for concrete with fly ash

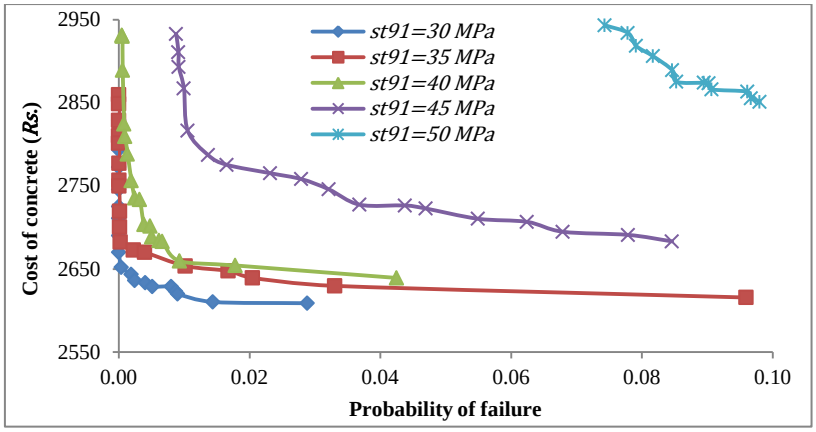

Figure 5.50(a) Pareto-optimal fronts based on LTRR/LOLSR model of 91 days compressive strength with P_f = 0.1 for concrete with fly ash

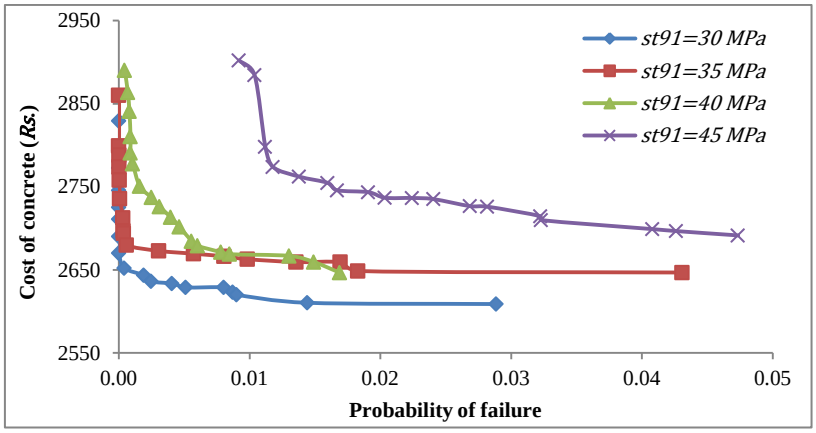

Figure 5.50(b) Pareto-optimal fronts based on LTRR/LOLSR model of 91 days compressive strength with P_f = 0.05 for concrete with fly ash

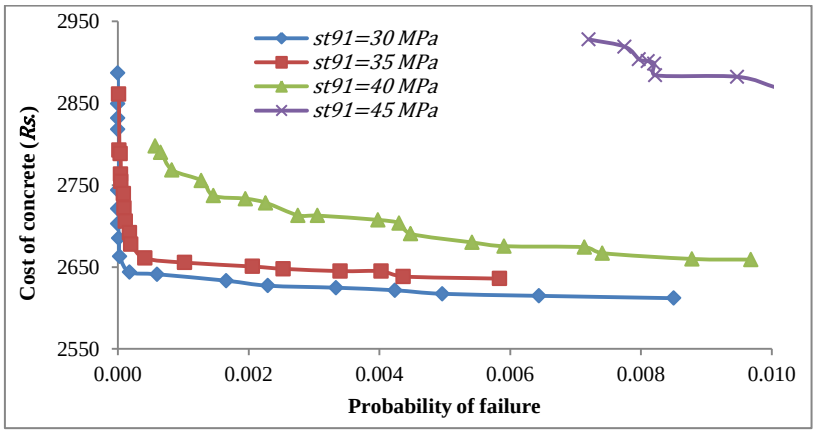

Figure 5.50(c) Pareto-optimal fronts based on LTRR/LOLSR model of 91 days compressive strength with P_f = 0.01 for concrete with fly ash

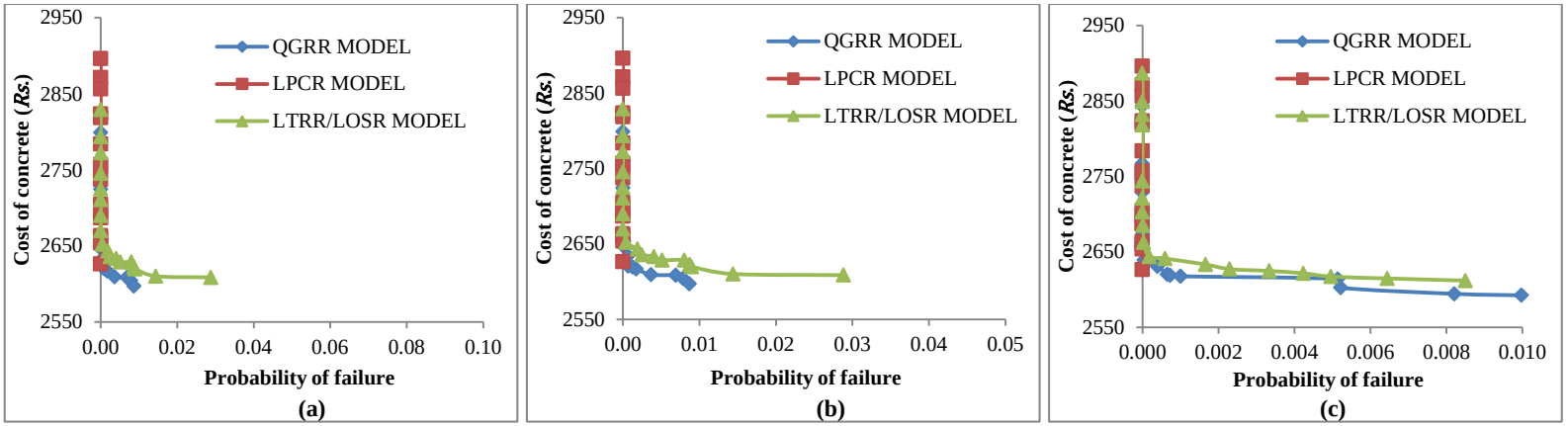

Figure 5.51 Pareto-optimal fronts obtained for different models of 91 days compressive strength for target $st91$ = 30 MPa with (a) P_f = 0.1 (b) P_f = 0.05 and (c) P_f = 0.01, for concrete with fly ash

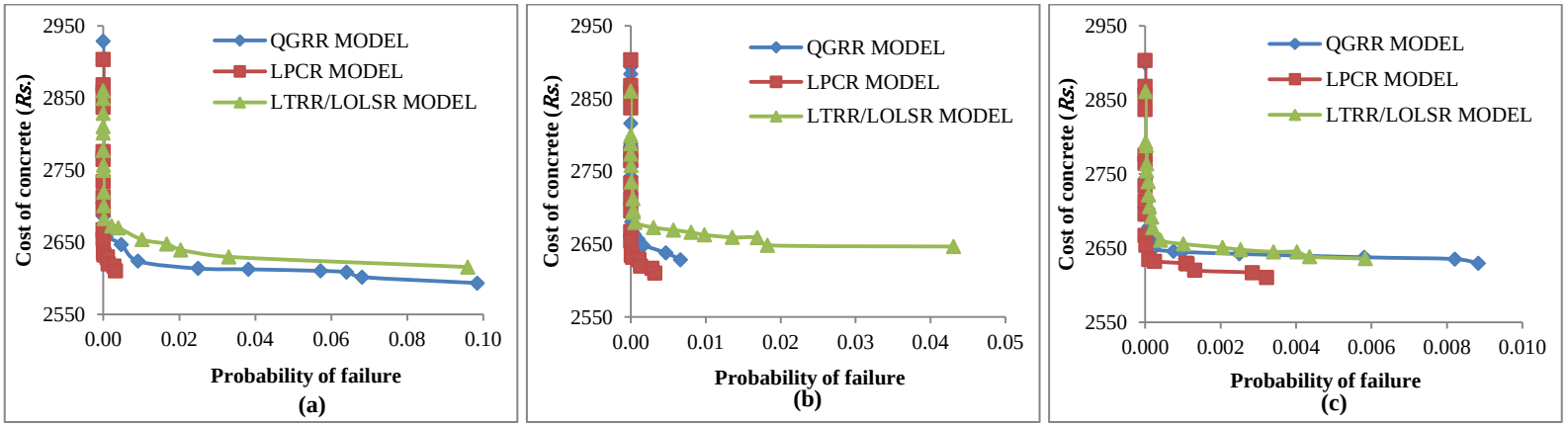

Figure 5.52 Pareto-optimal fronts obtained for different models of 91 days compressive strength for target $st91$ = 35 MPa with (a) P_f = 0.1 (b) P_f = 0.05 and (c) P_f = 0.01, for concrete with fly ash

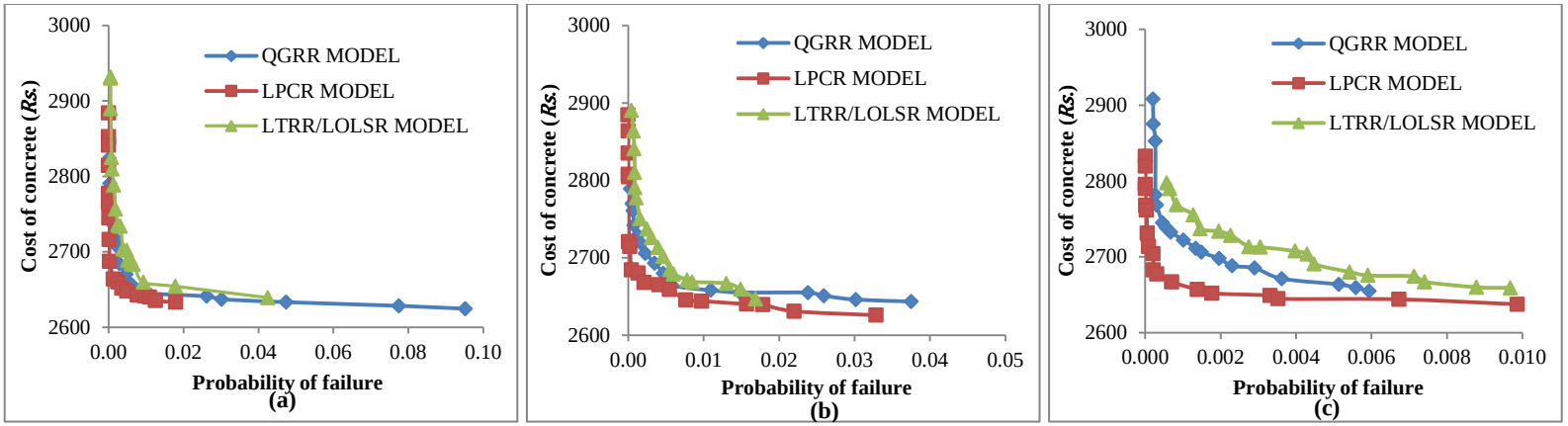

Figure 5.53 Pareto-optimal fronts obtained for different models of 91 days compressive strength for target $st91 = 40\ MPa$ with (a) $P_f = 0.1$ (b) $P_f = 0.05$ and (c) $P_f = 0.01$, for concrete with fly ash

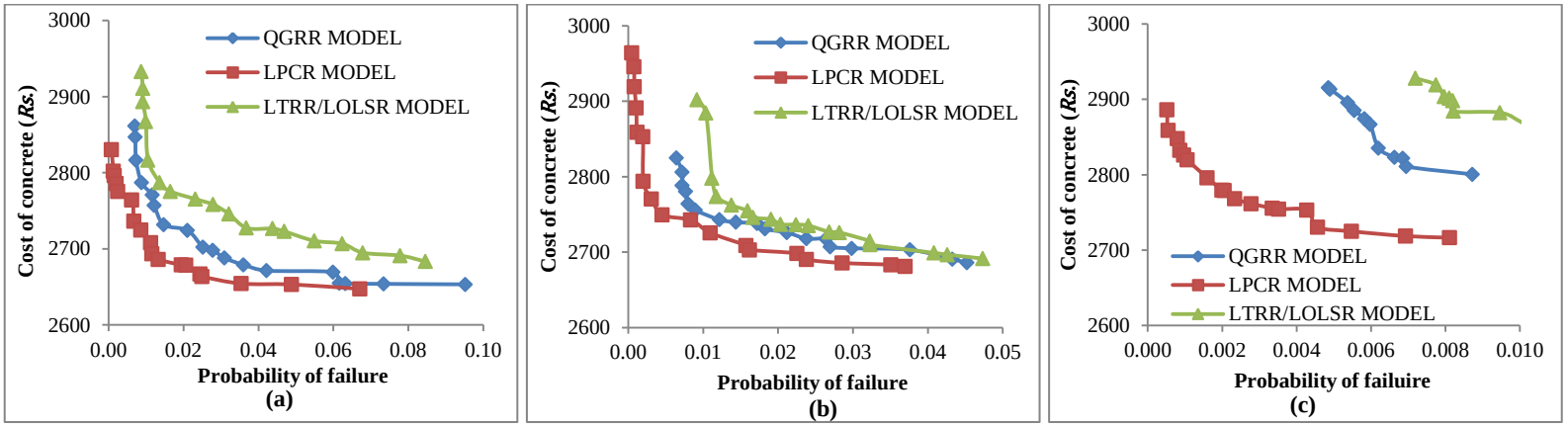

Figure 5.54 Pareto-optimal fronts obtained for different models of 91 days compressive strength for target $st91 = 45\ MPa$ with (a) $P_f = 0.1$ (b) $P_f = 0.05$ and (c) $P_f = 0.01$, for concrete with fly ash

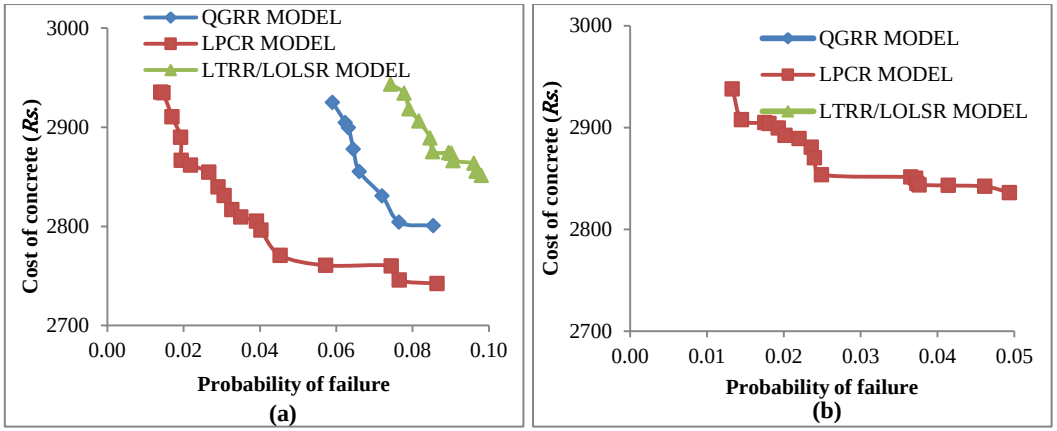

Figure 5.55 Pareto-optimal fronts obtained for different models of 91 days compressive strength for target $st91 = 50\ MPa$ with (a) $P_f = 0.1$ and (b) $P_f = 0.05$, for concrete with fly ash

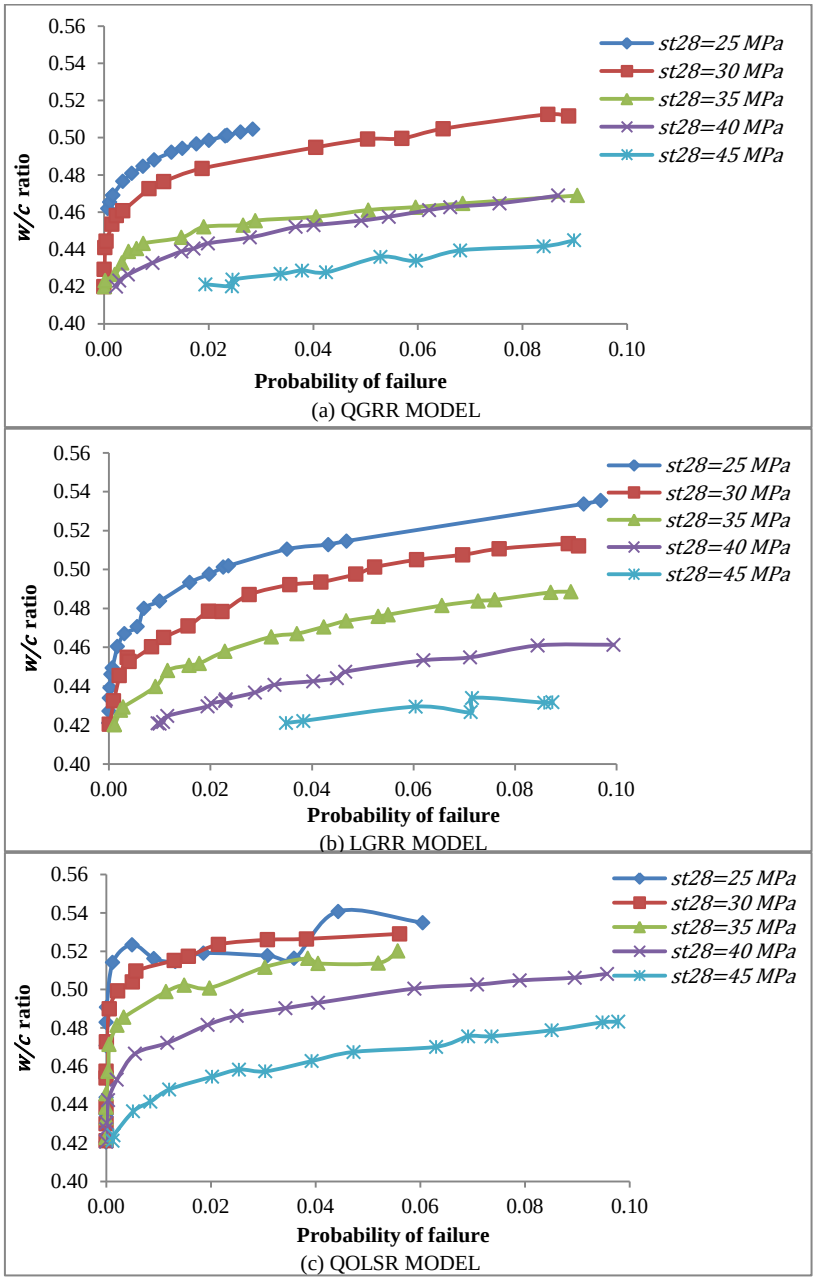

Figure 5.56 Variation of w/c ratio with probability of failure using different 28 days compressive strength models for concrete without fly ash

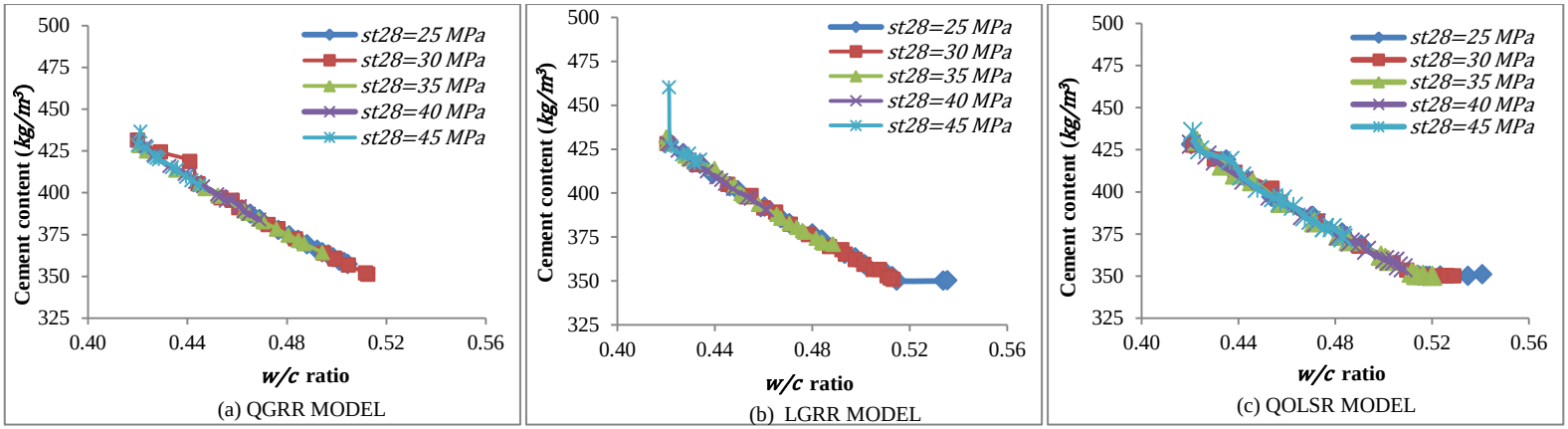

Figure 5.57 Variation of cement content with w/c ratio using different 28 days compressive strength models for concrete without fly ash

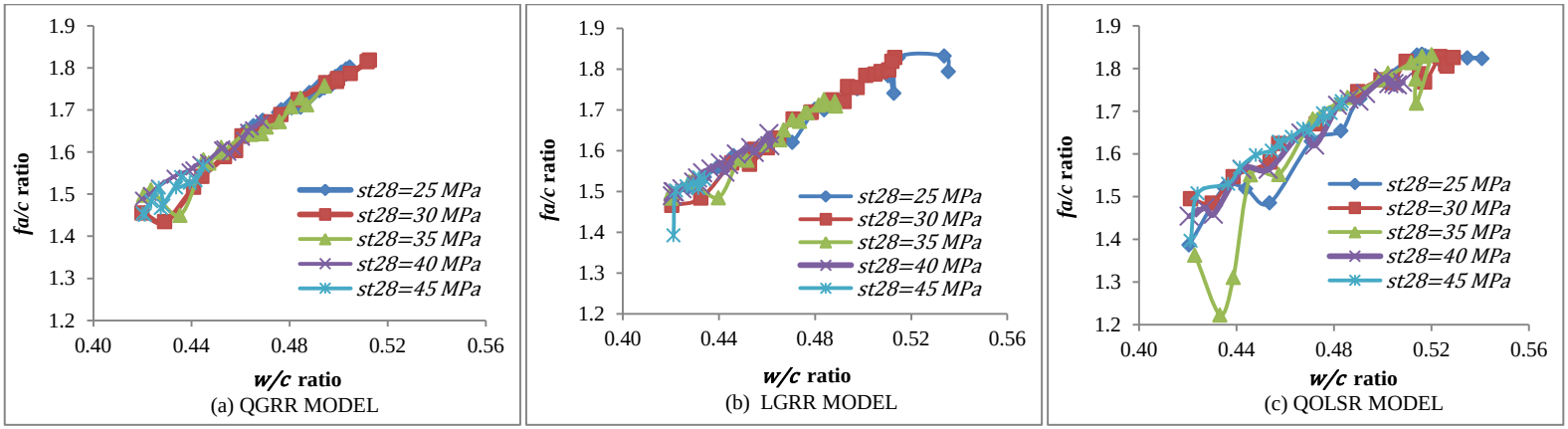

Figure 5.58 Variation of fa/c ratio with w/c ratio using different 28 days compressive strength models for concrete without fly ash

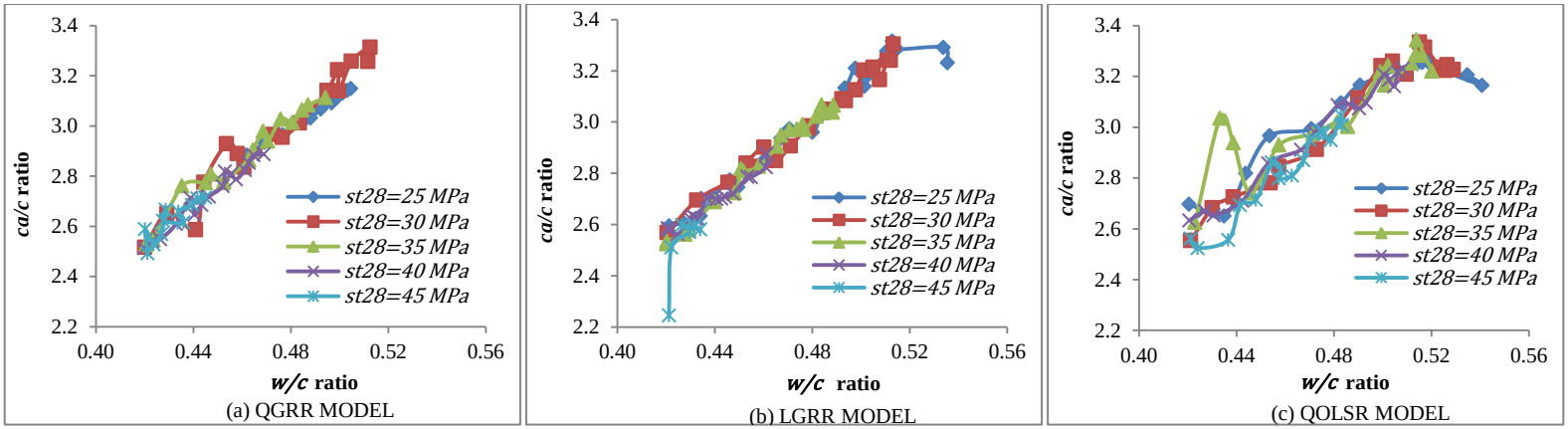

(a) QGRR MODEL (b) LGRR MODEL (c) QOLSR MODEL

Figure 5.59 Variation of ca/c ratio with w/c ratio using different 28 days compressive strength models for concrete without fly ash

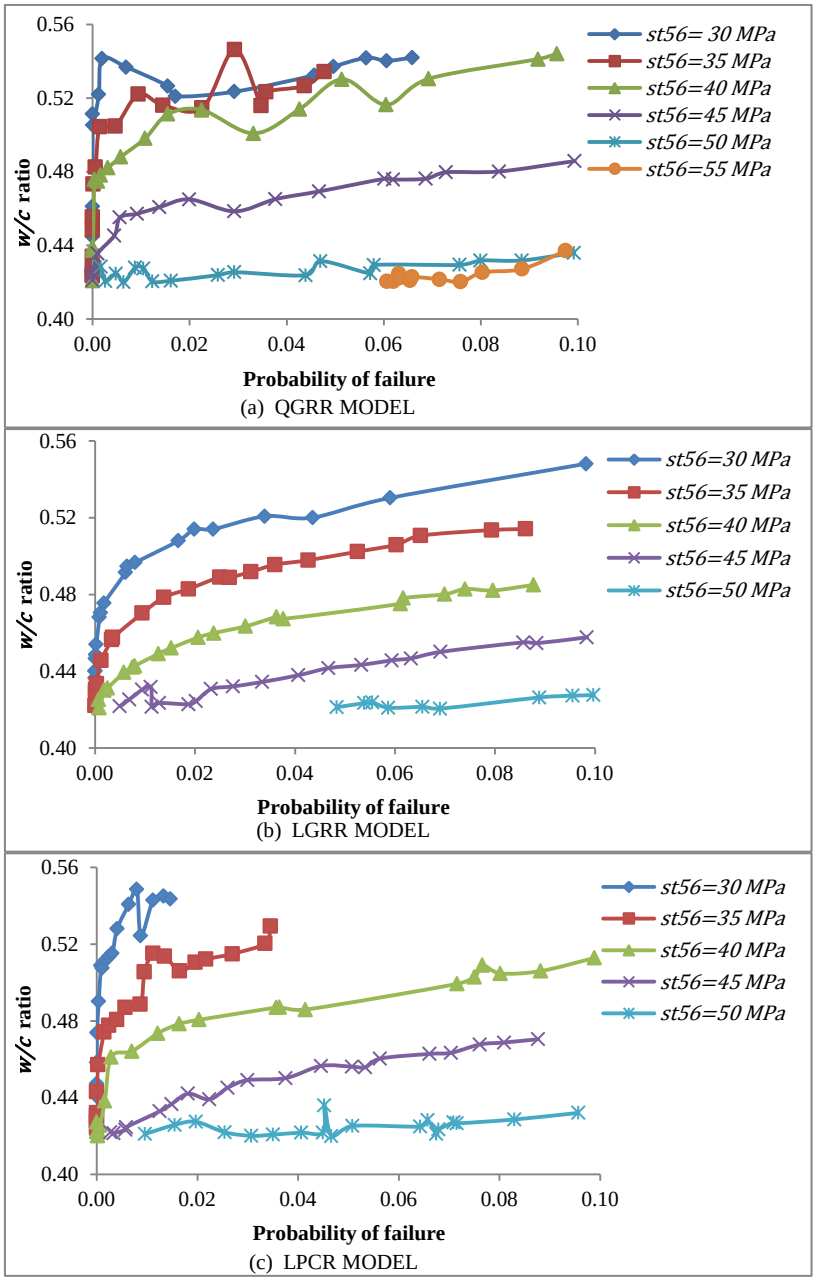

Figure 5.60 Variation of w/c ratio with probability of failure using different 56 days compressive strength models for concrete without fly ash

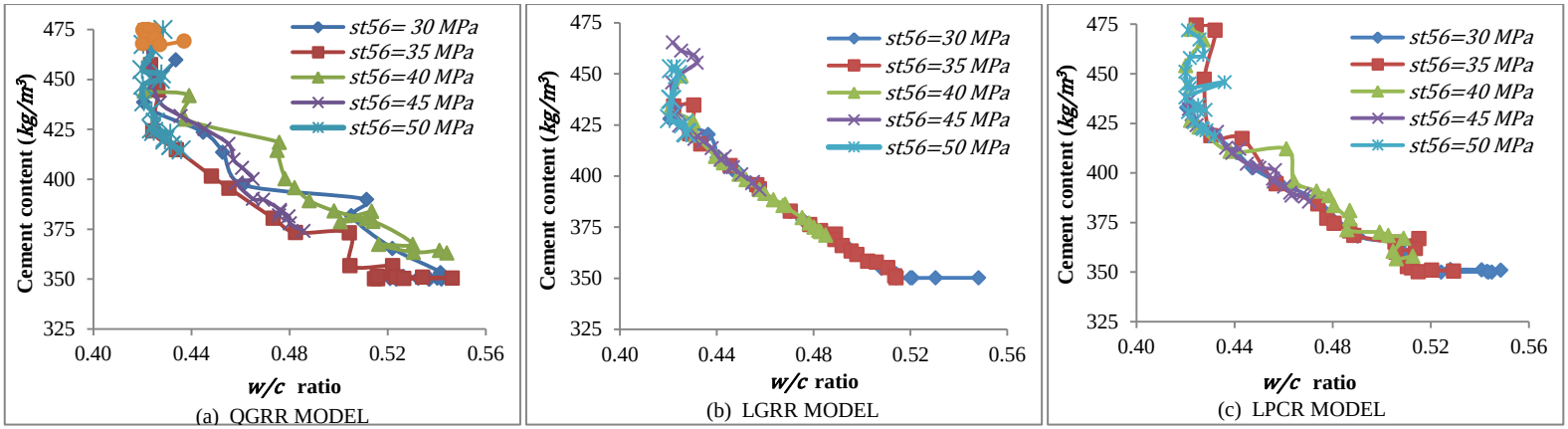

Figure 5.61 Variation of cement content with w/c ratio using different 56 days compressive strength models for concrete without fly ash

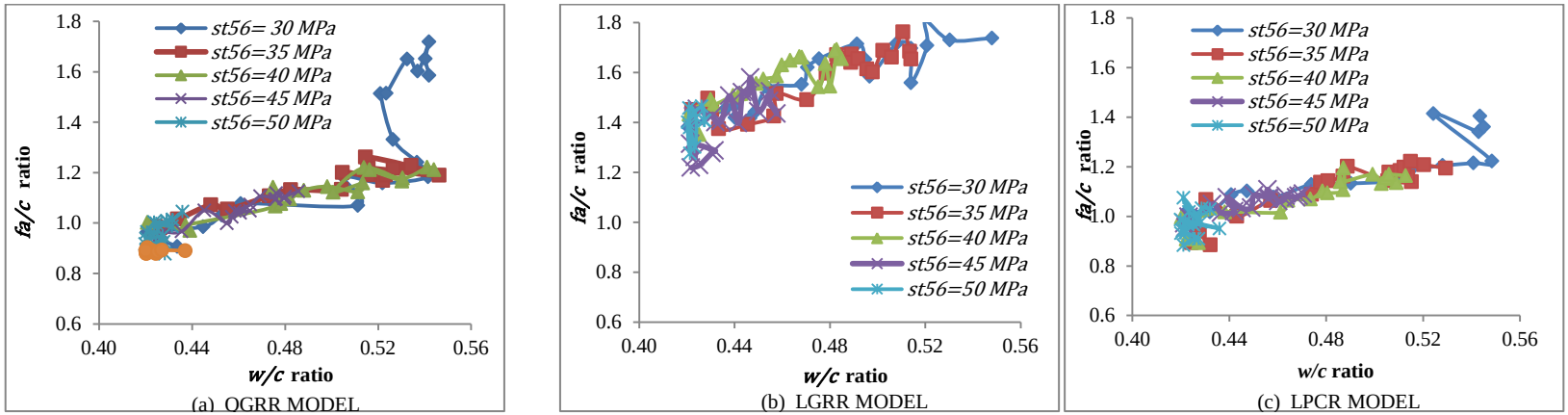

Figure 5.62 Variation of fa/c ratio with w/c ratio using different 56 days compressive strength models for concrete without fly ash

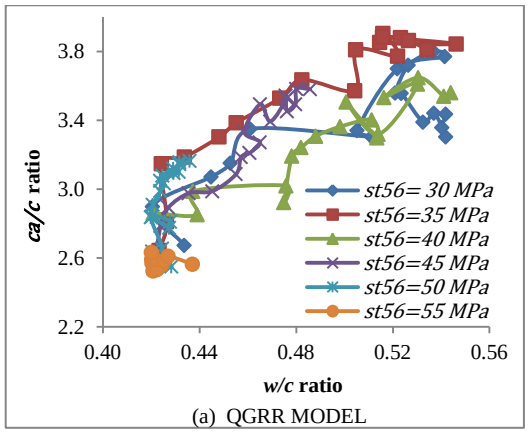

(a) QGRR MODEL

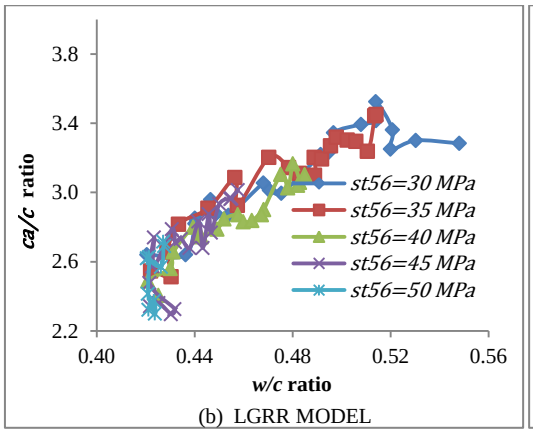

(b) LGRR MODEL

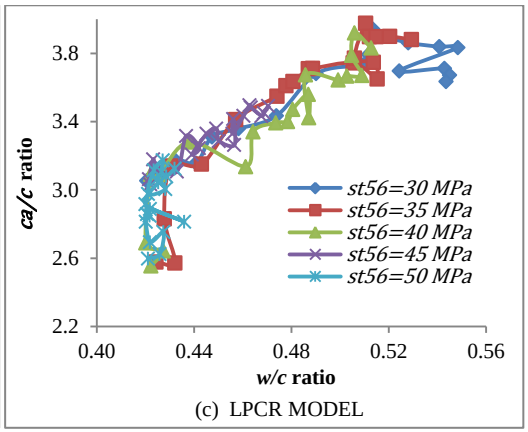

(c) LPCR MODEL

Figure 5.63 Variation of ca/c ratio with w/c ratio using different 56 days compressive strength models for concrete without fly ash

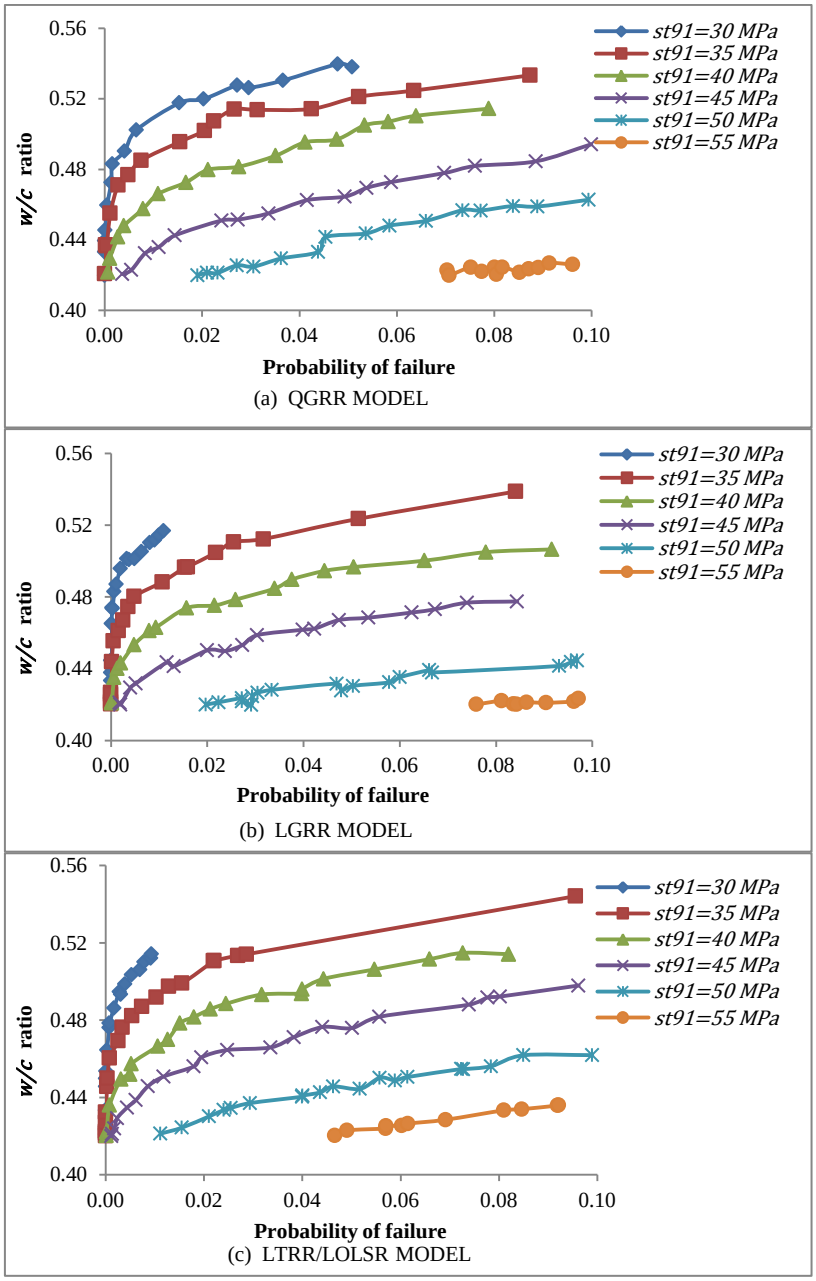

Figure 5.64 Variation of w/c ratio with probability of failure using different 91 days compressive strength models for concrete without fly ash

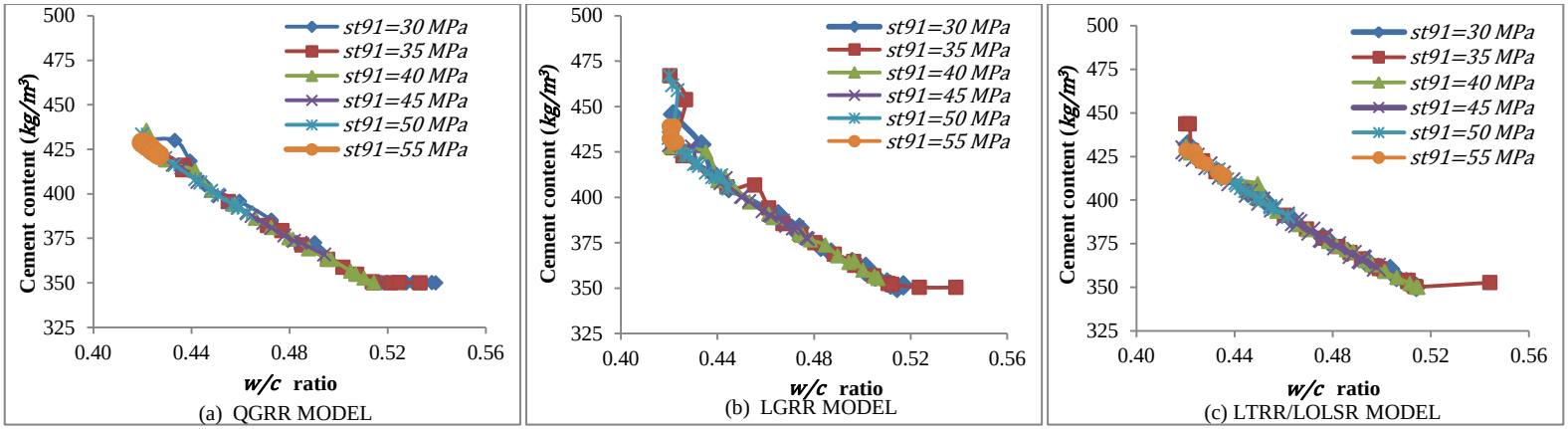

Figure 5.65 Variation of cement content with w/c ratio using different 91 days compressive strength models for concrete without fly ash

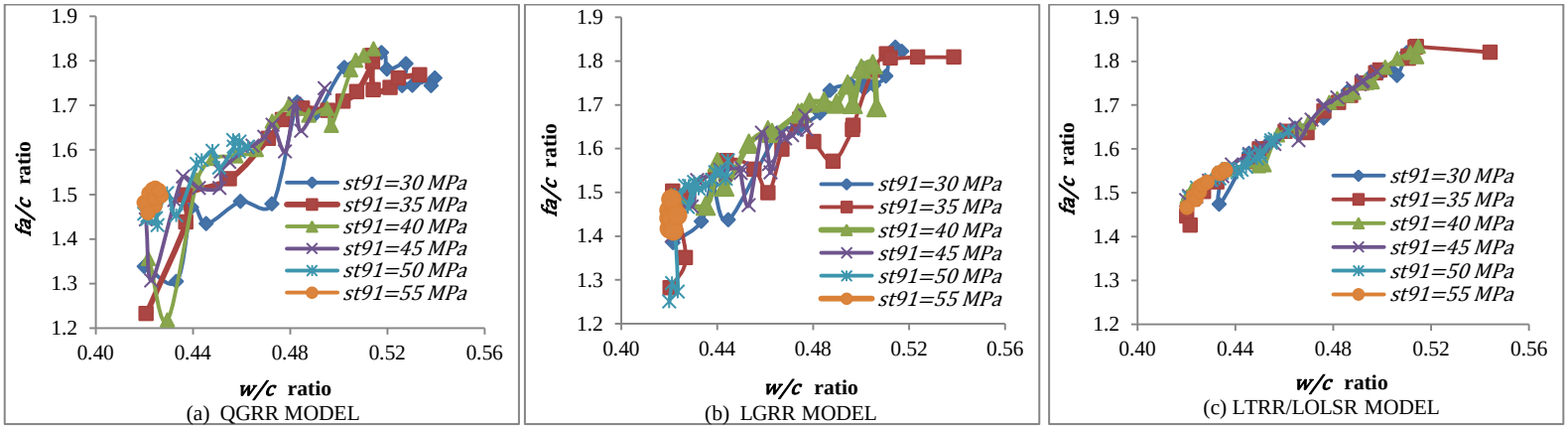

Figure 5.66 Variation of fa/c ratio with w/c ratio using different 91 days compressive strength models for concrete without fly ash

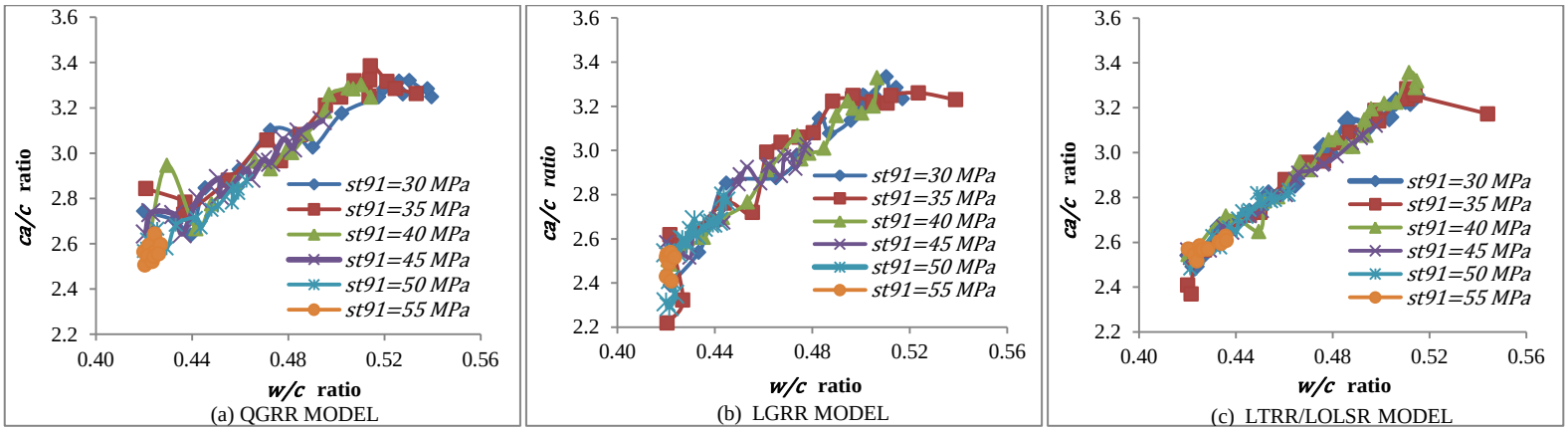

(a) QGRR MODEL (b) LGRR MODEL (c) LTRR/LOLSR MODEL

Figure 5.67 Variation of ca/c ratio with w/c ratio using different 91 days compressive strength models for concrete without fly ash

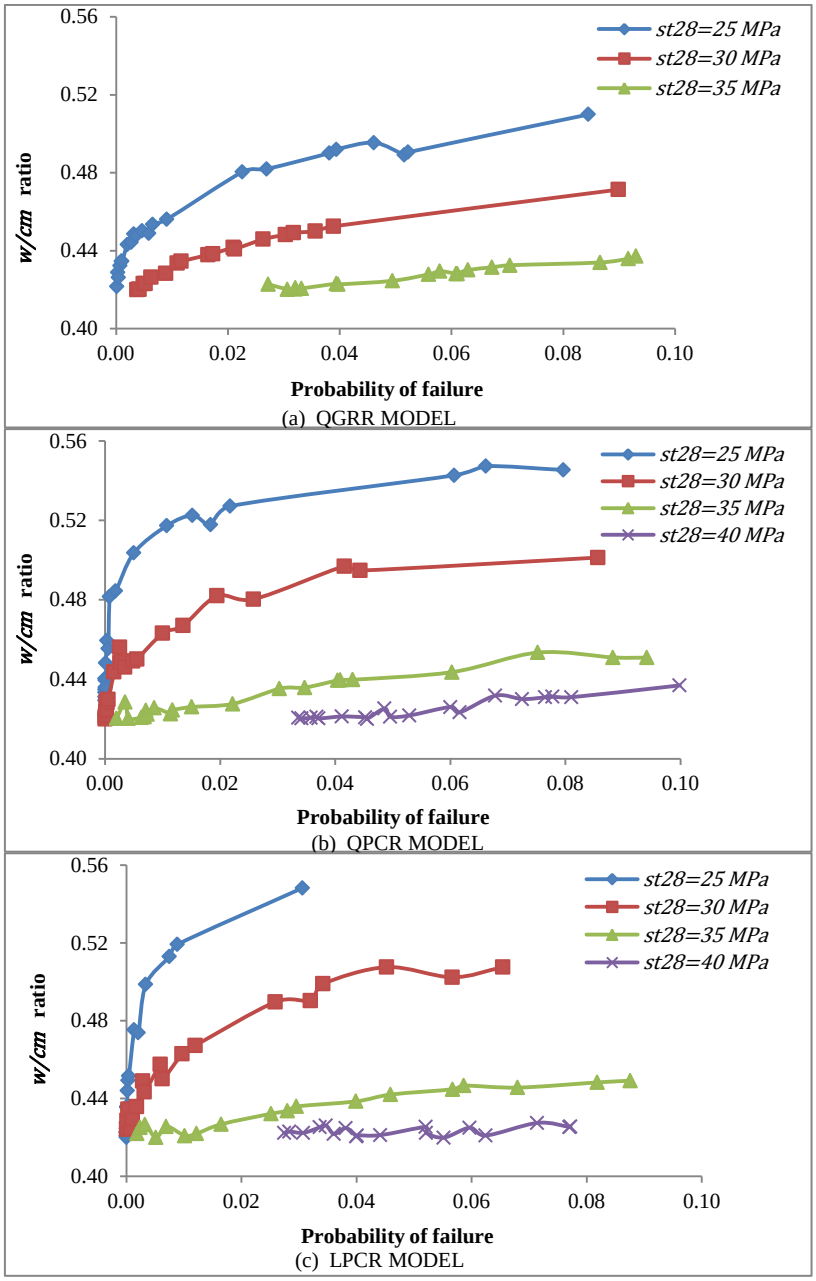

Figure 5.68 Variation of w/cm ratio with probability of failure using different 28 days compressive strength models for concrete with fly ash

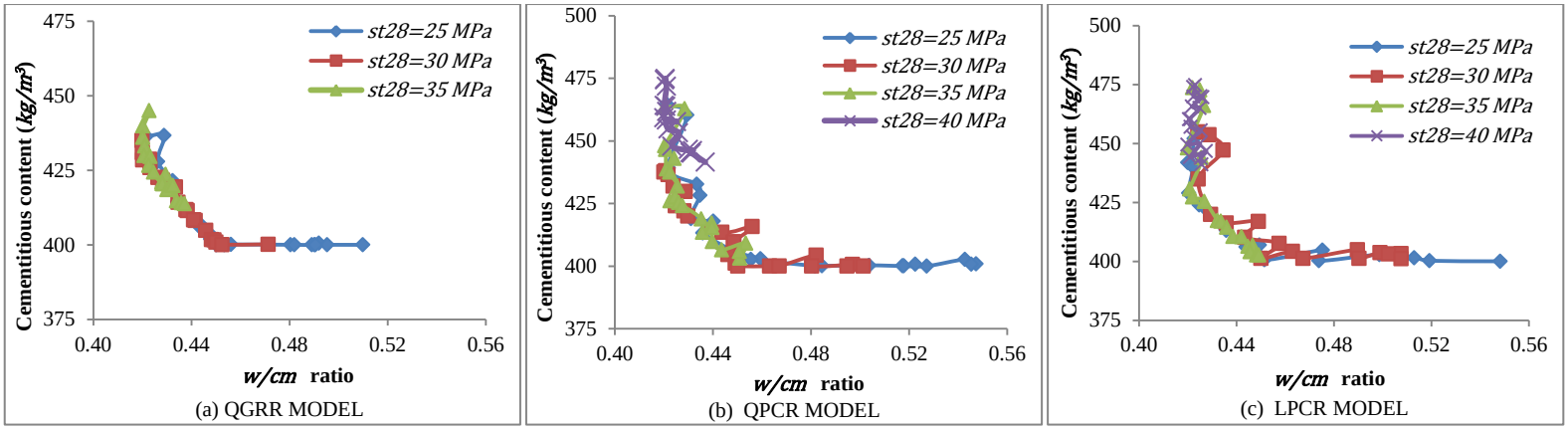

Figure 5.69 Variation of cementitious content with w/cm ratio using different 28 days compressive strength models for concrete with fly ash

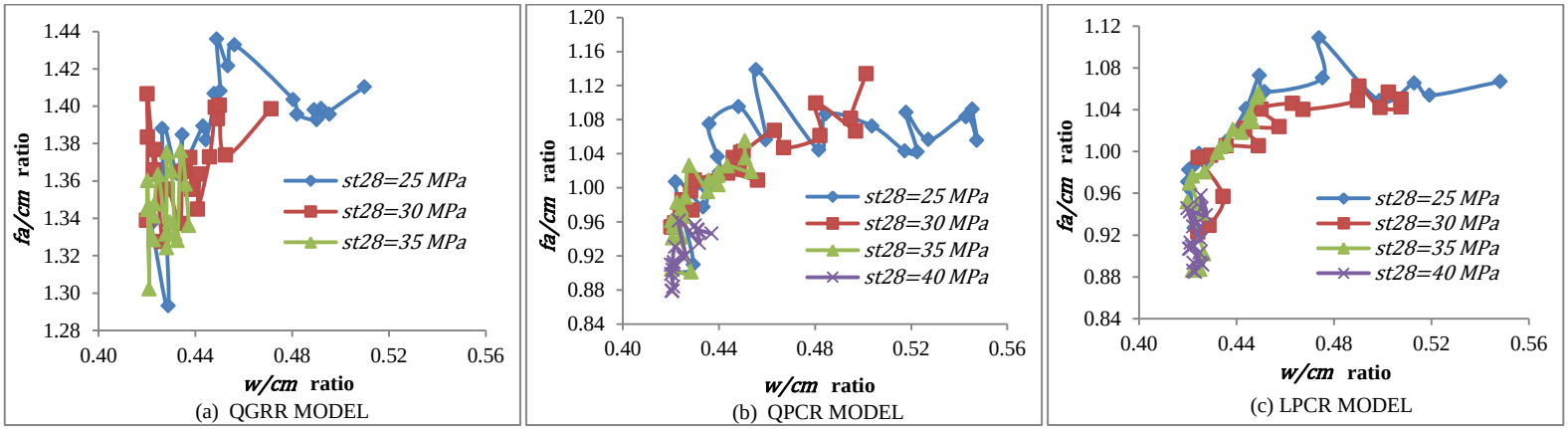

Figure 5.70 Variation of fa/cm ratio with w/cm ratio using different 28 days compressive strength models for concrete with fly ash

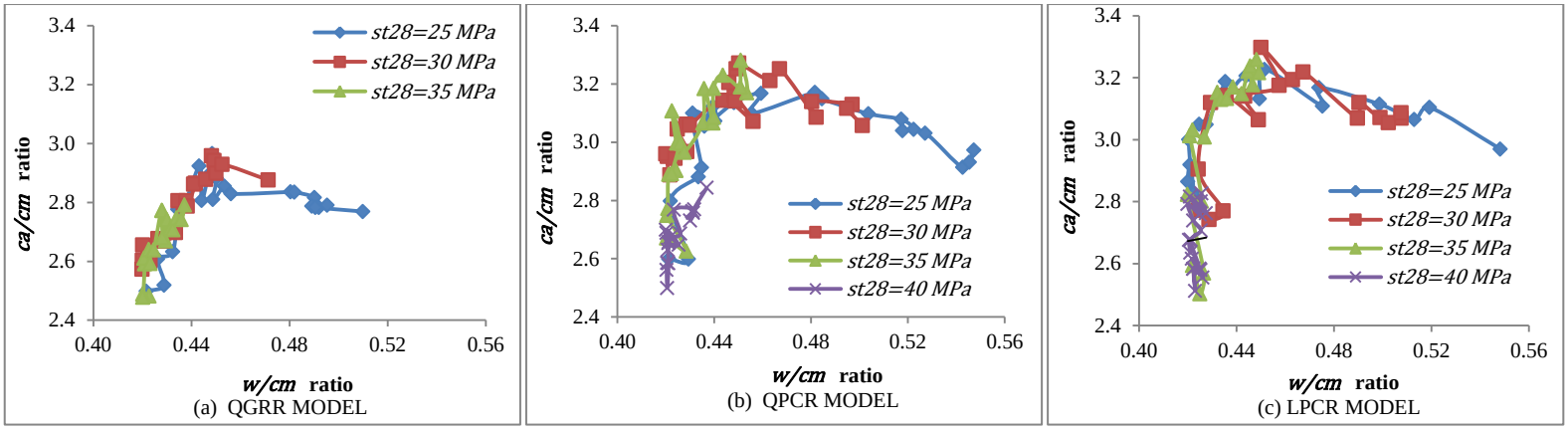

(a) QGRR MODEL (b) QPCR MODEL (c) LPCR MODEL

Figure 5.71 Variation of ca/cm ratio with w/cm ratio using different 28 days compressive strength models for concrete with fly ash

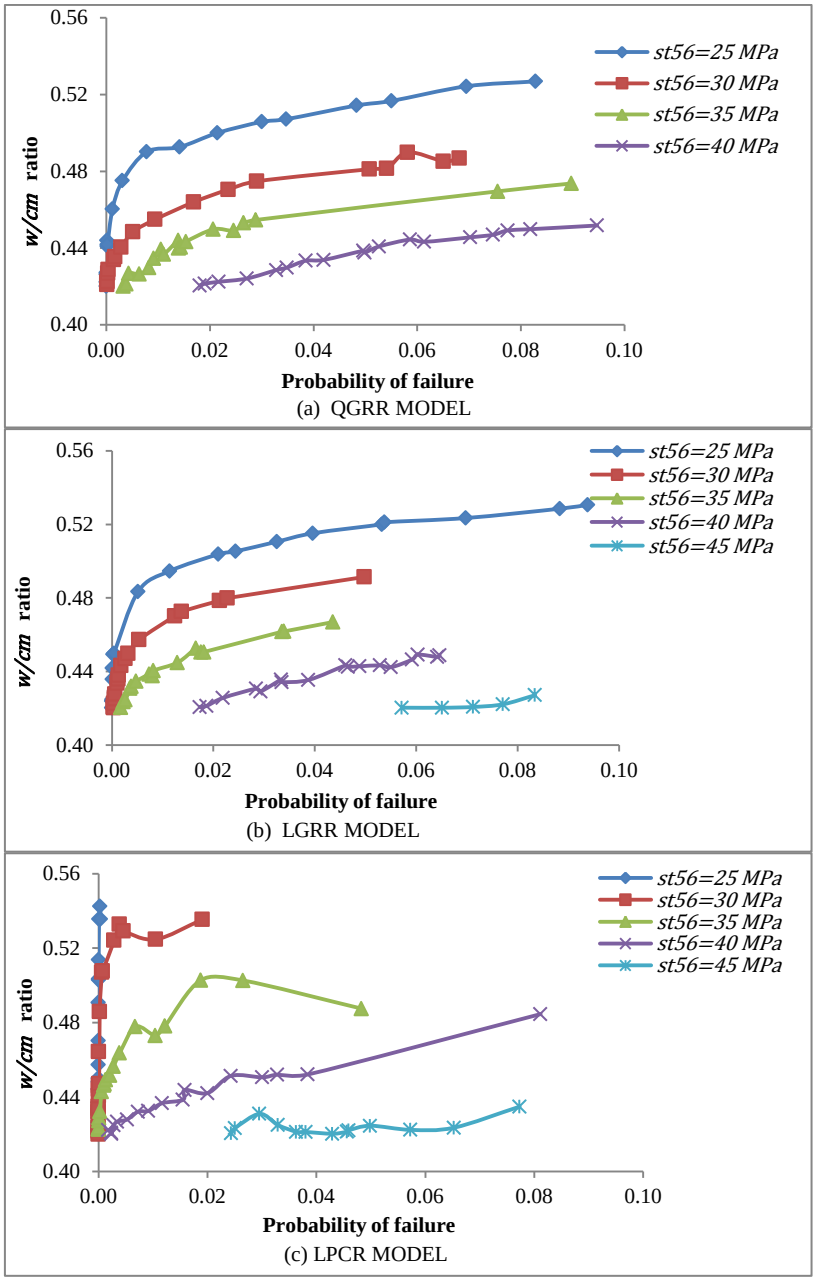

Figure 5.72 Variation of w/cm ratio with probability of failure using different 56 days compressive strength models for concrete with fly ash

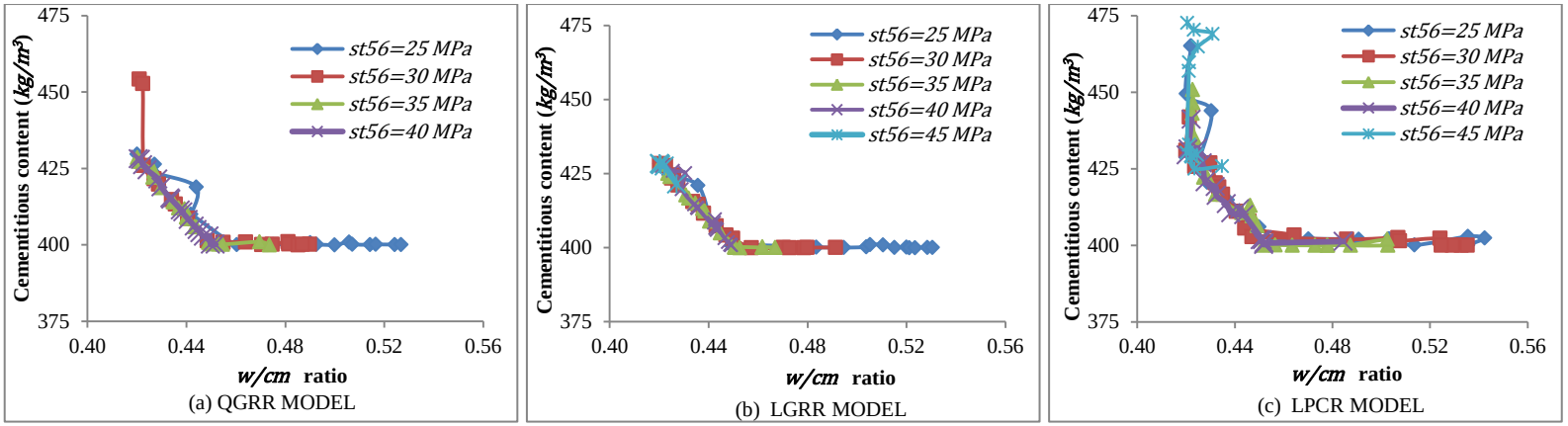

(a) QGRR MODEL (b) LGRR MODEL (c) LPCR MODEL

Figure 5.73 Variation of cementitious content with w/cm ratio using different 56 days compressive strength models for concrete with fly ash

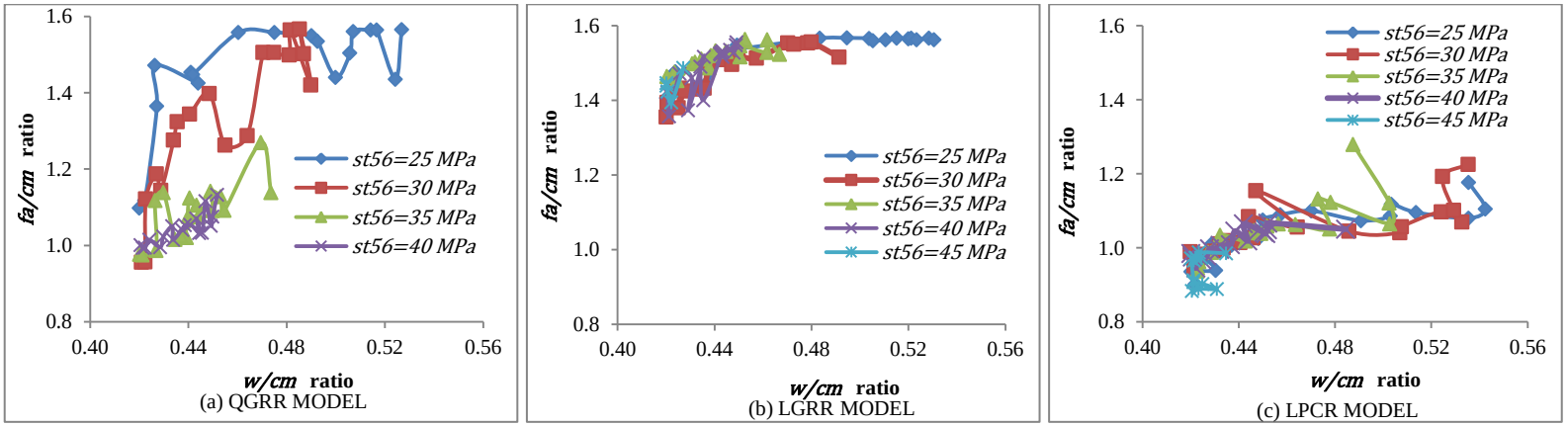

(a) QGRR MODEL (b) LGRR MODEL (c) LPCR MODEL

Figure 5.74 Variation of fa/cm ratio with w/cm ratio using different 56 days compressive strength models for concrete with fly ash

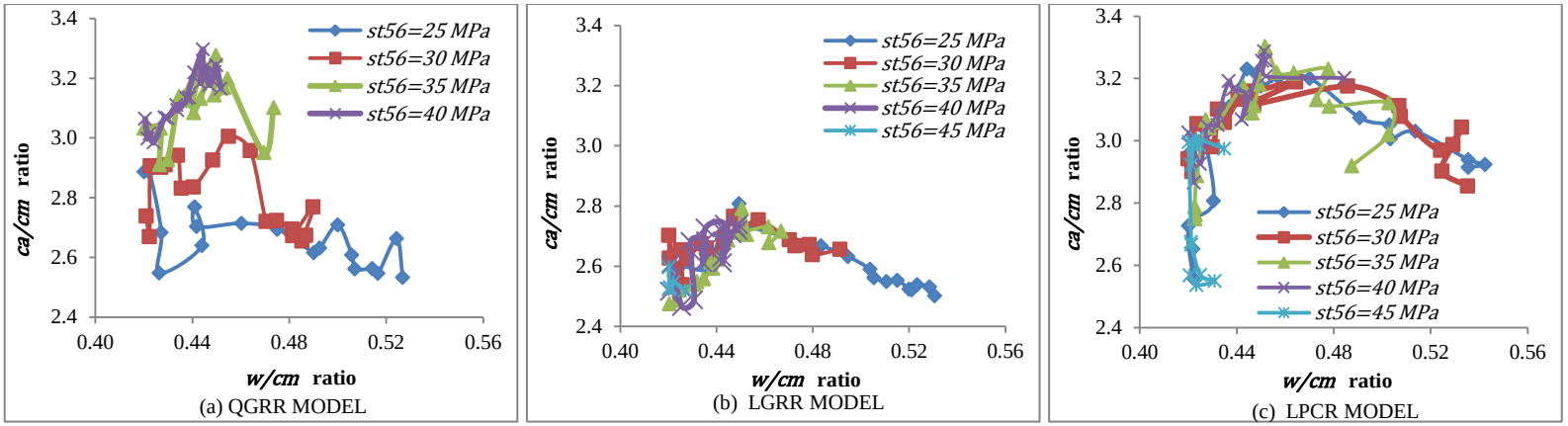

(a) QGRR MODEL (b) LGRR MODEL (c) LPCR MODEL

Figure 5.75 Variation of ca/cm ratio with w/cm ratio using different 56 days compressive strength models for concrete with fly ash

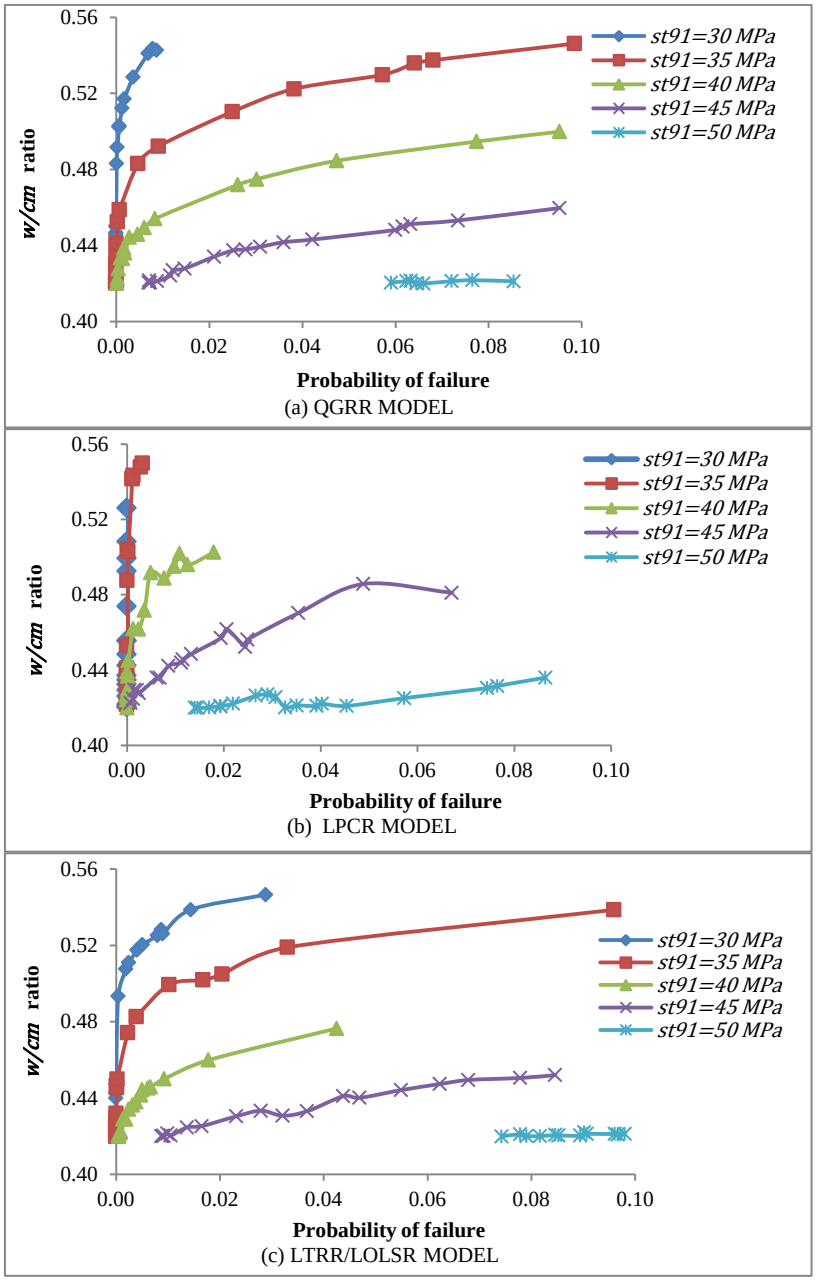

Figure 5.76 Variation of w/cm ratio with probability of failure using different 91 days compressive strength models for concrete with fly ash

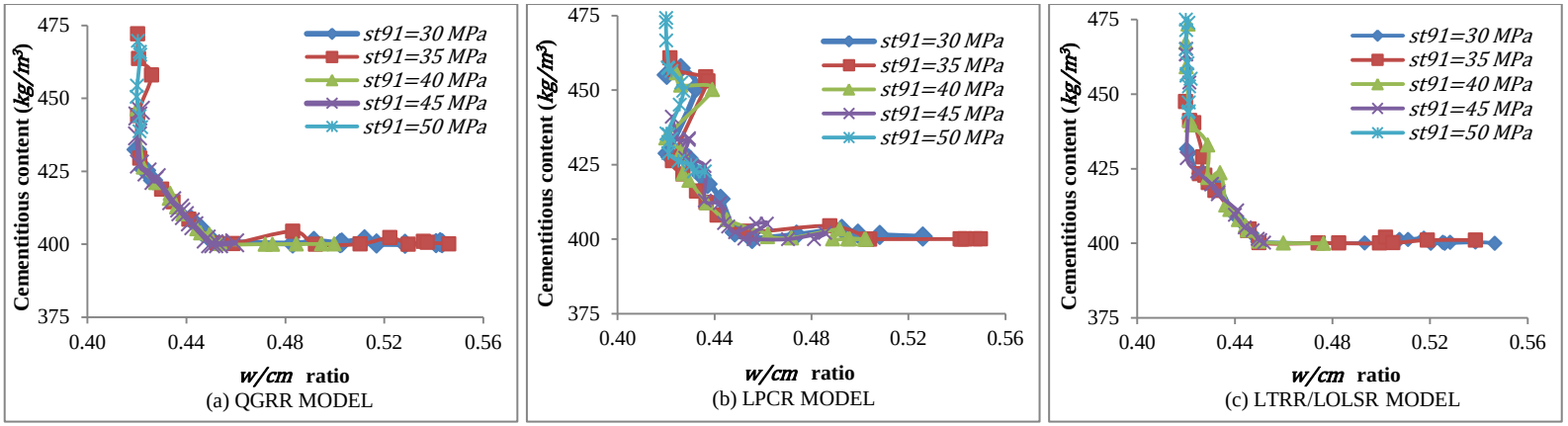

Figure 5.77 Variation of cementitious content with w/cm ratio using different 91 days compressive strength models for concrete with fly ash

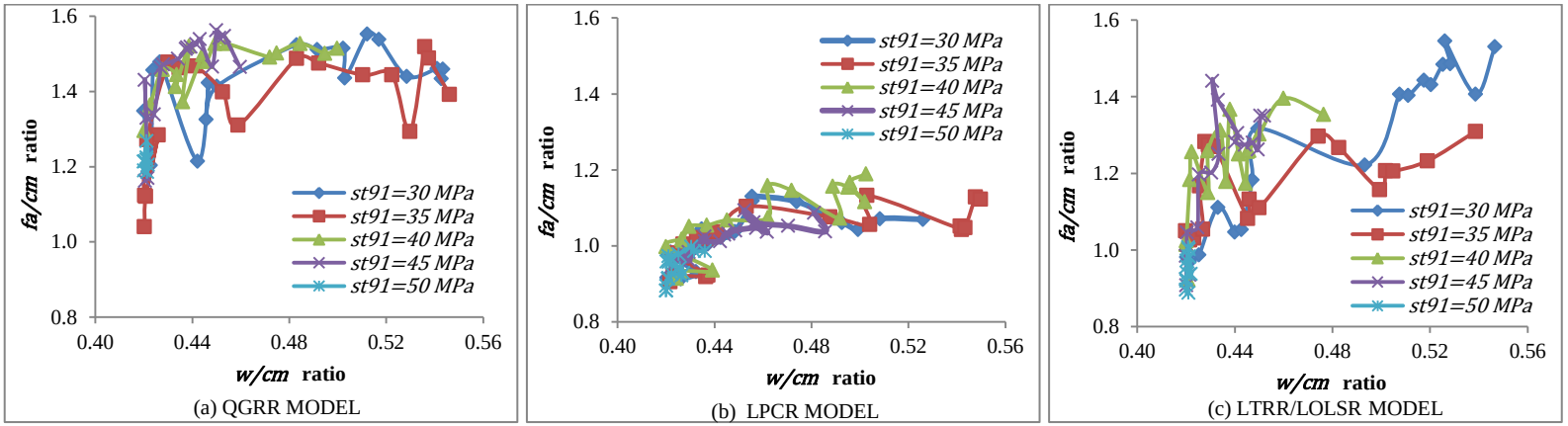

Figure 5.78 Variation of fa/cm ratio with w/cm ratio using different 91 days compressive strength models for concrete with fly ash

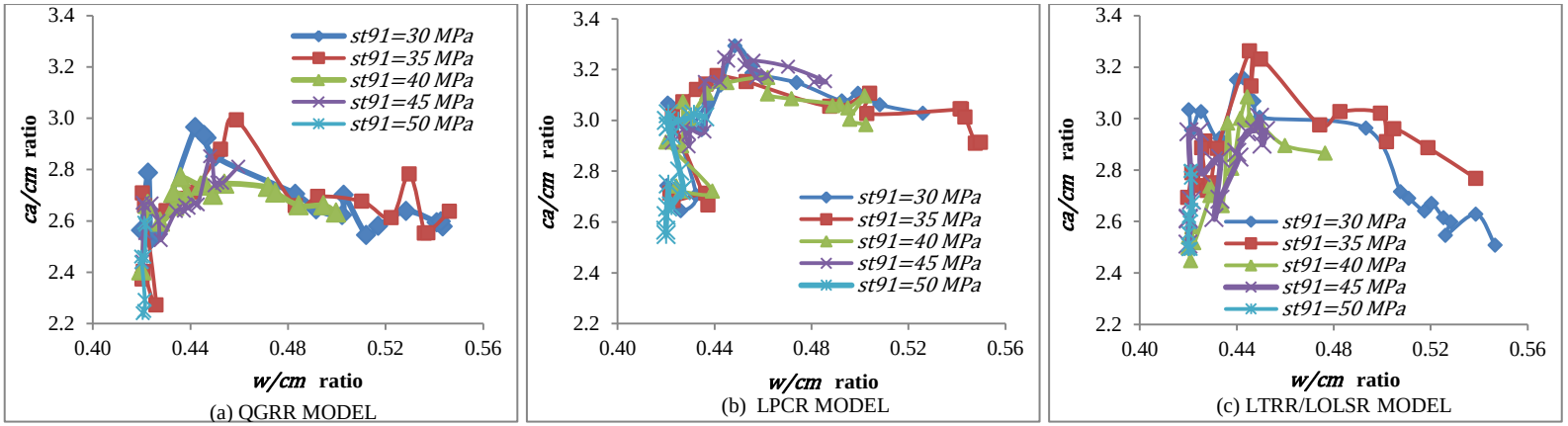

(a) QGRR MODEL (b) LPCR MODEL (c) LTRR/LOLSR MODEL

Figure 5.79 Variation of ca/cm ratio with w/cm ratio using different 91 days compressive strength models for concrete with fly ash

CHAPTER 6
CONCLUSIONS AND FUTURE SCOPE

==========

6.0 GENERAL

This chapter reports the conclusions drawn from this study on reliability based design optimization of concrete mix parameters. In addition, recommendations for further work are also included in this chapter.

6.1 PREDICTION MODELS FOR COMPRESSIVE STRENGTH OF CONCRETE

The following conclusions are drawn on comparing the various prediction models developed for compressive strength of concrete:

(i) For prediction of concrete compressive strength at curing ages of 28 and 91 days, QGRR model give the least value of MSE for concrete with or without fly ash, whereas, for 56 days concrete compressive strength, the least value of MSE is obtained for QTRR model.

(ii) The models that do not perform that well for prediction of concrete compressive strength at curing ages of 28, 56 and 91 days for concrete without fly ash are LPCR, LOLSR and QOLSR models, respectively.

(iii) The compressive strength prediction model that does not work efficiently for concrete with fly ash at curing ages of 28 and 91 days is QOLSR model, whereas, for curing age of 56 days, QPCR model shows the worst performance.

It is concluded that pure quadratic GRR models gave less value of MSE than other models in most of the cases.

6.2 RELIABILITY BASED SINGLE-OBJECTIVE OPTIMIZATION OF CONCRETE MIX PARAMETERS

Irrespective of their suitability, all the regression models developed for prediction of

concrete compressive strength are incorporated into RBDO model to assess their performance on the basis of optimization. Following conclusions have been arrived at in this work.

(i) QOLSR and QTRR models performed poorly in every case for concrete with or without fly ash and for each reliability level except for concrete without fly ash for 28 days curing age with all the three reliability levels.

(ii) Both linear and pure quadratic PCR models for 28 days compressive strength are not cost effective for concrete without fly ash although safety margins assumed by these models are moderate.

(iii) For 56 days concrete without fly ash, performance of QGRR, QPCR, LGRR, LTRR and LPCR models is more or less same for all the three reliability levels, while the remaining three models, namely, QTRR, QOLSR and LOLSR models failed to give workable concrete mix designs.

(iv) For concrete without fly ash at curing age of 91 days, QGRR model produces economical concrete mix designs in comparison to other models for reliability level of 0.90 and 0.95, whereas, for reliability level of 0.99, best cost effective designs are yielded by LPCR model.

(v) For concrete with fly ash at 28 days curing age, A single regression model could not be found that works well for each reliability level; however, QGRR and LPCR models perform better than other models for reliability levels of 0.95 and 0.99, respectively.

(vi) QTRR, QOLSR and LTRR/LOLSR models for 56 days concrete compressive strength produced infeasible optimal concrete mix designs for concrete with fly ash, whereas, performance of the remaining models is more or less same in this case.

(vii) QOLSR model failed to produce optimized concrete mix designs and QTRR model produced infeasible optimal designs for concrete with fly ash and 91 days curing age. Among remaining models, QGRR yields most economical concrete mix designs.

(viii) The TRR models fail to tackle the issue of multi-collinearity in almost all the cases.

(ix) 15% replacement of cement by fly ash results in a concrete having lower cost and same performance as that for concrete without fly ash.

(x) There is a non-linear relationship between reliability level and cost of concrete.

(xi) The safety factor based deterministic optimal concrete mix designs do not meet the reliability requirement for which they have been designed although they give optimal designs having lower cost than corresponding reliability based optimal designs for concrete with or without fly ash.

(xii) There is a reduction in w/b ratio with increase in target compressive strength and reliability level for concrete with or without fly ash. However, this reduction is more rapid for concrete without fly ash.

(xiii) The quantity of cement content in the optimal mixes increases with target compressive strength and reliability level for concrete with or without fly ash.

(xiv) The ratio of fine aggregate and binder content decreases with increase in compressive strength requirements for concrete with or without fly ash. Also, this ratio decreases with increase in reliability level for concrete without fly ash whereas reliability level does not affect this ratio for concrete with fly ash.

(xv) There is a slight reduction in ratio of coarse aggregates and binder content with increase in target compressive strength and reliability requirement for concrete with or without fly ash.

6.3 RELIABILITY BASED MULTI-OBJECTIVE OPTIMIZATION OF CONCRETE MIX PARAMETERS

Three best concrete compressive strength prediction models were selected on the basis of their performance in single-objective optimization for each curing age for concrete without or with fly ash. These selected models are then incorporated into multi-objective optimization of concrete mix proportions. Following conclusions have been drawn on the basis of multi-objective optimization results:

(i) Pareto-optimal fronts are not uniformly sensitive to change in compressive strength requirements, *i.e.*, rise in optimal cost for a unit rise in target compressive strength of concrete for a given reliability level is more in higher strength regions than lower strength regions for concrete with or without fly ash.

(ii) The rise in optimal cost is sharp as compared to the decrease in probability of failure for achieving a solution characterized by very low probability of failure requirements.

(iii) For concrete without fly ash and 28 days curing age, QTRR/QOLSR model provides a Pareto-optimal front much better than QGRR and LGRR models for each case of failure probability.

(iv) For concrete without fly ash and 56 days curing age, QGRR and LPCR models perform better than LGRR model.

(v) For concrete without fly ash and 91 days curing age, LTRR/LOLSR model and QGRR models perform better than other models for target strength ranging from 30 MPa - 40 MPa and from 45 MPa - 55 MPa, respectively.

(vi) For concrete with fly ash and 28 days curing age, both PCR models perform better than QGRR model. For curing ages of 56 days and 91 days, LPCR model yield best Pareto-optimal front.

(vii) w/b ratio increases with increase in probability of failure following a power curve in most of the cases for concrete with or without fly ash.

(viii) The amount of binder content in optimal mixes decreases with increase in w/b ratio for concrete with or without fly ash. However, this decrease is more rapid in optimal mixes for concrete without fly ash.

(ix) The ratio of fine aggregate and binder content is independent of w/b ratio, although this ratio decreases with increase in target compressive strength for concrete with or without fly ash.

(x) Coarse aggregate to binder content ratio is also independent of w/b ratio for concrete with or without fly ash.

Results from this study suggest that the RBDO methodology could be a valuable tool for minimizing the number of trial batches required to identify the optimal concrete mix proportions having desired properties and reliability.

6.4 SCOPE FOR FUTURE WORK

(i) Future work in this area should include using various techniques of optimization like particle swarm optimization and ant colony optimization that can lead to global optimum efficiently.

(ii) Soft computing models like ANN and GEP can be integrated with optimization techniques.

(iii) The work can be extended for high performance concrete and ultra high strength concrete.

(iv) The data used in the present work has been generated in controlled laboratory conditions. The compressive strength data from various construction sites can be collected and analyzed so that effect of other parameters like temperature of

curing, nature of curing, climatic conditions and degree of compaction can also be studied on compressive strength of concrete.

REFERENCES

[1] A.E. Hoerl, and R.W. Kennard.(1970). Ridge regression: Biased estimation for nonorthogonal problems. *Technometrics. 12*, pp. 55-67.

[2] A.M. Hasofer and N.C. Lind. (1974). Exact and invariant second moment code format. *J. Eng. Mech. Div. 100(1)*, pp. 111–121.

[3] A.M. Pande and L.M. Gupta. (2007). Proportions of concrete ingredients and their significance in compressive strength development. *The Indian Concr. J. 81 (6)*, pp. 15-36.

[4] A. Mohsine, G. Kharmanda and A. El-Hami A. (2006). Improved hybrid method as a robust tool for reliability-based design optimization. *Struct. Multidisc. Optim. 32(3)*, pp. 203–213.

[5] A.F. Almeida, E.V. Luiz and M.S.L.Velasco, "Deterministic and reliability-based design optimization of reinforced concrete plane frames," presented at Int. Conf. Engineering Optimization, Rio de Janeiro, Brazil, June 01 – 05, 2008.

[6] A. Chateauneuf, "Principles of reliability-based design optimization," in *Structural design optimization considering uncertainties*, Y. Tsompanakis, N. D. Lagaros and M. Papadrakakis Eds. London, UK: Taylor & Francis Group, 2008, pp. 3-30.

[7] A.N.S. Al Qadi, K.N.B. Mustapha, H. Al-Mattarneh and Q.N.S. Al-Kadi. (2009). Statistical models for hardened properties of self-compacting concrete. *American J. Eng. Appl. Sci. 2(4)*, pp. 764-790.

[8] A. Baykasoğlu, A. Öztas, and E. Özbay. (2009). Prediction and multi-objective optimization of high strength concrete parameters via soft computing approaches. *Expert Sys. Appl. 36*, pp. 6144 – 6155.

[9] A. Cevik, M.T. Göğüş, İ.H. Güzelbey, and H. Filiz. (2010). Soft computing based formulation for strength enhancement of CFRP confined concrete cylinders. *Adv. Eng. Softw. 41*, pp. 527-536.

[10] B.L. Karihaloo and D.L. Kornbak. (2001). Optimization techniques for the design of high performance fibre-reinforced concrete. *Struct.Multidisc.Optim. 21 (1)*, pp. 32-39.

[11] B.Y. Lee, J.H . Kim and J.K. Kim. (2009). Optimum concrete mixture proportion based on a database considering regional characteristics. *J. Comput. Civil Eng. 23*, pp. 258-265.

[12] B. Behnam and C. Eamon. 2013. Reliability-based design optimization of concrete flexural members reinforced with ductile FRP. *Construct. Build. Mater. 47*, pp. 942-950.

[13] C.M. Fonseca and P.J. Fleming, "Genetic algorithms for multi-objective optimization: Formulation, discussion and generalization," in *Proc. 5th Int. Conf. Genetic Algorithms*, 1993, pp. 416-423.

[14] C. Kirjner-Neto, E. Polak and A. der Kiureghian.(1998). An outer approximations approach to reliability-based optimal design of structures. *J. Optim.Theory Appl. 98(1)*, pp. 1-16.

[15] C.H. Lim, Y.S. Yoon and J.H. Kim. (2004). Genetic algorithm in mix proportioning of high–performance concrete. *Cem. Concr. Res. 34*, pp. 409-420.

[16] C. Y. Song, J. Lee and J. M. Choung. (2011). Reliability-based design optimization of an FPSO riser support using moving least squares response surface meta-models. *Ocean Eng. 38*, 304–318.

[17] D.M. Frangopol, "Reliability-based optimum structural design," in *Probabilistic structural mechanics handbook*, C. Raj Sundararajan, Ed. USA: Chapman Hall, 1995, pp. 352–387.

[18] D.M. Frangopol, K.Y. Lin, and A.C. Estes. (1997). Reliability of reinforced concrete girders under corrosion attack, *J. Struct. Eng. 123 (3)*, pp. 286-297.

[19] E. Nikolaidis and R. Burdisso. (1988). Reliability-based optimization: a safety index approach. *Comput. Struct. 28(6)*, pp. 781–788.

[20] E. Polak, R. J.-B.Wets and A. der Kiureghian, "On an approach to optimization problems with a probabilistic cost and or constraints," in *Nonlinear Optimization and related topics*, G.D. Pillo and F. Giannessi, Eds. US: Springer, 2000, pp. 299-316.

[21] E. Özbay, A. Baykasoğlu, A. Öztas, and H. Özbebek, "An experimental comparison of optimum mix proportions of high strength concrete proposed by Taguchi method and genetic algorithm," in *Proc. 5th Int. Symposium on Intelligent Manufacturing Systems*, Sakarya, Türkiye, 2006, pp: 1062-1070.

[22] E. Özbay, A. Baykasoğlu, A. and A. Öztas. 2010. Cost optimization of high strength concretes by soft computing approaches. *Comp. Concr. 7(3)*, pp. 221-238.

[23] F. Kursawe, "A variant of evolution strategies for vector optimization," in *Proc. Parallel Problem Solving in Nature I*, 1990, pp. 193-197.

[24] G. Kharmanda, A. Mohamed and M. Lemaire. (2002). Efficient reliability based design optimization using a hybrid space with application to finite element analysis. *Struct. Multidisc. Optim. 24(3),* pp. 233–245.

[25] H.O. Madsen, S. Krenk and N.C. Lind, *Methods of Structural Safety*. Englewood Cliffs, NJ: Prentice-Hall, 1986.

[26] H. Agarwal, "Reliability based design optimization: formulations and methodologies,". Ph.D. dissertation, Univ. Notre Dame, Indiana, 2004.

[27] H. Agarwal, C. Mozumder, J. Renaud and L. Watson. (2007). An inverse measure-based unilevel architecture for reliability-based design optimization. Struct. Multidisc. Optim. *33(3),* pp. 217–227.

[28] H.B. Nehzad, N.N. Zadeh and M.M. Ranjbar, "Multi Objective Optimization of Concrete Mix Design in Persian Gulf With Gmdh-type Neural Networks," in *Proc. 2nd Int. Conf. Engineering Optimization*, Lisbon, Portugal, 2010.

[29] I. Enevoldsen and J. D. Sørensen. (1994). Reliability-based optimization in structural engineering. *Struct. Safety. 15(3),* pp.169-196.

[30] I. Kaymaz, K. Marti. (2007). Reliability-based design optimization for elastoplastic mechanical structures. *Comput. Struct. 85(10),* pp. 615–625.

[31] I. Maruyama, M. Kanematsu, T. Noguchi and F. Tomosawa, "Optimization of mix proportion of concrete under various severe conditions by applying the genetic algorithm," in *Proc. 3rd Int. Conf. Concrete Under Severe Conditions Environment and Loading (CONSEC'01),* Vancouver, 2001.

[32] I. Maruyama, T. Noguchi and M. Kanematsu. (2002). Optimization of concrete mix proportion centered on fresh properties by genetic algorithm. *Indian Concr. J., 76*, pp. 567-573.

[33] I.C. Yeh. (1999). Design of high performance concrete mixture using neural networks and non linear programming. *J. Comput. Civil Eng. 13 (1),* pp. 36-42.

[34] *Indian Standard Plane and Reinforced Concrete- Code of Practice (Fourth Revision),* IS 456, 2000.

[35] I.T. Jolliffe, *Principal Component Analysis*. New York: Springer, 2002.

[36] I.C. Yeh. (2003). A mix proportioning methodology for fly ash and slag concrete using artificial neural networks. *Chung Hua J. Sci. Eng. 1 (1),* pp. 77-84.

[37] I.C. Yeh. (2007). Computer aided design of optimum concrete mixtures, *Cem. Concr. Compos. 29(3)*, pp. 193-202.

[38] I.C. Yeh. (2009). Optimization of concrete mix proportioning using a flattened simplex-centroid mixture design and neural networks. *Eng. Comput. 25 (2)*, pp. 179-190.

[39] *Indian Standard Concrete Mix Proportioning- Guidelines (First Revision), IS 10262*, 2009.

[40] J. Guiot, A.L. Berger and A.V. Munaut, "Response functions". in *Climate from tree rings*, M.K. Hughes, P.M. Kelly, J.R. Pilcher and V.C. LaMarche, Eds. Cambridge, UK: Cambridge University Press, 1982, pp. 38-45.

[41] J.D. Schaffer, "Some experiments in machine learning using vector evaluated genetic algorithms," Ph.D. dissertation, Vanderbilt Univ., Nashville, TN, 1984.

[42] J. Horn, N. Nafploitis and D. Goldberg, "A niched Pareto genetic algorithm for multi-objective optimization," in *Proc. 1st IEEE Conf. Evolutionary Computation*, 1994, pp. 82-87.

[43] J. A. Bland. (1998). Structural design optimization with reliability constraints using tabu search. *Eng. Optim. 30(1)*, pp. 55-74.

[44] J.O. Rawling, S.G. Pantula and D.A. Dickey, *Applied Regression Analysis: A Research Tool*. New York: Springer, 1998.

[45] J. Tu, K. K. Choi and Y. H. Park. (1999). A new study on reliability-based design optimization. *J. Mech. Des. 121(4)* pp. 557-564.

[46] J. O. Royset, A. D. Kiureghian and E. Polak. (2001). Reliability based optimal structural design by the decoupling approach. *Reliab. Eng. Syst. Safe. 73(3)*, pp. 213-221.

[47] J.F. Bonnans, J. Gilbert, C. Lemaréchal, C. Sagastizábal, *Numerical optimization*. Springer: Heidelberg, 2003.

[48] J. Namyong, Y. Sangchun and C. Hongbum. (2004). Prediction of compressive strength of in-situ concrete based on mixture proportions. *J. Asian Archit. Build. Eng., 3(1)*, pp. 9-16.

[49] J. Liang, Z.P. Mourelatos and J. Tu. (2008). A single-loop method for reliability-based design optimization. *Int. J. Product Development* 5, pp. 76-92.

[50] K. Deb, *Multi-Objective Optimization using Evolutionary Algorithms*. New York: Wiley, 2001.

[51] K. Deb, S. Agrawal, A. Pratap and T. Meyarivan, "A fast and elitist genetic algorithm for multi-objective optimization: NSGA-II," Kanpur Genetic Algorithms Laboratory, Indian Institute of Technology, Kanpur, India, Tech. Rep. 200001, 2000a.

[52] K. Deb, S. Agrawal, A. Pratap and T. Meyarivan, "A fast elitist non-dominated sorting genetic algorithm for multi-objective optimization: NSGA-II," in *Proc. the Parallel Problem Solving in Nature VI*, 2000b. pp.849-858.

[53] K. Marti and I. Kaymaz. (2006). Reliability analysis for elastoplastic mechanical structures under stochastic uncertainty. *ZAMM 86(5)*, pp. 358–384.

[54] L. Wang and S. Kodiyalam, "An effcient method for probabilistic and robust design with non-normal distribution," in *Proc. 43rd AIAA/ASME/ASCE/AHS/ASC Structures, Structural Dynamics, and Materials Conference*, Denver, Colorado, 2002.

[55] *Methods for Test for Strength of Concrete*, IS: 516, 1959.

[56] M. Hohenbichler and R. Rackwitz.(1981). Nonnormal Dependent Vectors in Structural Reliability. *J. Eng. Mechanics Division ASCE. 107(6)*, pp.1227-1238.

[57] M.V. Reddy, R.V. Grandhi and D.A. Hopkins. (1994). Reliability based structural optimization: a simplified safety index approach. *Comput. Struct. 53(6)*, pp. 1407–1418.

[58] M.L. Gambhir, *Concrete Technology*. New Delhi, India: Tata McGraw Hill Publishing Company Limited, 1995.

[59] M. Laumanns, G. Rudolph and H.P. Schwefel, "A spatial predator-prey approach to multi-objective optimization: A preliminary study," in *Proc. Parallel Problem Solving in Nature V*, 1998, pp. 241-249.

[60] M. Kumar, "Reliability based design of structural elements", Ph.D. Dissertation, Dept. Civil Eng., Thapar Univ., Patiala, India, 2002.

[61] M.K. Kazberuk and M. Lelusz. (2007). Strength development of concrete with fly ash addition. *J. Civil Eng. Manage. 13(2)*, pp. 115-122.

[62] M.A. Jayaram, M.C. Natraja and C.N. Ravikumar. (2009). Elitist genetic algorithm models: optimization of high performance concrete mixes. *Mater. Manuf. Process. 24*, pp. 225-229.

[63] M. Abdullahi, H.M.A. Al-Mattarneh, and B.S. Mohammed. (2009). Statistical Modeling of lightweight concrete mixtures. *European J. Sci. Res. 31(1)*, pp. 124-131.

[64] M.Y. Riad, S. Shoukry, E. Sosa and G. William. (2011). Prediction of concrete initial setting time in field conditions through multivariate regression analysis. *Mater. Struct. 44*, pp. 1063–1077.

[65] M.S. Ahmed. (2012). Statistical modeling and prediction of compressive strength of concrete, Concr. Res. Letters. *3(2)*, pp. 452-458.

[66] M. Khatibinia, E. Salajegheh, J. Salajegheh and M.J. Fadaee. (2013). Reliability-based design optimization of reinforced concrete structures including soil–structure interaction using a discrete gravitational search algorithm and a proposed metamodel. *Eng. Optim. 45 (10)*, pp. 1147-1165.

[67] M. Lofty, K.M.A. Hossain and M. Lachemi. (2014). Application of statistical models in proportioning lightweight self-consolidating concrete with expanded clay aggregates. *Construct. Build. Mater. 65*, pp. 450-469.

[68] N. Srinivas and K. Deb. (1994). Multi-objective function optimization using non-dominated sorting genetic algorithms. *Evol. Comput. J. 2(3)*, pp. 221-248.

[69] N. Kuschel and R. Rackwitz. (1997). Two basic problems in reliability-based structural optimization. *Math. Methods Oper. Res. 46(3)*, pp. 309–333.

[70] N. Kuschel and R. Rackwitz. (2000). A new approach for structural optimization of series systems. *Appl. Statis. Probab. 2(8)*, pp. 987-994.

[71] O. J. Koskisto and B. R. Ellingwood. (1997). Reliability-based optimization of plant precast concrete structures. *J. Struct. Eng. 123*, pp. 298-304.

[72] P. Hajela and C.Y. Lin. (1992). Genetic search strategies in multi-criterion optimal design. *Struct. Optim. 4(2)*, pp. 99-107.

[73] P.D. Ramugade. (2010). Estimating compressive strength. *The Indian Concr. J. 84 (7)*, pp. 35-44.

[74] P. Beaurepaire, M.A. Valdebenito, G.I. Schuëller and H.A. Jensen. (2012). Reliability-based optimization of maintenance scheduling of mechanical components under fatigue, *Comput. Methods Appl. Mech. Engrg. 221–222*, pp. 24–40.

[75] P. Kanakasabai and A.K. Dhingra, "An approach for uni-level reliability based design optimization using cross-entropy method," in *Proc. ASME 38th Design Auto. Conf. Information Eng. Conf.*, Chicago, Illinois, USA, 2012, pp. 1271-1279.

[76] R. Rackwitz and B. Fiessler. (1978).Structural reliability under combined random load sequences. *Comput. Struct. 9*, pp. 489-494.

[77] R.E. Steuer, *Multiple Criteria Optimization: Theory, Computation and Application*. New York: Wiley, 1986.

[78] R.V. Grandhi and L. Wang. (1998). Reliability-based structural optimization using improved two point adaptive nonlinear approximations. *Finite Elem. Anal. Des. 29(1)*, pp. 35–48.

[79] R. Rackwitz.(2001). Reliability analysis-a review and some perspectives. *Struct. Saf. 23(4)*, pp. 365-395.

[80] R.E. Melchers, *Structural Reliability Analysis and Prediction*. England: John Wiley & sons, 2002.

[81] R. Parichatprecha and P. Nimityongskul. (2009). An integrated approach for optimum design of HPC mix proportion using genetic algorithm and artificial neural networks. *Comp. Concr. 6(3)*, pp. 253-268.

[82] R. H. Lopez, D. Lemosse , J. E. Souza de Cursi , J. Rojas and A. El-Hami. (2011). An approach for the reliability based design optimization of laminated composites. *Eng. Optim. 43(10)*, pp. 1079-1094.

[83] *Specifications for Coarse and Fine aggregates from Natural Resourses of Concrete (Second Revision*), IS: 383, 1970.

[84] *Specifications for Fly ash for Use as Pozzolana and Admixture (First Revision)*, IS: 3812, 1981.

[85] *Specifications for High Strength Ordinary Portland Cement*, IS: 8112, 1989.

[86] S.K. Saluja, M.S. Sarma, A.P. Singh and S. Kumar. (1992). Compressive strength of fibrous concrete. *The Indian Concr. J. 66.*

[87] S. Bhanja and B. Sengupta B. (2002). Investigation on the compressive strength of silica fume concrete using statistical methods. *Cem. Concr. Res. 32*, pp. 1391-1394.

[88] S. Barakat, N. Kallas, M. Q. Taha. 2003. Single objective reliability-based optimization of prestressed concrete beams. *Comput. Struct.81*, pp. 2501-2512.

[89] S.H. Ngo, S. Kemény and A. Deák, A. (2004). Application of ridge regression when the model is inherently imperfect: a case study of phase equilibrium. *Chemometr. Intell. Lab. 72*, pp. 185-194.

[90] S. Tangtermsirikul, T. Kaewkhluab and P. Jitvutikrai. (2004). Compressive strength model for roller-compacted concrete with fly ash. *Mag. Concr. Res. 56(1)*, pp. 35-44.

[91] S. Rajasekaran. (2006). Optimal mix for high performance concrete by evolution strategies combined with neural networks. *Indian J. Eng. Mater. S. 13*, 2006, pp. 7-17.

[92] S. Chakraverty, H.Saini and S. K. Panigrahi. (2008). Prediction of product parameters of fly ash cement bricks using two dimensional orthogonal polynomials in the regression analysis. *Comp. Concr. 5(5)*, pp. 449-459.

[93] S. Chakraverty, H.Saini and S. K. Panigrahi. (2008). Prediction of compressive strength using simplex lattice design for mixture proportions in ternary systems of fly ash - cement - sand bricks. *The Indian Concr. J. 82(7)*, pp. 27-34.

[94] S. Shan S and G.G. Wang. (2008). Reliable design space and complete single loop reliability-based design optimization. *Reliab. Eng. Syst. Saf. 93(8)*, pp. 1218–1230.

[95] S.M. Abd, and M.F.M. Zain. (2009). Multiple regression model for compressive strength prediction of high performance concrete. *J. Appl. Sci. 9(1)*, pp. 155-160.

[96] S.S. Wu, B.Z. Li, J.G. Yang and S.K. Shukla, "Predictive modeling of high-performance concrete with regression analysis," in *Proc. IEEE Int. Conf. Industrial Engineering and Engineering Management*, Macao, 2010, pp.1009-1013.

[97] S. Salehghaffari , M. Rais-Rohani , E. B. Marin and D. J. Bammann. (2013). Optimization of structures under material parameter uncertainty using evidence theory, *Eng. Optim. 45(9)*, pp. 1027-1041.

[98] T.C. Palle and J.B. Michael, *Structural Reliability Theory and Its Applications*. Berlin, Heidelberg: Springer-Verlag, 1982.

[99] T.P. Ryan, *Modern Regression Methods*. New York: John Wiley & Sons, 1996.

[100] T. Noguchi, I. Maruyama and M. Kanematsu, "Performance-based design system for concrete mixture with multi-optimizing genetic algorithm". in *Proc. 11th Int. Congress Chemistry of Cement*, Durban, 2003, pp. 1921-1930.

[101] T.R. Gulati, I. Husain and A. Ahmed. (1997). Symmetric duality for multiobjective variational problems. *J. Math. Anal. Appl. 210(1)*, pp. 22-38.

[102] T.R. Gulati, I. Husain and A. Ahmed. (2005). Optimality conditions and duality for multiobjective control problems. *J. Appl. Anal. 11(2)*, pp. 225-245.

[103] T. Zou and S. Mahadevan. (2006). A direct decoupling approach for efficient reliability-based design optimization. *Struct. Multidisc. Optim.* 31, pp. 190-200.

[104] U. Atici. (2011). Prediction of the strength of mineral admixture concrete using multivariable regression analysis and an artificial neural network. *Expert Sys. Appl. 38 (8)*, pp. 9609-9618.

[105] W.F. Massy. (1965). Principal components regression in exploratory statistical research. *J. Amer. Statist. Assoc. 60*, pp. 234-256.

[106] W. Li and L. Yang. (1994). An effective optimization procedure based on structural reliability. *Comput. Struct. 52(5)*, pp. 1061–1067.

[107] W. Chen and X. Du. (2004) Sequential optimization and reliability assessment method for efficient probabilistic design. *J. Mech. Des. (ASME) 126(2)*, pp. 225–233.

[108] W. Park. (2013). Genetic-algorithm-based mix proportion design method for recycled aggregate concrete, *T. Can. Soc. Mech. Eng. 37 (3)*, pp. 345-354.

[109] W.J. Park, T. Noguchi and H.S. Lee. (2013). Genetic algorithm in mix proportion design of recycled aggregate concrete. *Comp. Concr. 11(3)*, pp. 183-199.

[110] X. C. Chen, T. K. Hasselman and D. J. Neill, "Reliability based structural design optimization for practical applications," in *Proc. 38th AIAA/ASME/ASCE/AHS/ASC Structures, Structural Dynamics, and Materials Conference, number AIAA-97-1403*, 1997, pp. 2724-2732.

[111] X. Du and W. Chen, W. (2000). Towards a Better Understanding of Modeling Feasibility Robustness in Engineering. *ASME J.Mech. Des. 122(4)*, pp. 357-583.

[112] X. Qu and R.T. Haftka. (2004). Reliability-based design optimization using probabilistic sufficiency factor. *Struct. Multidiscipl. Optim. 27(5)*, pp. 314–325.

[113] X. Yan. (2008). Modified nonlinear generalized ridge regression and its application to develop naphtha cut point soft sensor. *Comput. Chem. Eng. 32*, pp. 608-621.

[114] X.K. Zou, Q. Wang, J.Y. Fu and Y.W. Fan, " Integrated reliability-based design optimization of isolated concrete buildings under spectrum loading," in *Proc. 14th World Conf. Earthquake Engineering*, Beijing, China, 2008.

[115] Y.Y. Haimes, L.S. Lasdon and D.A. Wismer. (1971). On a bicriterion formulation of the problems of integrated systems identification and system optimization. *IEEE transactions on Systems, Man, and Cybernetics, 1(3)*, pp. 296-297.

[116] Y.T. Wu, H.R. Millwater and T.A. Cruse. (1990). Advanced Probabilistic Structural Analysis Method for Implicit Performance Functions. *AIAA J. 28(9)*, pp.1663-1669.

[117] Y.T. Wu. (1994).Computational Methods for Efficient Structural Reliability and Reliability Sensitivity Analysis. *AIAA J. 32(8)*, pp. 1717-1723.

[118] Y.T. Wu and W. Wang. (1998). Efficient probabilistic design by converting reliability constraints to approximately equivalent deterministic constraints. *J. Integr. Des. Process Sci. 2(4)*, pp.13–21.

[119] Y. Aoues and A. Chateauneuf. (2008). Reliability-based optimization of structural systems by adaptive target safety-Application to RC frames. *Struct. Saf.* 30, pp.144-161.

[120] Y. Luo, A. Li and Z. Kang. (2011). Reliability-based design optimization of adhesive bonded steel concrete composite beams with probabilistic and non-probabilistic uncertainties. *Eng. Struct. 33 (7)*, pp. 2110-2119.

[121] Y. Aoues, A. Chateauneuf, D. Lemosse and A. El-Hami. (2013). Optimal design under uncertainty of reinforced concrete structures using system reliability approach, *Int. J. Uncertainty Quantification. 3 (6)*, pp. 487–498.

[122] Z. You, S.W. Goh and J. Dong. 2012. Predictive models for dynamic modulus using weighted least square nonlinear multiple regression model. *Canadian J. Civil Eng. 39(5)*, pp. 589-597.

Appendix A

The experimental plan was designed by Kumar (2002) to generate compressive strength data for regression modeling and subsequent reliability based design optimizations. 49 concrete mixes were proportioned using four basic ingredients, namely, water, cement, coarse aggregate and fine aggregate. Also, 27 concrete mixes were proportioned using the four basic ingredients and fly ash. Fly ash is used as a replacement of cement by 15%. British DoE (Department of Environment) method of mix design (Gambhir 1995) was used for determining the proportions of materials for concrete mixes. The properties of the materials used by Kumar (2002) are presented in the succeeding sub-section.

A.1 MATERIALS

Ordinary Portland cement of 43 grade conforming to *IS 8112 -1989* was used. The average 7 and 28 days compressive strength of cement was found to be 35.6 MPa and 45.5 MPa, respectively. The physical properties of cement used in the study are given in Table A.1.

IS: 383-1970 defines the fine aggregate as the one passing through 4.75 mm IS sieve. The fine aggregate is often termed as a sand size aggregate. River bed sand with a fineness modulus of 2.09 and specific gravity of 2.54 was used as fine aggregate. The physical properties of fine aggregates are given in Table A.2. Also,

Percentage of fine aggregate passing 600 micron sieve = 71.8

The sand conforms to grading zone-III as per *IS: 383-1970*.

Three types of coarse aggregate *viz. CA-I, CA-II* and *CA-III*, were used in different proportions to increase the density of the resulting mix. Salient properties of these aggregates are listed in Table A.3. The aggregates used were washed and removed of any silt and then dried for 24 hours in an oven. The oven-dried aggregates were then used for casting of cubes for each type of concrete mix.

The fly ash used in the study was a low calcium Class F fly ash and it conforms to the requirements of *IS: 3812-1981*. Physical properties of fly ash are given in Table A.4.

A.2 CASTING OF SPECIMENS

A total of 49 different concrete mixes for concrete without fly ash and 27 concrete

mixes for concrete with fly ash as revealed in Tables A.5 and A.6, respectively, were prepared with varying water-binder ratio, binder content and aggregates fractions (Kumar 2002). Water-binder content ratio was kept between 0.42 and 0.55.

For each mix, 45 cubes of 150 mm size were cast and 15 each were tested at 28 days, 56 days and 91 days of curing period. The mixes produced were first tested for workability (vee-bee consistency test) and then the cubes were cast in moulds. The specimens were removed from the moulds after 24 hours and then cured in a temperature controlled curing tank at 27 ± 2º C.

A.3 TESTING OF SPECIMENS

The specimens, after the fixed curing period of 28 days, 56 days and 91 days were tested for compressive strength on an automatic compression testing machine (3000 kN capacity). The test was conducted in accordance *IS: 516-1959*. The mean values of compressive strength for each of the mixes are also reported in Table A.5 and A.6.

Also, cost of each concrete mix is calculated based upon the prices of ingredients in India. Cost of various ingredients of concrete per kg is given in Table A.7.

Table A.1 Physical properties of 43 grade ordinary Portland cement

S. No.	*Property*	*Observed values*
1	Normal consistency	28 to 30 percent
	Setting times (Vicat's apparatus)	
2	(a) Initial setting time	100-150 minutes
	(b) Final setting time	200-225 minutes
3	Specific gravity	3.10-3.15
4	Soundness	1.5 to 2.0 mm expansion
5	Fineness	3.0-5.0 percent
	Compressive strength	
6	(a) at 7 days	34-36.5 MPa
	(b) at 28 days	45-48.0 MPa

Table A.2 Physical properties of fine aggregates

S. No.	*Property*	*Observed values*
1.	Unit mass (compact)	1,680 kg/m^3
2.	Unit mass (loose)	1,590 kg/m^3
3.	Specific gravity (oven-dry basis)	2.54
4.	Percentage voids (compact)	33.7 percent
5.	Percentage voids (loose)	37.4 percent
6.	Percentage absorption	0.5 percent
7.	Fineness modulus	2.09

Table A.3 Physical properties of coarse aggregates

S.No.	*Property*	*Observed values*		
		CA – I	*CA - II*	*CA - III*
1.	Unit mass (compact)	1,580 kg/m^3	1,480 kg/m^3	2,150 kg/m^3
2.	Unit mass (loose)	1,380 kg/m^3	1,350 kg/m^3	1,980 kg/m^3
	Specific gravity			
3.	(a) Saturated surface dry	2.61	2.63	2.58
	(b) Oven-dry	2.68	2.68	2.60
4.	Percentage voids (compact)	41.2 percent	43.7 percent	17.3 percent
5.	Percentage voids (loose)	48.6 percent	48.7 percent	23.85 percent
6.	Percentage absorption	1.8 percent	1.18 percent	1.20 percent

Table A.4 Physical properties of fly ash

S. No.	*Property*	*Observed values*
1.	Specific gravity	1.99
2.	Lime reactivity-average compressive strength at Blaine 3389 cm^2/gm	47.87 kg/cm^2
3.	Colour	Grey (blackish)
4.	Fineness modulus	0.68

Table A.5 Mixture data for concrete without fly ash

S.No.	w/c ratio	Mix proportions ($c: fa: ca-I: ca-II: ca-III$)	Cement content (kg/m^3)	28 days Compressive strength (MPa)	56 days Compressive strength (MPa)	91 days Compressive strength (MPa)
1	0.514	1:1.392:2.181:1.074:0	350	39.52	43.31	46.13
2	0.543	1:1.497:2.294:1.130:0	350	31.66	37.18	43.92
3	0.480	1:1.245:2.001:0.986:0	375	42.73	48.23	52.23
4	0.507	1:1.354:2.134:1.051:0	375	40.69	44.46	46.42
5	0.533	1:1.581:2.042:1.006:0	375	36.84	40.92	44.52
6	0.450	1:1.100:1.811:0.892:0	400	47.99	52.95	55.51
7	0.475	1:1.210:1.953:0.962:0	400	44.89	51.20	53.85
8	0.500	1:1.430:1.892:0.932	400	43.13	50.22	51.97
9	0.525	1:1.543:2.005:0.988:0	400	38.58	45.51	47.49
10	0.423	1:0.981:1.650:0.813:0	425	51.25	57.55	59.50
11	0.447	1:1.087:1.794:0.883:0	425	49.05	54.14	57.35
12	0.471	1:1.275:1.725:0.850:0	425	47.16	51.25	54.27
13	0.494	1:1.397:1.858:0.915:0	425	45.05	50.72	52.85
14	0.422	1:0.977:1.644:0.810:0	450	53.69	57.77	59.89
15	0.444	1:1.140:1.576:0.776:0	450	49.63	54.48	58.04
16	0.467	1:1.254:1.702:0.839:0	450	47.42	51.34	55.30
17	0.421	1:1.045:1.470:0.724:0	475	54.01	57.91	60.15
18	0.442	1:1.192:1.650:0.813:0	475	50.05	55.72	58.31
19	0.543	1:1.497:1.712:1.712:0	350	36.64	43.46	46.55
20	0.507	1:1.354:1.593:1.593:0	375	41.57	46.81	50.04
21	0.533	1:1.581:1.524:1.524:0	375	37.81	43.50	47.55
22	0.475	1:1.210:1.458:1.458:0	400	46.22	52.58	53.07
23	0.500	1:1.430:1.412:1.412:0	400	44.11	50.98	52.56
24	0.525	1:1.543:1.497:1.497:0	400	40.90	46.56	51.07
25	0.447	1:1.087:1.339:1.339:0	425	50.35	56.02	58.32
26	0.471	1:1.275:1.288:1.288:0	425	47.51	52.92	54.47
27	0.494	1:1.397:1.387:1.387:0	425	45.30	51.47	53.09
28	0.518	1:1.511:1.473:1.473:0	425	42.54	49.05	51.19
29	0.422	1:0.977:1.227:1.227:0	450	54.11	58.52	62.28
30	0.444	1:1.140:1.176:1.176:0	450	52.03	56.26	59.19

Table A.5 (Continued) Mixture data for concrete without fly ash

S.No.	w/c ratio	Mix proportions ($c: fa: ca-I: ca-II: ca-III$)	Cement content (kg/m^3)	28 days Compressive strength (MPa)	56 days Compressive strength (MPa)	91 days Compressive strength (MPa)
31	0.467	1:1.254:1.271:1.271:0	450	48.74	53.42	55.03
32	0.489	1:1.370:1.365:1.365:0	450	46.59	53.21	53.61
33	0.421	1:1.045:1.097:1.097:0	475	54.49	58.65	63.07
34	0.442	1:1.192:1.231:1.231:0	475	53.06	56.67	62.57
35	0.463	1:1.230:1.255:1.255:0	475	49.18	54.04	57.10
36	0.533	1:1.473:0:1.206:1.206	375	37.30	43.51	46.63
37	0.500	1:1.321:0:1.106:1.106	400	44.04	50.53	52.55
38	0.525	1:1.436:0:1.182:1.182	400	39.61	46.09	48.17
39	0.471	1:1.191:0:0:1.016:1.016	425	47.37	51.31	54.77
40	0.494	1:1.294:0:1.088:1.088	425	44.69	50.69	52.75
41	0.518	1:1.426:0:1.009:1.009	425	40.02	46.92	48.48
42	0.444	1:1.069:0:0.928:0.928	450	50.93	55.71	59.05
43	0.467	1:1.171:0:1.002:1.002	450	48.08	52.63	55.61
44	0.489	1:1.288:0:0.930:0.930	450	45.25	50.43	53.09
45	0.511	1:1.393:0:0.991:0.991	450	42.68	48.54	49.63
46	0.421	1:0.954:0:0.841:0.841	475	54.14	58.21	61.11
47	0.442	1:1.059:0:0.921:0.921	475	51.31	56.37	59.51
48	0.463	1:1.167:0:0.858:0.858	475	48.67	53.48	56.50
49	0.484	1:1.264:0:0.915:0.915	475	45.52	50.97	53.63

Table A.6 Mixture data for concrete with 15% replacement of cement by fly ash

S.No.	w/cm ratio	Mix proportions $(cm: FA: fa: ca)$	Cement content (kg/m^3)	28 days Compressive strength (MPa)	56 days Compressive strength (MPa)	91 days Compressive strength (MPa)
1	0.450	1:0.15:1.100:1.811:0.892:0	400	39.04	47.65	52.20
2	0.423	1:0.15: 0.981:1.650:0.813:0	425	45.09	50.21	55.75
3	0.447	1:0.15:1.087:1.794:0.883:0	425	41.14	48.67	52.69
4	0.471	1:0.15:1.275:1.725:0.850:0	425	38.35	43.27	50.42
5	0.422	1:0.15:0.977:1.644:0.810:0	450	46.13	51.01	56.51
6	0.444	1:0.15:1.140:1.576:0.776:0	450	42.50	49.17	53.11
7	0.467	1:0.15:1.254:1.702:0.839	450	39.58	44.02	51.07
8	0.421	1:0.15:1.045:1.470:0.724:0	475	47.34	52.30	57.70
9	0.442	1:0.15:1.192:1.650:0.813:0	475	43.55	49.79	53.79
10	0.447	1:0.15:1.087:1.339:1.339:0	425	42.01	49.68	53.39
11	0.471	1:0.15:1.275:1.288:1.288:0	425	38.85	44.96	50.50
12	0.422	1:0.15:0.977:1.227:1.227:0	450	47.25	51.95	57.17
13	0.444	1:0.15:1.140:1.176:1.176:0	450	43.09	50.30	53.67
14	0.467	1:0.15:1.370:1.365:1.365:0	450	40.26	45.30	51.62
15	0.489	1:0.15:1.045:1.097:1.097:0	450	37.15	44.52	48.08
16	0.421	1:0.15:1.192:1.232:1.232:0	475	49.41	53.58	58.19
17	0.442	1:0.15:1.192:1.232:1.232:0	475	44.02	51.81	54.12
18	0.463	1:0.15:1.230:1.255:1.255:0	475	40.73	45.95	52.10
19	0.471	1:0.15:1.191:0:1.016:1.016	425	38.90	43.20	50.50
20	0.444	1:0.15:1.069:0:0.928:0.928	450	43.22	49.53	53.62
21	0.467	1:0.15:1.171:0:1.002:1.002	450	39.85	44.61	51.42
22	0.489	1:0.15:1.288:0:0.930:0.930	450	36.87	41.25	47.30
23	0.511	1:0.15:1.393:0:0.991:0.991	450	35.23	40.05	46.11
24	0.421	1:0.15:0.954:0:0.841:0.841	475	47.94	53.05	57.82
25	0.442	1:0.15:1.059:0:0.921:0.921	475	43.87	50.48	54.38
26	0.463	1:0.15:1.167:0:0.858:0.858	475	40.34	45.61	52.39
27	0.484	1:0.15:1.264:0:0.915:0.915	475	37.65	42.28	48.55

Table A.7 Cost of concrete mix ingredients

Ingredient	Cost per kg $(Rs.)$
Cement (c)	5.000
Fine Aggregate (fa)	0.500
Coarse aggregate-I $(ca-I)$	0.550
Coarse aggregate-II ($ca-II$)	0.570
Coarse aggregate-III ($ca-III$)	0.700
Fly ash	0.425